NASA Technical Memorandum 88223

Final Reports of U.S. Monkey and Rat Experiments Flown on the Soviet Satellite Cosmos 1514

Richard C. Mains and Edward W. Gomersall

May 1986

National Aeronautics and Space Administration

NASA Technical Memorandum 88223

Final Reports of U.S. Monkey and Rat Experiments Flown on the Soviet Satellite Cosmos 1514

Edited by
Richard C. Mains, Mains Associates, Berkeley, California
Edward W. Gomersall, Ames Research Center, Moffett Field, California

May 1986

NASA
National Aeronautics and
Space Administration

Ames Research Center
Moffett Field, California 94035

TABLE OF CONTENTS

SUMMARY

On December 14, 1983, the U.S.S.R. launched Cosmos 1514, an unmanned spacecraft carrying biological and radiation physics experiments from nine countries, including five from the United States. This was the fourth flight with U.S. experiments aboard one of the U.S.S.R.'s unmanned spacecraft. Earlier flights carried a variety of biological specimens and lasted 18.5 to 19.5 days. The Cosmos 1514 flight was limited to 5 days' duration because it was the first nonhuman primate flight for the U.S.S.R. Cosmos 1514 marked a significant departure from earlier flights both in terms of Soviet goals and the degree of cooperation between the U.S.S.R. and the United States. This flight included more than 60 experiments on fish, crawfish eggs, plants and seeds, 10 Wistar pregnant rats, and 2 young adult rhesus monkeys as human surrogates. After 5 days in orbit, the spacecraft landed in Central Asia where a Soviet recovery team began recovery operations. U.S. specialists participated in postflight data transfer and specimen transfer to the United States, and conducted rat neonatal behavioral studies. An overview of the mission is presented focusing on preflight, on-orbit, and postflight activities pertinent to the five U.S. experiments aboard Cosmos 1514.

PREFACE

On December 14, 1983, the Soviet Union launched Cosmos 1514, an unmanned spacecraft carrying biological and radiation physics experiments from nine countries, including five from the United States. The total number of investigators involved numbered at least sixty, and the experiments were more than four years in preparation. This launch was the fourth time the Soviet Union had flown U.S. experiments aboard one of its unmanned spacecraft. Earlier flights included Cosmos 782, 936, and 1129, launched in November 1975, August 1977, and September 1979, respectively.

A U.S./U.S.S.R. Science and Applications Agreement was signed in 1971 which initiated cooperation in the area of Space Biology and Medicine between the two countries. A Joint Working Group was established and has met periodically to exchange information obtained during spaceflights and to discuss problems and topics of mutual scientific interest. In October of 1974, the Soviets first offered to fly U.S. experiments aboard an unmanned spacecraft. U.S. experiment proposals were submitted to the Soviets, and subsequently a group of eleven experiments was flown on Cosmos 782, seven experiments on 936, and fourteen experiments on 1129.

Previous Cosmos flight experiments have used a variety of biological specimens including rats, plants and insects. This multispecies approach provided opportunities for investigators to examine questions of basic biology and problems common to man and animals that have been observed during and following sojourns in space.

Cosmos 1514 marked a significant departure from the earlier flights both in terms of Soviet goals and the degree of cooperation required between the two countries. This flight included rats, fish, crawfish eggs, plants and seeds, and for the first time, the Soviets decided to fly two young adult Macaques as human surrogates. This decision required the development of a sophisticated monkey restraint couch and life support system and allowed the U.S. to propose experiments with instrumentation to monitor physiological parameters on nonhuman primates. Also, the Soviets requested that the U.S. provide an adaptation of existing U.S. cardiovascular instrumentation to use as part of the monkey experiments. The Soviet goal to study rat gestation during this flight also provided unique opportunities to conduct postflight developmental and morphological studies on mothers and offspring.

These opportunities significantly increased the need for interaction among specialists from both countries, joint verification testing of hardware and experiments, and data sharing. Even though Cosmos 1514 was viewed by the Soviets as a hardware evaluation flight with a science-oriented follow-on flight planned, it can be seen by the results reported in this volume that significant scientific contributions to space biology and medicine were made.

In addition to the science results, Cosmos 1514 has contributed to the evolution of a model for the low-cost, systematic approach to development, testing and utilization of experimental hardware. This experience can be applied to the preparation of U.S. biological experiments for the Space Shuttle and the proposed Space Station.

For the many people involved in this venture within NASA, the Soviet Space Program, and the science and engineering specialists in both countries, there is a clear understanding that this accomplishment was possible only because of a determination to overcome all difficulties. The inevitable language, logistical and technological problems were surmounted by a team effort. The good will generated by this joint endeavor will remain. Our Soviet colleagues deserve our sincere admiration and thanks for their dedicated assistance in the execution of our experiments.

Edward W. Gomersall
Manager, Cosmos Project
NASA Ames Research Center

Contributors and Affiliations

U.S. Contributors

NASA Ames Research Center, Moffett Field, California, U.S.A.

R. R. Adachi
B. Benjamin
E. W. Gomersall
B. Halpryn
J. W. Hines
P. Patterson-Allen
D. N. Rasmussen
H. Sandler

J. R. Alberts, Indiana University, Bloomington, Indiana
C. E. Cann, University of California, San Francisco, California
C. A. Fuller, University of California, Riverside, California
J. R. Keefe, Case Western Reserve University, Painesville, Ohio
R. C. Mains, Mains Associates, Berkeley, California
M. C. Moore-Ede, Harvard Medical School, Boston, Massachusetts
F. M. Sulzman, State University of New York, Binghamton, New York
H. L. Stone,* University of Oklahoma, Norman, Oklahoma

*Deceased

U.S.S.R. Contributors

Institute of Biomedical Problems, Moscow, U.S.S.R.

A. M. Alpatov
Z. Apenasenko
V. Klimovitsky
Y. Kondratyev
I. B. Krasnov
V. Krotov
B. Kulaev
V. Magedov
A. N. Nazin
V. Oganov
A. Rachmanoff
L. V. Serova
A. Ushakov

V. Krilov, Academy of Sciences

COSMOS 1514 MISSION DESCRIPTION

Richard C. Mains
Science Consultant, Cosmos Project
Mains Associates
Berkeley, CA 94704

Edward W. Gomersall
Manager, Cosmos Project
Biosystems Division
National Aeronautics and Space Administration
Ames Research Center
Moffett Field, CA 94035

INTRODUCTION

The Cosmos Program uses the unique weightlessness* of spaceflight to determine the role of gravity in terrestrial biological phenomena and to study ways to support man during prolonged spaceflight. Human support areas of specific interest include artificial gravity, radiation shielding, and techniques for providing biological life support.

Earlier Cosmos flights have been launched by the Soviets approximately on a two-year cycle. The development time for Cosmos 1514 was more than four years primarily due to the time required by the Soviets for developing and testing a monkey BIOS capsule. This capsule had to provide adequate restraint, protection against launch and reentry stresses, and life support. In addition, a one-year training period was required for the monkeys to adapt to the BIOS, to learn to operate feeding, drinking, and psychomotor devices, and to fully recover from implantation of physiological sensors.

The last three Cosmos flights were approximately 19 days duration. Cosmos 1514 lasted only 5 days since this was the first nonhuman primate flight for the U.S.S.R. and they wished to ensure that the monkey subjects were able to adapt to the flight environment successfully. The launch occurred at 1000 hours on December 14, and the recovery was at 0700 hours on December 19, 1983 (table 1). The ten rat and two monkey subjects were judged to be in good condition at recovery.

The science interests of the many investigators were extremely diverse. A list of the more than sixty experiments and investigators is shown in table 2. Countries in addition to the U.S. and U.S.S.R. represented in this flight were Bulgaria, Hungary, German Democratic Republic, Poland, Rumania, Czechoslovakia, and France.

Mission Management Plan

The U.S. responsibilities for this flight can be divided into hardware development, training of Soviet specialists, hardware and experiment verification testing and postflight data transfer and analysis. The four U.S. experiments included monkey cardiovascular, biorhythm, and calcium metabolism studies, and a rat developmental study with both behavioral and neuroanatomical measurements.

---

* Although the term "weightlessness" is used here, it should be noted that complete weightlessness was not achieved. The spacecraft rotated in orbit and imparted accelerations to experiments near the perimeter of the spacecraft of 1.7×10^{-7} to 1.5×10^{-4} g. Accelerations to rats located near the center of the spacecraft were probably somewhat lower. These acceleration levels are presumed to be below the threshold of biological sensitivity.

1. Hardware Development

Flight hardware was developed for the cardiovascular and biorhythm experiments and special ground support equipment (GSE) for the calcium metabolism and the rat developmental study. This hardware is discussed in detail in a separate chapter in this report. It was developed with periodic formal Soviet evaluation of its proposed design and function. NASA conducted several internal hardware design reviews and submitted early prototypes to the simulated launch and reentry stresses specified by the Soviets. Eight units of flight acceptance-tested hardware were supplied to the Soviets to support all phases of experimentation. These phases were defined as flight, flight back-up, synchronous control, and vivarium control. Two units of flight hardware were required for each phase for the cardiovascular and biorhythm experiments.

2. Soviet Specialist Training

Soviet surgeons were trained at both NASA-ARC and at the Institute of Medical and Biological Problems in Moscow, the Soviet experiment integration and test facility, to implant a blood flow and pressure sensor in the monkey for the cardiovascular experiment. Soviet coinvestigators and engineering specialists were trained to calibrate and evaluate sensor performance using U.S.-provided GSE.

The Soviet coinvestigator for the biorhythm experiment was trained to apply three surface sensors on monkey subjects. Also, Soviet specialists were trained to transfer data from temporary memory in the biorhythm recorders to permanent storage. The rat development experiment which was to be conducted postflight was set up in Moscow to train the Soviet coinvestigator and to verify hardware performance on Soviet electrical power.

3. Hardware and Experiment Verification Tests

After successful bench tests, the hardware was evaluated during tests with monkeys and rats. Experimental procedures and data quality were also evaluated at this time. This testing was usually separate for the flight and GSE hardware. Flight hardware was evaluated extensively at NASA-ARC during an October 1981 flight simulation test conducted with two flight-size rhesus monkeys. The monkeys were placed in custom-designed, NASA-fabricated restraint systems to provide an approximation of the Soviet conditions for flight. These restraint systems allowed attachment of cardiovascular and biorhythm sensors for the estimated maximum 10-day flight duration.

Additional bioengineering and flight simulation tests of gradually increasing duration were conducted in Moscow with both Soviet experiment-unique and general flight-related equipment such as the BIOS capsule and Soviet data acquisition system. Soviet support of U.S./U.S.S.R. hardware interface testing was critical to the successful integration of the many special devices built for this flight.

Preliminary biological specimens were collected from Soviet monkeys in Moscow for the calcium metabolism experiment and transported to the U.S. prior to the actual flight to verify the sampling, storage, shipping, and analytical techniques. Radiographs of monkeys were also taken in Moscow for this experiment and transported to the U.S. to verify both the hardware and procedures.

4. Data Transfer/Analysis

U.S. specialists were in Moscow postflight to support data transfer from the flight hardware experiments. Data were transferred from solid state recorders used for the biorhythm experiment to a floppy disk and a permanent paper copy produced using experiment GSE. The cardiovascular experiment data from the various experiments were transferred from the Soviet analog tape recorder to a U.S. tape recorder for digitization and subsequent computer analysis in the U.S.

5. Documentation

An Experiment Management Plan (EMP) was written which included all critical information required for conducting each experiment. Each EMP contained a description of the experiment objectives, a listing of the joint investigators (U.S./U.S.S.R.) and their responsibilities, the flight, synchronous and vivarium experiment protocols, experiment verification test status, specimen collection and labeling procedures, animal preparation/test procedures, experiment data log sheets, data transfer and analysis requirements/procedures, and the equipment list, specifications and operating procedures. The EMP was the major document used to support training of the Soviet specialists.

Flight hardware units were delivered to the Soviets with a document titled "Biorhythm Specifications and Procedures Manual" or "Cardiovascular Specifications and Procedures Manual." These documents described the acceptance tests conducted for each flight hardware unit prior to delivery to the Soviets. They also contained all equipment specifications and operating instructions required for the Soviets to test, operate and maintain the hardware. Also included was a hardware use summary describing the operational history of each unit prior to delivery. A demonstration of each unit was conducted at ARC for Soviet engineers using these manuals to verify that the hardware met performance specifications and to assist them in verifying proper function of the equipment.

Spacecraft Description

A modified Vostok spacecraft similar to that used for the previous biological satellites as well as early Soviet manned spaceflights, was used for the Cosmos 1514 mission. It was a spherical craft approximately 2.5 meters in diameter with a 900-kg payload and a gross weight of approximately 2250 kg (fig. 1). The atmospheric pressure within the craft was maintained approximately at sea level and varied between 715 and 780 mm Hg with an average of 758. Air temperature ranged in the flight capsule between 20.5 and 24.0 deg C and in the primate BIOS capsule between 24.0 and 25.0 deg C. The pO_2 ranged from 150 to 210 mm Hg, and pCO_2 values

were 1.5 mm Hg or less. The relative humidity range was 30% to 50%. The flight light cycle was 16 hours light and 8 hours dark with a light level of approximately 60 ± 10 lux during light and less than 1 lux during dark. Lights on in the capsule occurred at 0800 Moscow time. Spacecraft power was supplied by onboard batteries.

The Soviet development of the monkey BIOS capsule, a combined life support and experiment system, was a major engineering effort. Each of the two capsules (fig. 2) included a restraint couch (figs. 3 and 4) with a remotely controlled chest restraint pad, a lap restraint plate with leg divider, upper and lower arm restraint straps and a deflector (fig. 5) which used unidirectional airflow to move excreta toward a centrifugal collector underneath the chair. The two capsules were placed so that the monkeys could view each other. A major design goal for the restraint couch was to provide monkey support adequate for the anticipated reentry shock of 20-60 g at ground impact after parachute descent.

The capsule also contained separate paste diet and juice dispensers (fig. 6). The dispensers were designed so that the presentation of food and water could be controlled via an up-linked signal from the ground. The paste and juice dispensers were monkey-activated by bite switches located in the spouts. When activated, they injected fixed quantities of paste or liquid into the monkey's mouth. A TV camera was mounted on each BIOS to monitor inflight behavior of the subjects.

A psychomotor system was built into the wall of the capsule which included leg response levers (fig. 5). The monkeys were trained to respond to light signals with lever presses to obtain a juice reward. The strength required for a lever press could be measured using the integrated EMG signals recorded from limb muscles. There was also a vestibular test which included an eye-tracking device with a semicircular array of programmed lights located in front of each monkey. A sensor was located in the skull cap of one monkey which, when pointed directly at the light on the panel, registered that a correct response was made by the monkey and a juice reward was presented. Part of the vestibular test included a slow sinusoidal motion of subjects in the head to foot direction produced by a motorized oscillator attached to the restraint couch.

The Soviet rat breeding chamber (BIOS) flown on Cosmos 1129 is shown in figure 7. It was modified for Cosmos 1514 by removing the partition that divided the males from the females. In this way a single compartment measuring 65 by 20 by 16 cm was provided for the pregnant female rats. Water and paste food were provided to the rats. The rat excreta management was accomplished by passage of a unidirectional airflow through the ceiling of the cage into a waste collector on the bottom which was rotated every two days.

The light/dark cycle in the rat chamber was 12:12 with an 8-lux intensity. Ten-gram quantities of the paste diet were provided to the rats four times/day at 6-hour intervals throughout the flight. Water was provided ad libitum.

The paste diet composition used for the rats is shown in table 3. The liquid presented to the monkeys was 60% water and the remainder fruit juice with a

preservative added to prevent fermentation at room temperature. The paste diets contained the same preservative to prevent spoilage and gas formation in the food line. The daily schedule of food, juice and psychomotor testing in the BIOS capsule is shown in figure 8.

Payload Description

1. U.S. Experiments

Four experiments were flown, with three designed for monkey subjects and one for rats. The monkeys were all laboratory bred Macaca mulatta males and the rats were all the Wistar strain of Czechoslovakian origin, bred at the Institute for Medical and Biological Problems in Moscow. All experiments focused on the effect of weightlessness as the prime experimental variable.

o Biorhythm Experiment

The experiment was conducted on the flight monkey subjects and was designed to measure and record the external synchronization of motor activity, body temperature and skin temperature rhythms to a fixed light/dark cycle and the internal synchronization of these rhythms to each other. Preflight control and postflight recovery data recordings were critical to the interpretation of flight data.

o Cardiovascular Study

The Soviets were provided with U.S.-developed, implantable instrumentation to monitor blood flow and pressure from the carotid artery of one of the flight monkeys and correlate this with other cardiovascular data recorded simultaneously. A major interest was to evaluate early flight versus long-term changes in these parameters. Ambient cabin pressure was also monitored to assist in interpretation of the vascular pressure data.

o Calcium Metabolism

This experiment was designed to measure the change in calcium metabolism for monkey subjects by comparing the flight with the preflight and postflight periods. A continuous stable isotope was used to differentiate dietary and skeletal calcium and evaluate the initial response of the skeleton to weightlessness. Correlated measurements of endocrine response and skeletal status were planned to aid in interpretation of the results.

o Neuro-ontogeny Experiment

This experiment was a postflight embryology study of neonatal rats and their mothers conducted post-delivery with one-third of the gestation period under flight conditions. A battery of postnatal behavioral tests was conducted to evaluate sensory development. Sacrifice of some mothers, fetuses and neonates during the recovery

period provided samples for a histomorphometric analysis of vestibular, olfactory, and visual organs and their central nervous system pathways.

2. U.S.S.R. Experiments

A complete list of experiments for Cosmos 1514 is given in table 2. More detailed descriptions of the Soviet experiments will be included in the Soviet Cosmos 1514 Final Science Reports.

The Soviet experiments required several monkey sensor implants which are diagrammed in figure 9. Brain and oculogram electrodes provided data correlated with inflight vestibular tests and sleep/wake studies. Electromyograms were recorded from the left leg to provide data on muscle strength recorded during psychomotor testing. Rheoplethysmographic electrodes were implanted on the thorax to provide signals related to cardiac stroke volume and blood distribution changes. Subcutaneous electrodes provided electrocardiograms for interpretation of cardiac function and circadian rhythms. Body temperature was recorded using a telemetry implant. Recordings were also made of inflight food and water consumption and monkey behavior was monitored via video.

No surgical implantation of sensors was conducted with the rats. The subjects flown were normal and all testing was done postflight. A Soviet schematic of the major hardware distribution in this biosatellite is shown in figure 10.

MISSION OPERATIONS

General Experiment Design

The overall Soviet design for Cosmos 1514 was similar to earlier missions and included flight, synchronous, and vivarium control experiments. In general, the synchronous control was designed to duplicate the flight experiment except for factors unique to the external spacecraft environment such as weightlessness. The vivarium control was designed to accumulate as much data as possible with subjects housed in normal laboratory conditions to control for all factors which were unique to the internal spacecraft environment. These experiments differed for the monkey and rat subjects and are described separately below.

1. Monkey Experiments

A single preflight group of monkeys formed the candidate pool from which to select flight subjects and synchronous and vivarium controls were selected. This group began training for the flight more than a year prior to launch. The subjects were all Macaca mulatta (rhesus) and laboratory-bred at the Soviet Primate Center in Sukumi to be about 3 years of age at launch. The goal was to have subjects which weighed 3.5-4.5 kg about 3 months prior to launch. Since a Soviet vestibular test required that the flight restraint seat oscillate vertically within the animal capsule, the major size constraint on flight candidates was height, which could not exceed 42 cm from top of head to seat.

The training consisted of conditioning subjects to sit in restraint couches and perform various kinds of tasks (lever pressing with feet and eye-tracking on a moving light) with food rewards. Subjects were trained to eat and drink from flight-type food and juice dispensers and also were evaluated on a centrifuge programmed to simulate launch and reentry g loads. In addition, subjects were evaluated for their ability to tolerate a several-hour stay in the right-lateral supine position which would be experienced during the prelaunch rocket maneuvers.

The Soviet goal was to have a group of 18 trained monkeys available for implantation of sensors beginning about L-90 (90 days prior to launch). Two separate surgeries were conducted on the subjects. The first was performed on half of the group about L-90 and consisted of brain electrodes with skull cap required for Soviet vestibular and sleep studies. The first surgery on the remaining half of the group was done at L-60 and consisted of implantation of the U.S.-provided carotid pressure and flow (CPF) cuff.

The second surgery was performed on the total group at about L-30 days and consisted of implantation of 15 subcutaneous electrodes for Soviet experiments including electromyogram, electrooculogram, electrocardiogram, and rheoplethysmogram measurements. Also, the Soviet subcutaneous, axillary temperature transmitter was implanted and the CPF cuff leads were exteriorized at this time.

A 10-day, preflight control data acquisition period began on the remaining acceptable flight candidates (about 14 monkeys) on L-16. At L-6, four flight subjects were chosen with two designated as prime and two as back-up candidates. This group was shipped to the launch site on this day and the remaining 10 monkeys formed the vivarium candidate pool. At L-3, a final selection of the 2 flight monkeys was made and the 2 back-ups were sent to Moscow as prime candidates for synchronous control subjects.

The synchronous control began 9 days postlaunch and was conducted with subjects in the BIOS capsule and the same Vostok spacecraft as was used for the flight. This control simulated all the major environmental and mission events which occurred for the actual flight including; flight duration, lift-off and reentry shock and vibration profiles, ambient temperature, humidity and atmospheric conditions. A 21-day recovery period was begun immediately after both the flight and synchronous control experiments for gathering postflight data.

The vivarium experiment had a variable protocol dependent on each investigator's experiment. Vivarium subjects were kept in colony cages during the entire period after selection of the flight and backup monkeys except for short-term restraint required to connect instrumentation for obtaining specific measurements. It was planned that all three monkey groups would receive the same flight diet and juice during the experiments to control for this variable.

Soviet specialists were ultimately responsible for conducting most aspects of the three U.S. monkey experiments. U.S. investigators were in Moscow after recovery mainly to support data transfer activities. Soviet specialists implanted the blood

pressure and flow cuff for the cardiovascular study, exteriorized the leads and assembled the experiment hardware in the BIOS capsule. They attached all sensors to the monkeys for the biorhythm experiment, assembled the flight hardware and activated the recorders prior to installation of the equipment into the BIOS. They collected all biological samples for the calcium metabolism experiment, prepared the fixatives and labeled, stored and shipped the samples to Moscow for delivery to the U.S. for analysis. The extensive training of Soviet specialists in most aspects of the experiments was critical for preparing them to assume their highly responsible role.

2. Rat Experiments

Three sets of pregnant female rats were established to provide candidates for the flight and the synchronous and vivarium control groups. Mating of these rats was scheduled so that on the actual or control experiment launch day, the females would be very close to gestation day 13 of their 21-day cycle.

The vivarium control group was meant to be a direct control for the flight group to allow, for example, postflight placement of tissues in the same fixative batch, and storage, transport and processing through all subsequent steps simultaneously. The only variation in this plan was the requirement that this group lag behind the flight group by 2 days to provide flight back-up candidates in case there was an unavoidable last-minute delay of the launch. Thus, the vivarium control group was 2 days behind the flight group and the synchronous control 13 days behind. Each of these groups consisted of 10 pregnant female rats.

The rat synchronous controls were placed in the flight rat BIOS within the ground-based spacecraft and exposed to the same environmental and mission-related events as were the flight subjects. The vivarium controls were kept in standard colony housing.

Soviet specialists sacrificed pregnant females at the recovery site and prepared the specimens for fixation and shipment to Moscow for histomorphometric analysis by the U.S. In addition, they actively supported the postflight neonatal behavior study. The major responsibility for conduct of the rat experiment was held by the U.S. investigator team since this was mainly a postflight effort.

Preflight Events

1. Monkey Experiments

At L-21, subjects were placed on the flight 16:8 light/dark cycle. The lights-off period was from 2400 to 0800 hrs Moscow time. On the same date, flight monkey candidates were placed on the flight-type paste diet. Subjects were presented with this diet for 2 hours at 1000 and 1600 hours. At L-15 monkey subjects were switched to an identical diet with no Calcium-48 present (termed the Calcium-40 diet) as part of the U.S. calcium metabolism experiment. The subjects not chosen for flight became synchronous control candidates and remained on the flight diet until

2 subjects were chosen for this experiment. After that time, only the 2 synchronous subjects continued the Calcium-40 diet.

Periodically during the preflight period, subjects were placed in the BIOS capsule and exposed to the psychomotor training procedure where they had to respond to presented stimuli with foot lever presses and head positioning in order to obtain juice rewards. Continued training on flight food dispensers was also conducted during this time. At no time were subjects left in the capsule for longer than a 48-hour period, and an attempt was made to minimize the restraint time during the preflight period to minimize any deconditioning effects.

During the time the flight candidates were out of restraint and housed in the colony cages they wore restraint jackets which protected the exteriorized leads connected to the implanted sensors. To ensure that these leads were not damaged, the Soviets monitored subjects 24 hours/day during the prelaunch period.

At L-5, four flight candidates were transported by airplane in special cages to the launch site on a five-hour trip. An attempt was made to provide expected spacecraft environmental conditions beginning at this time until launch. The synchronous and vivarium candidates were not transported to the launch site, but were exposed to a similar 5-hour airplane flight but then returned to Moscow.

From L-4 to L-3, the subjects recovered from their trip and were then placed in a BIOS capsule for continued preflight training. At L-2.5 the flight subjects were chosen and each BIOS was placed in the spacecraft with monkeys in the seated-upright position. During L-1 and within the normal daylight hours for monkey subjects, the spacecraft was attached to the rocket. This oriented the monkeys so that they were lying horizontal on their right sides for 8 to 10 hours. At 8 hours before launch, the entire rocket was tilted upright so that the subjects were again in the seated-upright position which they assumed until launch at 1000 hours on December 14th.

2. Rat Experiments

At L-21, the flight rats were switched from a pellet/seed diet fed ad libitum to the flight paste diet provided in a 40-gm quantity per animal once per day and water provided ad libitum. At this same time the flight light cycle and daily weighings were begun. At L-13, the 10 females were inseminated. The rats were transported to the launch site and installed in the spacecraft at the same time and in the same manner as the monkey subjects. The vivarium and synchronous control groups followed this sequence except for being delayed by 2 and 13 days, respectively, compared to flight subjects.

Launch, On-Orbit, Reentry Events

Soviet data show that acceleration was 4 g at launch (+Gz), about 10^{-6} on-orbit and 6 g (+Gz) during reentry.

1. Monkey Experiments

Immediately after achieving orbit, a Soviet up-linked signal activated the onboard cardiovascular U.S. signal conditioners. Thereafter, the units were activated every two hours by a Soviet signal for a 5-minute period of data acquisition. Shortly after insertion into orbit, the chest restraint straps on each monkey were loosened by a motor-driven device activated by an up-linked signal to provide more mobility for the subjects. These same straps were tightened shortly before reentry to secure each subject in the restraint couch to maximize support for the shock of landing. The monkeys followed the basic daily flight activity and experiment schedule diagrammed in figure 8.

On-orbit TV monitoring indicated the following (as quoted from a Soviet report). "During the first two days both primates were drowsy and inert, in particular Bion; they made no sharp movement with the head or body; their faces, especially the lips and the neck, were enlarged. By flight day 3 the behavior of Abrek became normal; he began to turn his head and showed interest in the surrounding objects; the edematous enlargement decreased significantly. The behavior of Bion also improved but became normal only by the end of flight day 4."

2. Rat Experiments

No special inflight activities were conducted with the rat chamber. The rat flight chamber performance characteristics have been described above under the description of the spacecraft.

Postflight Events

1. Monkey Experiments

Landing occurred at 0700 hours on December 19th (R-0). When the spacecraft was located, it was covered with a temperature-controlled portable field laboratory within which all animal removal procedures were conducted. The hatch was opened on the spacecraft by 0830 hours. All animal subject reactions appeared to be normal. At 0900 hours the Vestibular monkey (Abrek) was removed from the BIOS and by 1000 hours the Cardiovascular monkey (Bion) was removed. Postflight examinations of the monkey subjects were completed by 1600 hours on this day and revealed no unusual signs. The subjects were placed in transport cages on R+1 and flown to Moscow. Beginning on R+2 the flight monkeys were allowed to recover in vivarium cages.

Based on behavior and food and juice consumption it appeared that Abrek adapted to the flight faster than Bion. Abrek was more active during the flight and ate and drank shortly after achieving orbit. Bion began to drink juice only on the third day and did not consume food until the beginning of the fourth day of flight. Abrek consumed 396 gm of food and drank 616 ml of juice during the flight, and with a preflight weight of 3.5 kg, lost 260 gm (7.4%) in weight. Bion consumed 318 gm of food and drank 200 ml of juice, and with a preflight weight of 4.64 kg, lost 400 gm (8.6%) in weight. Due to the magnitude of the weight losses experienced during

flight, the Soviets decided to supplement the scheduled continuation of the post-flight paste diet with fresh food.

The Soviets observed body dehydration at recovery, and the circulating blood and plasma volume was decreased by 25-28%. Extracellular and interstitial fluid decreased and venous hematocrit increased by 9%. Data on monkey ECG amplitude-interval parameters, vestibular tests, myograms, leg circumference measurements and "higher nervous activity" (Soviet Programs 1 & 2 in fig. 8) are presented in separate Soviet papers.

Beginning at R+2, it was noticed that Bion was not in good health and this subject subsequently died at the 69th hour of recovery. A post-mortem analysis indicated that death was due to a strangulated bowel which may have been congenital in nature and appeared to be unrelated to either the implanted instrumentation or the spaceflight. The cardiovascular flow and pressure implant on Bion appeared to be properly placed and the enclosed artery was still patent. Flight experiment recovery studies continued with Abrek as planned. Two 48-hour periods of recovery physiological monitoring for the biorhythm experiment were conducted on Abrek beginning at R+5 and R+13.

The flight Calcium-40 paste diet was discontinued on R+7 and the Calcium-48 diet continued until R+21. The flight light cycle was maintained until R+15 when acquisition of the biorhythm recovery data was completed.

Two monkeys, Ariel (Cardiovascular) and Teuton (Vestibular), were chosen for the synchronous control study which began 9 days after the actual launch. This day was designated SL-0 (synchronous launch) and began the simulated flight period. Pre-synchronous and post-synchronous baseline data acquisition was conducted for all experiments to compare to the flight period. Additional postflight baseline studies were conducted by the Soviets to support their flight data interpretation.

U.S. specialists were in Moscow during the postflight period to transfer cardiovascular study data from the Soviet flight tape recorder to the U.S. ground-based recorder. In addition, data were transferred from the biorhythm experiment flight recorders to permanent copy for analysis in the U.S.

2. Rat Experiments

At R+0, all female rats were recovered in good condition. The five females allowed to deliver were transported to Moscow by airplane in individual cages and maintained in the rat colony until after delivery of litters at approximately R+5. The mothers plus newborns were then transferred into the specially designed cages to be used for conducting the U.S. behavior experiment. Four of the five females had at least twelve pups. The fifth female had a prolonged labor and delivered dead fetuses.

The remaining five female rats were sacrificed at the recovery site and specimens stored in fixative for transport to Moscow. The vivarium and synchronous control experiments were instituted as planned and begun at L+2 and L+9, respectively, at

the Institute of Medicine and Biological Problems in Moscow. Postflight data acquisition continued for 21 days for the flight experiment, and synchronous and vivarium controls.

U.S. specialists were in Moscow postflight to conduct the 21-day behavior studies for the three experiments and to transfer specimens to the U.S. Because of the 9-day lag of the synchronous control experiment, the postflight test phase was 30 days in duration.

As reported by the Soviets, weight gains of the dams was less during the flight period than in the comparable synchronous control period. Flight rats showed significant decreases in muscle mass. Liver mass, hemoglobin and amniotic fluid also decreased.

SPECIMEN TRANSFER

All biological specimens were hand-carried from Moscow to San Francisco by U.S. specialists at the end of the synchronous control experiment. Frozen monkey urine and fecal samples for the calcium metabolism experiment were placed in a metal container with dry ice and this package was placed in a larger container with the metal container surrounded with "blue ice" blocks designed to maintain a temperature of 4-8 deg C during transport.

Tissue specimens from the neuro-ontogeny experiment were stored in fixative in Moscow at 4-8 deg C. For shipment they were packed in "blue ice" in a transport case fitted with a thermometer which could be monitored during transit to ensure that this temperature range was maintained. All specimens were received in investigator's laboratories in good condition and at the proper temperature.

ACKNOWLEDGMENTS

Special thanks are owed to many individuals who contributed to the success of the U.S. experiments flown on Cosmos 1514. The U.S. investigators and all members of their experiment teams worked diligently on the preparation and execution of their experiments frequently against great time pressures and in the face of changing schedules. A small but dedicated group of U.S. Project personnel devoted themselves, sometimes at great personal sacrifice, to surmounting the many logistical and management problems inherent in an international mission of this nature. Our Soviet colleagues performed the U.S. experiments with great skill and a determination to overcome all obstacles. They ultimately deserve the major credit for the success of this mission.

TABLE 1.- SOVIET BIOLOGICAL SATELLITE MISSIONS WITH U.S. PARTICIPATION

Mission parameters	Cosmos 782	Cosmos 936	Cosmos 1129	Cosmos 1514
Launch date	25 Nov. 1975	3 Aug. 1977	25 Sept. 1979	14 Dec. 1983
Recovery date	15 Dec. 1975	22 Aug. 1977	14 Oct. 1979	19 Dec. 1983
Mission length	19.5 days	18.5 days	18.5 days	5.0 days
Period of revolution	90.5 min	90.7 min	90.5 min	89.3 min
Apogee	405 km (251 mi)	419 km (260 mi)	406 km (252 mi)	288 km (179 mi)
Perigee	226 km (140 mi)	224 km (139 mi)	226 km (140 mi)	226 km (140 mi)
Orbital inclination	62.8°	62.8°	62.8°	82.3°[a]

[a]Higher orbital inclination for radiation experiment.

TABLE 2. - DESCRIPTIVE TITLES AND PRINCIPAL INVESTIGATORS FOR THE EXPERIMENTS OF COSMOS 1514

Title	Principal investigators
I. EXPERIMENTS WITH MONKEYS	
A. Behavior, Central Nervous System, and Biorhythms of Primates	
1. Behavior and Higher Nervous Activity of Primates Before and during Space Flight	G. Shlyk I. Kozlovskaya V. Korolkov E. Ilyin V. Magedov M. Efimova
2. Functional State of Primates Measured by Instrumental Reflexes	E. Wachtel K. Hecht E. Drescher B. Shlyk I. Kozlovskaya V. Korolkov V. Magedov
3. Primate Adaptation to the Weightless State as Evaluated from Variations in Circadian Rhythms	V. Klimovitsky A. Alpatov V. Magedov F. Sulzman C. Fuller M. Moore-Ede
4. Synchronization of Primate Circadian Rhythms in the Flight of Cosmos 1514	F. Sulzman
5. Effect of Weightlessness on the Minute Rhythms of Sensory and Motor Functions	K. Hecht E. Wachtel E. Drescher G. Shlyk E. Ilyin V. Korolkov

TABLE 2.- CONTINUED

B. Vestibular Function and Vestibulo-Visual Interactions	
1. Gaze Fixation as a Method of Measuring the Vestibular Function in Primates	I. Kozlovskaya B. Babayev I. Beloozerova Yu. Kreidich M. Sirota V. Barmin
2. Effect of Weightlessness on the Vestibular Function of Primates	I. Kozlovskaya B. Babayev I. Beloozerova M. Sirota
3. Effect of Real and Simulated Space Flights on the Lifting Reaction of Primates	G. Aizikov Yu. Kreidich A. Lazarev V. Barmin F. Solodovnik
C. Effect of Weightlessness on Fluid-Electrolyte Metabolism	
1. Calcium Metabolism and Endocrine Factors in Primates during Space Flight	C. Cann A. Ushakov V. Korolkov Yu. Kondratyev A. Truzhennikov R. Rudneva E. Besedina
2. Flight-Induced Changes in Fluid-Electrolyte Metabolism of Primates	M. Dotsenko V. Korolkov V. Lobachek V. Zhidkov R. Rudneva E. Besedina
3. Bone Changes in Primates and Rats	C. Nogues M. Armand

TABLE 2.- CONTINUED

D.	Cardiovascular Studies. Environmental Control	
1.	Pressure-Flow Response in the Cosmos Monkey	H. Sandler L. Stone
2.	Changes in Blood Pressure and Flow in the Common Carotid Artery of Primates during Space Flight	V. Krotov B. Kulaev A. Badakva R. Kazakova S. Kholin N. Gorbatenkova V. Magedov
3.	Central Circulation of Primates during Space Flight	A. Badakva
4.	Cardiac Function of Primates during Space Flight Evaluated from ECG	V. Melnichenko B. Kulaev M. Goldovskaya E. Shulman
5.	Analysis of Heart Rate Variations from ECG Data of Two Rhesus Monkeys	C. Milhaud B. Blostin B. Cailler A. Seurra
6.	Environmental Control in the Primate Capsule	J. Cesnak B. Perepec
E.	Motor System	
1.	Electromyographic Evaluation of Skeletal Muscles of Cosmos 1514 Primates	A. Rakhmanov V. Oganov V. Magedov L. Murashko G. Shlyk
2.	Effect of Weightlessness on Motor Reactions of Primates (Experimental Goals, Conditions and Results)	I. Kozlovskaya I. Beloozerova N. Sirota

TABLE 2.- CONTINUED

II.	EXPERIMENTS WITH RATS	
A.	Growth and Development of Rats Exposed In Utero to Weightlessness. Behavior	
1.	Critical Stages in the Embryonic and Postnatal Development of Rats	Z. Drahota J. Helinek I. Richter
2.	Developmental Morphology of the Eye, Vestibular System and the Brain in 18-Day Fetuses and Newborn Rats Exposed In Utero to No-Gravity during the Flight of Cosmos 1514	R. Keefe I. Krasnov
3.	Early Postnatal Development of Rats Exposed to No-Gravity during Fetal Period	J. Alberts L. Serova Z. Apanasenko
4.	Behavioral Reactions and Performance of Higher Functions of CNS in Rats Exposed to Weightlessness during Fetal Period	Z. Apanasenko M. Kuznetsova V. Korotkova
5.	Postnatal Differentiation of Skeletal Muscles of Newborn Rats Exposed to Weightlessness during Fetal Period	S. Skuratova V. Oganov M. Shirvinskaya
B.	Effect of Weightlessness on the Metabolism of Rat Dams and Pups	
1.	Effect of Weightlessness on the Hormonal Status of Pregnant Rats	L. Macho
2.	Reactions of Sympatho-Adrenal System of Male and Female Rats to the Weightless State	R. Kwetnianski
3.	Effect of Weightlessness on Tissue Lipids of Pregnant Rats and Their Offspring	I. Alers L. Serova I. Alersova M. Toropil B. Smaida I. Djatlinka

TABLE 2.- CONTINUED

4.	Space Flight Effects on Nucleic Acid Synthesis in Tissues of Pregnant Rats, Fetuses and Newborns	G. Komolova V. Makeyeva I. Egorov L. Serova
5.	Effect of Weightlessness on Tissue Nucleic Acids in Pregnant Rats and Their Pups	E. Misurova
6.	Characteristics of the Gastro-Intestinal Tract of Rats Flown in Weightlessness	P. Groza K. Smirnov A. Bordeanu I. Medkova A. Boka N. Goncharova
7.	Characteristics of Structure and Metabolism of the Heart of Female Rats Exposed to Weightlessness and Their Pups	B. Oschadal F. Kolarz
C.	Radiobiological Investigations	
1.	Frequency of Morphological Changes in Neurons of the Rat Cortex Exposed to Accelerated Carbon Ions	B. Fedorenko R. Kabitsina G. Krivitskaya V. Derevyagin N. Ryzhov
D.	Effect of Weightlessness on Fluid-Electrolyte Metabolism	
1.	Fluid-Electrolyte Metabolism of Dams, Fetuses, and Newborns after Cosmos 1514 Flight	Yu. Nabochin L. Denisova E. Lavrova L. Serova E. Shakhmatova
2.	Application of Atomic-Emission Spectrometry to Mineral Studies of Flight Rats and Their Offspring	P. Luederiz D. Markwirt K. Hecht M. Belakovsky E. Wachtel J. Prosser I. Sergeev

TABLE 2.- CONTINUED

3.	Effect of Weightlessness on Skeletal Development of Rat Fetuses	L. Denisova
4.	Mineral Content and Mechanical Properties of Humeruses of Pregnant Rats after 5-Day Flight	A. Bakulin E. Ilyin V. Oganov
5.	Bone Changes in Primates and Rats	C. Nogues M. Armand
6.	Collagen Metabolism in Bones and Skin of Flight Rats and their Offspring	I. Pospisilova M. Pospisil L. Serova
E.	Effect of Weightlessness on the Nervous System. Morphological Examinations	
1.	Cyto- and Histogenesis of the Brain of Rats Exposed to Weightlessness during Gestation	S. Olenev
2.	Quantitative Analysis of Stereo-architectonics of the Brain Cortex of Rats Exposed to Weightlessness during Gestation	V. Kesarev
3.	Concentration of Neuropeptides in the Posterior Pituitary, Epiphysis, Retina, and Gardner's Gland of Weightless Rats	G. Gauquelin
4.	Electron-Microscopic Analysis of Neurosecretory Structures of the Brain of Rats Exposed in Utero to Weightlessness	I. Babichenko
5.	Morphology of Cerebellar Cell Structures of Rats Exposed In Utero to Weightlessness	A. Privat I. Viktorov A. Shashkova
6.	Stereological Analysis of Cerebellar Purkinje Cells of Weightless Rats	M. Bouteille
F.	Remote Effects of Weightlessness on the Mother-Fetus System	
1.	Genetic Structures of Sex Cells of Rats Exposed to Weightlessness in Utero	D. Behova A. Bairakova

TABLE 2.- CONTINUED

2.	Morphometric Analysis of the Yellow Body of Pregnant Rats after Exposure to Weightlessness	W. Baranska W. Baran M. Kuawa S. Lancewski
3.	Evaluation of the First Order Oocytes of Rats after Space Flight	W. Baranska W. Pisarek
4.	Effect of Short-Term Weightlessness on Hemopoietic Stem Cells of Pregnant Rats and Their Offspring	A. Vacek N. Khurshchev T. Michurina E. Domoratskaya L. Serova O. Pryanishnikova
G.	Motor System	
1.	Effect of Weightlessness on Skeletal Muscles of Rats Exposed to Weightlessness	M. Rapcsak T. Szilagyi A. Szoor V. Oganov S. Skuratova
2.	Biochemical Adaptation of Muscle Proteins in Rats	O. Takacs F. Guba M. Rapcsak T. Szilagyi
3.	Intramuscular Calcium Movements: Experiment on the Soviet Biosatellite Cosmos 1514	Y. Mounier C. Goblet X. Holy
4.	ATP-ase Activity of Skeletal Muscles of Rats after Cosmos 1514 Flight	M. Grandmontagne
5.	Creatine Phosphate and ATP in Skeletal Muscles of Rats Flown on Cosmos 1514	D. Desplanches
6.	Contractile Properties of Myofibers of Pregnant Rats after 5-Day Flight	V. Oganov S. Skuratova M. Shirvinskaya

TABLE 2.- CONTINUED

III.	EXPERIMENTS WITH PLANTS AND SEEDS	
A.	Plant Studies. Maize, Crocus	
1.	Energy Metabolism of Maize Seedlings in in Weightlessness	M. Tairbekov A. Devyatko
2.	Anatomical-Morphological Characterization and Ultrastructure of Cells of the Maize Root Meristem	V. Grif E. Valovich M. Danilova E. Barbicheva M. Tairbekov
3.	Chemical Composition of Cell Walls of Maize Seedlings	V. Lozovaya O. Zabotina M. Tairbekov
4.	Meiosis of Plants in Space Flight	Yu. Bogdanov G. Parfyonov
5.	Embryogenesis of Crocusi in Space Flight	T. Petrova G. Parfyonov
B.	Radiobiological Investigations	
1.	Space Flight Effects on Lettuce Leaves	L. Nevzgodina A. Miller E. Maksimova
2.	Study of Developmental Abnormalities of Artemia Salina Cysts and Genetic Effects of Tobacco Seeds Induced by Radiation and Nonradiation Space Flight Factors	H. Planel I. Gaben M. Delpoux B. Pianezzi G. Gasset
3.	Space Flight Effects on Genetic Lesions in Crepis Capillaris and Arabidopsis Seeds	E. Vaulina I. Anikeeva A. Balayeva L. Kostina
4.	On the Mechanisms of Radiation Lesions in Seeds of Higher Plants Induced by Accelerated Carbon Ions	E. Vaulina I. Anikeeva A. Balayeva L. Kostina

TABLE 2.- CONCLUDED

IV.	EXPERIMENTS WITH FISH	
	A. Study of the Otolith Apparatus of the Fish Grown in Weightlessness	Ya. Vinnikov D. Lychakov E. Cherdantseva
	B. Embryonic Development of Guppi in Weightlessness	E. Cherdantseva
V.	MISCELLANEOUS EXPERIMENTS	
	A. Origin of Gravity Receptors	Ya. Vinnikov
	B. Inactivation of Bac. subtilis Spores as a Result of Hits of Heavy Nuclei of GCR (Biostack Data)	H. Buecker

TABLE 3.- COMPOSITION OF THE PASTE DIET FED TO RATS DURING THE COSMOS 1514 MISSION

INGREDIENTS[a]

Name	Quantity in gm
Casein (milk)	3.0
Cornstarch	3.0
Sucrose	6.7
Sunflower seed oil	1.7
Dry Brewers yeast	1.0
Salt mixture	0.6
Water	24.0

Food Content

Name	Quantity in gm
Protein	3.06
Fats	1.79
Carbohydrates	9.61

Mineral Content

Name	Quantity in mg
Sodium	60.9
Chlorine	15.5
Potassium	67.1
Phosphorus	86.3
Calcium	84.26
Iron	3.19
Iodine	0.07
Zinc	0.08
Copper	0.08
Cobalt	0.008
Fluorine	0.13
Aluminum	0.0008
Magnesium	6.96
Sulfur	11.17
Manganese	0.90

TABLE 3.- CONCLUDED

Vitamin Content

Name	Quantity in μg
B_1	64.8
B_2	62.4
B_6	50.5
Pantothenic acid	240.0
Nicotinic acid	493.6
E	1380.0
A	20.0
D	6.0
Folic acid	32.0
Inosine	800.0
B_{15} Biotin	16.0
P-amino benzoic acid	800.0
B_{12}	0.48 mg
Choline	16000.0
K	16.0

[a]Sorbic acid 0.5% to weight of feed added as preservative.

Note: Quantities are those provided by Soviet scientists and are for 40 gm of diet, wet weight.

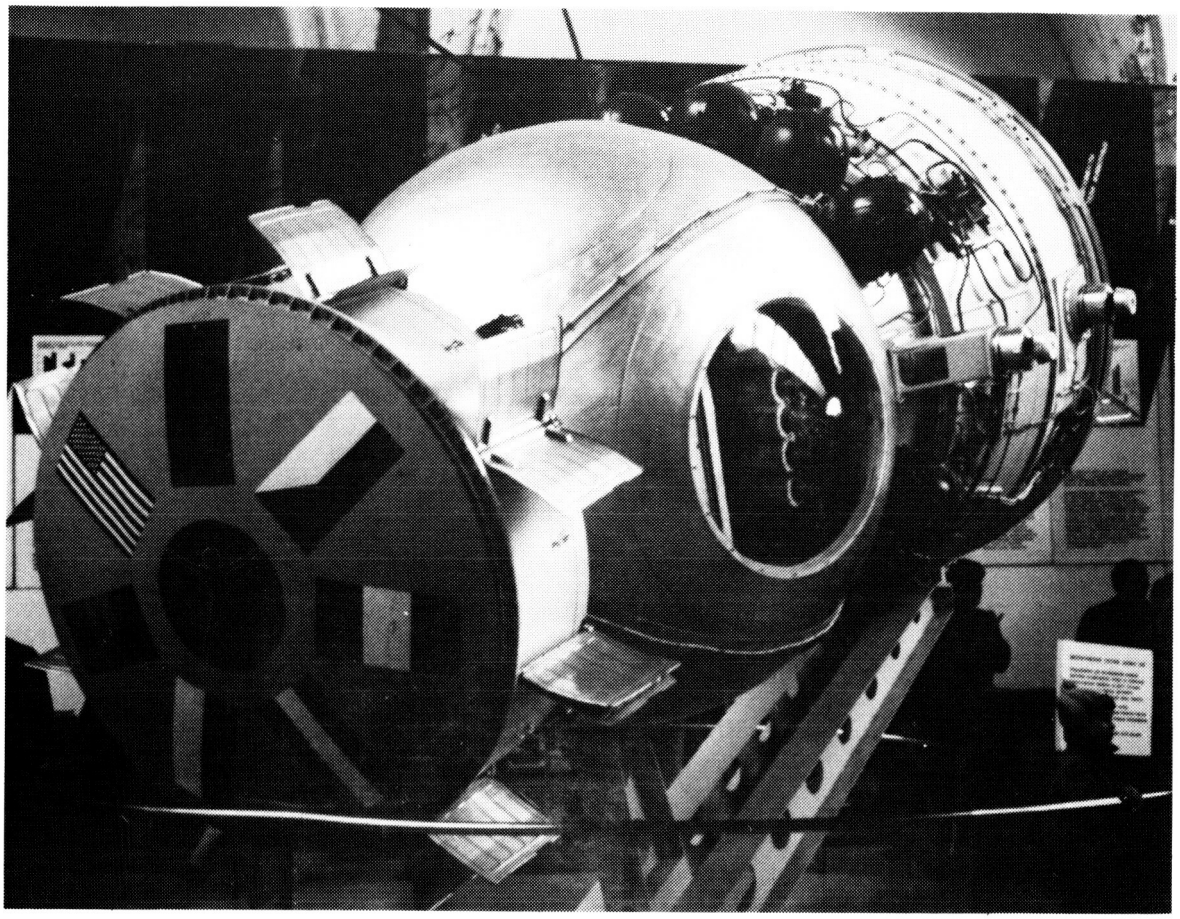

Figure 1.- Cosmos 782 spacecraft on display in the Moscow Space Museum. The circular viewport was installed for display purposes.

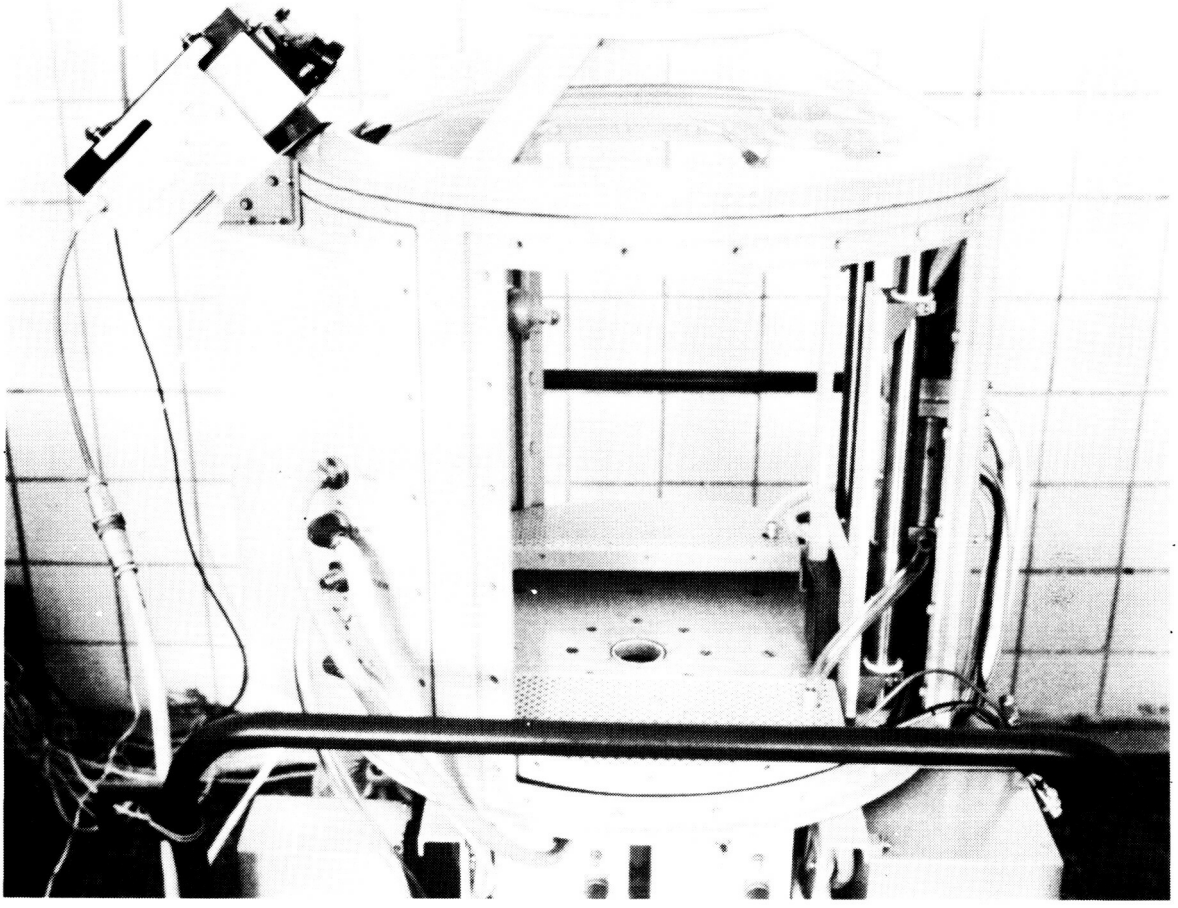

Figure 2.- Soviet monkey BIOS capsule.

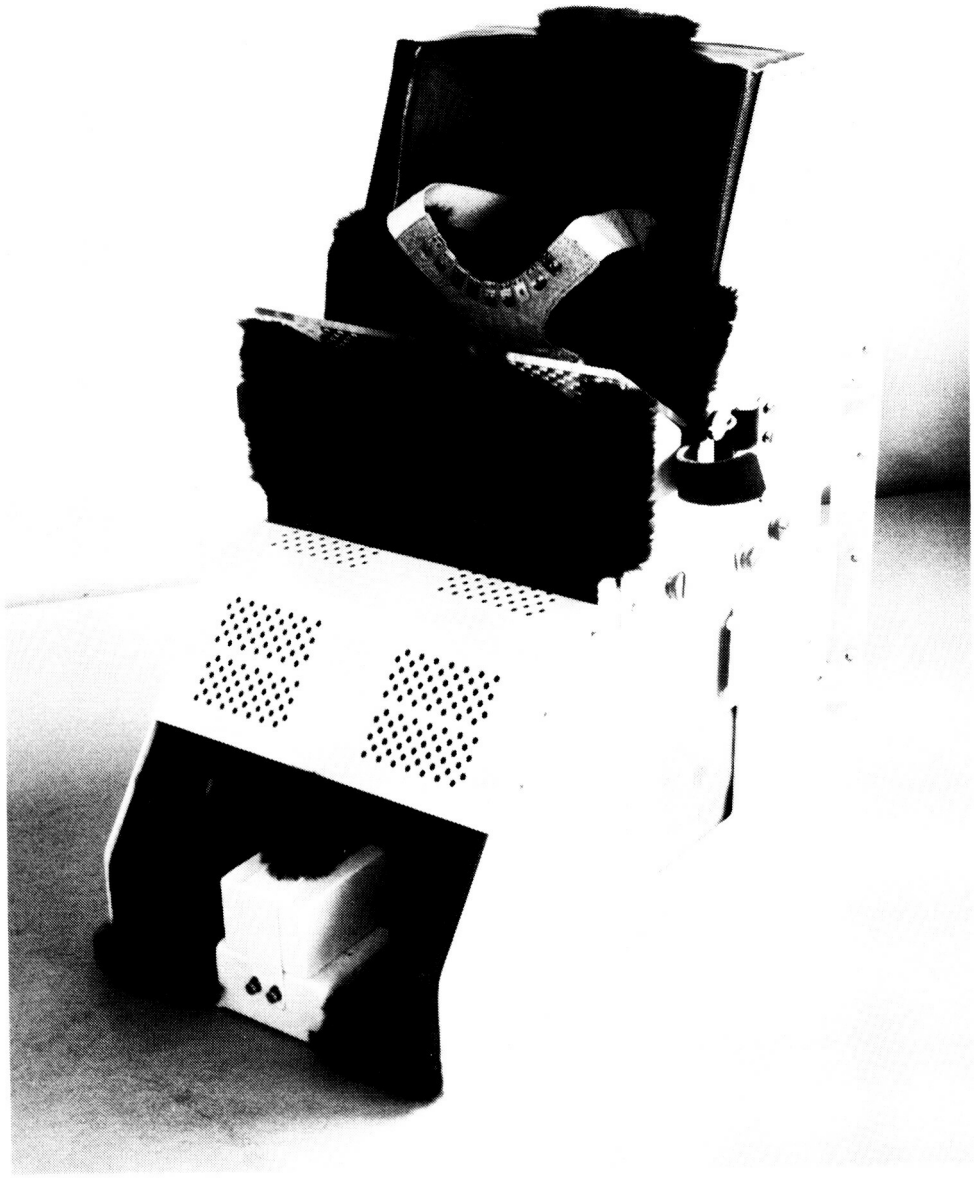

Figure 3.- Monkey restraint chair.

Figure 4.- Monkey in BIOS restraint chair.

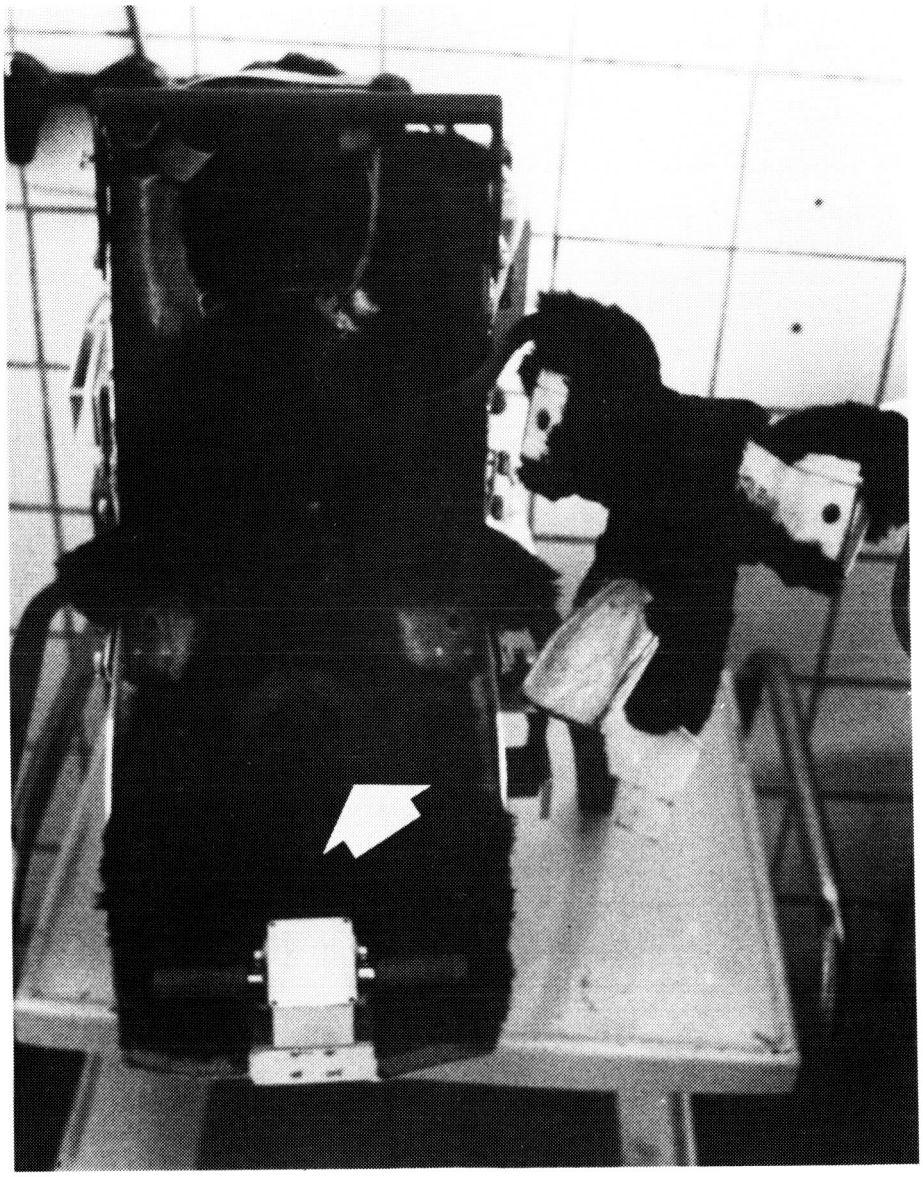

Figure 5.- Monkey restraint chair showing excreta orifice (arrow), lap restraint and foot psychomotor response lever.

Figure 6.- Paste feeder and juice dispensers.

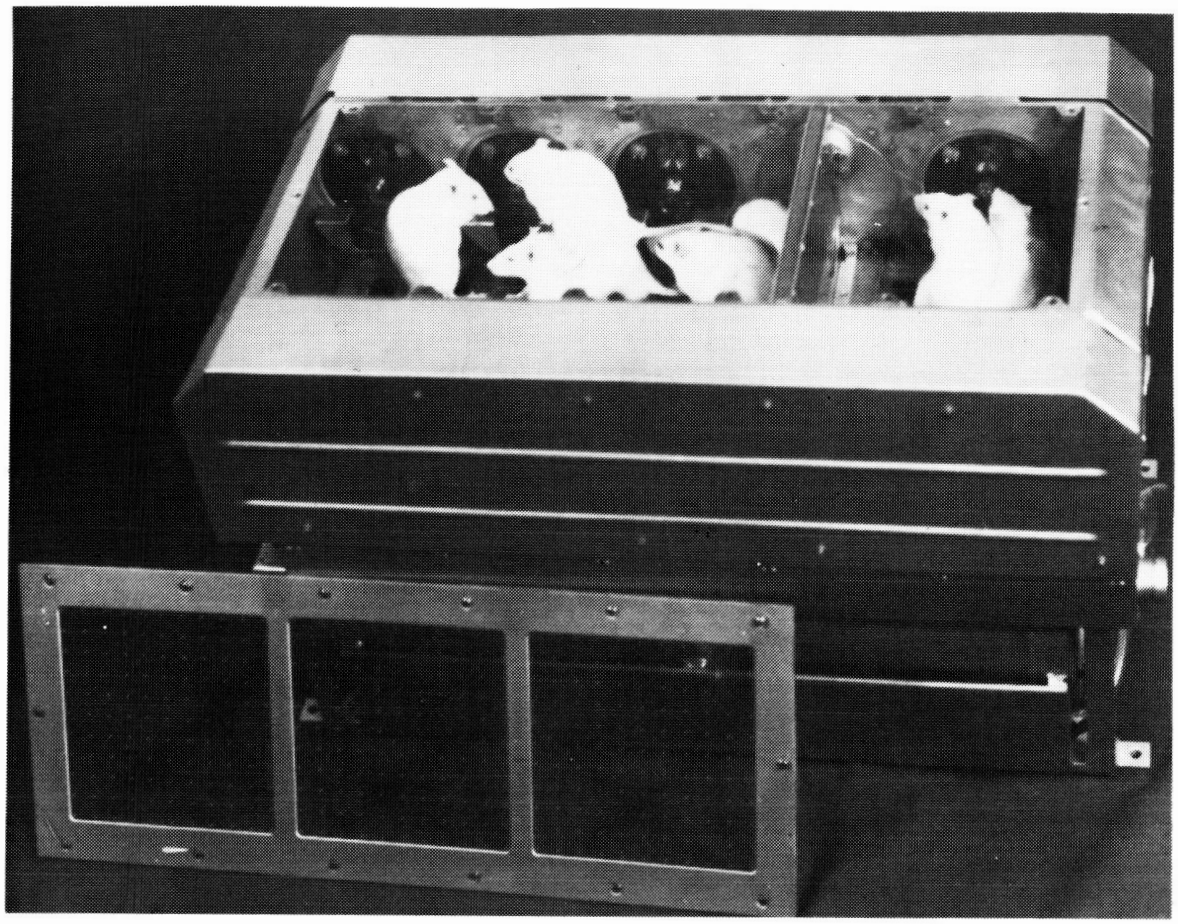

Figure 7.- Rat BIOS with separator as in Cosmos 1129.

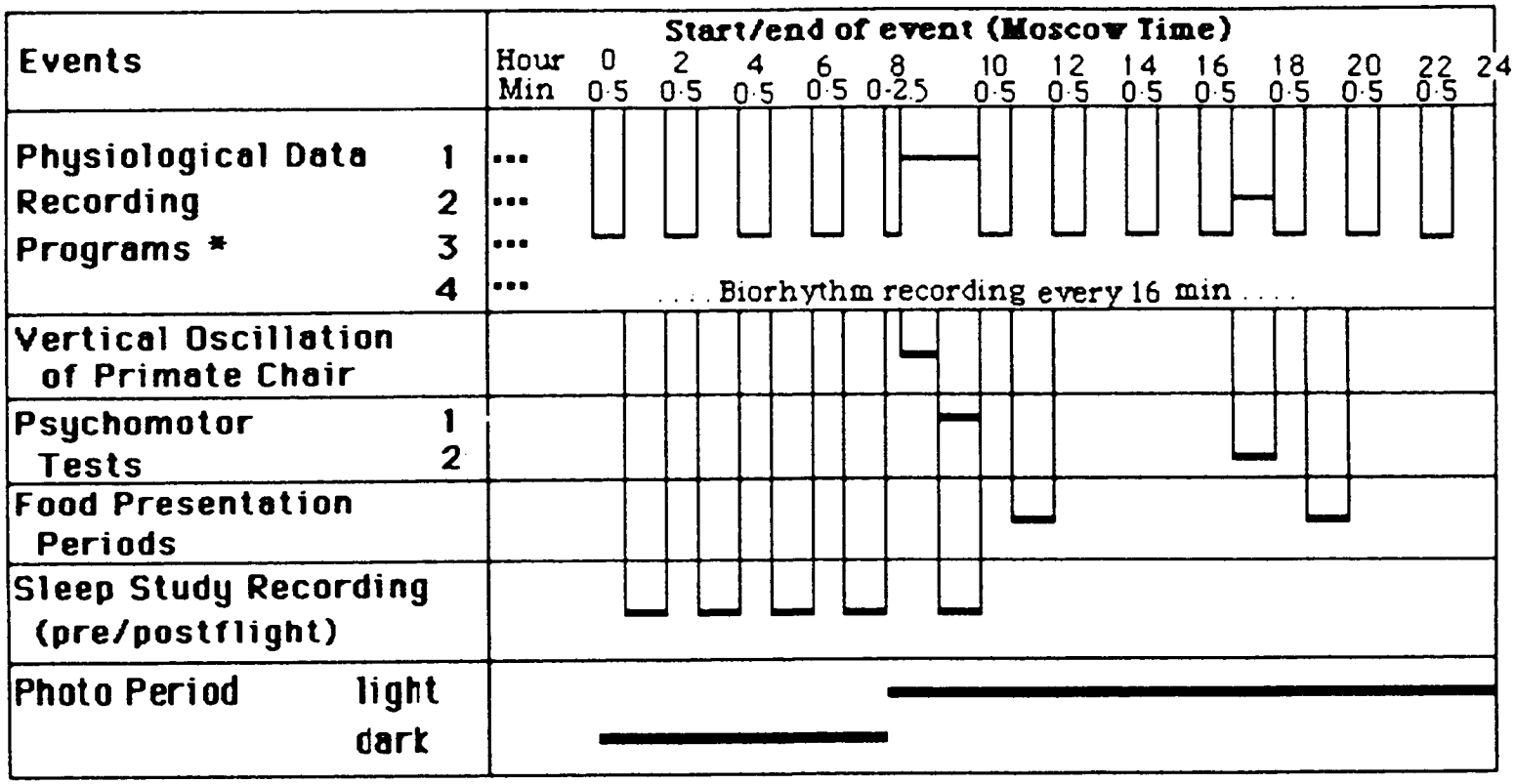

* Program Explanation

1 - Vestibular Test, A.M.
2 - Vestibular Test, P.M.
3 - Cardiovascular Study recording 5 min/2 hour
4 - Biorhythm Experiment recording every 16 min.

Figure 8.- Daily schedule of major events in primate study.

DEFINITIONS

ECOG - ELECTROCORTICOGRAM
NG - NEUROGRAM
RPG - RHEOPLETHYSMOGRAM (4 POLAR)
$2RPG_C$ - TWO CURRENT ELECTRODES FOR RHEOPLETHYSMOGRAM

BTT - BODY TEMPERATURE TRANSMITTER (AXILLARY)
RPG_V - RHEOPLETHYSMOGRAM (FOR VOLTAGE)
ECG - ELECTROCARDIOGRAM
EOG - ELECTROOCULOGRAM
CG - COMMON GROUND (PERIPHERAL ELECTRODES)
EMG - ELECTROMYOGRAM
DMG - MUSCLE TENSION - LIKE EMG BUT MEASURES CONTRACTIVE FORCE

ST - SKIN TEMPERATURE
AS - ACTIVITY SENSOR (INITIAL SITE)

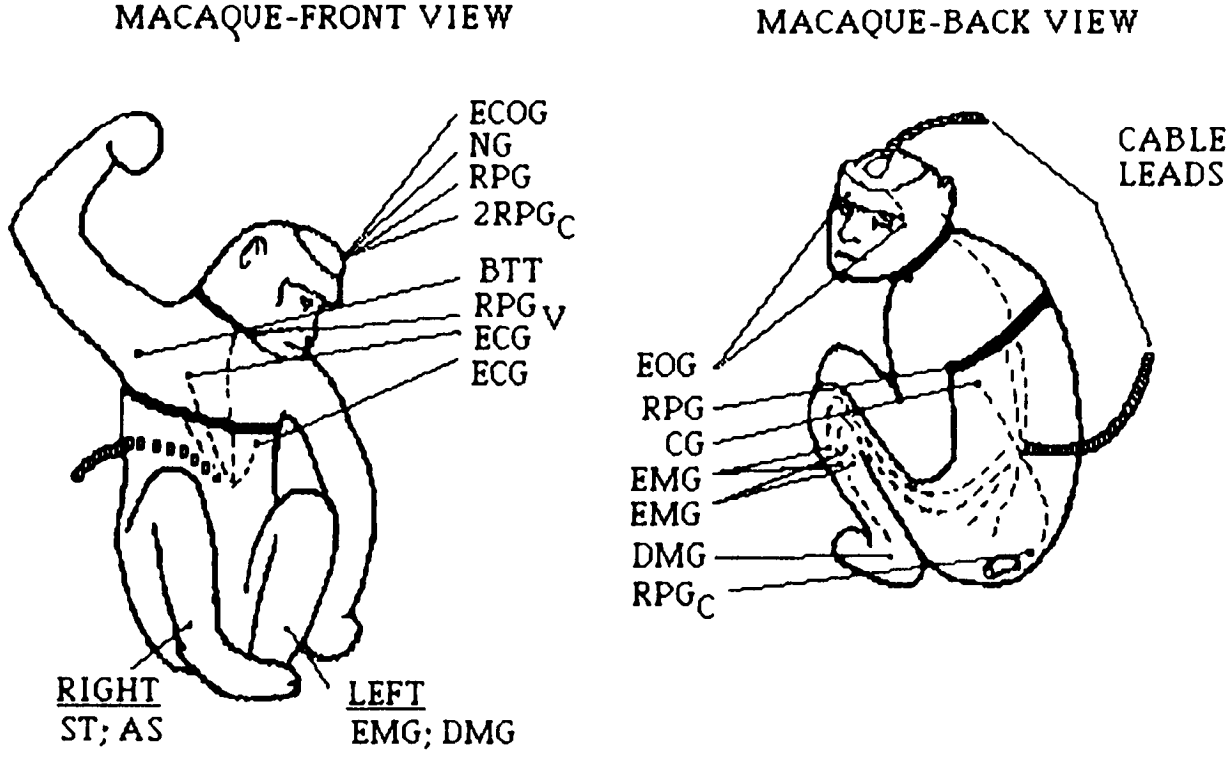

Figure 9.- Diagram of implanted monkey instrumentation excluding carotid blood flow and pressure sensor.

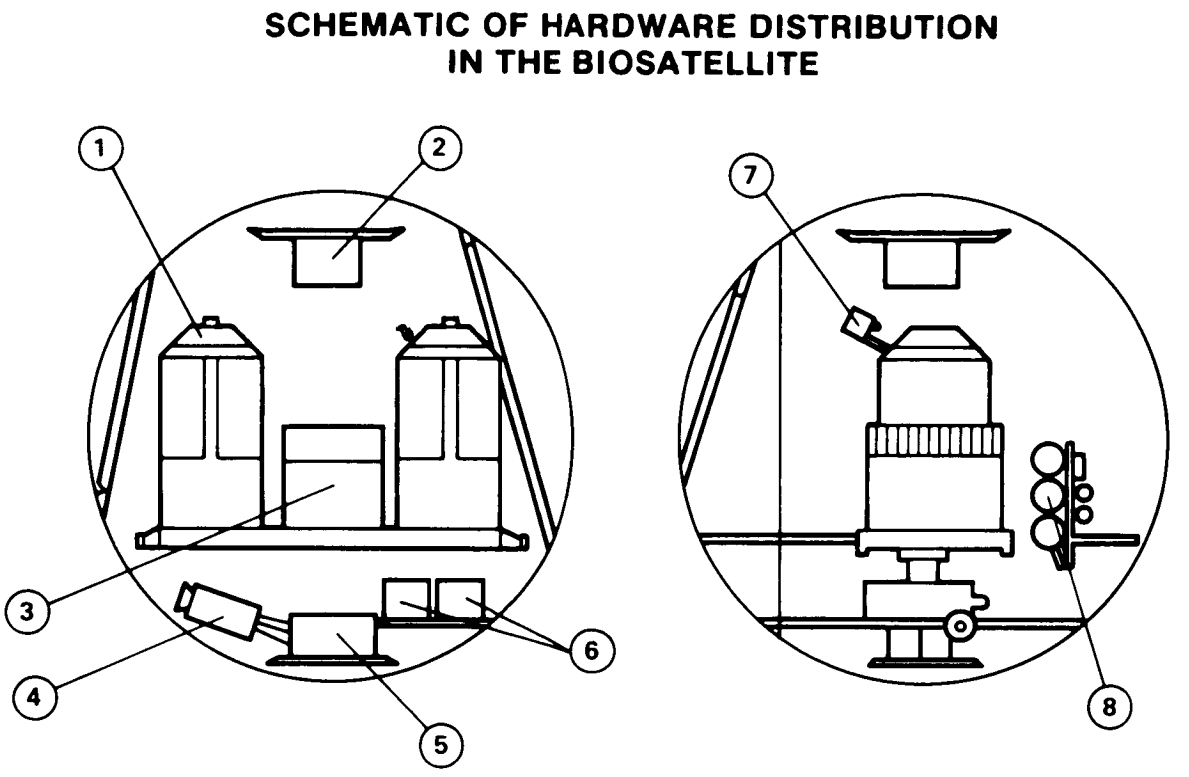

Figure 10.- Schematic of hardware distribution in the Biosatellite.

U.S. BIOINSTRUMENTATION ON COSMOS 1514

Daryl N. Rasmussen
Project Engineer, Cosmos Project
Biosystems Division
Ames Research Center
Moffett Field, CA 94035

Richard C. Mains
Science Consultant, Cosmos Project
Mains Associates
Berkeley, CA 94704

INTRODUCTION

This chapter describes the development of U.S. flight and ground support hardware. A description is provided of hardware definition, development, test, and integration with the Soviet spacecraft. An assessment is presented of the hardware performance as determined by the quality of the data recorded and postflight calibration tests. Recommendations are made for future efforts of this type based on the experience of this mission. This chapter expands on the brief hardware development description provided in the Mission Description chapter of this report.

Previous Flight History

U.S. flight hardware developed for former Cosmos missions included only plant tissue holding containers and radiation dosimeters which were provided to the Soviets preflight and returned to the U.S. postflight for analysis. These hardware items were nonelectronic and required only mechanical support and environmental control from the Biosatellite.

Cosmos 1514 Hardware Requirements

This mission required a significantly increased level of hardware integration and cooperation between the two countries since the flight hardware included U.S. biosensors, signal conditioners, and recorders. U.S. biosensors were implanted or attached to monkey subjects preflight by Soviet specialists. In addition, the monkey body temperatures monitored inflight via Soviet telemetry were recorded on U.S. recorders. Significant development and testing of U.S. ground support equipment (GSE) was also required for conducting postflight data transfer between the two countries and joint postflight developmental behavior studies on rat subjects.

The Soviet requirements for hardware reliability were the same for this mission as for their human missions due to the inclusion of monkey subjects. NASA conducted formal hardware design reviews for the flight hardware and submitted early prototypes to the simulated stresses of launch and reentry at levels equal to or greater than those specified by the Soviets. The actual flight hardware was formally flight qualified to these same stress levels prior to delivery to the USSR.

The high level of hardware integration and reliability required correspondingly high levels of Soviet support in several areas. These included: biosensor implantation and attachment to monkey subjects; operation of U.S. flight and GSE hardware; conduct of experiment procedures; U.S. hardware reliability and quality assurance testing review; integration of hardware with the Cosmos Biosatellite; postflight transfer of data from Soviet to U.S. magnetic tape; and development of documentation for U.S. hardware appropriate to use by Soviet specialists.

FLIGHT HARDWARE DESCRIPTION

Hardware Definition Process

This process consisted of submission of written proposals by the U.S. with counter-proposals by the Soviets which were negotiated primarily during joint meetings. These proposals included descriptions of overall requirements including hardware volume, weight and location, data to be recorded on U.S. and Soviet recorders, hardware verification testing, flight hardware acceptance testing in the U.S. and U.S.S.R. and documentation requirements. The Soviets provided specifications for acceleration, shock, vibration and temperatures to which the hardware should be exposed to ensure survival of launch and reentry stresses and ambient temperatures during shipment from the U.S. to Moscow and Moscow to the launch site.

This process was similar to that used during previous flights but much more extensive and detailed due to the complexity of the instrumentation. The hardware drawings and the documentation provided to the Soviets during the hardware development process were critical to the success of this effort.

For simplicity, the four U.S. experiments which required hardware development are referred to in the discussion below with the abbreviated titles used earlier in this report. For reference, the experiment abbreviations with the associated primary investigators are, Biorhythm (Sulzman), Cardiovascular (Sandler), Calcium Metabolism (Cann) and Neuro-ontogeny (Alberts).

Biorhythm Hardware

A general schematic for the Biorhythm Experiment equipment is shown in figure 1. Data output from the equipment is discussed in detail in the enclosed report by Sulzman et al. The hardware was based on a commercial data recorder manufactured by Solicorder, Inc., of Long Island, New York. The Solicorder was recommended by Sulzman who had earlier experience with it in his laboratory. The Solicorder was a solid state, single channel recorder available either in temperature or event-counting models. Three of these units were repackaged into a single volume for the flight by L & M Electronics of Daly City, California. The flight version used only the commercial circuit boards which were custom-manufactured by Solicorder, Inc., to NASA standards. A flight power supply was developed by NASA using lithium batteries manufactured by Electrochem Industries, Clarence, New York. The flight hardware assembly is shown in figure 2 (a,b).

The three recorders measured skin temperature, body temperature and motor activity. The activity sensor and an associated signal conditioner were developed by L & M Electronics. The activity sensing system required extensive testing with monkey subjects to determine the proper sensitivity setting and sensor location.

Body temperature was obtained from a subcutaneous sensor implanted in the axilla of the monkey. This device was developed by Dr. V. Poleschuk of the Soviet team. It transmitted a radio signal to a Soviet receiver which provided a pulse train whose

frequency was proportional to temperature. An event-counting Solicorder was used to count the pulses and store a frequency in memory for later conversion to temperature. This recorder was modified to be compatible with the Soviet receiver signal characteristics. Electrical isolation from the Soviet receiver was achieved with an optical coupling to avoid ground-loop problems.

The standard temperature Solicorder was used with a skin thermistor manufactured by Yellow Springs Instruments, Inc., in Yellow Springs, Ohio, to measure skin temperature. A data readout and control unit (DRCU) commercially available from Solicorder, Inc., was used to start the Solicorders at the beginning of an experiment and to read out recorded data in engineering units at the end.

It was planned that the ambient temperature of the BIOS monkey flight capsule would be measured and recorded by a NASA-developed solid state recorder (DeBoo et al., 1981). This device (shown in fig. 2c) had been flown on earlier Cosmos missions and was already flight qualified. A temperature readout unit (TRU) was available for reading out the stored values in degrees Centigrade.

A general purpose readout unit was developed which would act as a backup to the DRCU and the TRU. This system was based on an Apple II Computer and could be used for a range of functions including recorder diagnostics, data transfer, data analysis and reporting.

Cardiovascular Hardware

The Cardiovascular Experiment equipment is shown schematically in figure 3. Data output examples are presented and discussed in the chapter in this report by Sandler et al. The system consisted of blood pressure and velocity transducers, their associated signal conditioners and a control circuit. The pressure transducer was commercially available from Konigsberg, Inc., of Pasadena, California. The remainder of the system was a modification of equipment commercially available from L & M Electronics, Inc. This equipment was recommended by Dr. H. Sandler and J. Hines based on their experience with it in their laboratory at the NASA Ames Research Center.

L & M Electronics repackaged the sensors and signal conditioners to meet the Soviet integration requirements and provided support during the bioengineering testing and flight qualification activities. The Soviets offered to provide spacecraft power for the signal conditioners but the extreme sensitivity of the U.S. signal conditioners dictated an isolated power supply. This was accomplished with a NASA-developed battery pack based on the same lithium batteries used for the biorhythm experiment. The flight hardware assembly is shown in figure 4 (a,b).

The pressure and velocity transducers were mounted in a common plastic cuff as shown in figure 5. This cuff was adjustable in size and was surgically placed over the carotid artery and the leads passed under the skin and exteriorized at the monkey's lower back. Extensive work was required to make the cuff and leads biocompatible with the artery and adjacent tissues for the approximate two- to four-month period

of implantation. Because of this long implantation period it was important that the drift of the transducers and associated electronics be minimal and characterizable.

The U.S. signal conditioner had to accept a "start pulse" from the Biosatellite on reaching orbit to become activated and also had to transmit pressure and velocity signals to the onboard Soviet tape recorder. Electrical isolation from the recorder was achieved through a high impedance design. Isolation of the start pulse was achieved through an optical coupling. Soviet flight recorder data were transferred to a U.S. recorder manufactured by Honeywell, Inc. Signals were preconditioned by a special offset and gain amplifier manufactured by L & M Electronics. Sketches of the biorhythm and cardiovascular flight hardware and its interconnections are shown in figure 6 (a-e).

GROUND SUPPORT EQUIPMENT (GSE) DESCRIPTION

Calcium Metabolism Experiment

The U.S. provided a portable x-ray machine for use in Moscow to take skeletal radiographs of flight candidate monkey subjects for evaluation of skeletal age. In addition, a calcium carbonate isotope was provided to the Soviets with which to prepare the flight monkey paste diet. This isotope served as a natural easily monitored tracer to study calcium loss.

Neuro-ontogeny Experiment

Several items of custom test hardware were developed by the primary investigator for this experiment including; maternity cages with data output provided from rat dams and pups and videomonitoring capabilities, rotational and tilt devices for vestibular and righting tests, and an olfactory, respiration, auditory and visual testing system. Details of this hardware are presented and discussed in the enclosed report by Alberts et al.

GSE for Flight Hardware

In addition to the ground-based equipment described above for the biorhythm and cardiovascular experiments, many items of test and calibration equipment were required. These included custom-made biological signal simulators to use during system integration tests when it was not practical to have animal subjects present. General-purpose commercial test equipment was required for diagnosis of system problems and conducting on-site repairs. This included oscilloscopes, signal generators, impedance meters and RF receivers. One of the challenges in supporting hardware integration was anticipating the GSE needs in the U.S. and U.S.S.R. and shipping the required items to and from Moscow in a timely fashion.

SPACECRAFT ENVIRONMENT, RESOURCES AND INTERFACE REQUIREMENTS

The spacecraft environment and resources including power, mass, volume and the interface requirements for the biorhythm and cardiovascular experiments are listed

in table 1 (a-e). The dimensions and labels for all cables and connectors were specified exactly but are not included here. The U.S. was given the option to select the types of connectors and cables to be used as long as they met NASA reliability and safety requirements.

The operating specifications for the biorhythm and cardiovascular experiment hardware are given in tables 2 and 3, respectively. The sensor interfaces to the two flight monkeys were also specified initially and then modified to optimize the data quality and noninterference of measurements between experiments.

HARDWARE DEVELOPMENT, INTEGRATION AND TEST PLANS

A. Development Plan

This flight required the development of detailed hardware development plans to meet the increased U.S. and U.S.S.R. integration and bioengineering and hardware test requirements. The hardware development methods of the two countries differed. The U.S. emphasized documentation and design reviews whereas the U.S.S.R. emphasized testing and demonstration. Therefore, project management in the U.S.S.R. did not specify safety, reliability and quality assurance (SR & QA) requirements for the U.S. because they planned to verify the U.S. equipment during bioengineering and BIOS integration tests prior to flight.

The U.S. engineers chose to develop the hardware under the standard NASA design review process (NASA SP-6502, 1967), but to use SR & QA staff support in a design rather than a policing role. Thus SR & QA staff reviewed materials, parts and systems to identify any questionable items, and the Cosmos Project Manager could waive SR & QA requirements based on project engineering staff recommendations. This approach reduced documentation requirements to a minimum and allowed the flight hardware to be developed for a cost only slightly above that of the commercial versions.

The Soviets requested eight sets of hardware for each of the two flight hardware experiments. One set of ground support equipment was supplied with each two flight sets. Table 4 (a,b) lists the items included in each equipment set. Table 5 lists the U.S.S.R. equipment set labels, purpose, testing required and delivery dates.

Typical NASA change control procedures involve either a formal written request from the Project Engineer or a formal directive to him resulting from a formal design review. Due to travel and time limitations, it was not possible to have Soviet specialists attend the several NASA design review meetings, and therefore change control procedures were needed that maintained order but did not remove the flexibility necessary to respond to unexpected Soviet requirements. In this joint program, documentation and communication can be difficult because of; differences in language, inevitable communication and transportation delays, limited access to facilities of the other side, and differences in technical standards such as variability in the power line frequencies (50 versus 60 Hz/sec).

It was therefore essential for the U.S. Cosmos Project management to have the authority to make its own assessments and to act on these quickly with higher management review. This allowed U.S. engineers to accommodate unexpected Soviet changes which were required to solve either a communication or a technical problem. It was decided that formal U.S./U.S.S.R. approval was required for changes to the basic interface specifications listed in table 1. The changes made for the U.S. flight hardware specifications were managed by a control board made up of the U.S. Cosmos Project Manager, Project Engineer, and the Principal Investigator.

Changes were regularly discussed and reviewed with the Soviets during monthly U.S./U.S.S.R. telephone conferences, in person during periodic trips, or through the mail. Documents sent by mail were of limited value because they either did not provide enough information or were out of date by the time they reached their destination. Telephone calls were useful for simple logistical matters but were inadequate for technical discussions of any depth. Direct, in-person contact between engineers worked very well and was found to be absolutely essential to the success of this complex mission. Ideally, both sides would have exchanged a technical specialist for perhaps six months at a time. This would have significantly aided communication and improved the quality of training by both sides in each other's methods.

B. Integration Plan

The major concern of both sides was that the U.S. and U.S.S.R. equipment required for the joint experiments would work well separately but not together. The potential problems included; electrical ground loops (conductive noise), radio frequency interference (radiated noise), and equipment failures which could not be clearly diagnosed and repaired by the Soviets without direct U.S. assistance. The best solution to this concern appeared to be high-quality Soviet training, common essential documentation, ground support equipment development and periodic joint testing.

Cosmos Program requirements demanded that the most critical tests be conducted by the Soviets in a Biosatellite mockup about three months before the flight and in the actual spacecraft several days prior to launch. During these tests, U.S. specialists could not be present to diagnose any problems that might arise since the tests were located in an area off-limits to foreigners. Because complete electrical specifications for the Biosatellite mockup and the spacecraft were not available to the U.S., testing could not be done in the U.S. to assure there would be no problems of the sort described above. The consequences of failure in these final two tests were serious since U.S. equipment would have to be eliminated if the hardware failed to perform to specifications. Because of this concern, the following hardware development guidelines were chosen to reduce the possibility of electrical interference:

1. Shield all cables against radio frequency transmission and reception

2. Isolate all connections to Soviet equipment either with an optical isolator or high impedance

3. Operate at a distance from any known Soviet frequencies and alert them to the frequencies being used by the U.S.

4. Provide backup flight units

5. Provide documents and equipment for testing all flight equipment

6. Provide training to the Soviets on equipment and problem diagnosis

7. Minimize connections to Soviet equipment by using self-contained power supplies and data storage

C. Test Plan

A summary of the major flight and GSE hardware tests conducted in the U.S. and U.S.S.R. is presented below.

1. Commercial Acceptance Test - conformance to functional specifications, physical dimensions, mass, power, materials, and workmanship.

2. Flight Acceptance Test - conformance to the commercial test plus flight environment tests for vibration, acceleration, and shock. The environment tests were conducted at 100% of the expected flight level as listed in table 1e.

3. Qualification Test - conformance to the commercial test plus flight environment tests for vibration, acceleration, and shock at 150% of the expected flight levels.

4. Independent U.S. and U.S.S.R. Science Verification Tests - verification by the principal investigators that the hardware met the functional specifications (see tables 2 and 3). Testing was designed to ensure that the animal/hardware interfaces were adequate for acquiring high-quality data and with no trauma to the subjects.

5. U.S. Mission Simulation - a two-week verification test of flight-type hardware functioning with two monkey subjects in a simulated Soviet couch.

6. U.S. GSE Testing - a short test to assemble all GSE for each of the experiments which required electrical power to ensure that it functioned properly on the U.S. power transformers.

7. U.S.S.R. Bioengineering Test - a four-day test using U.S. and U.S.S.R. flight hardware installed in the primate BIOS capsules.

8. U.S.S.R. Acceptance Test - functional tests of all U.S. hardware using jointly agreed-upon acceptance tests. These tests were conducted by the Soviets using procedures written by the Americans prior to delivery of hardware to the Soviets.

9. U.S.S.R. Bioengineering Test and Final Readiness Review - a six-day test using two closed primate BIOS capsules with all U.S. and U.S.S.R. hardware operating simultaneously.

10. Preflight Calibration - bench tests in the U.S.S.R. to verify that all flight units were interchangeable, regardless of which monkey flight candidates were chosen for the flight and synchronous control experiments.

11. Postflight Evaluation and Calibration - a repeat of the Commercial Acceptance Test. Sensors and instruments were recalibrated to measure any instrument drift that may have occurred during the flight.

DOCUMENTATION

Documentation was kept to a minimum because of the tight Cosmos Project schedule, the many required hardware changes, and the small budget. Documents were primarily needed for the core U.S. Project personnel and their counterparts in the U.S.S.R. The exceptions to this were the Hardware Development Plans for NASA Headquarters and the Materials Lists for the Johnson Space Center Safety Office. The documents produced are listed in table 6.

A description is given in the Mission Description chapter of the contents of the hardware User Manuals and the Experiment Management Plans. An attempt was made throughout the preflight hardware development period to keep these key documents current, and at least three editions were produced to this end.

SOVIET TRAINING

The training of Soviet specialists in using U.S. hardware is described in the Mission Description chapter of this report. This training was conducted for the Soviet Cosmos Project management staff, the Soviet coinvestigators and various Soviet engineers. Since it could not be determined who would actually conduct the critical immediate preflight evaluation, installation, and activation of the flight hardware, it was very important that the documentation be accurate and the procedures as simple as possible. Special care was taken to label equipment clearly and to design equipment to make assembly as foolproof as possible.

DATA TRANSFER

Detailed data transfer procedures were written for both the biorhythm and cardiovascular experiments for technical and personnel reasons. As for the preflight hardware checkout, assembly and activation, it was essential that various U.S. and U.S.S.R. specialists be able to conduct data transfer procedures. In the end, the

principal investigators were involved in the data transfer process since they were available in Moscow.

Biorhythm Experiment

It was planned that U.S. specialists would conduct the biorhythm experiment data transfer from the flight recorders using the general-purpose Apple computer system. When U.S. specialists were given the flight units in Moscow, it was learned that the Soviets had already completed a data transfer using the commercial DRCU system on which they had been trained. They had accomplished this by hand-writing numbers from the digital display. An apparent failure of the Apple computer system occurred when the U.S. principal investigator attempted to conduct an additional data readout directly to a magnetic disk. Data from the sychronous control experiment were transferred at the same time.

Cardiovascular Experiment

This experiment required transfer of taped inflight data from a U.S.S.R. flight recorder to a ground-based U.S. tape recorder, postflight. Also, pre- and postflight calibration, tilt-test and synchronous control data were transferred to the U.S. recorder for digital analysis using a Digital Equipment Corporation PDP 11/30 computer at the NASA ARC Cardiovascular Research Laboratory.

Calcium Metabolism Experiment

Flight candidate skeletal x rays, flight diet samples and fecal and urine samples were transferred postflight for analysis in the U.S. Serum samples were not available as planned due to the Soviet decision to eliminate the blood sampling procedures based on their concern for the health of the monkey subjects.

Neuro-ontogeny Experiment

Most of the data were obtained directly by the U.S. primary investigator and his assistant in Moscow in the immediate postflight period. Additional preflight and postflight data and tissue samples were obtained from the Soviets who were trained in all the U.S. procedures. Videomonitoring data of high quality were not obtained as planned for the maternal cages due to a hardware problem which is addressed in the section below.

HARDWARE PERFORMANCE

Biorhythm Experiment

1. Flight Hardware

The flight hardware including the customized Solicorder, activity and skin temperature sensor systems developed for this experiment worked according to specification for the flight and synchronous control experiments. A decision was made by the

Soviets just prior to launch not to include the NASA Ambient Temperature Recorder with the payload. This decision was based on their not having a method at the launch site to check out the recorder performance. The Cosmos Project Manager attempted to solve this potential problem preflight by providing a check-out system in Moscow which could be used prior to shipment of the recorder to the launch site, but found out postflight that this was not sufficient to meet the final payload integration requirements. Ambient temperature data were obtained, therefore, from a Soviet ambient temperature recorder which provided values every 2 hours instead of every 30 minutes as would have been provided by the U.S. recorder.

2. GSE Hardware

The Apple computer data readout unit apparently did not work properly when the principal investigator attempted to transfer the data to magnetic disk immediately postflight. A postflight test of the system after shipment of the system to the U.S. did not clarify this problem as the system appeared to function normally. As noted above, the data were transferred successfully by reading values from the DRCU digital display.

Cardiovascular Experiment

1. Flight Hardware

The flight hardware system, including sensors and signal conditioner, functioned according to specification for the flight and synchronous control experiments. The postflight calibrations of equipment showed only minor changes from preflight values.

2. GSE Hardware

Supporting hardware for this experiment was provided for each of the flight units and performed according to specification. The data transfer hardware worked very well postflight even though the process was time consuming.

Calcium Metabolism Experiment

The ground-based hardware and materials including the portable x ray, Ca-40 diet tracer and a frozen sample shipment container worked according to specification. No equipment problems were encountered.

The several ground-based hardware systems developed by the primary investigator worked according to specification except the videomonitoring system which produced poor-quality images. These systems are described in the enclosed science report by Alberts et al.

As a guideline, no hardware, including all GSE, was shipped to the U.S.S.R. without conducting a systems test using simulated Soviet power. Two of the above-mentioned, commercial videomonitoring systems were therefore tested at NASA Ames Research

Center prior to shipment. This was done by providing 220 volt/50 Hz power input to a U.S. transformer which provided 110 volt/50 Hz as output.

Due to the necessity of conducting this test at a remote Ames Center site, the two hardware systems were transported on separate trips by car. Inadvertently, complete tests were not conducted on all hardware and cables, and at least one component was apparently not tested. As was learned postflight, the two video systems were not identical as thought, and the component not tested was incompatible with 50-Hz power resulting in the recording of poor-quality images.

RECOMMENDATIONS FOR FUTURE FLIGHTS

The guidelines discussed in the above sections were found to be highly valuable for making this mission an engineering success. The design of hardware systems so that experiments or portions of experiments could be deleted or fail without effecting the entire payload was found to be very advantageous. Providing the Soviets with options for sensor and recorder attachment sites allowed them to make changes in the design of the restraint couch which optimized monkey subject welfare based on their test results.

It was critical to this mission that the attached U.S. instrumentation not be detrimental to the monkey subjects, and much work was required by the U.S. and U.S.S.R. specialists to develop systems which were determined by tests to be benign. Past flights with monkeys such as the U.S. Biosatellite III mission have been criticized for not conducting flight duration bioengineering tests with all equipment operating simultaneously. Special effort was therefore made by both countries to conduct mission duration simulation tests with all hardware, first separately and then integrated, to identify problems early in the development phase. The U.S. test lasted fourteen days to ensure that the mission simulation would be at least as long as any proposed spaceflight. This effort was instrumental to the success of the hardware and the science.

The electrical isolation of U.S. hardware from the Biosatellite by the use of lithium battery packs worked well. It would have been better, however, if the packs had been designed to be easily removable and include an elapsed time meter to provide good estimates of remaining battery life. This technique would also have allowed an inexpensive power supply to be substituted during the many ground-based bioengineering tests.

A complicating factor in U.S./U.S.S.R joint spaceflight hardware development is that the U.S. does not have access to integrated testing with the actual Biosatellite. This means that U.S. hardware must be operable and testable by the Soviets during the final integration process. This can only be done with high quality training of Soviet specialists by U.S. specialists. The several joint bioengineering tests were critical for developing this Soviet capability. These tests also served to train the U.S. specialists in the procedures which would be used during the preflight integration process and postflight data transfer. The willingness of the Soviet

specialists to devote many hours and much diligence to this effort was a decisive factor in the joint success of this mission.

BIBLIOGRAPHY

1. Deboo, G. J., Westbrook, R. M.; Bennett, L. D.; and Steinhaver, R. A.: A Solid-State Digital Temperature Recorder for Space Use. NASA TM 81267, 1981.

2. Elements of Design Review for Space Systems. NASA SP-6502, 1967.

TABLE 1.- U.S.S.R. RESOURCES AND INTERFACE REQUIREMENTS

TABLE 1a.- DIMENSIONS AND POWER

Experiment	Parameter				
	Length (mm)	Width (mm)	Height (mm)	Mass (kg)	Power
Biorhythm	160	80	150	2.0	U.S. supplied
Cardiovascular	160	160	150	4.5	U.S. supplied

TABLE 1b.- RECEPTION OF U.S.S.R. INTERNAL BODY TEMPERATURE RECEIVER

Parameter	Value
Amplitude	3.5 volts +/- 20%
DC offset	+/- 0.3 volts
Pulse width	70 microseconds +/- 20%
Frequency ranges	100 Hz to 2000 Hz
Current drive	1.8 milliamperes
Receiver isolation	optical coupling

TABLE 1c.- U.S. INSTRUMENT CONNECTIONS TO U.S.S.R. TAPE RECORDER

Parameter	Value
Input voltage	0 volts to 5 volts
Limits	negative voltage must not be supplied by U.S.
Output impedance	2000 ohms maximum
Input impedance	100,000 ohms minimum

TABLE 1d.- U.S.S.R. START PULSE FOR CARDIOVASCULAR EQUIPMENT

Parameter	Value
Switch closure	dry contact (no voltage)
Duration	0.1 seconds to 0.8 seconds
Contact current	100 MA maximum
Pulse interval	2 hours

TABLE 1e.- OPERATING ENVIRONMENT SPECIFICATION FOR FLIGHT AND GROUND USE OF BIORHYTHM AND CARDIOVASCULAR EQUIPMENT

Parameter	Value
Operating temperature	22°C +/- 2°C
Storage temperature	0°C to 40°C
Shock	40 g for 50 milliseconds in any direction
Vibration	random motion for 300 seconds 20 to 2000 Hz at approx. 0.02 g/Hz
Acceleration	5.1 g +/- 10% for 300 seconds, in 3 axes

TABLE 2.- BIORHYTHM HARDWARE SPECIFICATIONS

Parameter	Instrument			
	Limb Activity Monitor	Skin Temp. Monitor	Body Temp. Monitor	Ambient Temp. Mon.
Unit	Number of motion events in any axis above 10 mV threshold	°C	Hz (U.S.S.R. to supply °C/Hz table)	°C
Range	0 - 3584 events	23°-39°C	0 - 2000 Hz	-10° to +50°C
Sampling frequency	1 sample/ 16 min	1 sample/ 16 min	1 sample/ 16 min	1 sample/ 16 min
Transducer accuracy	TBD	+/- 0.1°C	+/- 0.1°C	+/- 1°C
Readout resolution (using control unit)	4,12,36,44, 68,76,100, 108 counts	0.252°C	8.53 Hz	+/- 0.1°C
Readout resolution (using computer)	1,3,9,11,17, 19,25,27 counts	0.063°C	2.13 Hz	+/- 0.1°C
Flight duration	15 days	15 days	15 days	15 days
Mission duration	26 days	26 days	26 days	26 days
Operational life (battery pack)	120 days	120 days	120 days	120 days

TABLE 3.- CARDIOVASCULAR HARDWARE SPECIFICATIONS

Parameter	Instrument	
	Blood Velocity Signal Conditioner	Blood Pressure Signal Conditioner
Output voltage (volts)	0.0 - 5.0	0.0 - 5.0
Range (ml/sec)	0.5 - 5.0	0.0 - 200.
Accuracy (%)	Flow = 20[a] Velocity = 1	10
Artery diameter (mm)	2.0 - 5.0	2.0 - 5.0
Calibration	1 V = 0 kHz 5 V = 4 kHz	1 mV = 0.1 mm Hg
Drift	0 ml/sec/month	3 mm Hg/month
Operational life of battery pack	60 hours of continuous operation, or 60 days for a duty cycle of 5 minutes every 2 hours	

[a]Due to estimation of vessel diameter.

TABLE 4(a).- BIORHYTHM HARDWARE DESCRIPTION

Hardware Type	Item
1. Flight (8 sets for U.S.S.R. use)	Digital recorder (3 Solicorders) Skin thermistors Activity sensors Interconnection cables and boxes Digital recorder (ARC ambient temperature)
2. Ground Support Equipment (4 sets for U.S.S.R. use)	Battery pack tester Signal simulator Solicorder data readout unit ARC ambient temperature readout unit Thermistor tester Activity sensor tester Battery pack spares 220/110 V transformer
3. Test equipment (1 set for U.S. use)	Activity sensor calibration Thermistor calibration Core temperature sensor calibration
4. Support equipment (1 set for U.S. use)	Spare parts kit Tools General purpose data transfer system (Apple computer-based)

TABLE 4(b).- CARDIOVASCULAR HARDWARE DESCRIPTION

Hardware Type	Item
1. Flight (8 sets for U.S.S.R. use)	Signal processor (includes controller, pressure and flow signal conditioners) Combined pressure/flow cuffs Interconnection cables and boxes
2. Ground support equipment (4 sets for U.S.S.R. use)	Battery pack tester Signal simulator Battery pack spares 220/110 V transformer
3. Test equipment (1 set for U.S.S.R. use)	Pressure sensor calibration Flow sensor calibration
4. Support equipment (1 set for U.S. use)	Spare parts kit Tools Data transfer (tape recorder, time code generator, cables, connectors, etc.) Interference Test (spectrum analyzer, frequency generator, etc.) Cross-Calibration (L&M 1012, 2007 signal conditioners, etc.) Rechargeable/switchable power supply

TABLE 5.- EQUIPMENT SET DESIGNATIONS, PURPOSE, REQUIRED TESTING AND SCHEDULE OF DELIVERY TO U.S.S.R. FOR BIORHYTHM AND CARDIOVASCULAR FLIGHT HARDWARE

Equipment Set Labels	Purpose	Testing Required	Delivery Date
A & B	Laboratory tests and backup to C & D	Commercial acceptance	After PDR[a] (9/80)
C & D	Synchronous control experiment	Qualification level (150%)	After CDR[a] (12/82)
E & F	Backup for flight units	Flight level (100%)	After FRR[a] (3/83)
G & H	Flight experiment	Flight level (100%)	After FRR[a] (9/83)

[a]PDR = Preliminary Design Review
CDR = Critical Design Review
FRR = Final Readiness Review

TABLE 6.- PROJECT DOCUMENTATION SUMMARY

Function	Title
1. Hardware Development Plans	o Biorhythm experiment o Cardiovascular experiment
2. Preliminary Design Requirements	o Biorhythm experiment o Cardiovascular experiment
3. Critical Design Requirements	o Biorhythm experiment o Cardiovascular experiment
4. U.S./U.S.S.R. Meeting Protocols	o Session summaries o Interface agreements o Procedures o Schedules
5. Hardware User Manuals	o Flight equipment o Ground support equipment
6. Hardware Acceptance	o Development phase (U.S.) - Vendor acceptance - Flight qual. or acceptance for battery packs, cables, and flight units - Calibration o Mission integration - Specifications & procedures manuals (U.S.S.R. acceptance) - Simulation test plans and results (U.S. and U.S.S.R.)
7. Experiment Management Plans	o Biorhythm o Cardiovascular o Calcium metabolism o Neuro-ontogeny
8. Integrated Experiments Plan	o Integrated timeline for all U.S. experiments

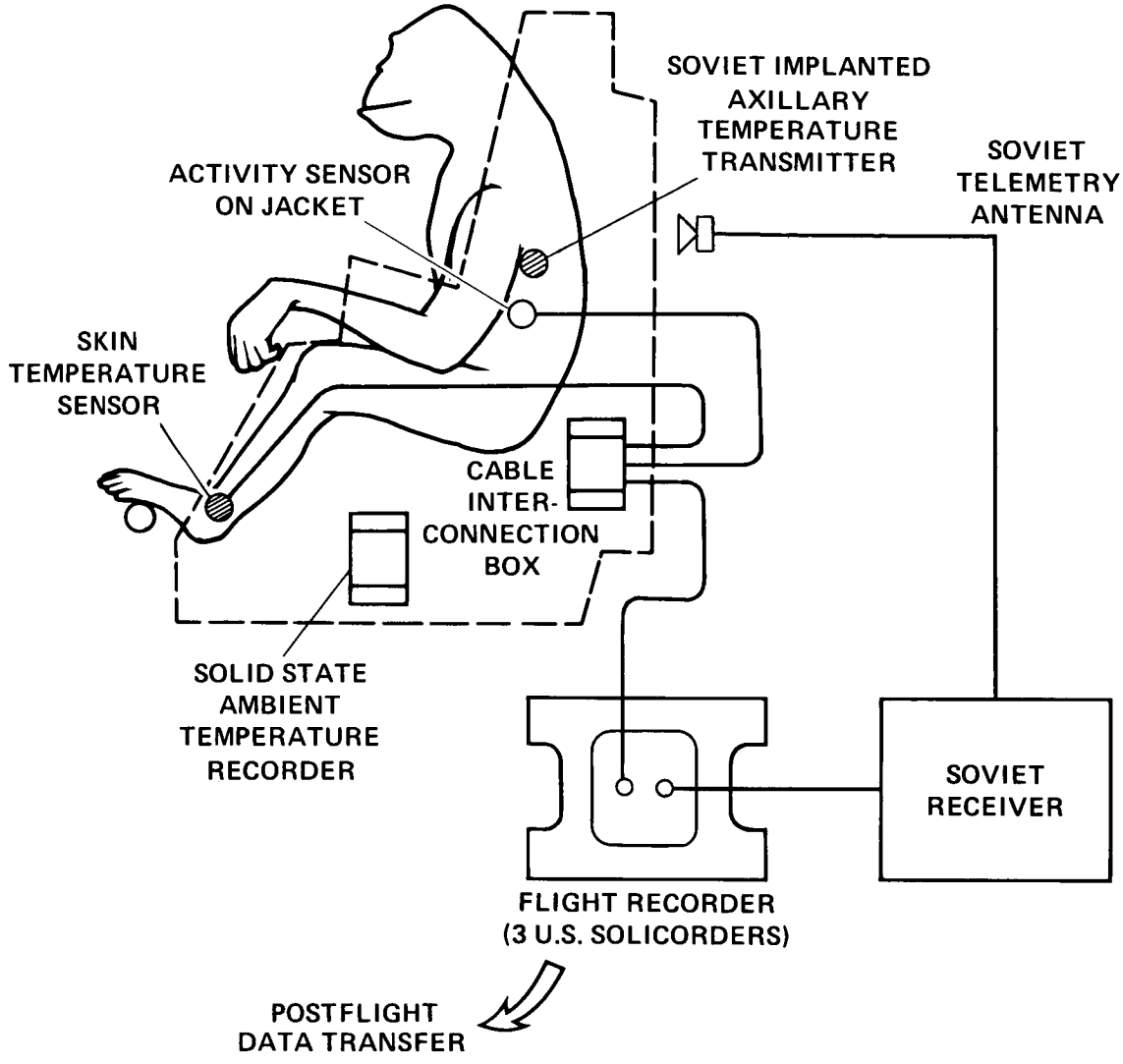

Figure 1.- Biorhythm experiment equipment schematic showing sensor attachment points.

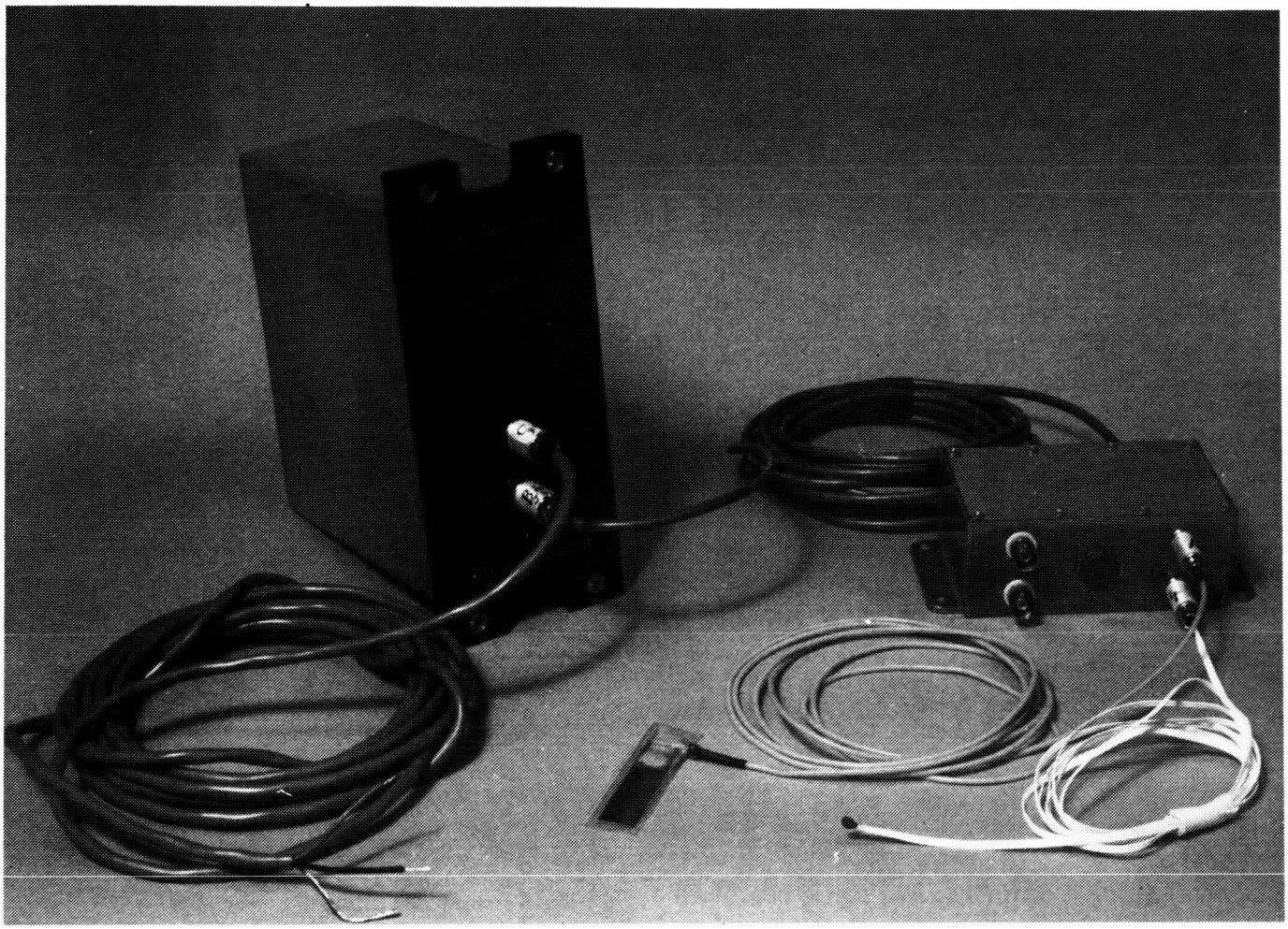

Figure 2a.- Biorhythm flight hardware assembly including activity and skin temperature sensors and input cable from Soviet body temperature telemetry receiver.

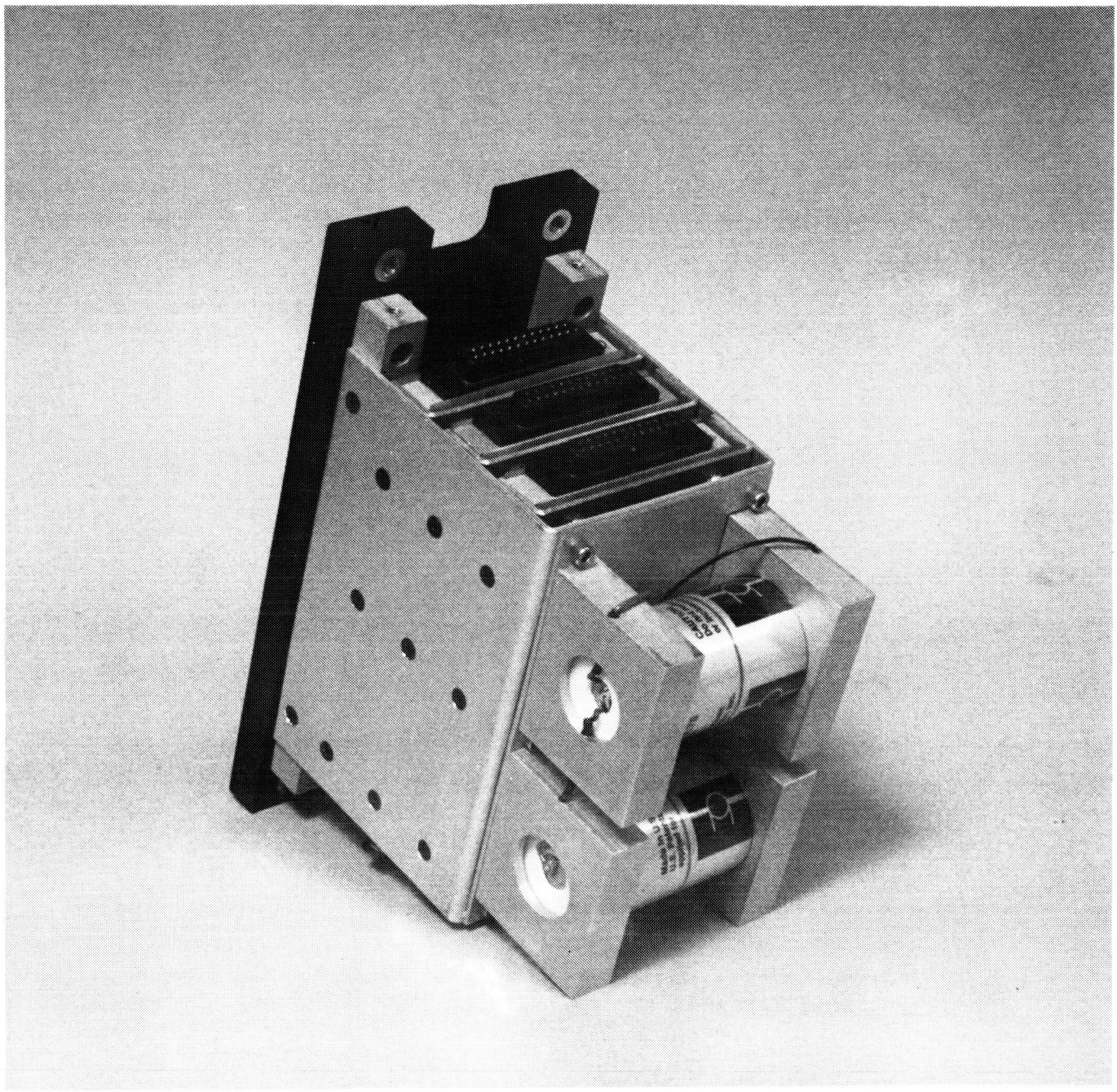

Figure 2b.- Biorhythm experiment flight unit with outer case removed showing three Solicorder data interface ports and lithium battery power supply.

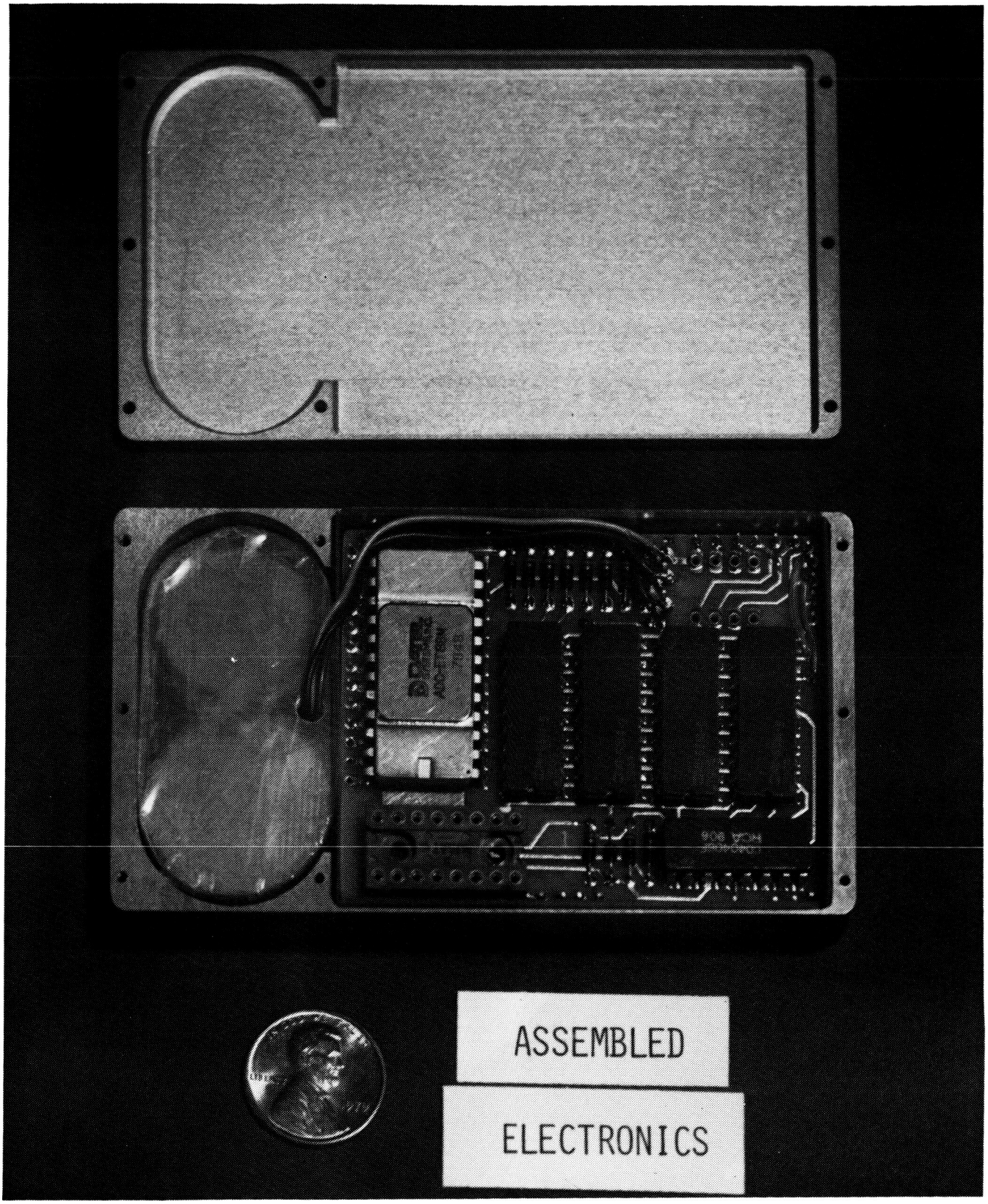

Figure 2c.- Cosmos digital ambient temperature recorder (top removed).

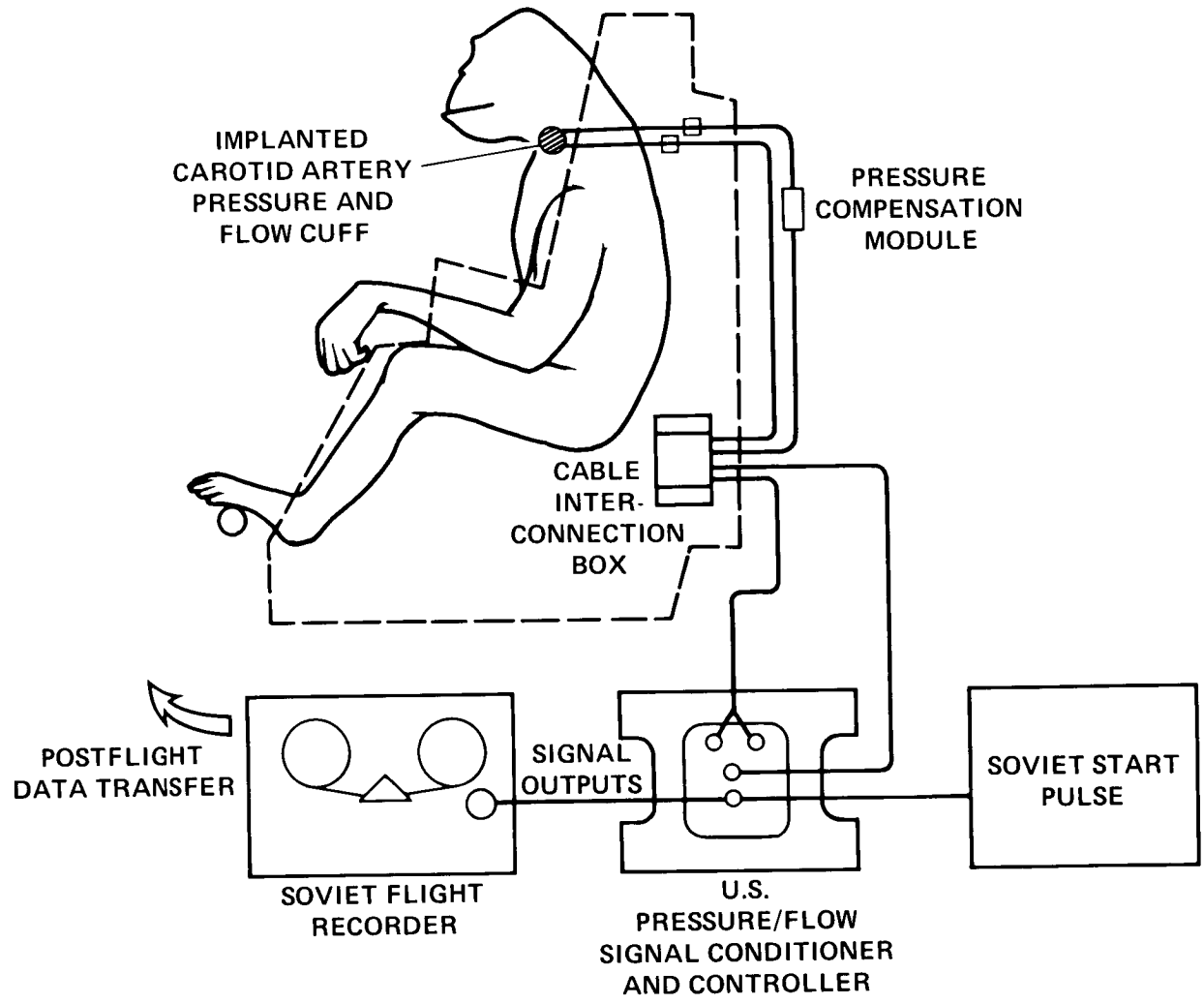

Figure 3.- Cardiovascular experiment equipment showing sensor attachments and data recording.

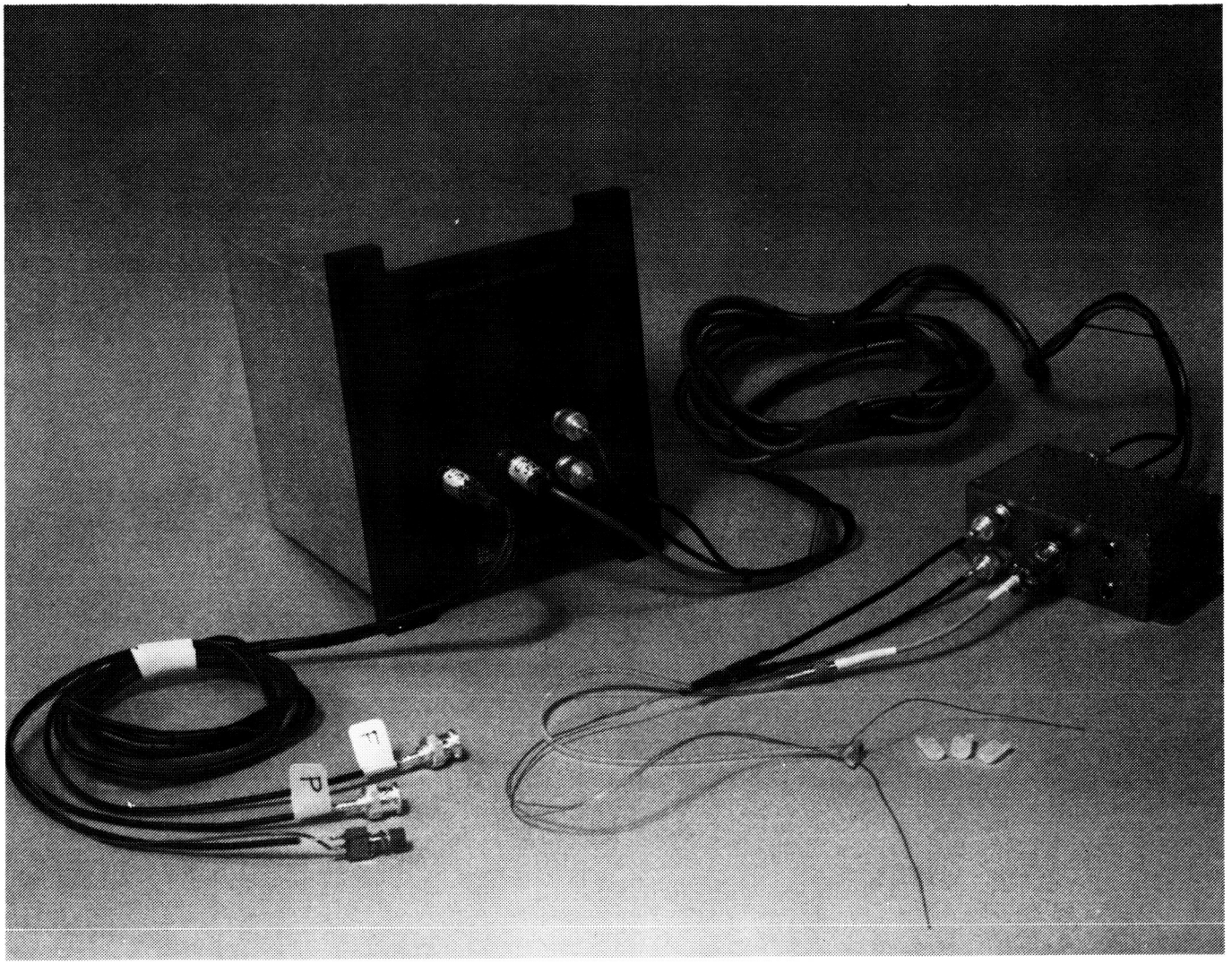

Figure 4a.- Cardiovascular flight hardware assembly including combined pressure/flow cuff sensor with three upper housings.

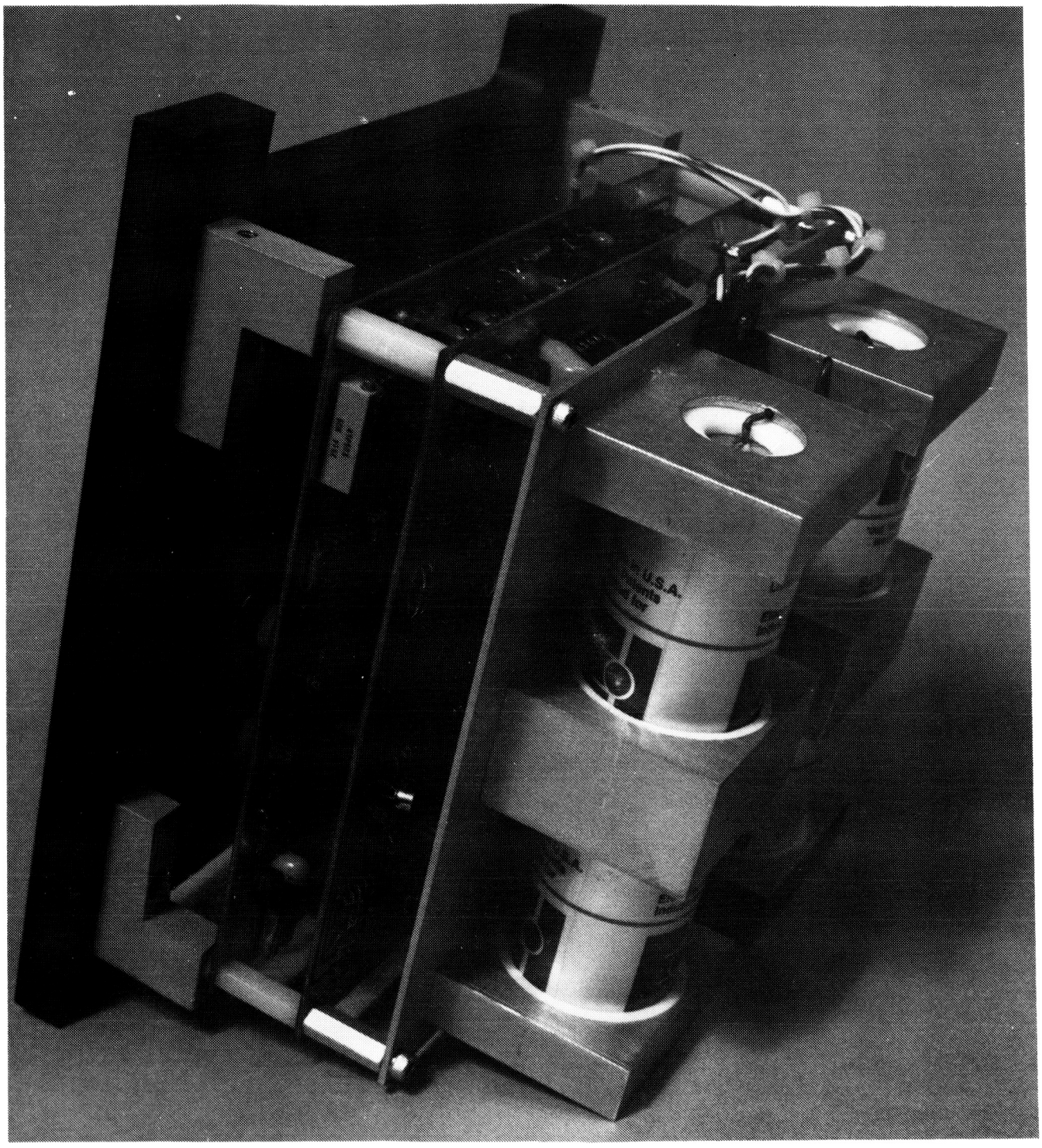

Figure 4b.- Cardiovascular experiment flight unit showing pressure and flow PC boards and lithium battery power supply.

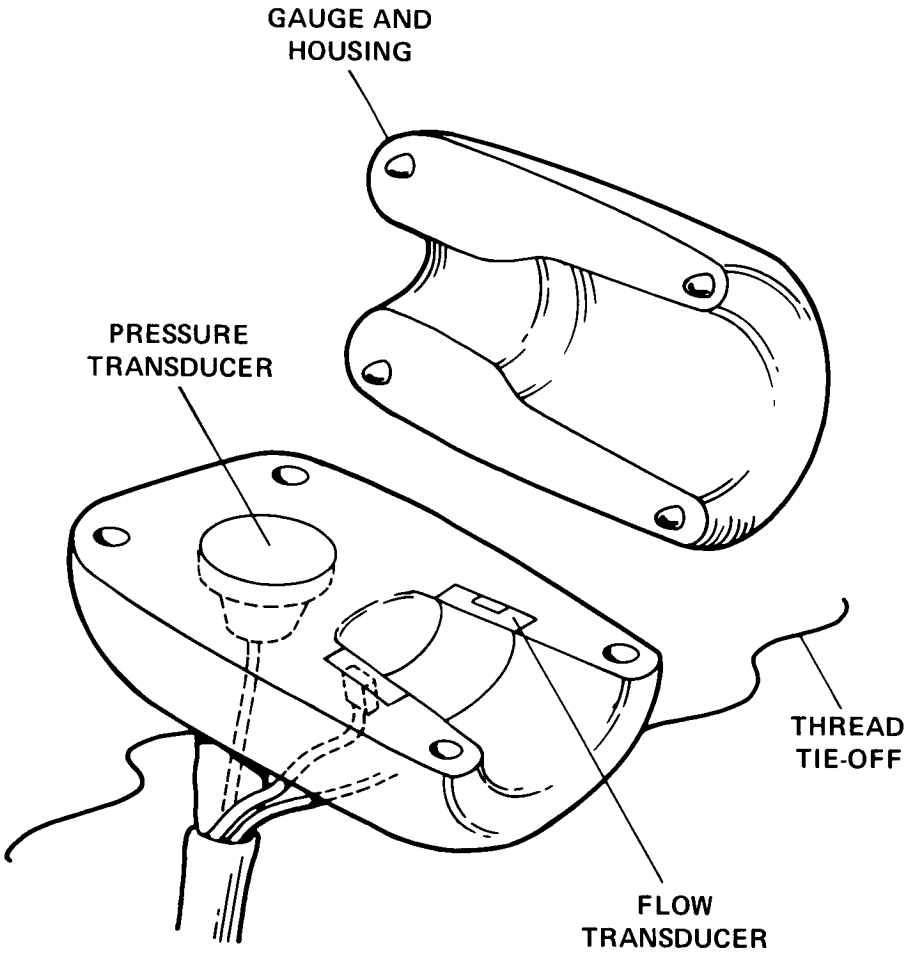

Figure 5.- Combined pressure/flow cuff which is attached to the carotid artery.

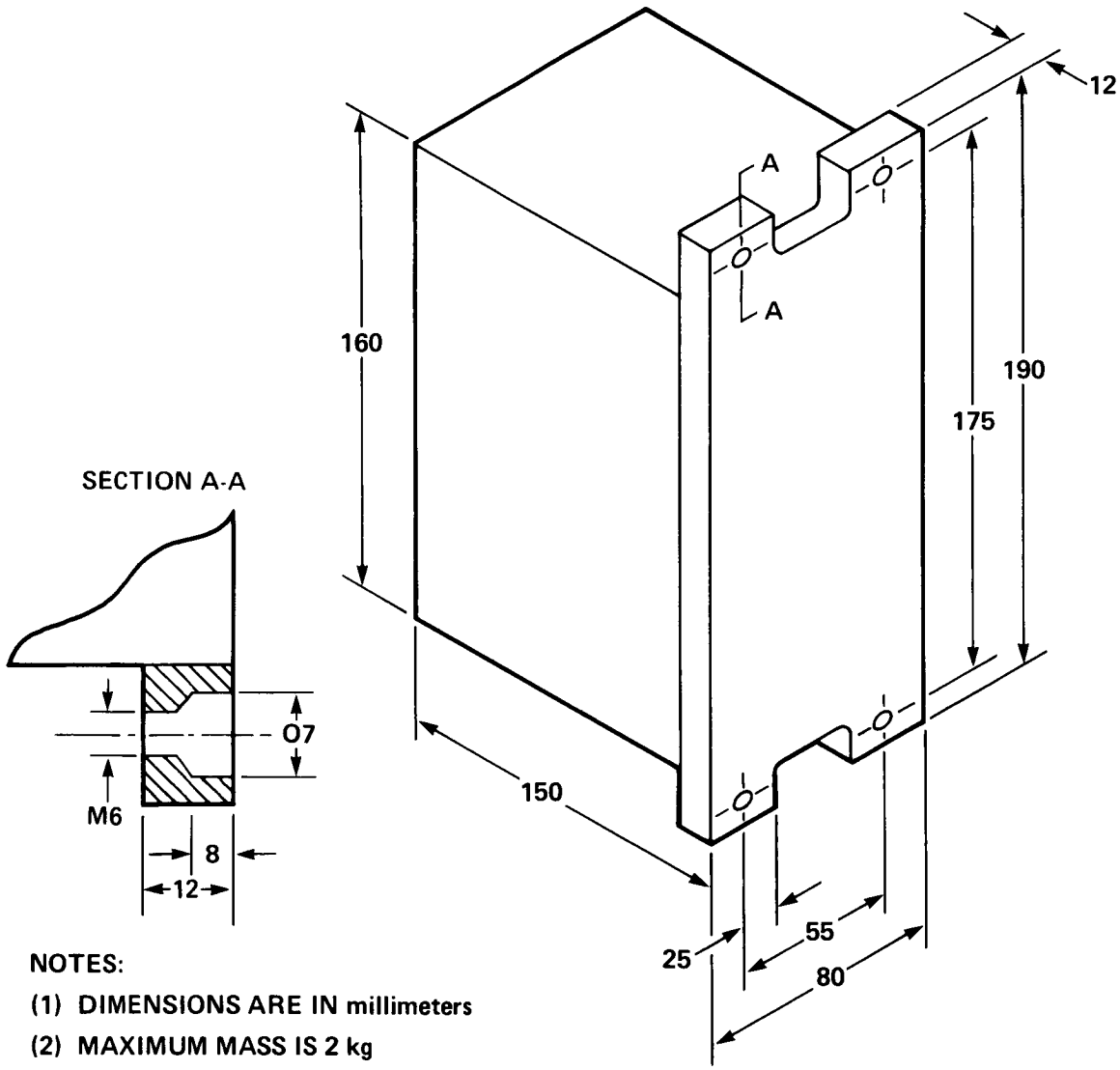

Figure 6a.- Biorhythm flight unit physical dimensions specified by the Soviets.

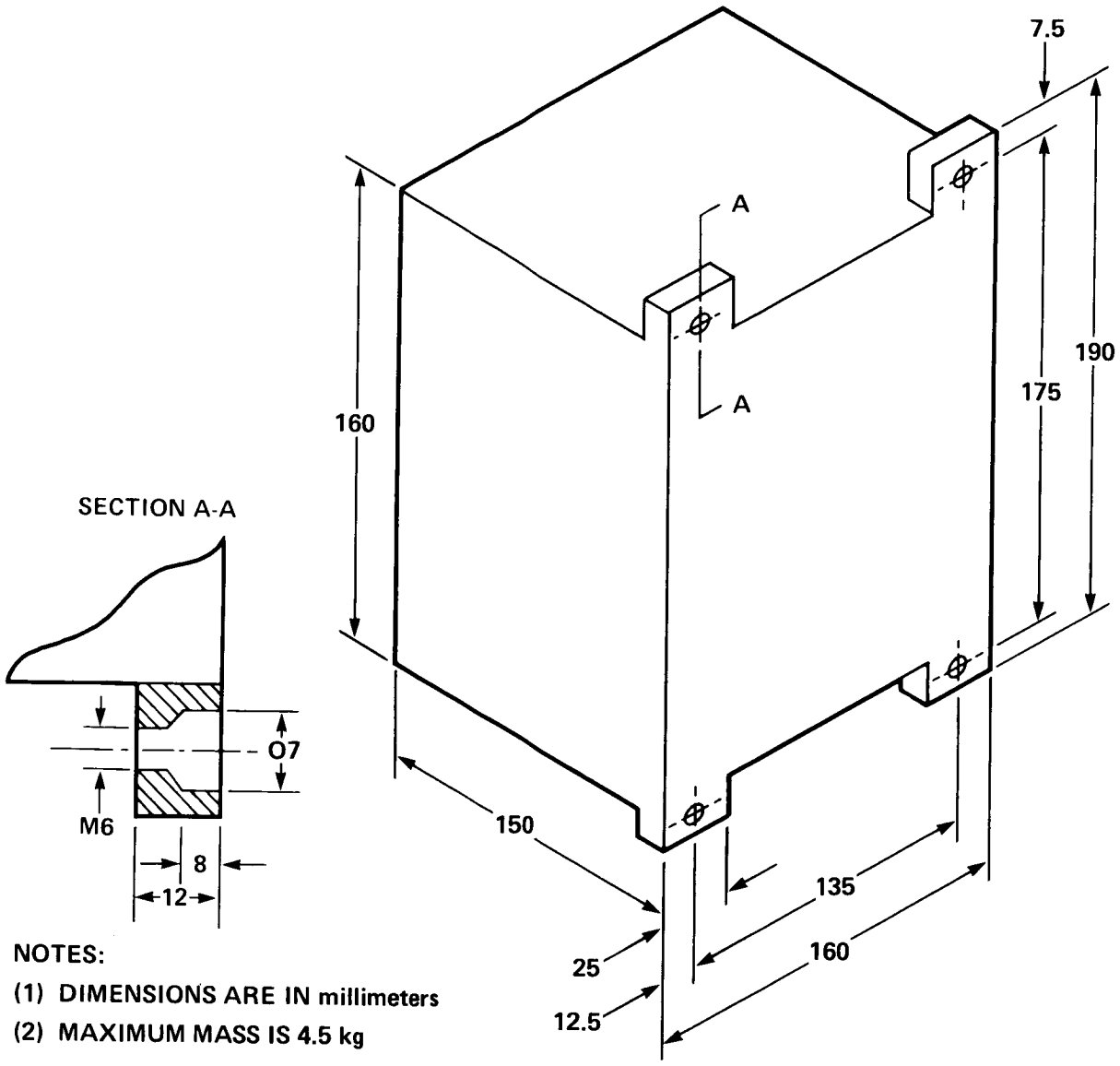

Figure 6b.- Cardiovascular flight unit physical dimensions specified by the Soviets.

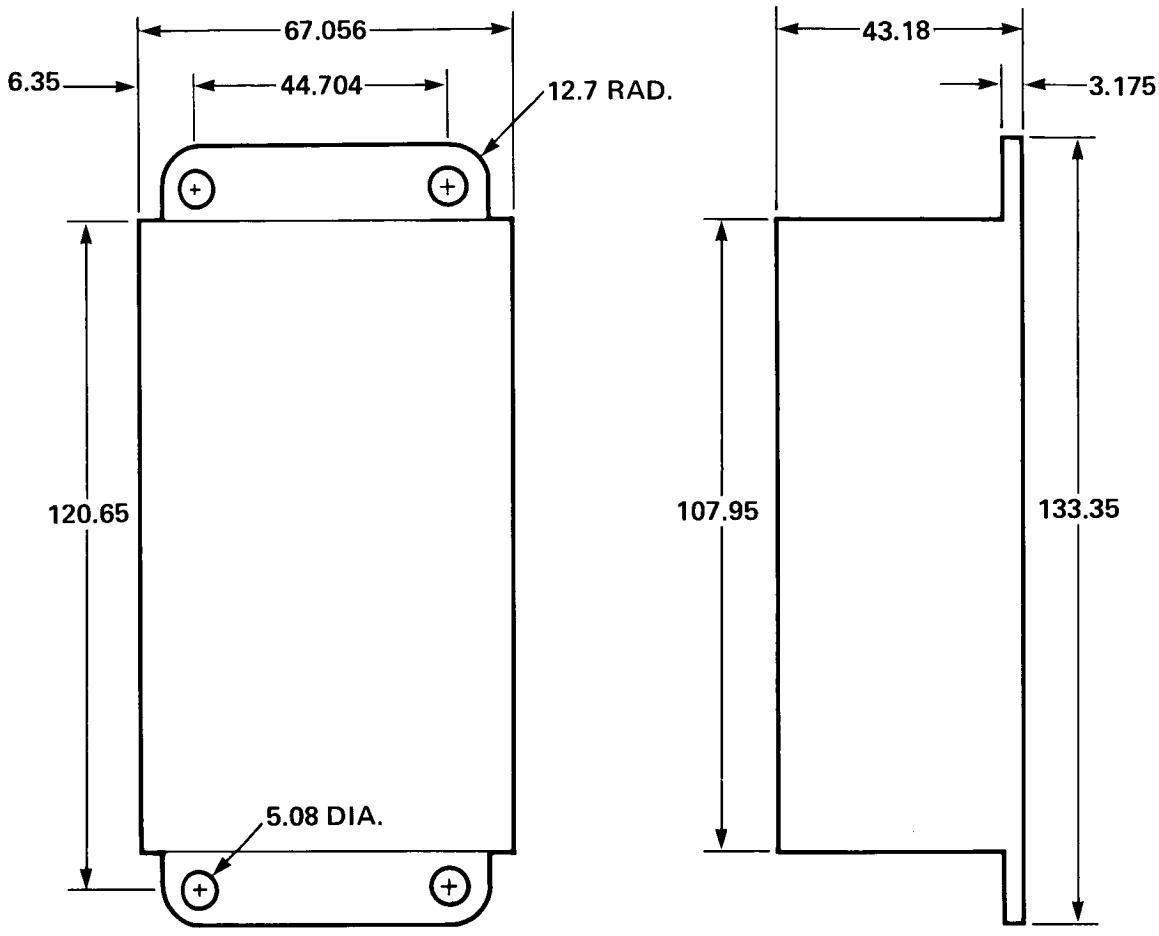

NOTES:

(1) DIMENSIONS ARE IN millimeters

(2) MAXIMUM MASS IS 300 g

Figure 6c.- Physical dimensions of the sensor interconnection box for the biorhythm and cardiovascular experiments.

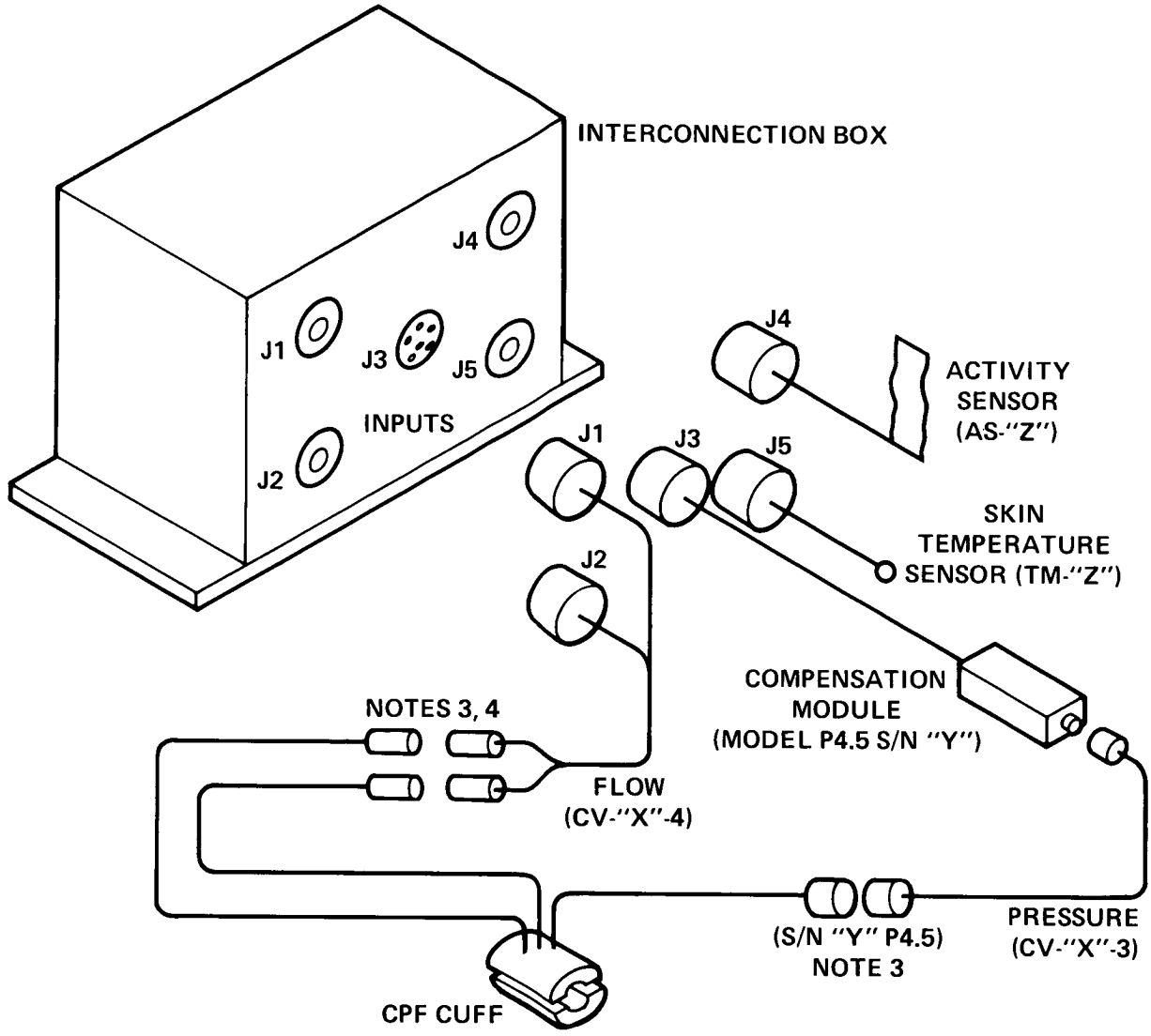

NOTES:

(1) "X" IS THE UNIT SERIAL LETTER (A, B, C, D, E, F, G, H)

(2) "Y" IS THE CUFF SERIAL NUMBER

(3) UNLABELED CABLE ENDS ARE UNIQUELY KEYED TO THEIR MATING CONNECTOR

(4) THE FLOW CABLE CONNECTORS, J1 AND J2, ARE INTERCHANGEABLE

Figure 6d.- Biorhythm and cardiovascular cable connections at the input side of the interconnection box.

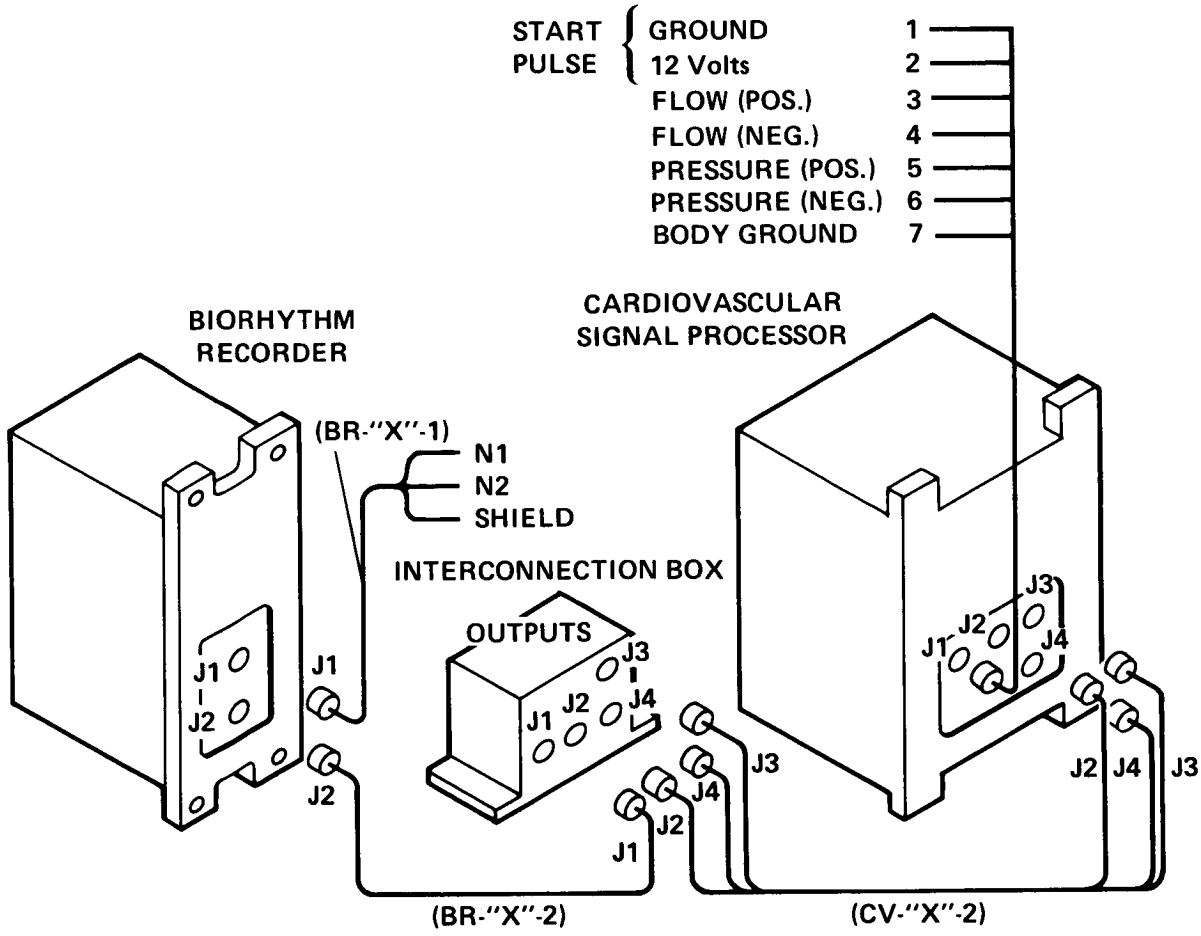

NOTES:

(1) "X' IS THE UNIT SERIAL LETTER (A, B, C, D, E, F, G, H)

(2) CONNECTORS ARE KEYED SO THEY CAN ONLY BE INSERTED IN ONE PLACE

Figure 6e.- Biorhythm and cardiovascular cable interconnection box for the biorhythm and cardiovascular experiments at the output side.

SYNCHRONIZATION OF PRIMATE CIRCADIAN RHYTHMS IN SPACE

Prepared by:

Frank M. Sulzman
Department of Biological Sciences
State University of New York
Binghamton, NY 13901

U.S. INVESTIGATORS

Frank M. Sulzman
Principal Investigator
Department of Biological Sciences
State University of New York
Binghamton, NY 13901

Charles A. Fuller
Division of Biomedical Sciences
University of California
Riverside, CA 92521

Martin C. Moore-Ede
Department of Physiology and Biophysics
Harvard Medical School
25 Shattuck Street
Boston, MA 02115

U.S.S.R. INVESTIGATORS

V. Klimovitsky
Principal Investigator
Institute of Biomedical Problems
Moscow, U.S.S.R.

V. Magedov
Institute of Biomedical Problems
Moscow, U.S.S.R.

A. M. Alpatov
Institute of Biomedical Problems
Moscow, U.S.S.R.

SUMMARY

To evaluate the function of the thermoregulatory and circadian timing systems during spaceflight, body movement, axillary temperature, and ankle skin temperature were monitored in the two rhesus monkeys flown on the Soviet biosatellite COSMOS 1514. The axillary temperatures of both monkeys were lower in space than on Earth, with the largest difference (approximately 0.7° to 0.8°C) occurring during the night. Ankle skin temperature was uniformly low in microgravity, indicating cutaneous vasoconstriction. As expected, the circadian rhythms in all three parameters persisted during spaceflight.

INTRODUCTION

For many years it has been known that there are prominent daily variations in diverse behavioral, physiological and biochemical parameters. The timing of these diurnal rhythms is under the control of the circadian timekeeping system, an endogenous, multioscillator, self-sustained mechanism, which is capable of measuring approximately 24-hour intervals even in the absence of temporal information from the environment (Moore-Ede et al., 1982). In natural conditions, mammalian circadian rhythms are normally both externally and internally synchronized. Several environmental factors normally interact with the circadian timekeeping system in such a way as to entrain the period of these rhythms to 24.0 hours. As a consequence of this entrainment process, various rhythms are maintained at appropriate phase relationships with the environment. The action of pacemakers in the circadian timekeeping system usually produces internal synchronization of circadian rhythms so that all of the diverse rhythms exhibit identical periods and characteristic phase angle relationships.

In certain situations external desynchronization occurs and three such examples are listed below. First, Stroebel (1969) has reported external desynchronization of the circadian rhythm of brain temperature of rhesus monkeys exposed to behaviorally stressful conditions. Second, a more common form of external desynchronization is observed when individuals travel across time zones. As a result of this temporal dislocation, environmental time differs from internal body time and several days are required for resynchronization of the body's rhythms to the new local time. There are numerous reports of diminished performance resulting from this condition. The decrements may be due, at least in part, to the external desynchronization. Third, an additional type of external desynchronization has been reported in man where the circadian rest-activity and body temperature rhythms were not synchronized to the solar day (Kokkoris et al., 1978). These rhythms showed a period greater than 24 hours, with periodic sleep difficulties evident when the individual's subjective day was out of phase with the solar day.

Internal desynchronization has also been observed in both human and nonhuman primates. This condition was first described by Aschoff (1965). He reported that humans maintained in environments devoid of temporal information could show internal desynchronization in which the period of the rest-activity cycle was significantly different from the period of the body temperature rhythm. We have shown that this breakdown in the organization of the circadian timekeeping system is not a consequence of man's volitional control over the rest-activity cycle. Nonhuman primates maintained in isolation, in conditions of constant light and temperature, also show spontaneous internal desynchronization (Sulzman et al., 1977a).

Uncoupling of the temporal organization of the circadian timing system can have important consequences to the organism. We have shown that components of the thermoregulatory system can become uncoupled when individuals are maintained in an environment without circadian time cues (Fuller et al., 1979). This uncoupling can lead to thermoregulation dysfunction as manifested by an inability to maintain core

body temperature in the face of mild exposures to cool temperatures (Fuller et al., 1978).

Thus in certain conditions there can be a breakdown of the normal coupling of the circadian timekeeping system, both externally to environmental cycles and internally among the various rhythms. Furthermore, this uncoupling can result in decrements in performance both on behavioral and physiologic levels. The question thus arises: what are the factors in the environment that normally provide synchronizing cues to the circadian system of primates? In an examination of several different natural factors, we have identified those cycles which are capable of providing meaningful temporal information to the circadian timekeeping system of primates (Sulzman et al., 1977b). Cycles of light and dark are the most effective synchronizers of circadian rhythms, and on Earth, in natural unstressed conditions, this would certainly be sufficient to provide adequate external and internal circadian synchronization. However, it is not certain whether light-dark cycles alone are sufficient to synchronize primate rhythms in space.

Whereas the majority of researchers feel that the circadian timekeeping system is endogenous, an alternative explanation for these persisting circadian rhythms has been argued for many years by Brown (see Brown, Hastings, and Palmer, 1970). He proposed that subtle changes in geophysical variables provide temporal information to organisms in otherwise constant conditions. In other words, the timing system is exogenous, and the organism perceives daily timing signals such as periodic fluctuations in air pressure or slight variations in gravity associated with the rotation of the Earth in relation to the Sun and Moon. A test of this exogenous hypothesis would be to determine if circadian rhythms persist outside of the Earth's environment. In fact, we conducted such an experiment in Spacelab I (Experiment INS007) with a microbial experimental package (Sulzman et al., 1984). While this experiment showed that microbial circadian rhythms can persist in space, there were some indications that microgravity may alter daily cellular timekeeping. At the present time, we have little data on how the circadian timekeeping system of higher organisms, especially primates, will function outside of the Earth's environment. For this reason it is important to examine the effectiveness of environmental synchronizers (viz., light-dark cycles) in maintaining external and internal synchronization.

These issues have further import in light of the results of Biosatellite III. In this mission it was clear that there were serious problems with the circadian timing system of the experimental monkey. There was evidence that the normal synchronization to 24-hour time cues that is seen in ground-based controls did not occur during the mission. Rather, external desynchronization was evident (Hahn et al., 1971).

Thermoregulatory Rhythms

The daily rhythm in body temperature has been known for over 200 years (Hunter, 1778). The first extensive studies on the temperature rhythms of nonhuman primates were undertaken by Simpson and Galbraith (1906) who demonstrated that not only was

body temperature higher in the day than at night, but also the rhythm was synchronized by light-dark cycles. While activity levels and sleep can influence body temperature, they do not generate the rhythm. More than 100 years ago Jurgensen (1873) showed that the temperature rhythm persists in humans during continuous bed rest with either normal meals or complete fasting. It has also been known for many years that the body temperature rhythm can persist in the absence of the sleep-wake cycle. Studies by Aschoff and co-workers have shown that the rhythm in human body temperature is primarily generated by day-night differences in heat loss, and that metabolism plays only a minor role in the rhythm (Aschoff et al., 1974).

Thermoregulation in Space

There is some evidence that thermoregulation is altered in the absence of the normal gravitational fields found on Earth. Fuller and colleagues have shown that hypergravity can produce a transient hypothermia in rats (Fuller et al., 1977) and monkeys (Fuller et al., 1981). There is also some evidence that zero gravity affects thermoregulation since hypothermia has been observed in the rats flown aboard the Soviet biosatellite COSMOS '82 (Klimovitsky et al., 1979) and the macaque that was flown aboard the U.S. Biosatellite III (Hahn et al., 1971). Temperature changes and thermal discomfort were also reported for the Soviet cosmonauts in Salyut spaceflights (Novak et al., 1980; Koslovskaya, 1982 personal communication).

The absence of gravity that is encountered during spaceflight produces some well-known physiological changes in the body. Particularly germane to the thermoregulatory system are the cephalic fluid shifts. The normal pooling of blood in the lower extremities that occurs on Earth is absent in zero gravity. Humans in space show this fluid redistribution by a puffy face, a feeling of fullness, reduced calf girth, and a reduction in leg volume by about 1 liter (Nicogossian and Parker, 1982). The headward fluid shift in space has been hypothesized to be responsible for several physiological responses including: space motion sickness, changes in fluid and electrolyte balance, and perhaps decreased muscular function. On Earth, recumbency has frequently been used to simulate the headward fluid shifts that occur in space (Nicogossian and Parker, 1982; Hargens et al., 1983). For many years it has been known that antiorthostasis can alter both skin and core body temperature. Recumbency of humans during the daytime produces an elevation in skin temperature and a lowering of core temperature (e.g., Nielsen et al., 1938; Aschoff, 1944; Goetz, 1950).

Usefulness of Primate Model

At this stage in evaluating the effectiveness of light-dark cycles in providing external and internal synchronization, it is important to use an animal model with a circadian timekeeping system similar to that of man. Our experience has indicated that certain nonhuman primates are excellent for such studies, and certainly preferable to common laboratory rodents for several reasons. First, obvious phylogenetic similarities with man allow many direct comparisons of the specific mechanisms involved in rhythmic functions. Second, the organization of the rest-activity cycle of primates is comparable to man in that both are diurnal and have consolidated

sleep patterns. The prominent ultradian rhythms in rodents can act to obscure longer period rhythms. Third, since the overall architecture of the circadian timing systems of man and monkeys is similar, the internal temporal order, internal and external phase relations are comparable. The use of a diurnal organism is preferable. Because there are many similarities between the thermoregulatory systems of rhesus monkeys and humans, results on thermoregulation in space should have human applicability.

Animals

In all of the spaceflight and ground-based studies rhesus monkeys (Macaca mulatta) were used. The monkeys were young (3 kg to 5 kg) and extensively trained to accept restraint in metabolism chairs for periods of 1 to 2 weeks.

Spaceflight Data

Activity was monitored via a sensor (L & M Electronics, Foster City, CA) attached to the monkey's restraint jacket. The output of the sensor was filtered and amplified, then fed into a digital data collection unit (Ambulatory Monitoring, Inc., Ardsley, NY) and totalled over 16-minute intervals.

Axillary temperature was monitored with a Soviet biotelemetry system. The transmitters were calibrated and then implanted in the left axilla several weeks before the experiment. The output of the transmitter was recorded at 16-minute intervals on another data collection unit (Ambulatory Monitoring, Inc.).

Ankle skin temperature was measured by YSI thermistors (Yellow Springs Instruments, Yellow Springs, OH). The thermistor was attached to the ankle skin by cyanoacrylate glue, and then covered with tape. The output of the thermistor was recorded on a digital data collection unit (Ambulatory Monitoring, Inc.).

Ground-Based Control Studies

Baseline data were collected at 1 g with the same procedures used in the spaceflight experiment. However, in some of the experiments conducted in the U.S., ankle temperature was measured with copper-constantan thermocouples (Omega Instruments, Stamford, CN) calibrated to 0.1°C against an NBS certified mercury thermometer. Axillary temperature was also monitored with surface thermocouples taped to the axilla, and these data were identical to the axillary temperatures measured by telemetry. Colonic temperature was also monitored with thermocouples to evaluate how well axillary temperature reflected core body temperature. The thermocouples were coated with plastic, inserted approximately 10 cm past the anus, and the lead was then taped to the base of the tail. The output of the thermocouples was amplified and the temperature data were recorded on a millivolt strip chart recorder. These data were digitized at 16-min intervals with an Apple II digitizer.

Oxygen Consumption

Oxygen consumption was continuously monitored with an oxygen analyzer (Amtek/Thermax, Instruments Div., Pittsburgh, PA). The monkeys were placed in a Plexiglas chamber that was approximately 80 by 80 by 20 cm, and 8 liters/min of air were pulled through the chamber. The air flow maintained the chamber oxygen above 20%, carbon dioxide below 1%, and the relative humidity between 50% and 60%. The outflowing air was dried, carbon dioxide removed, and then passed into the oxygen analyzer. The dc output of the calibrated analyzer was recorded on a millivolt strip-chart recorder and then digitized on an Apple II+ microcomputer. Data were digitized at 1-min intervals and then averaged over 16 min for further analysis.

Heart Rate

Heart rate was measured by a Vitalog PMS-8 solid state recorder (Vitalog Corp., Palo Alto, CA). Two Ag/AgCl electrodes (3M No. 2259, 3M, St. Paul, MN) were applied to both sides of the chest and a reference electrode was applied to the back. Before application of the electrodes the sites were shaved and then cleaned with 70% alcohol. Data were averaged over each minute and stored in the recorder. The values presented in this report are the 16-min averages of the recorded data.

Data Analysis

Data were analyzed on an Apple II+ microcomputer and plotted on a digital Hi-Plot plotter (Model DMP-4, Houston Instruments, Houston, TX). To evaluate the underlying repetitive circadian characteristics of the data, a waveform eduction was performed. The data were reduced to a single cycle by averaging the data points at each clock time. In other words, the 08:00 points on each day were averaged together to give the mean value for that time. This procedure was repeated at 16-min intervals to give 96 average values. The circadian period of these rhythms was determined using the chi square periodogram method of Sokolov and Bushell (1978).

RESULTS

The data that will be described in this report include the flight data from COSMOS 1514, synchronous control data, and vivarium control data. The ground-based data were collected at the Institute of Biomedical Problems in Moscow and at the State University of New York at Binghamton. The data set is summarized in table I.

Since the monkey Abrek was a subject in a preflight test in November 1983, there is reasonably good control data from this animal. These data are shown in figure 1 and are fairly representative of the limited data set for 1 g measurements. Activity (top panel) is generally high in the day and low at night. The high activity counts on the first night of the experiment probably reflect adaptation to the restraint chair. Axillary temperature (middle panel) is also high during the day and low at night. In control situations, we have shown that axillary temperature has the same temporal pattern as core body temperature. Ankle skin

temperature (bottom panel) showed a highly variable pattern, but there was a trend for elevated skin temperature around the time when axillary temperature was declining. Other ground-based studies have shown that an increase in heat loss is reflected by an elevation in peripheral skin temperature. This is an important determinant of the nightly decline in core body temperature.

The average daily patterns in these three variables are more clearly shown in figure 2. These waveform eductions of activity (top panel) and axillary temperature (middle panel) confirm the general patterns seen in figure 1. In this experiment, there is not a significant circadian rhythm in ankle skin temperature. The absolute level of the activity counts reflects both the movement of the monkey and the method of sensor attachment; hence, only the relative differences are important. On the other hand, the level of the temperature values reflects thermoregulatory function. The typical range of axillary temperature is from a high of about 38.2°C during the day to a low of about 37.0°C during the night. The average ankle skin temperature of about 32.8°C reflects relatively high heat loss through cutaneous vasodilation. The ambient temperature for this experiment is summarized in table II.

The data from Abrek during spaceflight were quite good and are shown in figure 3. The raw data here are presented in the same way as in figure 1. Launch occurred on December 14, 1983, at the time indicated by the arrow, and recovery occurred on December 19, 1983, at the time indicated by the second arrow. Clear rhythms were evident in both activity and axillary temperature. Ankle skin temperature (bottom panel) showed normal day-night changes on the two prelaunch days, but while Abrek was in space, ankle skin temperature was uniformly low and just above ambient temperature.

Figure 4 shows the waveform eductions of the data from figure 3. Only the data while the monkey was in space were used in this eduction. These data are presented in the same manner as figure 2. Activity shows a very prominent circadian pattern, as does axillary temperature. Ankle skin temperature shows very little day-night difference. The axillary temperature in space ranged from about 37.5°C in the day to about 36.3°C in the night. Ankle skin temperature remained around 26°C. The ankle skin temperature and ambient temperature data are summarized in table II.

There were two postflight monitoring sessions on Abrek. Data from these sessions are plotted in figure 5. The changes in activity levels probably reflect differences in activity sensor attachment. The average waveforms of these postflight data are shown in figure 6. The activity waveform does not indicate a circadian rhythm, but if the raw data were normalized, a circadian trend might be evident. Axillary temperature shows a similar pattern to that seen in figure 2. Ankle skin temperature shows a peak just before lights off, and a trough at the time of lights on.

The most significant differences between the flight data and the pre- and postflight data are in axillary and skin temperatures. Figure 7 plots the average 1 g data (both pre- and postflight) and the 0 g data. Although the waveforms are

quite similar, axillary temperature in space averages about 0.7°C lower than on the ground. This difference is highly significant. The differences in ankle skin temperature are quite evident in table II. While the ambient temperatures were approximately the same for preflight and flight, ankle skin temperature of Abrek averaged almost 7°C lower in space than on Earth.

Data from Bion, the second monkey on COSMOS 1514, are shown in figure 8 and are very similar to the data from Abrek. The first arrow indicates the time of launch and the second arrow indicates the time of recovery. The activity levels of Bion are much lower than those of Abrek. Axillary temperature of Bion in space is clearly rhythmic and low. Ankle skin temperature was typically rhythmic before the flight. In space the skin temperature was low except for one period on the third day. The average patterns of these three variables are plotted in figure 9. The educed temperature waveforms for Bion in space are quite similar to those of Abrek in space: Ankle skin temperature is low, indicating peripheral cutaneous vasoconstriction, and axillary temperature is lower than ground-based control animals. Unfortunately, the death of Bion after recovery and transport back to Moscow prevented any postflight circadian rhythm monitoring, so we do not have control axillary temperature data from Bion on Earth. Figure 10 shows the average axillary temperature of Bion during spaceflight and the average axillary temperature of 6 other rhesus monkeys monitored on Earth for a total of 30 monkey days. The reduction in axillary temperature in space is highly significant.

The periods of the axillary temperature and activity rhythms were examined in order to evaluate the external synchronization to the LD cycle, and the internal synchronization to each other. As an example of this analytical procedure, figure 11 shows the period spectrum of the space flight data of Abrek. The data are arranged with activity on top, axillary temperature in the middle and ankle temperature on the bottom. The line in each panel shows the confidence ($p = 0.01$) level of the spectrum. Table III shows the results of this analysis. All rhythms were statistically significant ($p < 0.01$) except for the preflight activity rhythm of Abrek ($p > 0.05$). This table shows that the six ground-based studies showed rhythms that were externally synchronized to the 24.0-hour light-dark cycle. In contrast to the controls on Earth, the rhythms in space all had peaks in the period spectrum at values other than 24.0 hours. The largest deviations from 24.0 were seen in the activity rhythm of Abrek. Inspection of the raw data (fig. 3) tends to confirm this result. It appears that the distribution in the activity counts changes. On December 14 and 15, the lowest activity occurs in the middle of the dark period, whereas on December 16 and 17, the lowest counts occur around the time of lights off.

To evaluate the axillary temperature as a measure of core body temperature, studies were conducted in which axillary temperature and colonic temperature were simultaneously monitored in 4 monkeys. Figure 12 shows the average colonic and axillary temperature patterns on Earth, and these data are summarized in table IV. The mean day, night, and 24-hr average temperatures were not statistically different ($p > 0.05$), and the waveforms are identical. Table IV also shows that there was excellent agreement between the U.S. and U.S.S.R. axillary temperature measurements at 1 g. Although the 24-hr average axillary temperature is approximately 0.5°C

lower in space than on Earth, the nighttime difference is greater. Figure 13 shows the average rhesus axillary temperature on Earth and in space. The waveforms are quite similar but there is a larger difference between the rhythms at night (0.7°C) than in the day. Since both Abrek and Bion showed very similar temperature patterns, we do not think that Bion's mild hypothermia was related to his death.

Two monkeys, Ariel and Teuton, served as subjects in synchronous control experiments. Unfortunately, the axillary temperature telemetry system did not function on either of these animals. Consequently there are no axillary temperature data for the synchronous controls. The data from the presynchronous control are too limited to permit any detailed analysis. The synchronous control data for Ariel are quite variable and of dubious value. Because of the absence of axillary temperature data and the poor quality of the skin temperature data from Ariel, no further analysis was performed on the data from the synchronous control monkeys.

To compare the mean ankle skin temperature on Earth and in space, the average ankle skin temperature and ambient temperature are shown in table II. While there were some differences in mean ambient temperature (23.0°C to 24.6°C), the mean ankle skin temperature is lower in space than on the ground. As noted above, this is particularly evident for Abrek in the preflight and flight data. Since ambient temperature data for the postflight monitoring sessions were not recorded, the mean skin temperature postflight are not included in this table.

In humans there is an excellent correlation between metabolism and heart rate (Astrand and Rodahl, 1977). Since there was a reduction in the heart rate of Bion during spaceflight (Sandler et al., 1985), this may indicate that metabolism was lower in space. To determine if heart rate is correlated with metabolism in rhesus monkeys, experiments were conducted with 4 monkeys in which oxygen consumption and heart rate were simultaneously monitored. Figure 14 shows the data from one monkey who had a higher mean heart rate and oxygen consumption during the day than at night. The correlation (r) between heart rate and metabolism in this monkey was 0.84. Two of the 4 monkeys showed a good correlation. Figure 15 shows the patterns of another monkey who showed a little day-night difference and a poor correlation between metabolism and heart rate ($r = 0.24$). It should be noted that the core temperature patterns of the monkeys shown in figures 14 and 15 are almost identical. The average temperature, oxygen consumption and heart rate patterns for the 4 monkeys are shown in figure 16. Core body temperature showed the typical rhythmic pattern, and mean heart rate was higher during the day than at night. However, the mean oxygen consumption was not rhythmic, and the overall correlation between metabolism and heart rate was 0.52. This indicates that only about 25% of the variance in the 24-hr heart rate is due to changes in metabolism. Closer inspection of the raw data indicated that the nighttime metabolic and heart-rate patterns were fairly similar, and so a correlation between metabolism and heart rate during the night was done, and this is shown in figure 17. It is quite evident that there is an excellent correlation between the nighttime oxygen consumption and heart rates, with $r = 0.86$. This indicates that more than 70% of the variance in nighttime heart rate is due to changes in metabolic rate. Therefore, the nighttime heart rate of rhesus monkeys is a good indicator of metabolic rate.

CONCLUSIONS

As a result of COSMOS 1514 several conclusions can now be made. First, it is clear that the circadian rhythms of activity and axillary temperature persist in space. There may be changes in mean level and amplitude, but as expected, rhythmicity is still quite evident. Second, the axillary temperature of monkeys in space appears to be maintained at a lower level than on the ground. The lower temperature is evident at all times of the day and night, and averaged between 0.5°C and 1.0°C below temperatures on the ground. Third, ankle skin temperature is low in space, and maintained just above ambient temperature. This probably reflects a decrease in peripheral cutaneous blood flow in space. Fourth, the results of the period analysis suggest that entrainment to the light-dark cycle is not as strong in space as it is on Earth. Each of these conclusions is discussed below.

Persistence of Rhythms

As noted above, the observation that the activity and temperature rhythms persist in space was expected. These rhythms are quite robust on Earth, and the presence of a light-dark cycle probably contributed to the amplitude of these rhythms in space. This observation, though expected, is important since it validates the instrumentation that was used to monitor the rhythmic parameters. The COSMOS 1514 mission clearly demonstrates the successful development of the data collection system.

Reduced Axillary Temperature

As noted in the Introduction, it was expected that there would be a reduction in core body temperature in space. This expectation was confirmed by the results from both Abrek and Bion. The data from Abrek are particularly significant since sufficient ground-based data were available to construct an average daily temperature pattern from this monkey at normal gravity. The temperature records from both Abrek and Bion suggest that axillary temperature declines during the first three days in space.

In order for core body temperature to be regulated at a set level, there must be a balance between metabolic heat production and heat loss. The low ankle temperatures seen in space suggest that heat loss is minimized by reduced cutaneous blood flow. Although metabolism was not measured in the monkeys flown in space, we have shown that there is an excellent correlation between the nighttime metabolic rate and heart rate. Since the cardiovascular experiment on COSMOS 1514 showed that there was a reduction in heart rate in space (Sandler et al., 1985), this suggests that a reduction in metabolism may be the cause of the lower axillary temperature in space.

While the reduction in body temperature seems real, two things should be kept in mind. First, the resolution of the axillary temperature data from the spaceflight experiment was not as good as for the ground-based studies. This is due to problems with the U.S. microcomputers after the flight. Although the data values

are correct, the flight data are accurate to only about 0.3°C, whereas the ground-based data are accurate to 0.1°C. Since the average reduction in axillary temperature was greater than 0.5°C, we are confident that this observation is real. Nevertheless, the reduced resolution of the spaceflight data is unfortunate.

Second, although axillary temperature was lower in space, it is not definite that core body temperature was reduced. In ground-based studies, we have shown that the axillary temperature is a good indicator of core body temperature, and that the axillary temperature rhythm has the same waveform as colonic temperature. The restricted movement of the monkeys' arms in restraint chairs provides significant thermal insulation so that the axillary temperature value is close to core body temperature. However, the reduced ankle skin temperature may indicate a general reduction in cutaneous blood flow, including the trunk. Although unlikely, it is possible that changes in cutaneous blood flow in space may alter the validity of axillary temperature as an indicator of core body temperature. A more direct measurement of core body temperature in space would resolve this doubt.

Reduced Ankle Skin Temperature

The observation that ankle skin temperature is low in space is important. Within the thermal neutral zone, the circadian rhythm of core body temperature of primates is regulated to a large extent by changes in vasomotor heat loss. This is accomplished by blood flow to various anatomical sites, and in monkeys the face, ears, tail, hands and feet are especially important. The fact that the ankle skin temperature was low in space suggests that increased heat loss was not the cause of the probable reduction in core body temperature. It should be noted that the average ambient temperature in COSMOS 1514 was between 23.5°C and 24.0°C. This temperature is just below the reported thermoneutral zone for rhesus monkeys (Johnson and Elizondo, 1979). Although the ambient temperature during spaceflight was quite similar to that of ground-based control experiments (see table II), the fact that 23.0°C to 24.0°C is at the lower border of the thermoneutral zone may produce some unexpected results. If possible, it would probably be better to raise the spacecraft ambient temperature to 26°C for future primate spaceflights.

Circadian Period

As expected, the circadian period measurements in the ground-based studies were all 24.0 hours. The non-24 hour periods of the spaceflight data could be due to several reasons: (1) It could be that because of the short time series that were being analyzed (less than 5 days), the observed values were not really different from 24 hours. This is quite possible since the observed values were so close to 24 hours. (2) The non-24-hour periods could reflect a changing waveform in space, an alteration in the phase relationship to the light-dark cycle, or some other phenomenon that results in a nonstationary time series. (3) The non-24 hour periods could be real and indicate some sort of stress-induced desynchronization (see Introduction). In view of the fact that Abrek, the monkey with the largest deviation from 24 hours, tolerated space flight quite well and showed relatively normal physiological responses, stress is probably an unlikely explanation for this result.

(4) It could be that some condition of space causes an alteration in the function of the circadian timing system so that the potency of environmental synchronizers is attenuated.

Unfortunately, the relatively brief spaceflights such as COSMOS 1514 make it difficult to resolve these various alternatives. A longer spaceflight (e.g., 7 to 10 days) would facilitate the resolution of circadian synchronization.

General Conclusions

The joint U.S.-U.S.S.R. primate circadian rhythm experiment on COSMOS 1514 should be considered a success for several reasons. First, the main engineering goals of this flight were accomplished. The usefulness of the nonhuman primate model and verification of the spacecraft and data collection systems were well established. Second, some important observations were made about the function of the circadian timekeeping system and the thermoregulatory system in space. However, for various reasons, at the present time these observations are only preliminary and require confirmation from additional studies.

ACKNOWLEDGMENTS

We would like to thank our Soviet colleagues for their involvement and support of this project, especially Dr. E.A. Ilyin at the Institute of Biomedical Problems. In the U.S., the role that Mr. Edward Gomersall played as Project Manager was key to the successful U.S. participation in the flight. We also wish to acknowledge the participation of other individuals at Ames Research Center, especially Daryl Rasmussen, Kenneth Souza and Vernon Yearwood-Drayton; support personnel, especially Richard Mains, John Zicker and Edward Luzzi; and the staff at SUNY-Binghamton: Mark Haley, Bruce Bailey, Sharon Sickles, Ellen Wurster and Scott Organ were essential in developing the equipment, procedures and tests necessary for this project. Dr. James S. Ferraro, Keith Halperin, Denise Dino, Gary Wassmer, Robert Chasin and Jean Garrett conducted the baseline studies. This work was supported by NASA contract NAS 2-10621.

BIBLIOGRAPHY

Aschoff, J.: Uber die Interferenz temperaturregulationischer und kreislaufregulatorischer Vorgange in der Extremitat des Menschen. Pflugers Arch., vol. 248, 1944, pp. 197-207.

Aschoff, J.: Circadian Rhythms in Man. Science, vol. 148, 1965, pp. 1427-1432.

Aschoff, J; Biebach, H.; Heise, A.; and Schmidt, T.: Day-Night Variation in Heat Balance. Heat Loss From Animals and Man. J. L. Montieth and E. L. Mount, eds., Butterworths (London), 1974, pp. 147-172.

Astrand, P. O.; and Rodahl, K.: Textbook of Work Physiology. McGraw-Hill (New York), 1977.

Brown, F. A.: Hypothesis of Environmental Timing of the Clock. The Biological Clock: Two Views. F. A. Brown, J. W. Hastings, and J. D. Palmer, Academic Press (New York), 1970, pp. 15-59.

Fuller, C. A.; Horowitz, J. M.; and Horwitz, B. A.: Effects of Acceleration on the Thermoregulatory Responses of Unanesthetized Rats. J. Appl. Physiol., vol. 42, 1977, pp. 74-79.

Fuller, C. A.; Sulzman, F. M.; and Moore-Ede, M. C.: Thermoregulation is Impaired in an Environment Without Circadian Time Cues. Science, vol. 199, 1978, pp. 794-796.

Fuller, C. A.; Sulzman, F. M.; and Moore-Ede, M. C.: Circadian Control of Thermoregulation in the Squirrel Monkey, Saimiri sciureus. Am. J. Physiol., vol. 236, no. 3, 1979, pp. R153-R161.

Fuller, C. A.; Tremor, J.; Connolly, J. P.; and Williams, B. A.: Temperature and Behavioral Responses of Squirrel Monkeys to 2 g Acceleration. The Physiologist, vol. 24, 1981, pp. S111-S112.

Goetz, R. H.: Effect of Changes in Posture on Peripheral Circulation, with Special Reference to Skin Temperature Readings and the Plethysmogram. Circulation, vol. 1, 1950, pp. 56-75.

Hahn, P. H.; Hoshizaki, T.; and Adey, W. R.: Circadian Rhythms of the Macaca nemestrina Monkey in the Biosatellite III, 1971.

Hargens, A. R.; Tipton, C. M.; Gollnick, P. D.; Mubarak, S. J.; Tucker, B. J.; and Akeson, W. H.: Fluid Shifts and Muscle Function in Humans During Acute Simulated Weightlessness. J. Appl. Physiol., vol. 54, 1983, pp. 1003-1009.

Hunter, J.: Of the Heat of Animals and Vegetables. Phil. Trans. R. Soc. Lond. (Biol.) vol. 68, 1778, pp. 7-49.

Johnson, G. S.; and Elizondo, R. S.: Thermoregulation in Macaca mulatta: a Thermal Balance Study. J. Appl. Physiol., vol. 46, 1979, pp. 268-277.

Jurgensen, T.: Die Korperwarme des gesunden Menschen. Ph.D. thesis, Leipzig, 1873.

Klimovitsky, V. Ya.; Organov, V. S.; Il'in, Ye. A.; Noskin, A. D.; Verigo, V. V.; Magedov, V. S.; Murashko, L. M.; Rastopshin, Yu. A.; and Skuratova, S. A.: Temperature Homeostasis and Motor Activity of the Animals During Flight. Vilyaniye dinamicheskikh factorov kosmicheskitgo poleta na organism zhivotnykh. A. M. Genin, ed., Nauka (Moscow), 1979, pp. 13-16.

Kokkoris, C. P.; Weitzman, E. D.; Pollak, C. P.; Apielman, A. J.; Czeisler, C. A.; and Bradlow, H.: Long-Term Ambulatory Monitoring in a Subject with a Hypernyethermeral Sleep-Wake Cycle Disturbance. Sleep, vol. 1, no. 2, 1978, pp. 177-190.

Moore-Ede, M. C.; and Sulzman, F. M.: The Physiological Basis of Circadian Timekeeping in Primates. Physiologist, vol. 20, 1977, pp. 17-25.

Moore-Ede, M. C.; Sulzman, F. M.; and Fuller, C. A.: The Clocks That Time Us: Physiology of the Circadian Timing System. Harvard University Press, 1982.

Nicogossian, A. E.; and Parker, J. F.: Space Physiology and Medicine. NASA SP-447, (Washington, D.C.: U.S. Government Printing Office), 1982, 324 pp.

Nielsen, M.; Herrington, L. P.; and Winslow, C. E. A.: The Effect of Posture upon Peripheral Circulation. Am. J. Physiol., vol. 127, 1938, pp. 573-580.

Novak, L.; Genin, A. M.; and Kozlowski, S.: Skin Temperature and Thermal Comfort in Weightlessness. The Physiologist, vol. 23, 1980, pp. S139-S140.

Sandler, H.; Stone, H. L.; Hines, J. W.; Benjamin, B.; Halpryn, B. M.; Krotov, V. P.; Kulayev, B. P.; Krilov, V.; Magedov, V.; and Nazin, A. N.: Cardiovascular Results from a Rhesus Monkey Flown Aboard Cosmos 1514, Spaceflight and Ground-Based Controls. NASA TM-88223, 1986.

Simpson, S.; and Galbraith, J. J.: Observations on the Normal Temperature of the Monkey and its Diurnal Variation, and on the Effect of Changes in the Daily Routine on this Variation. Trans. Roy. Soc. Edinburg, vol. 45, 1906, pp. 131-160.

Sokolov, P. G.; and Bushell, W. N.: The Chi-Square Periodogram: its Utility for Analysis of Circadian Rhythms. J. Theor. Biol., vol. 72, 1978, pp. 131-160.

Stroebel, C. F.: Biologic Rhythm Correlates of Disturbed Behavior in the Rhesus Monkey. Bibl. Primat., vol. 9, 1969, pp. 91-105.

Sulzman, F. M.; Fuller, C. A.; and Moore-Ede, M. C.: Spontaneous Internal Desynchronization of Circadian Rhythms in the Squirrel Monkey. Comp. Biochem. Physiol., vol. 58A, 1977a, pp. 63-67.

Sulzman, F. M.; Fuller, C. A.; and Moore-Ede, M. C.: Environmental Syncronizers of Squirrel Monkey Circadian Rhythms. J. Appl. Physiol. vol. 43, no. 5, 1977b, pp. 795-800.

Sulzman, F. M.; Fuller, C. A.; and Moore-Ede, M. C.: Feeding Time Synchronizes Primate Circadian Rhythms. Physiol. Behav., vol. 18, 1977c, pp. 775-779.

Sulzman, F. M.; Ellman, D.; Fuller, C. A.; Moore-Ede, M. C.; and Wassmer, G.: Neurospora Circadian Rhythms in Space: A Reexamination of the Endogenous-Exogenous Question. Science, vol. 225, no. 4658, 1984, pp. 232-234.

TABLE I.- NUMBER OF DAYS IN EACH DATA SET OF SOVIET COSMOS 1514 RHYTHM EXPERIMENTS

Monkey	Activity	Axillary Temperature	Ankle Temperature	Ambient Temperature
Abrek				
Preflight	4	5	5	5
Flight	5	4+	5	5
Postflight	5	5	5	0
Bion				
Flight	5	5	5	5
Ariel				
Presynch. Control	2+	0	2+	0
Synchronous Control	6	0	6	6
Postsynch. Control	6	0	6	0
Teuton				
Presynch. Control	3	1	3	0
Synchronous Control	6	0	6	6
Postsynch. Control	6	0	6	0
Anonymous				
Vivarium Control	9+	8	0	9+
MM3				
Vivarium Control	8+	6+	6+	6+
MM4				
Vivarium Control	0	4	4	4
MM5				
Vivarium Control	0	4	4	4
MM6				
Vivarium Control	0	4	4	4

TABLE II.- SUMMARY OF ANKLE SKIN AND AMBIENT TEMPERATURE

	Ankle Skin Temperature		Ambient Temperature	
Experiment	Mean	S E.M.	Mean	S.E.M.
Abrek Flight	25.9	0.1	24.0	0.1
Bion Flight	26.9	0.1	23.5	0.1
Abrek Preflight	32.8	0.2	23.7	0.1
Ariel Synch.	32.8	0.4	24.4	0.1
Teuton Synch.	28.3	0.2	24.6	0.1
MM3 Vivar.	32.6	0.1	23.0	0.1
MM4 Vivar.	26.7	0.1	23.3	0.1
MM5 Vivar.	27.7	0.1	23.3	0.1
MM6 Vivar.	30.9	0.1	23.3	0.1

S.E.M. = standard error of the mean

TABLE III.- CIRCADIAN PERIOD OF ACTIVITY AND AXILLARY TEMPERATURE RHYTHMS

	Circadian Period	
	Activity	Axillary Temperature
Abrek Preflight	NS	24.0
Teuton Synchronous Control	24.0	ND
Vivarium Control	24.0	24.0
MM3 Vivarium	24.0	24.0
MM4 Vivarium	ND	24.0
MM5 Vivarium	ND	24.0
MM6 Vivarium	ND	24.0
Abrek Flight	23.5	23.7
Bion Flight	24.2	24.2

NS = no statistically significant circadian period ($p > 0.05$)
ND = no data available

TABLE IV.- CORE TEMPERATURES

	Day Maximum	Night Minimum	24-hr Mean
Colonic 1 g (U.S.)	38.1	37.0	37.6
Axillary 1 g (U.S.)	37.9	37.0	37.5
Axillary 1 g (U.S.S.R.)	38.1	36.9	37.5
Axillary 0 g (U.S.S.R.)	37.6	36.3	37.1

Day Maximum = 60-min average for highest hour of day
Night Minimum = 60-min average for lowest hour of night
24-hr Mean = Average for all data points in day and night

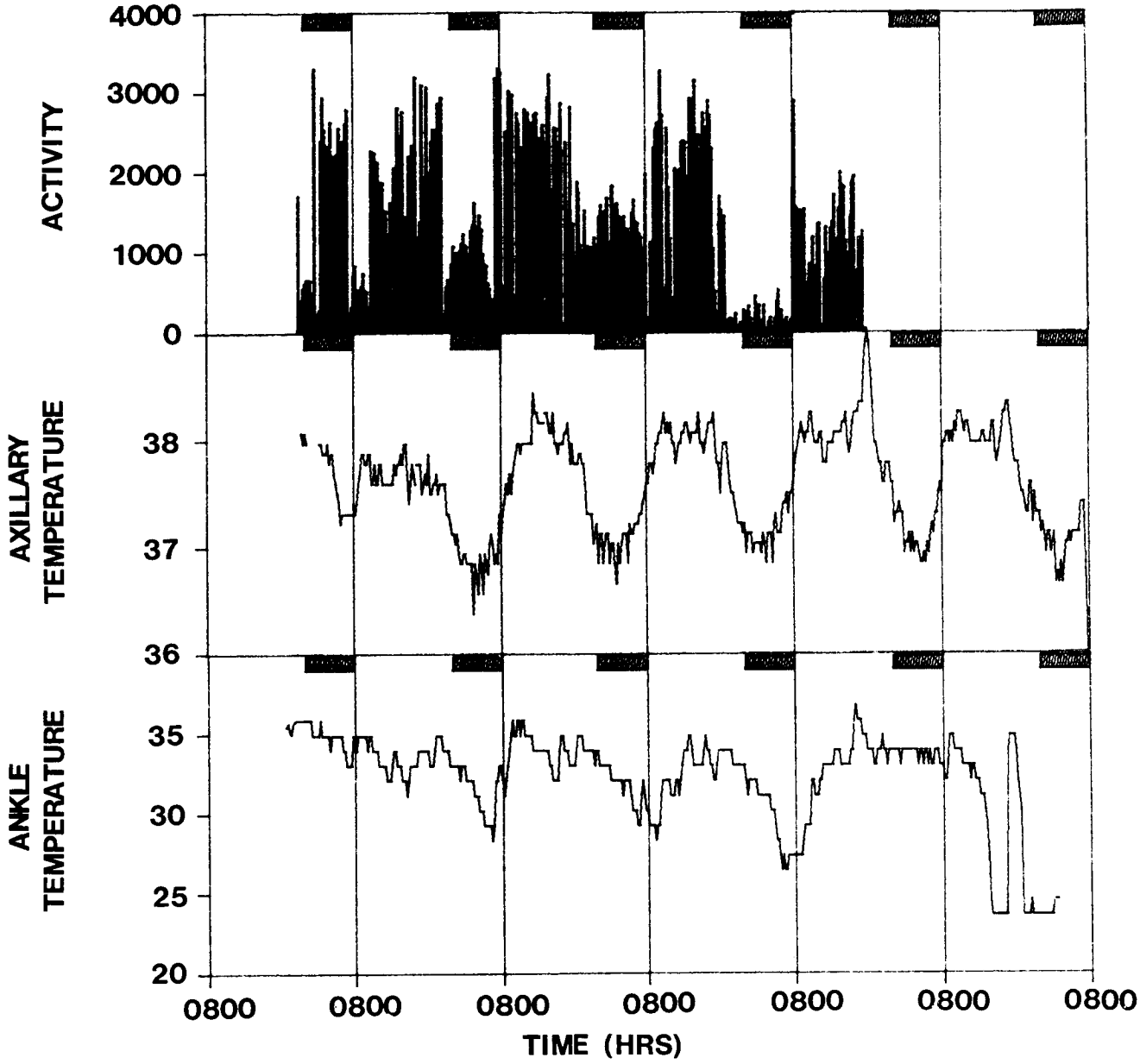

Figure 1.- A plot of activity (top panel), axillary temperature (middle panel) and ankle skin temperature (bottom panel) of the monkey Abrek in a preflight test conducted in November 1983. The activity data are total counts per 16-minute interval. The axillary and ankle skin temperatures are in degrees centigrade. The dark bars in the top of each day represent the eight-hour daily dark period. Time of day (Moscow time) is indicated on the bottom of the figure.

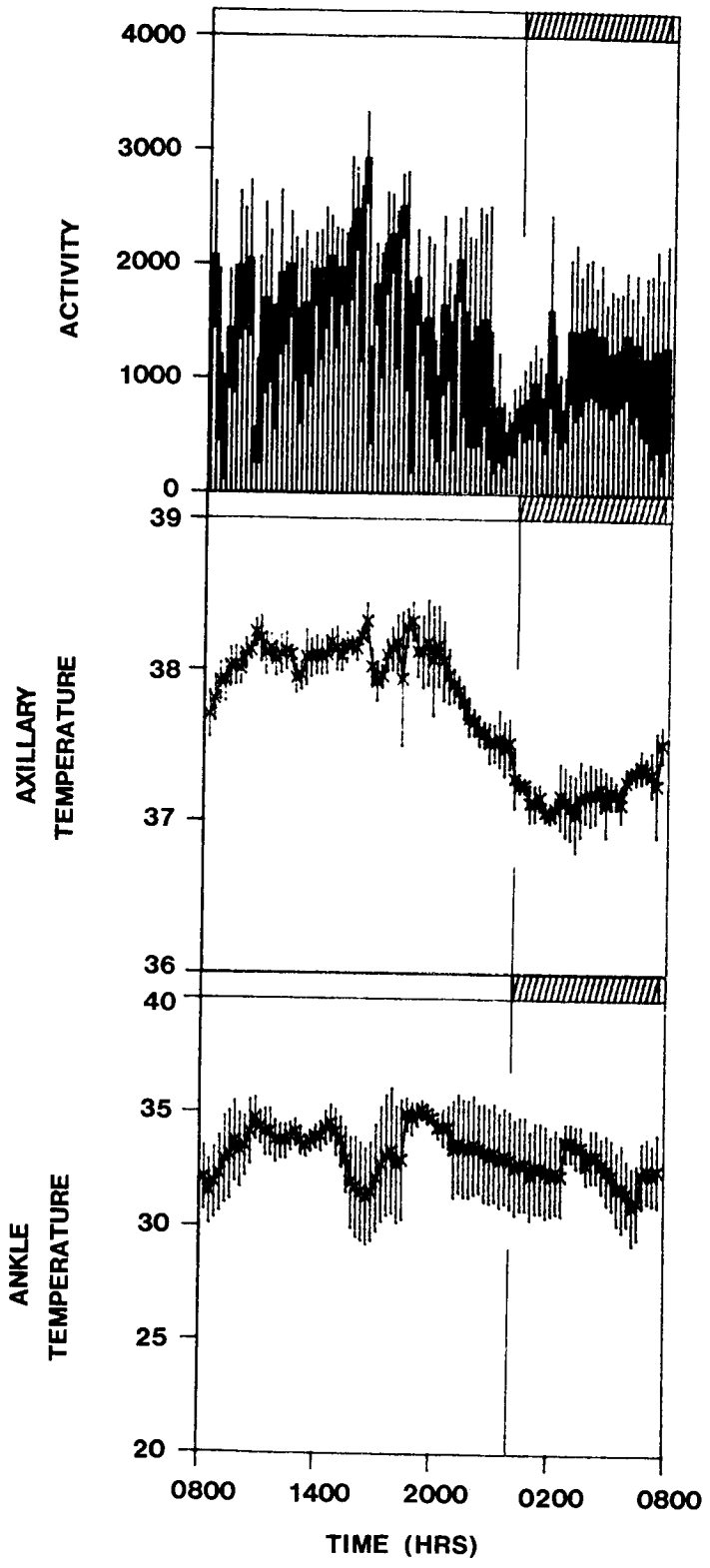

Figure 2.- The educed waveforms of the data from figure 1. The data are presented in the same order and units as figure 1. The mean value (± standard error of the mean) are plotted at 16-minute intervals.

C-2

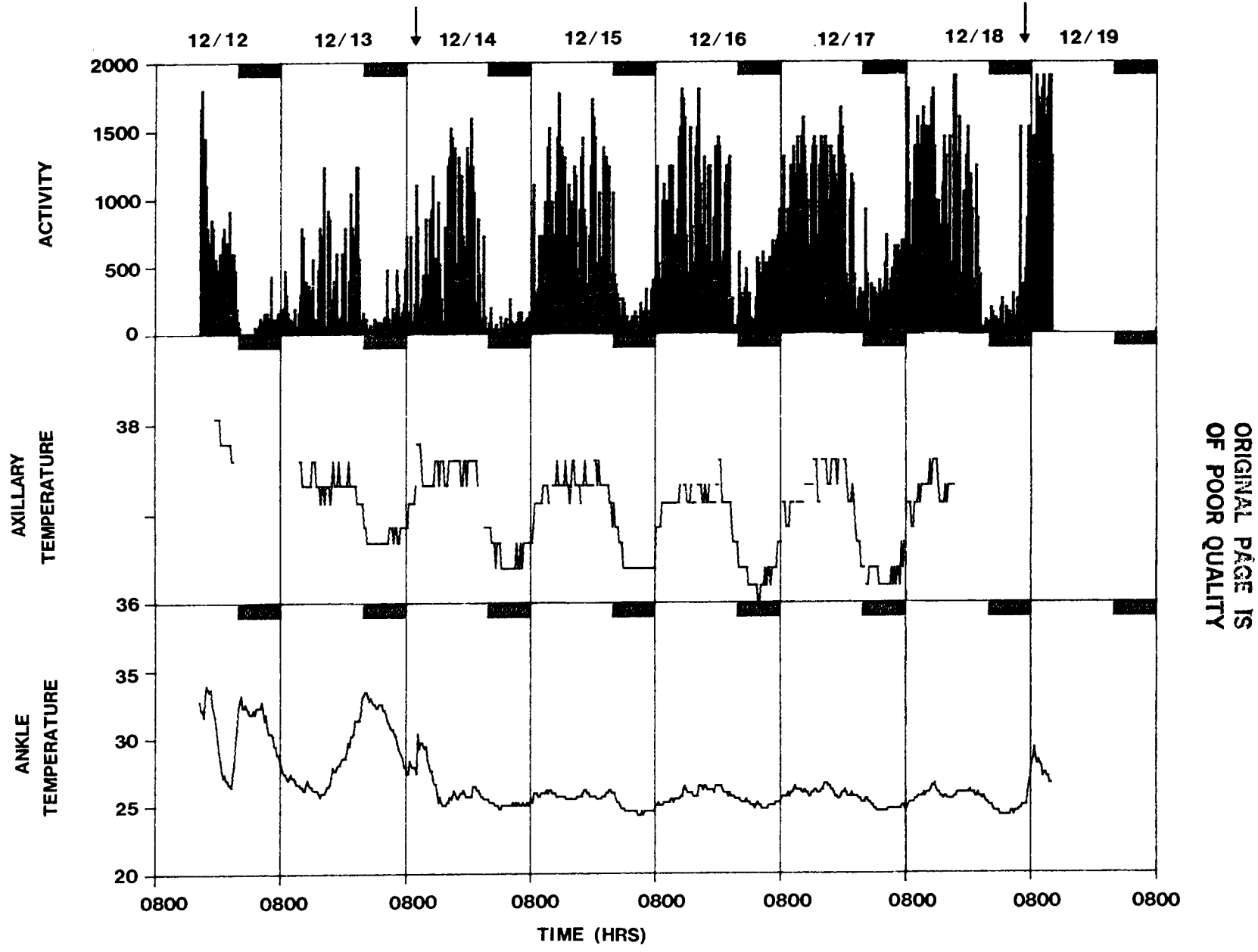

Figure 3.- The data from Abrek before and during COSMOS 1514. The data are presented in the same format as in figure 1. Launch occurred on December 14, 1983, at the time indicated by the arrow at the bottom of the figure. Recovery occurred on December 19, 1983, at the time indicated by the arrow.

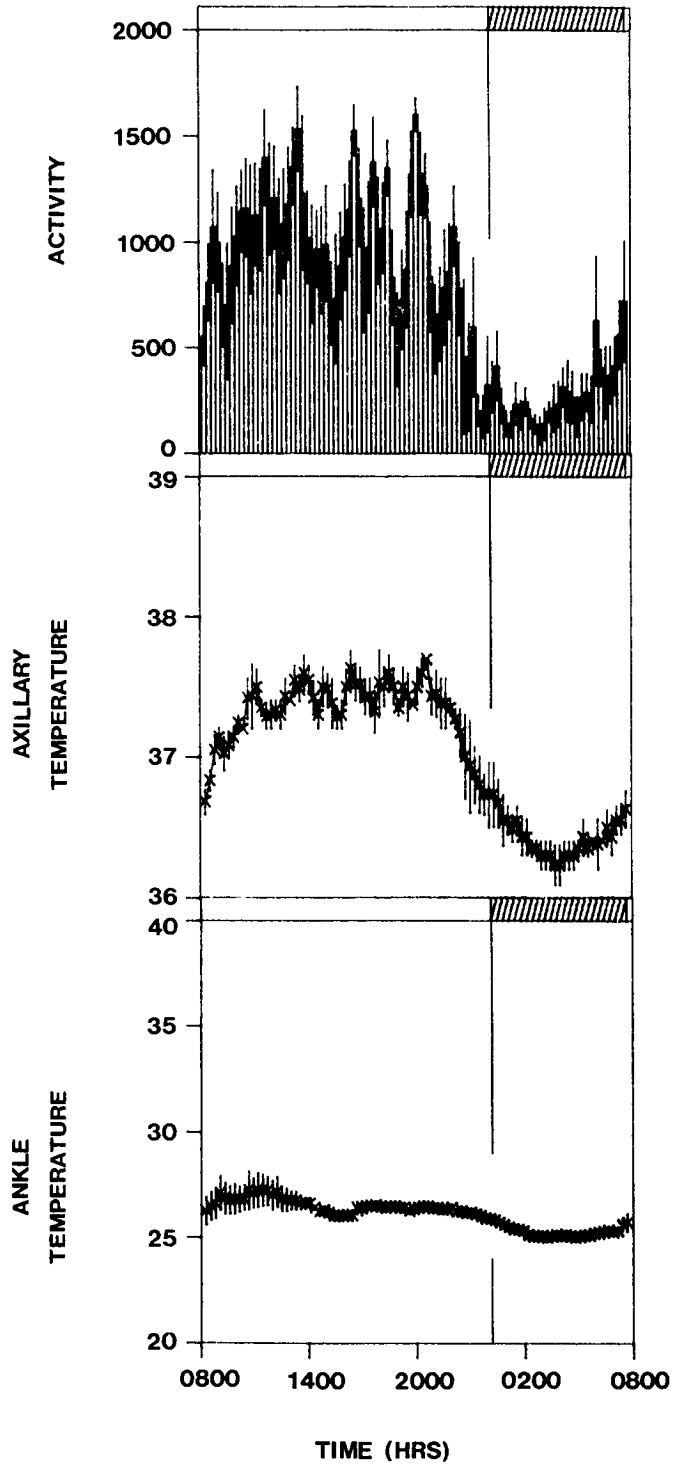

Figure 4.- Educed waveforms of the data from figure 3. Only the data collected while in space were used in the eductions. The data are presented in the same way as figure 2.

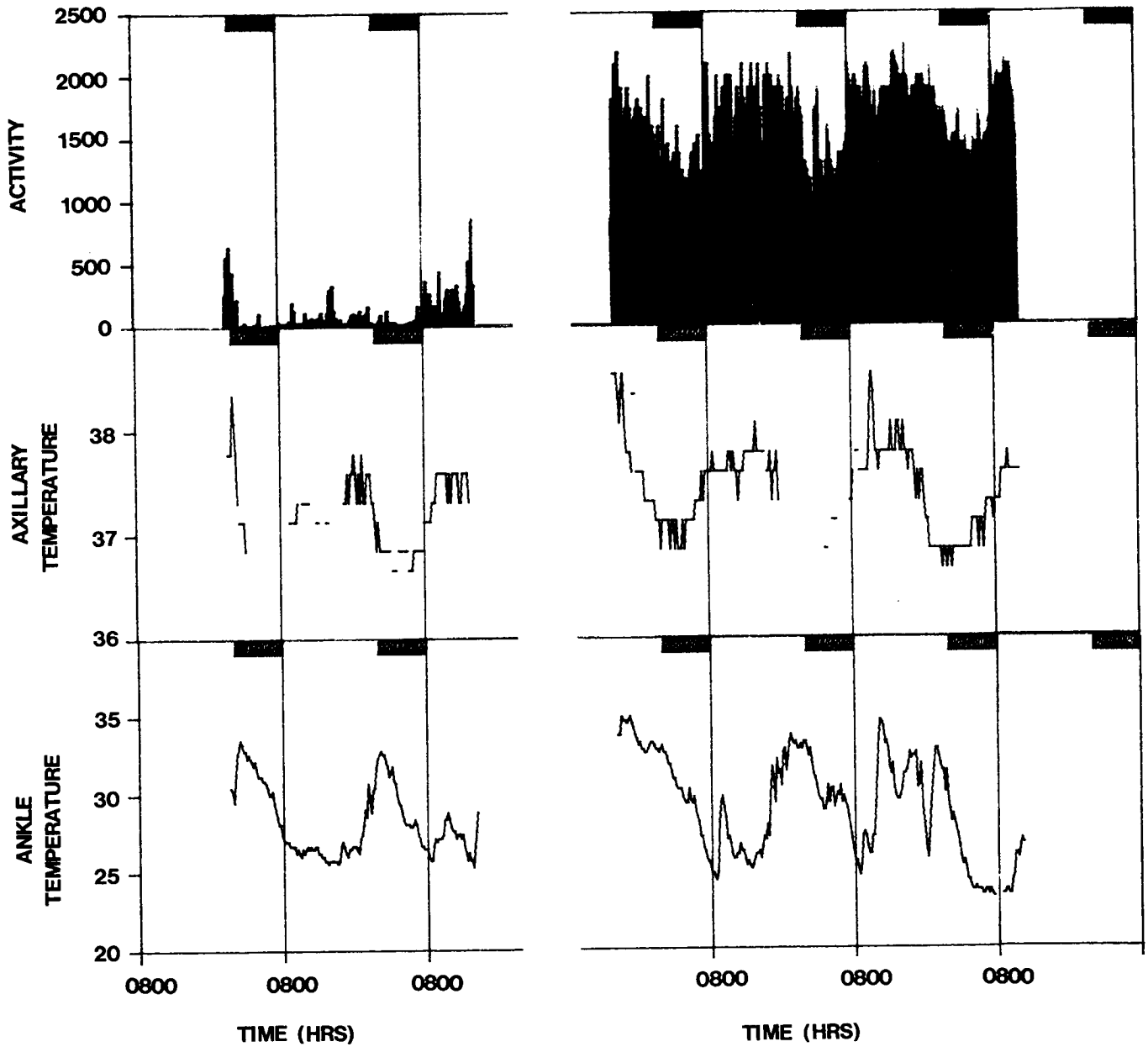

Figure 5.- Postflight data from Abrek. Two monitoring sessions were conducted and both are plotted in this figure. Otherwise, the data are presented in the same format as figure 1.

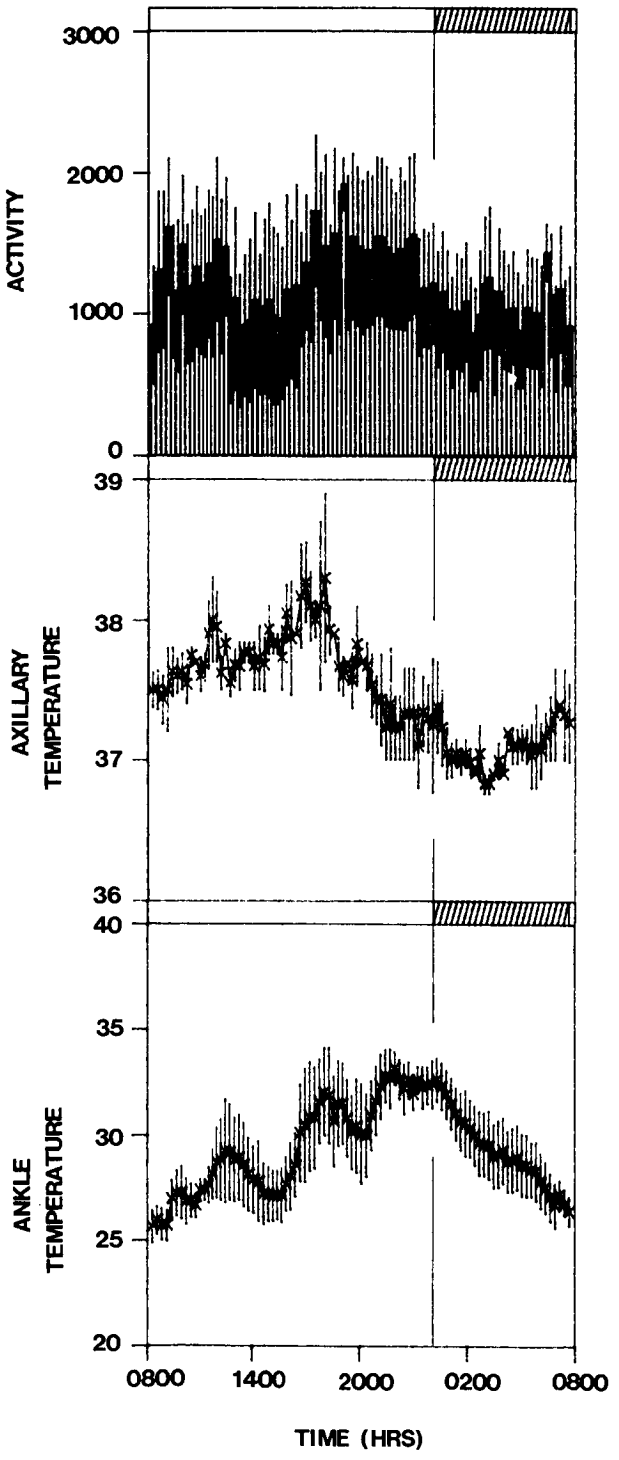

Figure 6.- Educed waveforms of the data from figure 5. The data are presented in the same format as figure 2.

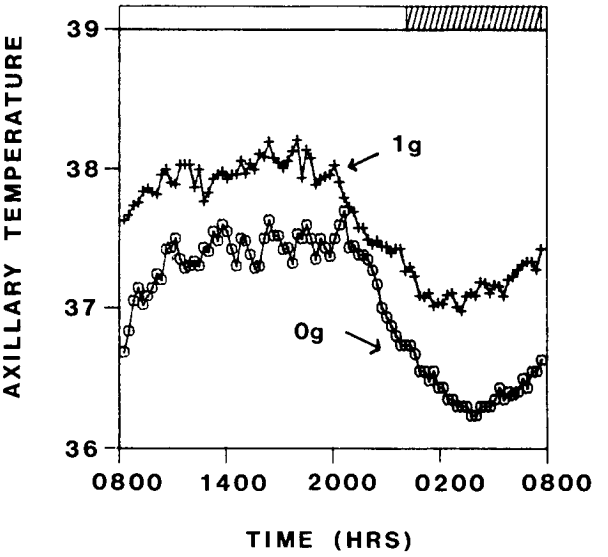

Figure 7.- A comparison of the average daily waveform of axillary temperature of Abrek monitored on Earth (upper curve) and in space (lower curve).

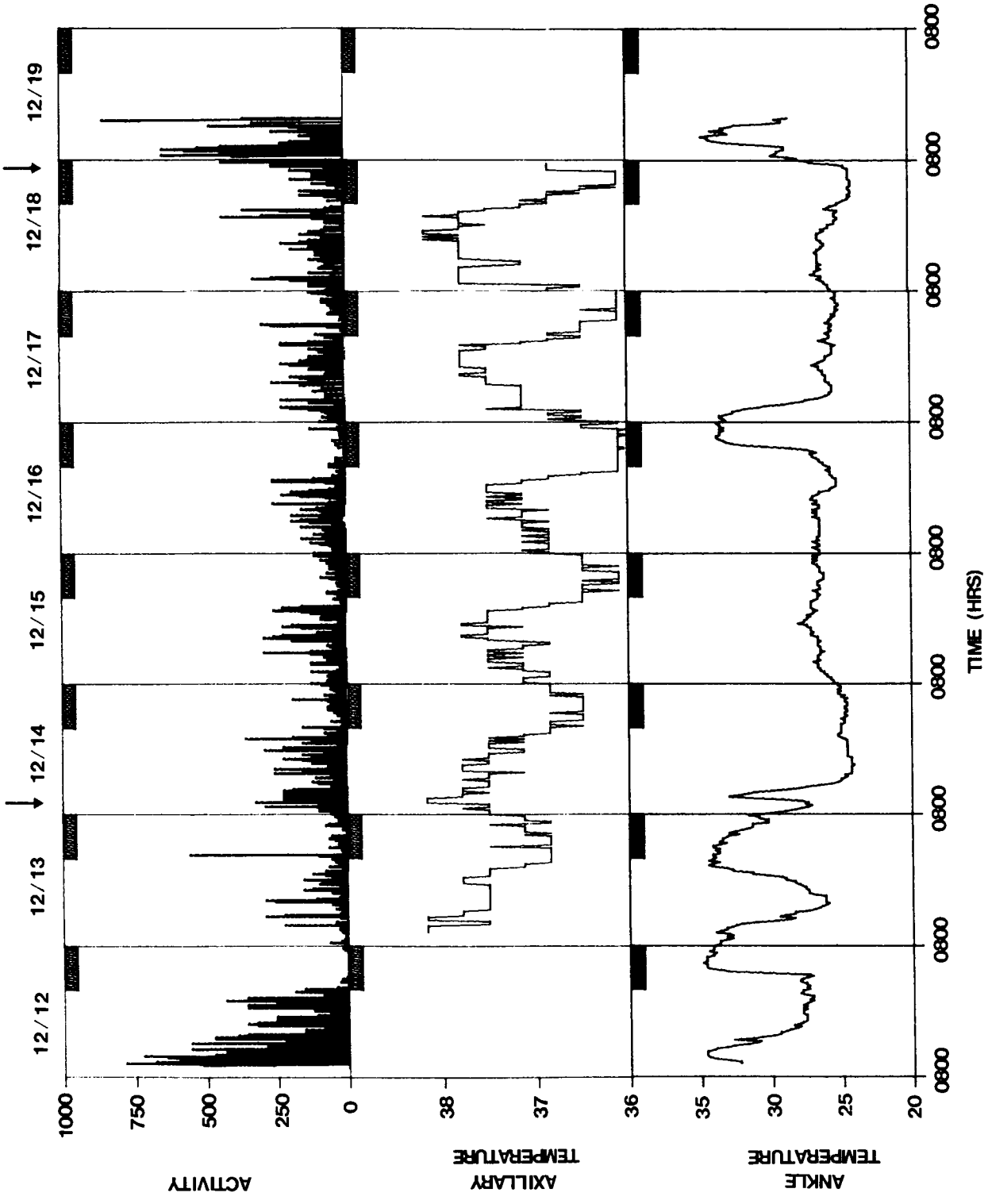

Figure 8.- The data from Bion before and during COSMOS 1514. The data are presented in the same format at figure 3.

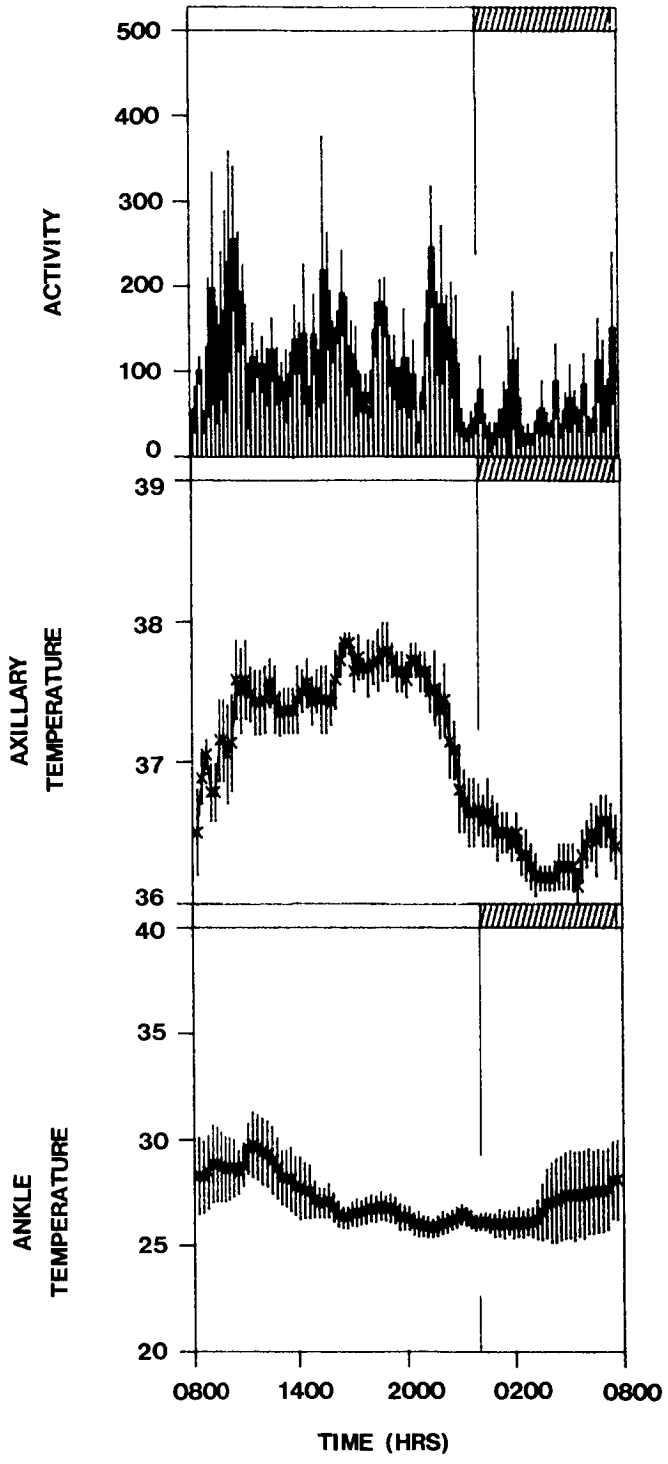

Figure 9.- Educed waveforms of the data from figure 8. Only the data collected while in space were used in the eductions. The data are presented in the same way as figure 2.

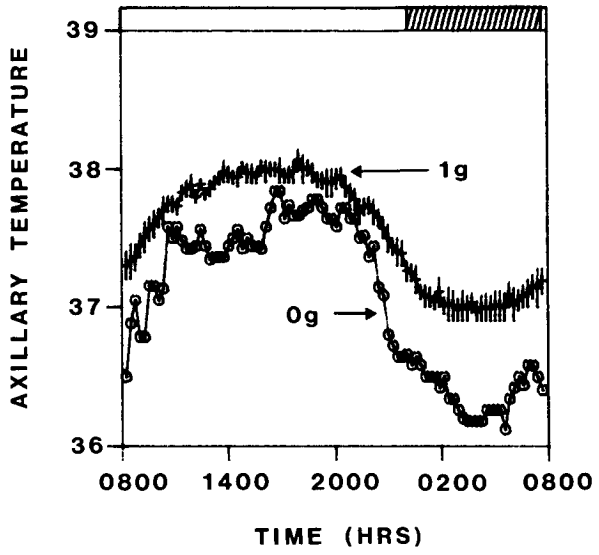

Figure 10.- A comparison of the average daily waveform of axillary temperature (mean ± S.E.M. of Bion in space (lower curve) and the average daily pattern (mean ± S.E.M.) of 6 other rhesus monkeys monitored for a total of 30 days on Earth (upper curve).

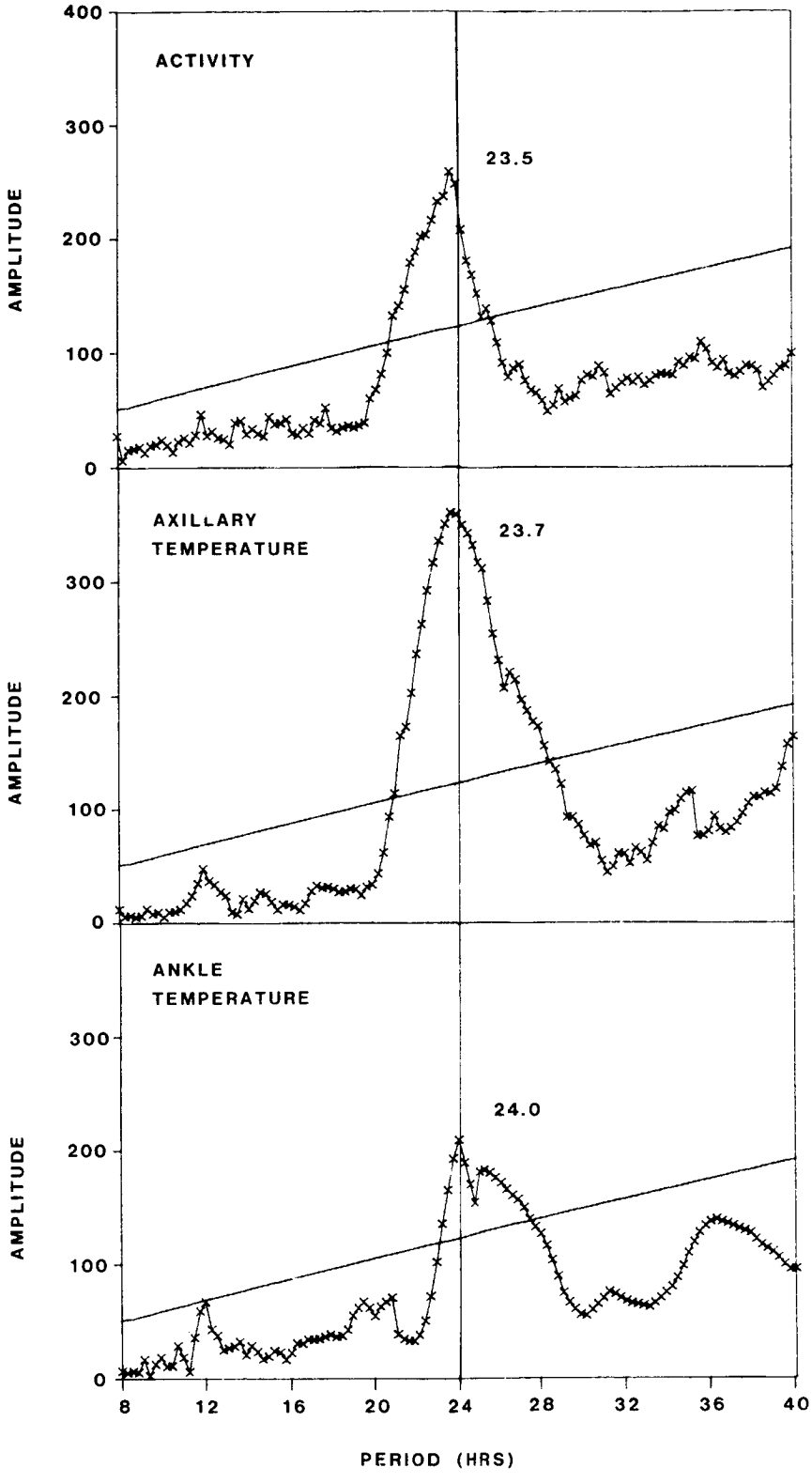

Figure 11.- Period spectra of the spaceflight data from Abrek. The three panels show the spectra for activity (top), axillary temperature (middle) and ankle skin temperature (bottom). The solid diagonal line in each panel shows the significance line at p = 0.01.

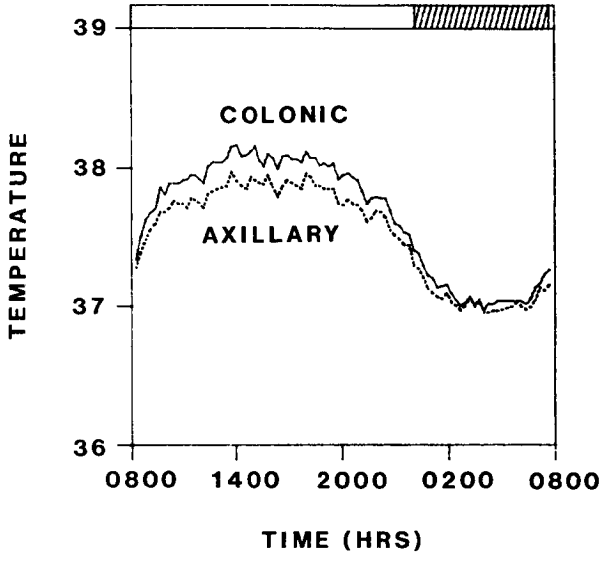

Figure 12.- A comparison of the average waveform of rhesus colonic temperature and axillary temperature measured simultaneously in 4 monkeys.

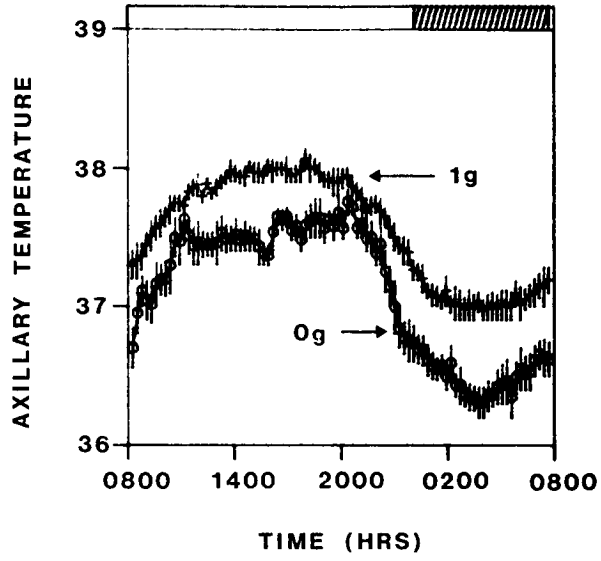

Figure 13.- A comparison of the average waveform of rhesus axillary temperature (mean ± S.E.M.) on Earth (upper curve) and in space (lower curve).

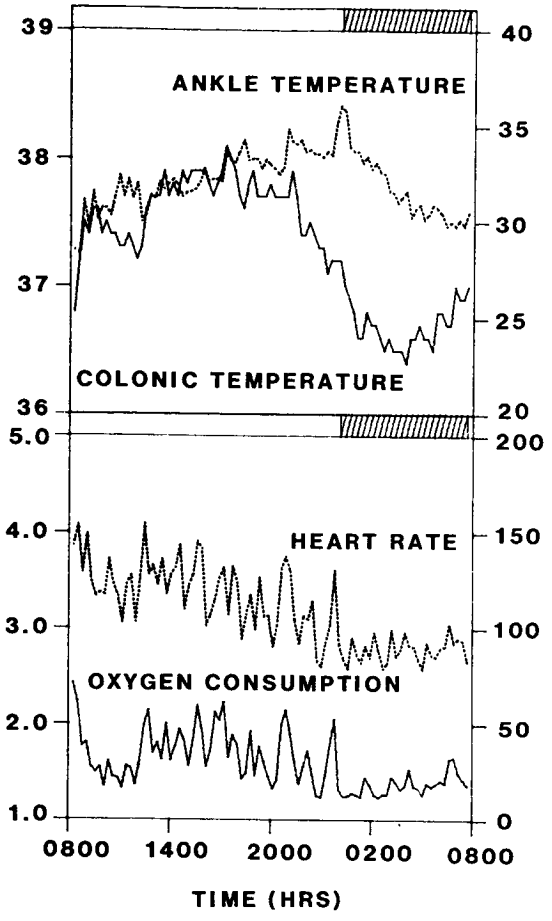

Figure 14.- A plot of the colonic temperature (°C), ankle skin temperature (°C), heart rate (beats per min), and metabolism (liters of oxygen consumed per hour) of a rhesus monkey (MM5) maintained at 25°C on an LD 16:8 cycle.

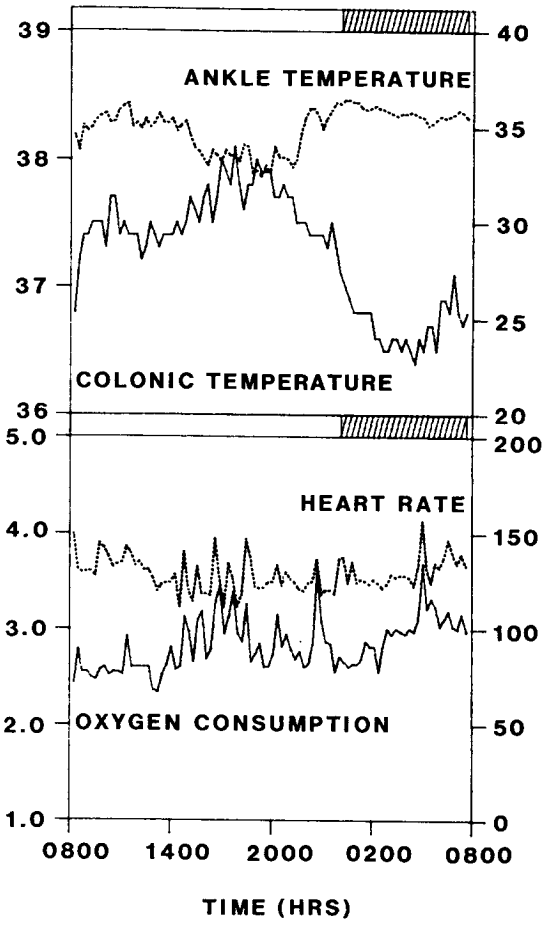

Figure 15.- A plot of the colonic temperature (°C), ankle temperature (°C), heart rate (beats per min), and metabolism (liters of oxygen consumed per hour) of a rhesus monkey (MM3) maintained at 25°C on an LD 16:8 cycle.

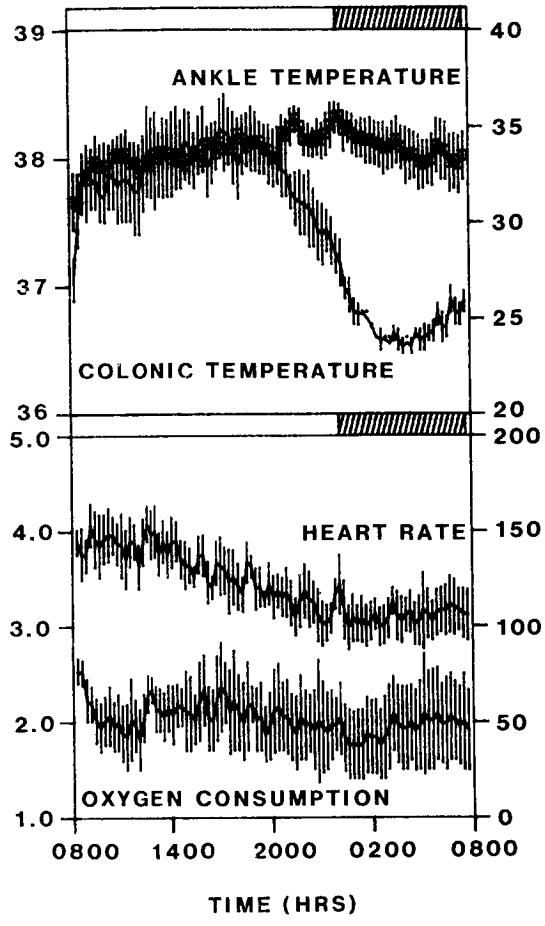

Figure 16.- A plot of the average (mean ± S.E.M) colonic temperature (°C), ankle temperature (°C), heart rate (beats per min) and oxygen consumption (liters of oxygen consumed per hour) of 4 rhesus monkeys.

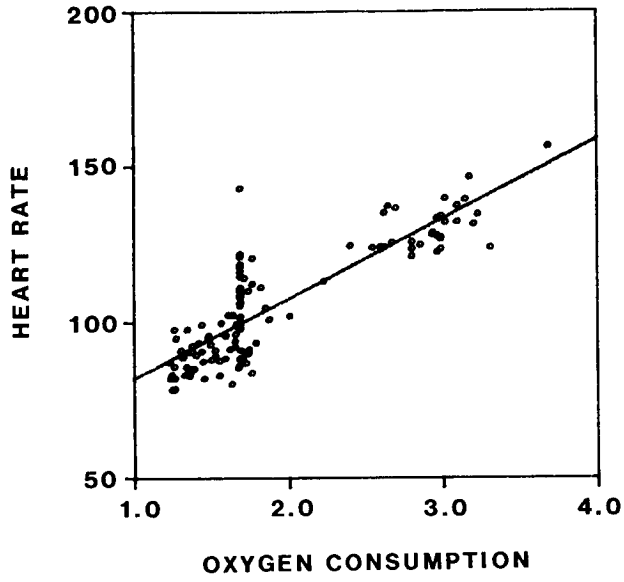

Figure 17.- A regression plot of nighttime oxygen consumption (liters of oxygen consumed per hour) against nighttime heart rate (beats per min). The correlation coefficient for the regression line is 0.86.

CARDIOVASCULAR RESULTS FROM A RHESUS MONKEY FLOWN ABOARD THE COSMOS 1514 SPACEFLIGHT, AND GROUND-BASED CONTROLS

Prepared by

Cardiovascular Research Laboratory
National Aeronautics and Space Administration
Ames Research Center
Moffett Field, California 94035 (USA)

U.S. Investigators:

Harold Sandler
Biomedical Research Division
NASA/Ames Research Center

H. Lowell Stone*
Department of Physiology and Biophyics
University of Oklahoma

John W. Hines
Cardiovascular Research Laboratory
NASA/Ames Research Center

Bruce Benjamin
Cardiovascular Research Laboratory
NASA/Ames Research Center

Bruce M. Halpryn
Cardiovascular Research Laboratory
NASA/Ames Research Center

U.S.S.R. Investigators:

V. Krotov
Institute of Biomedical Problems

B. Kulaev
Institute of Biomedical Problems

V. Krilov
Institute of Surgery
Academy of Sciences

V. Magedov
Institute of Biomedical Problems

A.N. Nazin
Institute of Biomedical Problems

*Deceased

INTRODUCTION

The successful completion of the Cosmos 1514 spaceflight clearly demonstrated the feasibility and scientific merit of studying the effects of spaceflight on the cardiovascular system of a chronically instrumented rhesus monkey. The Cosmos cardiovascular flight experiment was designed to determine whether blood pressure and flow relationships to the head change with weightlessness. This decision was based on the previous observations in man, that zero gravity causes a headward shift of body fluid which persists regardless of flight duration. Transcutaneous flowmeter measurements of left carotid arterial flow in French cosmonaut J.P. Chretien, taken aboard Salyut 7 (Pourcelot et al., 1982), demonstrated 1% to 6% increases in flow over the duration of the 7-day flight. The present experiment represents the first attempt to directly measure similar data in an animal model during weightlessness. The objectives of the cardiovascular portion of the Cosmos experiment were: (1) to develop a conscious rhesus monkey model to record carotid pressure and flow in a nonstressed animal: (2) to determine the effects of weightlessness on pressure-flow relationships to the head; and (3) to correlate cardiovascular findings with other simultaneously recorded physiologic information before, during, and after flight.

MATERIALS METHODS

A single cylindrical probe containing both flow and pressure transducers, shown in figure 1, was chronically implanted as a cuff around the left common carotid artery (CPF cuff) of five rhesus monkeys (M. mulatta) approximately 55 days before flight. One animal was subsequently chosen as the prime flight candidate (Bion) and another (Ariel) as backup. Both animals were treated and tested similarly except for exposure to weightlessness. Two monkeys flew aboard Cosmos 1514. Bion was used to measure pressure and flow changes in the left common carotid artery. The second animal (Abrek) was used for neurovestibular studies. Ariel was used to record cardiovascular parameters in an identical fashion to the flight animal during ground-based, synchronous control experiments. EKG recordings were obtained before, during, and after flight or simulation in all three animals.

The Pressure and Flow Cuff

A cross-sectional drawing of the cuff is shown in figure 2. The cuff consisted of two parts: the upper (top) portion of the assembly which contained both pressure and flow transducers, and the lower portion of the assembly consisting of several interchangeable shells capable of fitting about vessels ranging from 2.5 mm to 5.0 mm in diameter. The cuffs were constructed of injection-molded plastic to ensure that cuff surfaces were smooth and that upper and lower sections mated closely.

Pressure was measured using a 4.5-mm diameter and 1.2-mm thick titanium disk transducer (manufactured by Konigsberg Instruments, model P4.5) capable of chronic

implantation within the body. Pressure was sensed by imbalance of solid state strain gauge elements cemented to the inner (nonexposed) surface of the transducer diaphragm in a wheatstone bridge configuration. To improve longevity of the preparation and minimize damage to the transduced vessel, the pressure cell was placed on the vessel's external surface rather than intravascularly. This approach required at least 20% compression of the vessel wall (aplanation) to obtain optimal surface area contact between the transducer and the vessel wall. In figure 3, mean blood pressure as measured by the CPF cuff is compared with mean blood pressure measured in the descending thoracic aorta, using an identical pressure transducer implanted intravascularly. Three separate measurement comparisons are plotted and a near-linear relationship can be seen (slope 1.005). Such tests were conducted in six animals, with findings similar to those indicated in figure 3. Tests were also done in four animals using a manometer-tipped catheter to directly measure blood pressure at the same site (just proximal to the CPF cuff) in the carotid artery. There was very close correlation between the waveforms measured by the two pressure measurement systems, as shown in figure 4.

Flow was measured using Doppler ultrasonic crystals and the continuous wave technique (fig. 2). Crystals were placed in the cuff so as to lie on the leading edge of the cuff, proximal to the pressure transducer. The crystals were inserted at a compound angle, 45 degrees to the long axis of the vessel and 45 degrees towards its center. The placement of the crystals, so as to isonify the blood before it entered the cuff, minimized any turbulance effects from the decreased vessel cross section caused by the distally located pressure transducer. Extensive in vitro testing was done to ensure the accuracy of the flow measurement system. The apparatus and system used are shown in figure 5.

A great majority of cuffs used for ground-based studies functioned well after implantation and provided useful physiologic information. Of 31 monkeys implanted in the U.S., there were no cuff-related deaths. Four of the 31 cuffs were not functional 30 days after surgery due to lead damage by the monkey, infection, or because of inadequate alignment of the cuff in relation to the artery. Five of the 31 monkeys provided useful physiologic information for 30 to 60 days. Twenty-two of the 31 monkeys (71%) had cuffs that were functional between 60 and 365 days. A detailed breakdown of cuff history (U.S. and U.S.S.R.) is given in table 1.

Surgery

Cuffs were implanted under sterile conditions using Halothane-O_2 anesthesia (U.S. investigators) or pentobarbitol (U.S.S.R. investigators). Skin was incised from the angle of the left mandible to the left claviculo-sternal border. The sternohyoid and sternothyroid muscles were separated from the peritrachial fascia, revealing the carotid sheath. The vagosympathetic trunk and surrounding tissues were dissected away from the common carotid artery, proximal to its bifurcation into the internal and external branches, to the level of the clavicle. The cuff was placed around the common carotid artery proximal to the carotid sinus. The flow crystals were positioned proximal to the aorta. The cuff leads were passed under the sternothyroid and sternohyoid muscles before tunneling up to the subcutaneous

tissues in the intrascapular region. Enough slack was allowed so that the transducer did not distort the vessel. All incision sites were sutured closed. Routine postsurgical care was given to the animal, including 10 days of antibiotics. The transducer leads were exteriorized on the back in the low midscapular region 2 to 3 weeks following surgery. Characteristic pressure and flow waveforms four months after lead exteriorization from the back are shown in figure 6.

In Vivo Pressure Calibration

Changes in zero offset and gain over time are intrinsic characteristics of the strain gauge pressure transducer used for this experiment. The gradual growth of fibrous tissue over the pressure cell diaphragm also affects the transducer. For these reasons, a quantitative measurement of intravascular pressure could only be assured by periodic in vivo calibration of the implanted cuff. A cross-calibration technique was developed using direct measurement of pressure. Voltage output from the CPF cuff was compared with mean arterial blood pressure as measured from a precisely calibrated reference pressure transducer (Ailtech transducer connected to a 25-gauge needle). The needle was inserted transcutaneously into the left femoral artery just below the inguinal ligament. Mean blood pressure was measured at rest and after a bolus of phenylephrine (100 μg to 200 μg) was injected, which increased mean blood pressure by 30 mm Hg to 40 mm Hg. This procedure allowed detection of zero pressure level and determination of a calibration coefficient to convert voltage output of the CPF cuff into mm Hg. This latter value was calculated by comparing the voltage output at rest and peak pressure (Points A and C, fig. 7) from the implanted transducer with the direct pressure measured by the Ailtech at the same two points (Points B and D, fig. 7). This approach provided accurate, comparable physiologic data over the 60-day periods required by the present protocols.

Experimental Protocol

Five animals were instrumented with a CPF cuff over a 10-day period two months prior to flight, with one chosen as the flight candidate and the others used during ground-based test procedures. The flight animal, Bion, was instrumented 53 days before flight (F-53), and the leads were exteriorized from the back 20 days later at F-33. The cross-calibration procedure for the pressure transducer was performed on F-15. A cardiovascular stress test consisting of tilts (+70°, 0°, -70°) was performed immediately after the cross-calibration procedure. A 36-hour ground-based control study associated with the biorhythm experiment was performed on F-13 and F-12. The second flight animal, Abrek, was not instrumented with the CPF cuff, but EKG was monitored during the spaceflight. One of the animals instrumented with the CPF cuff (Ariel) served as subject for ground-based, synchronous control studies conducted three weeks postflight. These studies followed, as closely as possible, everything that occurred to the flight animals, except exposure to weightlessness.

Instrumentation Configuration

Although only one animal (Bion) was instrumented with the CPF cuff, two cardiovascular signal conditioners were flown, with one dedicated to each animal

capsule. One unit was used to measure pressure and flow from the CPF cuff implanted in Bion. The other unit (along with a separate CPF cuff) measured capsule ambient pressure required for correction and normalization of the implanted pressure sensor to 760 mm Hg. The outputs of each signal conditioner were recorded on separate, dedicated, on-board analog tape recorders.

Each cardiovascular physiologic monitoring system consisted of a blood flow measurement subsystem, a pressure measurement subsystem, and a timer/controller subsystem. Each data collection event was initiated by a ground-based start pulse. Upon receipt of this start pulse, the internal timer provided approximately 20 seconds each of high- and low-calibration signals followed by about 4.5 minutes of continuous, pulsatile data. At the end of the data collection period, the controller disabled power to the timer until receipt of the next start pulse.

All reference and measured signals were conditioned for the 0- to 5-volt input range of the on-board tape recorder. Electrical calibration values were 2 volts for the high level and 0 volts for the low level. These corresponded to ideal physiological ranges of 0 mm Hg to 200 mm Hg for pressure and a +/- 1 kHz frequency shift for Doppler flow. Actual calibration values were transducer-dependent, requiring precise in vitro calibration of each sensor to ascertain correct physiological levels prior to implantation.

Flow was measured using continuous wave (CW) Doppler measurement techniques. The output signal was conditioned for an idealized physiological range of -1 kHz to +4 kHz frequency shift over the 0- to 5-volt allowable range. For transducer Number 268, implanted in Bion, the calibration values corresponded to 26.5 cm/sec for the high level and 27.17 cm/sec for the low level, when converted from frequency to velocity.

The semiconductor strain gauge pressure cells were excited by a 5-mA constant-current source. The output was conditioned for an idealized -200 mm Hg to +300 mm Hg physiological pressure range over the 0- to 5-volt span provided by the tape recorder. The negative range was selected to allow for interchangeability of pressure cells and to accommodate the maximum drift expected from the sensor. Actual calibration values for transducer Number 268 were -41.5 mm Hg (High) and -457.6 mm Hg (Low).

The cardiovascular flight signal conditioners were designed and constructed by L & M Electronics, Inc. (Daly City, California), to specifications provided by Soviet coinvestigators. These units were based on previously used laboratory grade models developed for NASA-Ames Research Center's Cardiovascular Research Laboratory (L & M Model 1012 for flow, L & M Model 2007 for pressure). In vivo pressure cross-calibration was performed using an Ailtech (Electromedics) sensor with an interface to the Model 2007 pressure signal conditioner. The laboratory instruments were used in both U.S. and U.S.S.R. ground-based studies.

Data Analysis

Data collection before, during, and after flight consisted of five minutes of continuous recording every two hours. All data were recorded on analog tape and subsequently transferred to an American tape recorder (Honeywell 101), including reference data on timer synchronization (start and stop pulses for the tape recorder). Received data were digitized, stored, and processed using a Digital Equipment Corporation (DEC) PDP-11/34 computer (with an AR-11 analog-to-digital converter) and programs and additional procedures developed at the Automatic and Electronic Processing Institute of the Academy of Sciences, U.S.S.R. The data sampling rate was 200 Hz with 10-bit resolution. The primary purpose of the experiment was to acquire useful recorded information over a period of 20 cardiac cycles. Analysis of the recorded data revealed, in general, that portions of each 5-minute data section contained signals distorted by motion-related noise (animal head movements, eating artifacts, or general body movements); therefore, a method was developed for data reduction using waveform analysis of rheoplethysmographic signals and their first derivatives to select portions of the record where the animal was in a quiet state. In cases where there were more than three such intervals available in a 5-minute period, data were averaged to calculate mean, standard deviation and standard error. Additionally, to facilitate automatic processing of data by the computer, each 5-minute period was divided into fifteen 20-second intervals. Due to uncertainties related to start and stop pulses and calibration signals on the tapes, at least three 20-second intervals were discarded (the first two and the last) to avoid detection problems. This potentially allowed sampling and derivation of average data for the entire 4- to 5-minute period (maximum of eleven to thirteen 20-second intervals). The ability to analyze all intervals in a given 5-minute segment was dependent on the nature and the quality of the rheoplethysmographic signals and was rarely realized. Data could only be sampled for a 1-minute period during the 0800 hours interval each day, due to the performance of the vestibular experiment. A majority of intervals (6 to 10) were analyzable from the other eleven daily-occurring 5-minute periods only on the fourth day of spaceflight. Data derived from 20-second interval analysis were used to derive information on the 24-hour variations of parameters as shown in figures 8, 9, 10, 11.

For pressure, each beat was analyzed with respect to value at peak systolic (maximum) and diastolic (minimum) levels. Systolic and diastolic pressures were determined by averaging all values detected in respective intervals. Mean blood pressure was derived as the average (integrated area under the curve) for the entire 20-beat or 20-second interval. Carotid blood velocity was calculated as the mean, integrated area under the curve, for each beat, representing the sum of systolic and diastolic flow periods.

The implanted pressure transducers measure absolute pressure and must be corrected for barometric pressure changes. All of the blood pressures measured were corrected to an ambient pressure of 760 mm Hg using data from pressure transducers contained aboard the capsule. Barometric pressure varied by 52 mm Hg over the course of the flight.

Detected blood velocity (cm/sec) was multiplied by the cross-sectional area of the vessel lumen (cm^2) and 60 sec/min to obtain flow (ml/min). A 3-mm-diameter cuff was used in both Bion and Ariel. The inner diameter of the carotid vessel was assumed to be 2.6 mm (allowing 0.4 mm for vessel wall thickness and fibrous tissue growth). The conversion factor for velocity-to-flow was calculated to be 3.19. Peripheral resistance was calculated by dividing respective mean blood pressure values by mean flow.

Calibration data for the synchronous control animal (Ariel) indicated unphysiologically low levels of blood pressure due to use of the wrong electronic compensation equipment. Data are, therefore, not presented in this animal for comparison.

RESULTS

Information obtained during flight is compared with data obtained prelaunch and from the 1.5-day ground-based control study conducted a week before flight. Figures 12 through 14 show dynamic measurements of carotid blood pressure, flow velocity and common carotid artery peripheral vascular resistance taken from Bion over the course of the study. The X-axis indicated time of study in hours and days. Data were recorded each two hours. To the left are data recorded during the ground-based phase, and to the right are data obtained during flight. The heavy vertical line indicates rocket launch at 10:00 a.m. Each point represents a measured value obtained from originally recorded data. The heavier-lined curve, drawn to represent composite changes, was derived by employing a three-point average between successive points.

Blood pressure and flow values changed over the course of the ground-based observations in comparison to their initial levels. These changes are consistent with an adaptation in physiological state due to psychoemotional arousal from chairing and placement in the "Bio-primate" capsule. During the prelaunch period, there was a gradual decrease in blood pressure and slight increase in blood flow velocity compared to the previous ground-based control period. Of note is the fact that blood flow velocity fell initially from a much higher starting level and gradually returned to higher and more stable baseline levels. Blood pressure levels were much lower than expected since elevated parameter levels were anticipated during the prelaunch period. Higher pressure levels are consistent with an expected state of stress for the animals due to lack of sleep during the two-day period inside the launch capsule. During this interval, the capsule was transported to the launch site and raised atop the launch rocket. The animals were totally unaccustomed to these procedures, since they had not received prior exposure or training to these events.

Upon launch, the animals were exposed to two conditions: first, launch accelerations, and second, the loss of gravity. As noted in figures 12 and 13, blood pressure increased initially about 10% and blood flow velocity fell slightly by almost 4%. It is not possible to gauge exactly the physiological importance of these changes, since data were not sampled continuously during launch and insertion into orbit. Based on previous ground-based experiments, it would be expected that

slight increases in blood pressure and decreases in flow would occur during the period of acceleration (Stone and Sandler, 1977). Under ground-based conditions, such changes return to baseline level rapidly--in all cases within 1 to 2 minutes after cessation of acceleration stress. This is further supported by data obtained during synchronous control experiments using Ariel, where blood pressure did not increase during the first hour after inserting the animal into the capsule. A hemodynamic reaction was observed in Bion during the first few hours of flight, resulting undoubtedly from the headward redistribution of blood. In addition, all parameters showed persistence of change from prelaunch levels during the first few measurements (4 to 6 hours) of flight--blood pressure increasing 16% to 27%, blood flow velocity decreasing 47%--and were interpreted to indicate adaptation to the weightless state. There was a tendency for all values to return towards preflight levels by the end of the first day of flight.

During ground-based experiments performed on Bion two weeks prior to flight, the effects of postural change were determined under the influence of ketamine anesthesia (see fig. 15). During 70° head-down tilt (used to simulate flight conditions), blood flow velocity exceeds baseline levels by 10% to 20% during the first 5 to 10 seconds of tilt, falling towards baseline after 30 seconds. Blood flow velocity was within 90% to 95% of baseline after one minute and remained at that level to the end of the 3-minute test period. In Bion one can assume that, immediately after insertion into orbit, blood flow velocity in the common carotid artery increased for a short period of time. If changes during spaceflight followed a similar course to the ground-based studies, values decreased rapidly after insertion into orbit and fell to values lower than when on the launch pad. During the first hours of spaceflight there was a considerable increase in common carotid artery peripheral vascular resistance. The increase probably represented a reaction to the headward fluid shift by secondary resistance vessels of the brain, as well as by soft tissues of the head.

Figures 8 to 11 illustrate the average daily variance of hemodynamic parameters over the course of the entire flight and compare changes with launch pad and preflight levels. Each point represents the average of measureable data (no motion or noise artifacts) from each 5-minute record interval at the same hour each day of flight. The standard error bars in these graphs represent variations in the mean of each parameter from the second to the fifth day of flight, at a given time of day. Since the control and launch pad data represent only single points (the last 24 hours of the control study were used and only 18 hours of launch pad data were available), error bars are not given. Heart rates during flight were lower late in the day and at night (2200 to 0800 hours) than during the control or launch pad periods. Blood flow velocity was lower during flight from 1000 to 2400 hours, but otherwise it was similar to launch pad and preflight values. Control mean blood pressure was higher than blood pressures observed on the launch pad or during flight. Mean carotid peripheral resistance was lower inflight than during control. A 24-hour rhythm was present in all parameters and generally followed patterns seen before flight. Blood pressure showed peak points during periods of activity, which in some instances involved successful performance of tasks; in others, it occurred when the animal could not perform required training procedures

with enough success to receive a quantity of reward (food and juice). In the end, other factors may have had a greater bearing on the increase in blood pressure; one cannot exclude stress effects of flight, isolation and confinement and the effects from viewing a partner in the other biocapsule. To support this, one may note that after the 4th day of flight, Bion, on command from the ground, drank a whole dose of juice (100 ml). On the next day the range of 24-hour blood pressure change decreased, resulting in a much reduced range of blood pressure fluctuation during the period of operational task performance.

At the same time, it is not possible to exclude effects on measured hemodynamic parameters from adaptation of the animal to spaceflight conditions. Bion did not eat until the end of the third day of flight. In the last two days of flight, the amount of food consumed increased several-fold. If one assumes that the animal's anorexia was induced by vestibular effects, then the lessening of effects may also be reflected in an improvement in registered blood pressure curves.

There is, in general, a correlation between overall blood supply to the body and blood flow velocity, blood flow per minute to the brain and to a lesser extent the soft tissues of the head. Taking into account that the magnitude of head blood flow/minute is, in general, determined by the oxygen demand of the brain and upper body tissues, the magnitude of flow fluctuations should be predictable--increasing with periods of increased motor activity and decreasing during periods of inactivity, particularly when lights are off. This occurred during flight (see fig. 13).

An analysis of Abrek's heart rate immediately before and during spaceflight is shown in figure 16. A comparison with Bion's flight values is give in figure 17. Abrek's heart rate varied over the course of the flight from a low of 80 bpm to a maximum of 187 bpm. Abrek's heart rate was very close to Bion's at night during the flight, but it was higher during the day.

Figures 18 and 19 represent data obtained during Ariel's synchronous control study. Data were analyzed in an identical manner to the flight animal. Ariel's heart rate ranged from a minimum of 81 bpm to a maximum of 145 bpm. Ariel's carotid blood velocity varied from 24 cm/sec to 38 cm/sec. Blood flow in ml/min can be derived by multiplying blood velocity by 3.19.

DISCUSSION

The cardiovascular experiment on Cosmos 1514 evaluated heart rate and carotid pressure and flow relationships to the head in a rhesus monkey during spaceflight. Results from the flight clearly demonstrate the feasibility and scientific merit of studying the effect of spaceflight on the cardiovascular system in a chronically instrumented rhesus monkey. However, the data presented in this report were obtained from a single animal and, therefore, no statistically significant conclusions can be drawn. In examining the results, trends in data were observed indicating that blood pressure and blood flow relationships to the head are altered in weightlessness.

Data must be interpreted cautiously since the animal may require several days to adapt to a new environment (chair restraint, biocapsule, weightlessness). During this initial period of stress, measured variables may change erratically. Also, the transducer was placed around the common carotid artery in this experiment without ligation of the external carotid artery branch. Under these conditions, measured flow represents the sum of flow to the brain (internal carotid) and flow to the muscles and skin of the head and face (external carotid). Changes in flow must be interpreted with caution, since it is impossible to determine which vascular bed is influencing changes under these circumstances.

In general, heart rate was lower at night and higher during the day inflight. The heart rate variability observed at 0800 hours and 1600 hours may be due to feeding and test procedures carried out at these times. When compared to launch-pad and preflight controls, heart rates at night during flight were lower and may be explained in several ways: First, the difference between flight and control could be erroneous, since not enough control data were collected to establish a valid sample of 24-hour variations. (If such data were available, it might show that heart rates did decrease at night, as would be expected if the animal was in a steady state condition during the control period.) Second, decreases in heart rate could be due to decreases in metabolism and body temperature. And third, the lowered heart rates could represent altered sympathetic-parasympathetic nervous system interaction, with possible dominance of parasympathetic influence occurring during flight. Due to the short duration of the preflight and launch-pad controls and limited data during flight, it is hard to determine the significance of the heart rate response or the mechanism for the change. Definite answers must await data collection on longer missions.

Mean heart rate comparisons between Bion and Abrek during flight can be seen in figure 17. Abrek's heart rate was higher than Bion's from 0800 to 2000 hours daily. Heart rate for the two animals reached their lowest levels and approached similar values during the lights-off period.

The prevailing heart rates during flight (80 bpm to 130 bpm) provide evidence that the animal model developed for this flight represents a normal (nonstress) state for the monkey. Forsyth and Baireuther (1967) and Reichfott, Forsyth and Melmon (1971) have reported average heart rates in conscious, chair-restrained monkeys ranging from 140 bpm to 180 bpm. Others (Malinow, Hill, and Ochsner, 1974) have reported heart rates greater than 180 bpm as normal for the rhesus monkey. These values appear to be high, considering that chair restraint represents a hypokinetic environment and may indicate a state of chronic stress on the animal. Telemetry data from caged rhesus monkeys supports this idea. Malinow et al. (1974) observed heart rates as low as 78 bpm at night, and daytime values averaging between 110 bpm and 150 bpm in caged (nonhypokinetic) monkeys. Higher heart rates were observed when activity increased, especially during feeding and cage cleaning. Using the chair restraint and training techniques developed for this experiment (and limiting the amount of instrumentation), we have monitored heart rate from conscious, chair-restrained rhesus monkeys and found that heart rates vary between 80 bpm and 130 bpm. The importance of this is evident in reviewing data from

Biosatellite III. Heart rates routinely averaged around 190 bpm, indicating that the animal was stressed (Meehan and Rader, 1971). Interpretation of the data must take such findings into account.

Pressure-flow relationships in the carotid artery appear to be different inflight when compared to the preflight control. Average carotid blood velocities were higher, with lower pressures, than during control. Decreases in carotid peripheral resistance inflight support this finding. However, pressure-flow relationships on the launch pad were very similar to inflight values. The significance of these observations is not clear. The carotid flow measurement may have been altered by several factors which could influence data interpretation. Two important variables are the vascular beds distal to the common carotid and the environment that influences the monkey's behavior and physiology. It is expected that presure-flow relationships would be altered by the known headward fluid shifts that occur with weightlessness. Pressure-flow relationships in the common carotid artery are determined by intra- and extracranial vascular beds. The internal carotid (predominantly) carries intracranial blood flow, and the external carotid artery supplies the muscles of the face and scalp. Alterations in flow and resistance patterns may reflect changes related to cerebral hemodynamics and/or extracranial hemodynamics. If a change in resistance occurred, it would be difficult to determine which vascular bed was responsible and to what degree. It is also possible that cerebral or extracranial hemodynamics could be altered with little or no change in carotid pressure or flow. If pressure-flow relationships to the head are altered in weightlessness, it would be important to determine the relative contributions of the intra- and extracranial vascular beds to the change. Any alteration in cerebral hemodynamics, in particular a shift in cerebral autoregulation, could effect vestibular as well as cardiovascular function.

Relative levels of blood flow velocity and blood flow per minute decreased during days 2 to 3 of flight and included a decrease of signal amplitude fluctuations. This allows one to conclude that there was significant stress on the animal during this period, inducing a disruptive influence on circultory-regulatory mechanisms at different control levels. Starting with the third day of weightlessness, there was a relative increase in amplitude of 24-hour fluctuations for all parameters. This most likely signified the development of circulatory adaptive processes and associated neuro-endocrine mechanisms for adapting to the conditions of flight. One cannot draw conclusions about the completeness of this adaptation process due to the short flight period (5 days).

In summary, the monkey demonstrated from the first hour of weightless flight an increase in blood pressure, a decrease in blood flow velocity to the head and an increase in common carotid artery peripheral vascular resistance. Following this, compensatory mechanisms were invoked leading to rapid adaptation of regional hemodynamics in response to general hemodynamic changes.

Cardiovascular system changes due to weightlessness were maximal on Day 2 of flight. They were most clearly indicated by a decrease in amplitude for circadian

patterns of measured circulatory parameters. Signs of adaptation to weightlessness appeared on Days 3 to 5 of flight.

BIBLIOGRAPHY

Forsyth, R.; and Baireuther, R.: Systemic Arterial Blood Pressure and Pulse Rate in Chronically Restrained Rhesus Monkeys. Amer. J. of Physiol., vol. 212, 1967, p. 1461.

Malinow, L.; Hill, J.; and Ochsner, A.: Heart Rate in Caged Rhesus Monkeys (Macaca mulatta). Laboratory Animal Science, vol. 24, no. 3, 1974, p. 537.

Meehan, J. P.; and Rader, R. D.: Cardiovascular Observations of the Macca nemestrina Monkey in Biosatellite III. Aerospace Medicine, vol. 42, 1971, pp. 322-326.

Pourcelot, L.; Pottier, J. M.; Patat, F.; Arbeille, Ph.; Kotovskaya, A.; Genin, A.; Savilov, A.; Bistrov, U.; Golovkina, O.; Bost, R.; Simon, P.; Guell, A.; and Charib, C.: Cardiovascular Exploration in Microgravity. French-Soviet Flight Aboard Salyut VII, June 1982.

Reichfott, M.; Forsyth, R.; and Melmon, K.: Effects of Bradykinin and Autonomic Nervous System Inhibition on Systemic and Regional Hemodynamics in the Unanesthetized Rhesus Monkey. Circulation Research, vol. 29, 1971, p. 367.

Stone, H. L.; and Sandler, H.: Cardiovascular Studies in the Rhesus Monkey. The Use of Nonhuman Primates in Space. NASA Conference Publication 005, 1977, pp. 83-103.

TABLE 1.- U.S.-SOVIET CPF CUFF IMPLANT PERFORMANCE, 1980-83

Period Functional, Postsurgery	U.S. Monkeys	Soviet Monkeys
Less than 30	4	7
Between 30-60	5	12
Between 60-100	11	12
Between 100-365	11	5
Total number of monkeys	31	36

Figure 1.- A single cylindrical probe, containing both flow and pressure transducers, chronically implanted as a cuff around the left carotid artery of five rhesus monkeys.

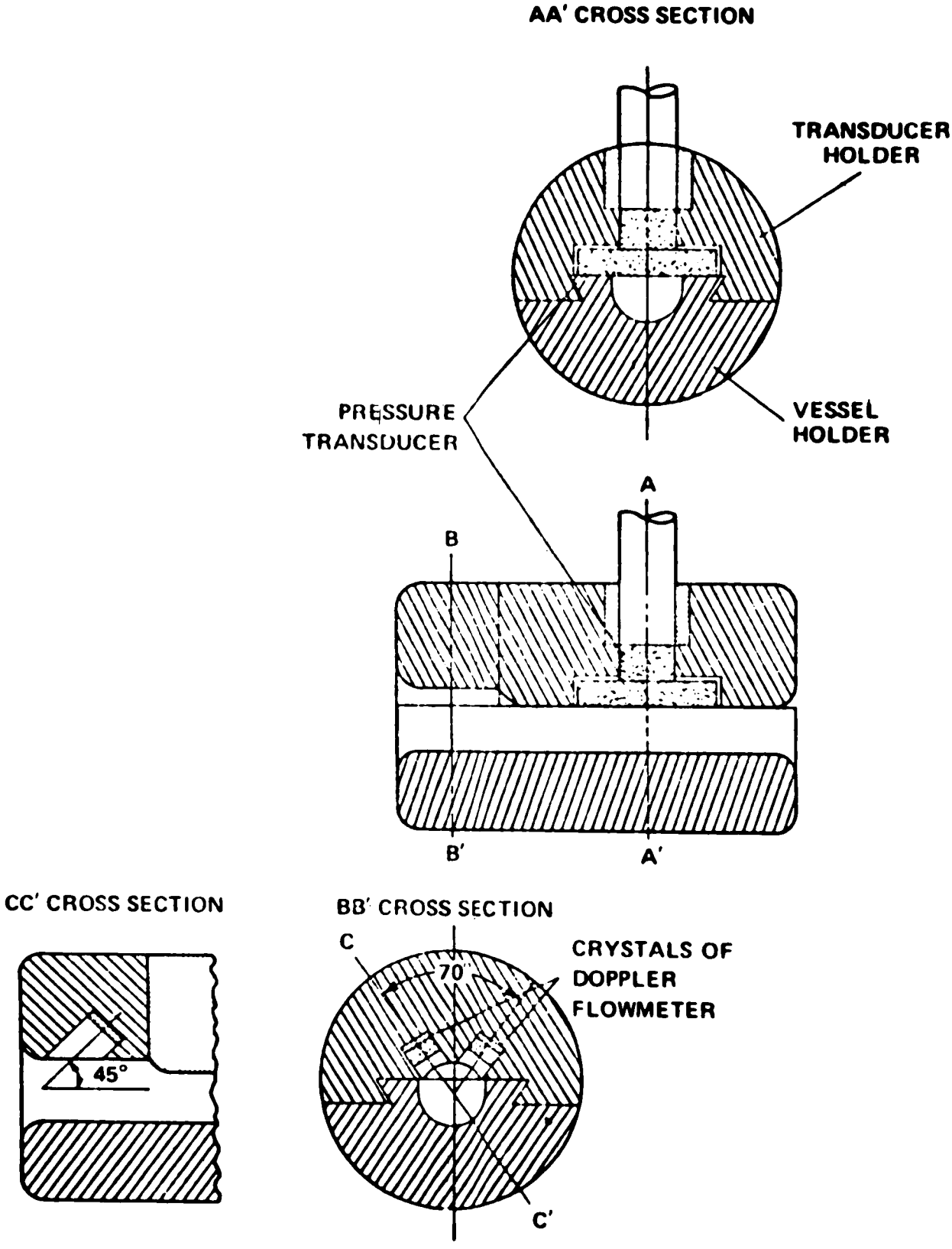

Figure 2.- Cross-sectional drawing of the arterial pressure and flow-measuring cuff.

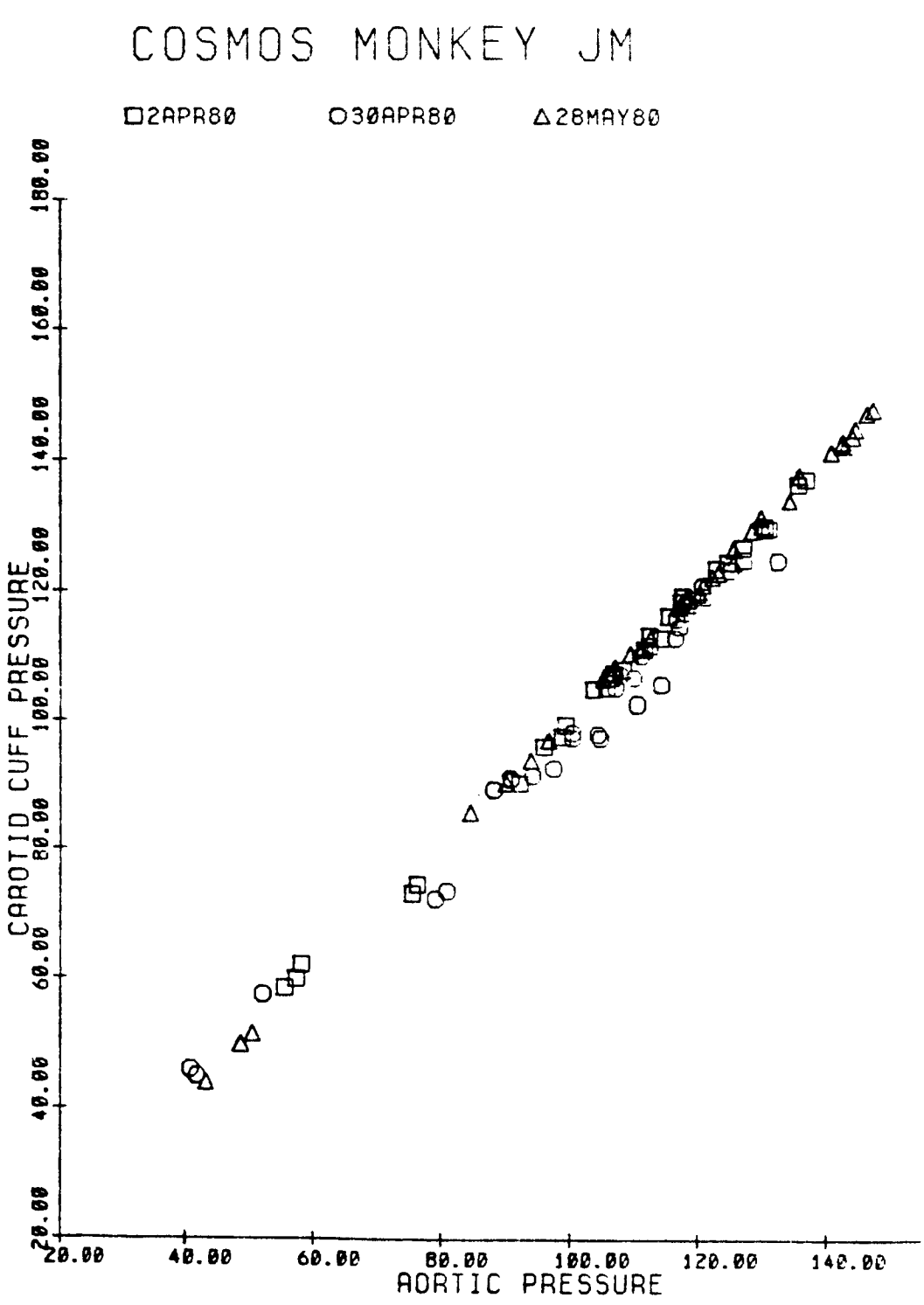

Figure 3. - Mean blood pressure measured in the descending thoracic aorta, using an identical pressure transducer implanted intravascularly. (Three separate measurement comparisons are plotted; April 2, April 30, and May 28, 1980.)

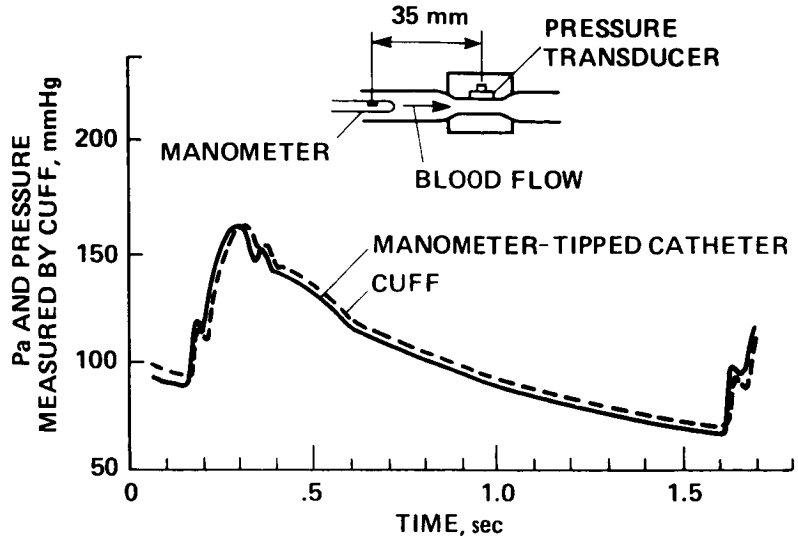

Figure 4.- In-vivo pressure calibration; comparison of blood pressure using manometer-tipped catheter placed just proximal to the CPF cuff.

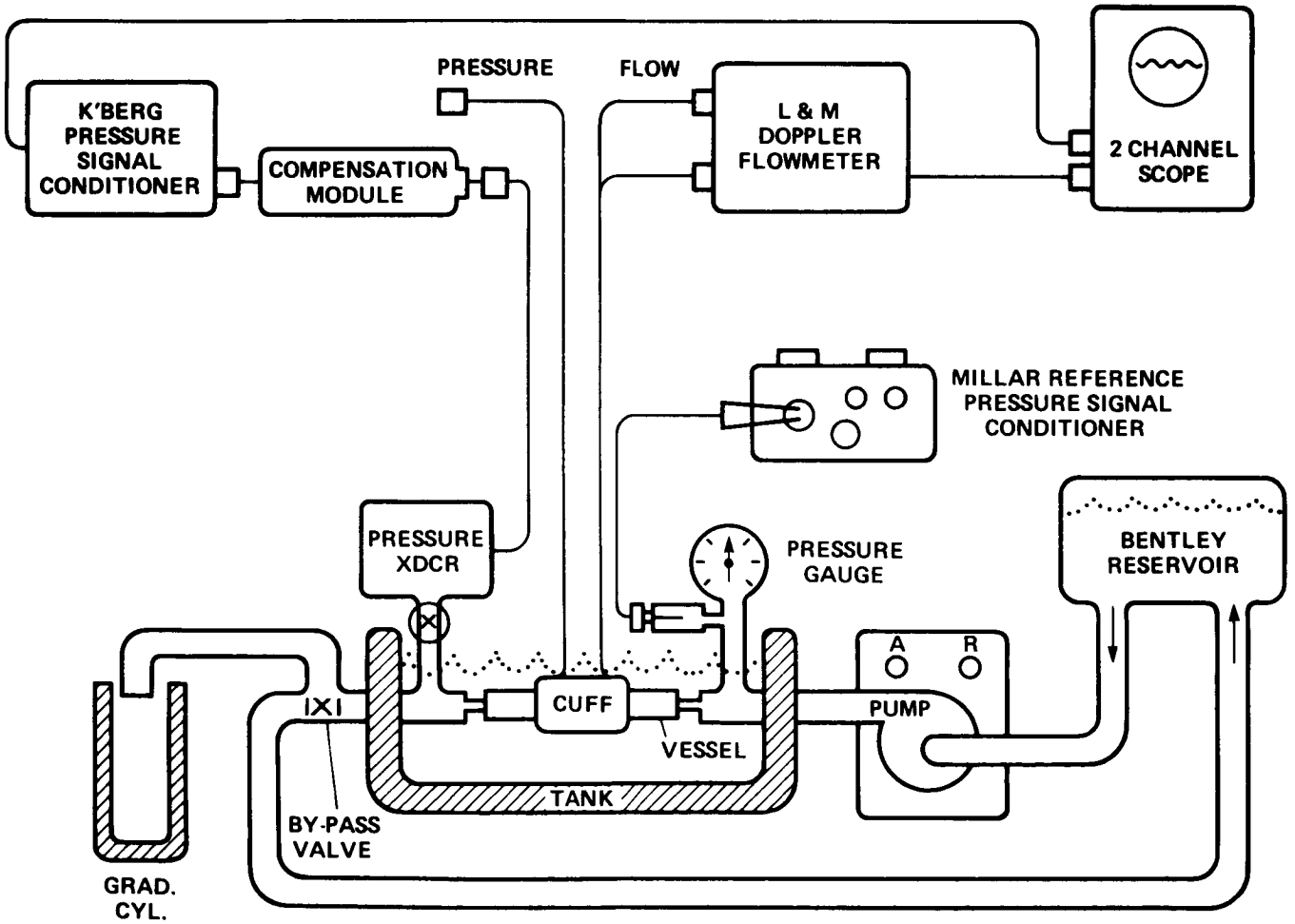

Figure 5.- CV measurements study demonstration unit used for extensive in-vitro testing to ensure accuracy of the flow measurement system.

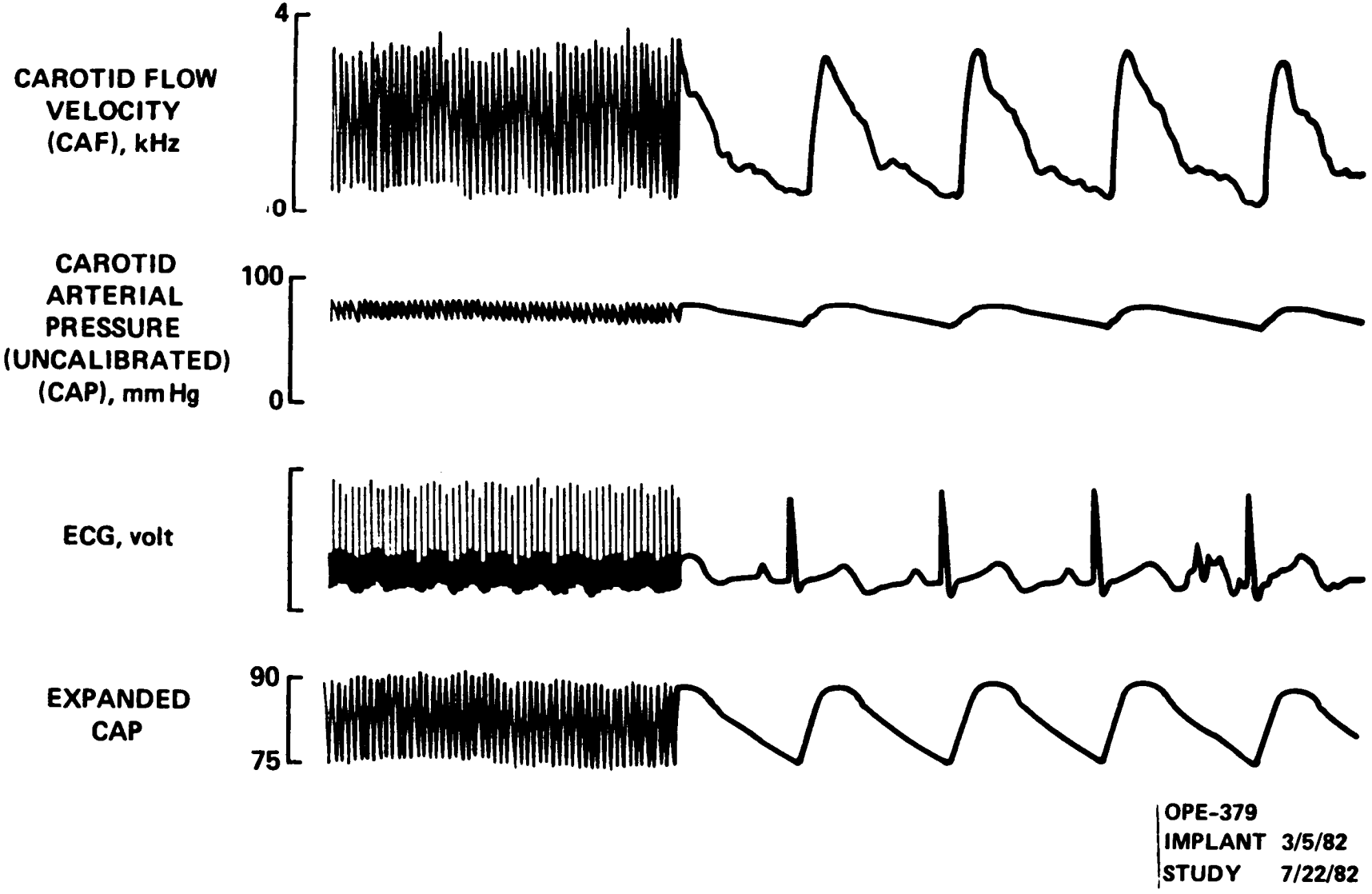

Figure 6.- Representative pressure and flow waveforms four months after lead exteriorization from the back.

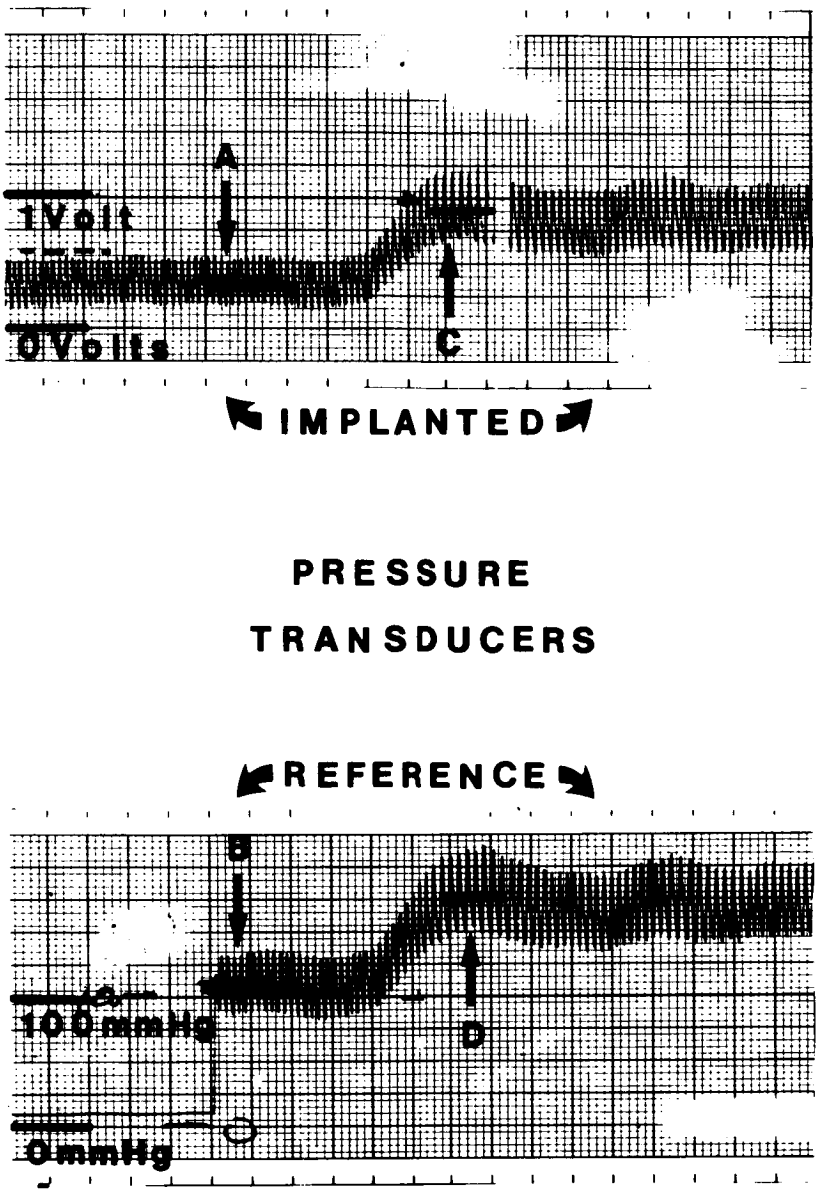

Figure 7.- In-vivo cross-calibration procedure using direct measurement of pressure to convert voltage output of the CPF cuff into mm Hg.

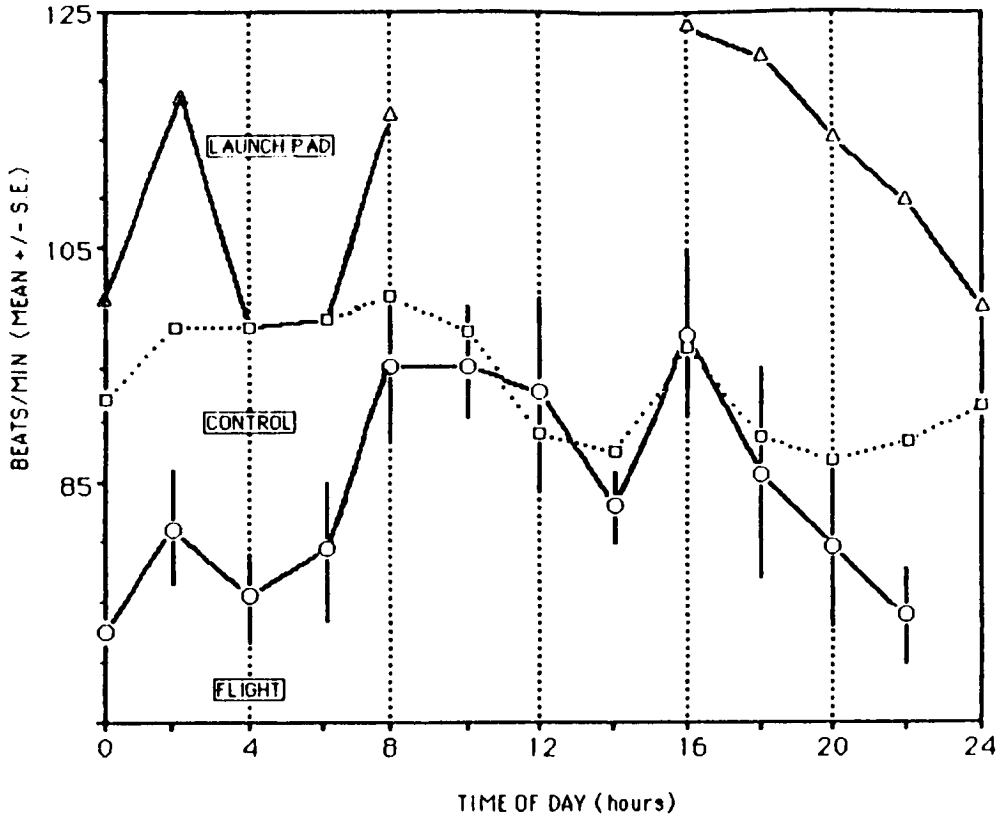

Figure 8.- Bion - Heart rate: flight vs. launch pad vs. control.

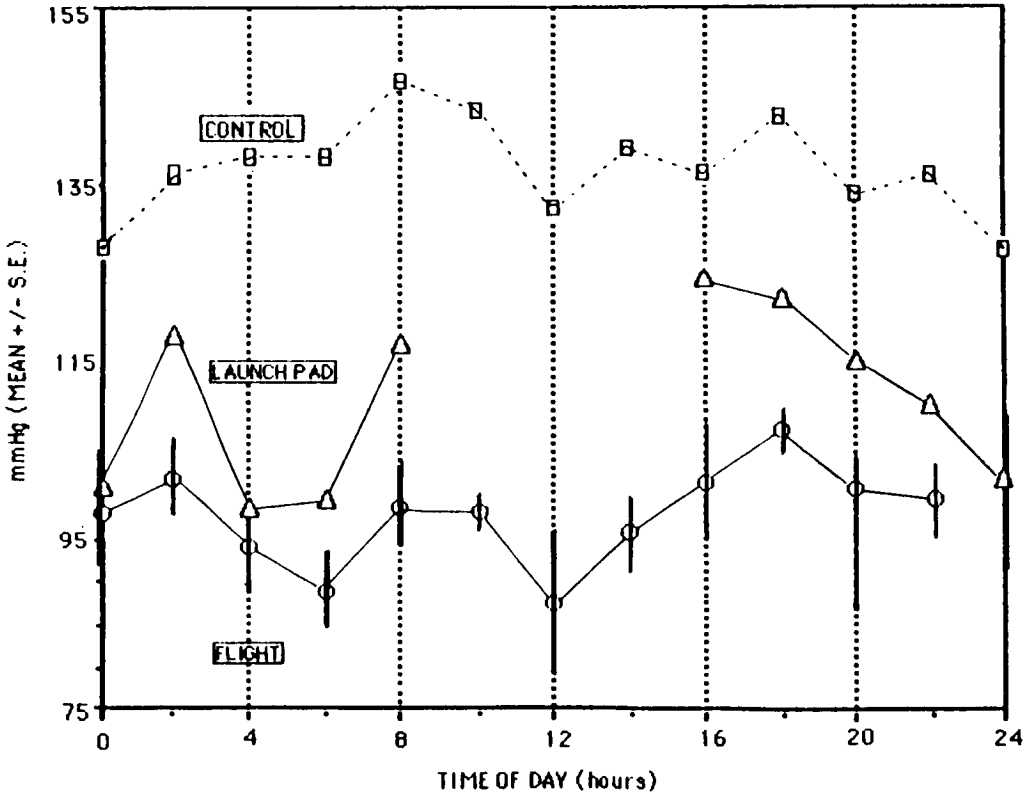

Figure 9.- Bion - Mean blood pressure: flight vs. launch pad vs. control.

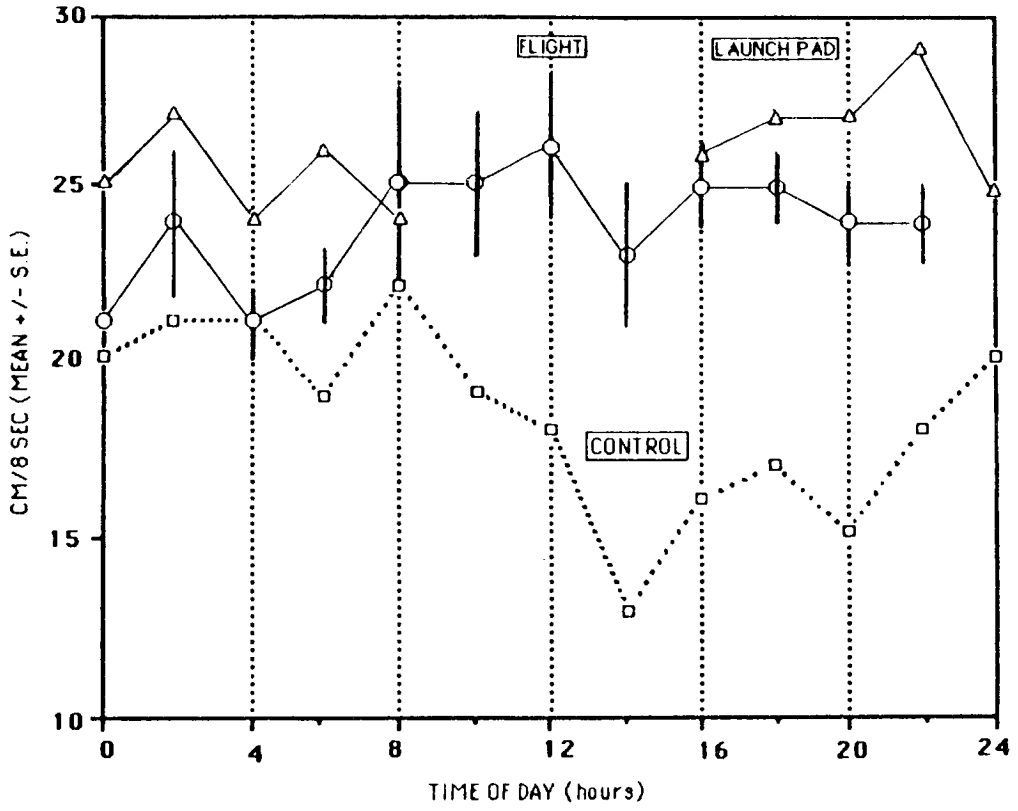

Figure 10.- Bion - Mean flow velocity: flight vs. launch pad vs. control.

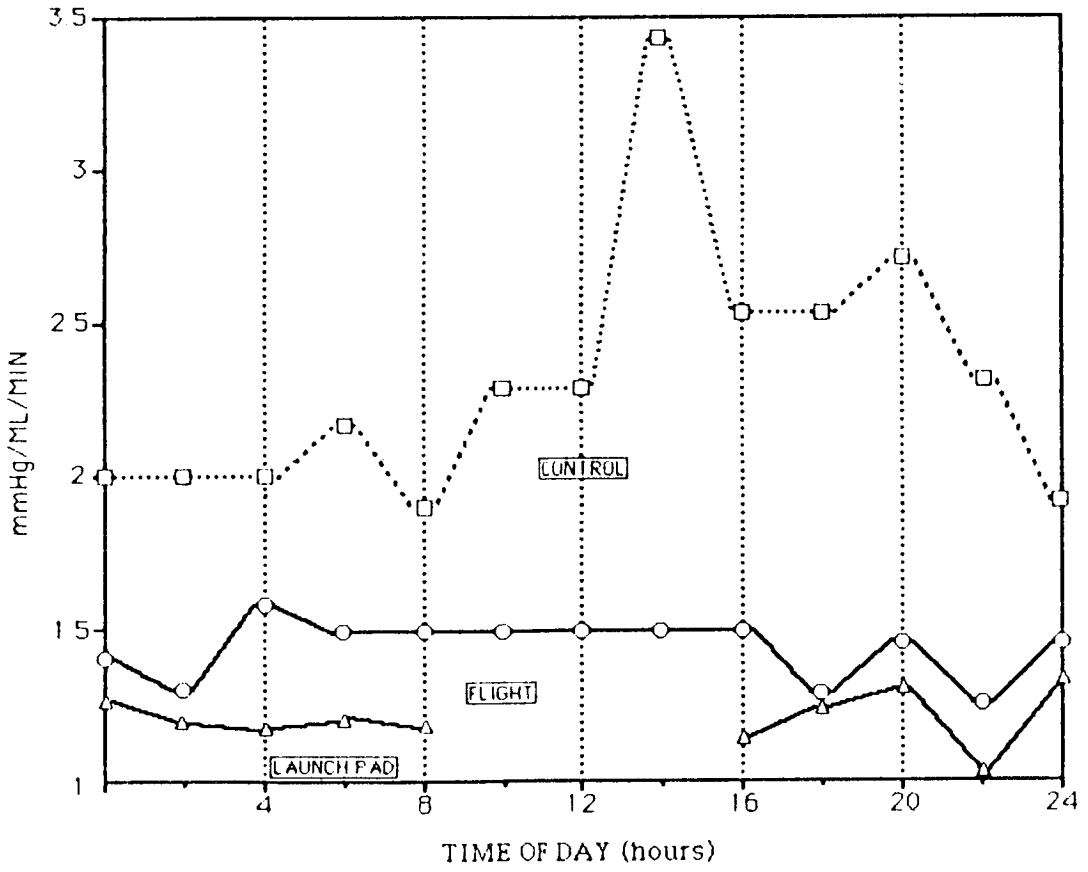

Figure 11.- Bion - Mean resistance: flight vs. launch pad vs. control.

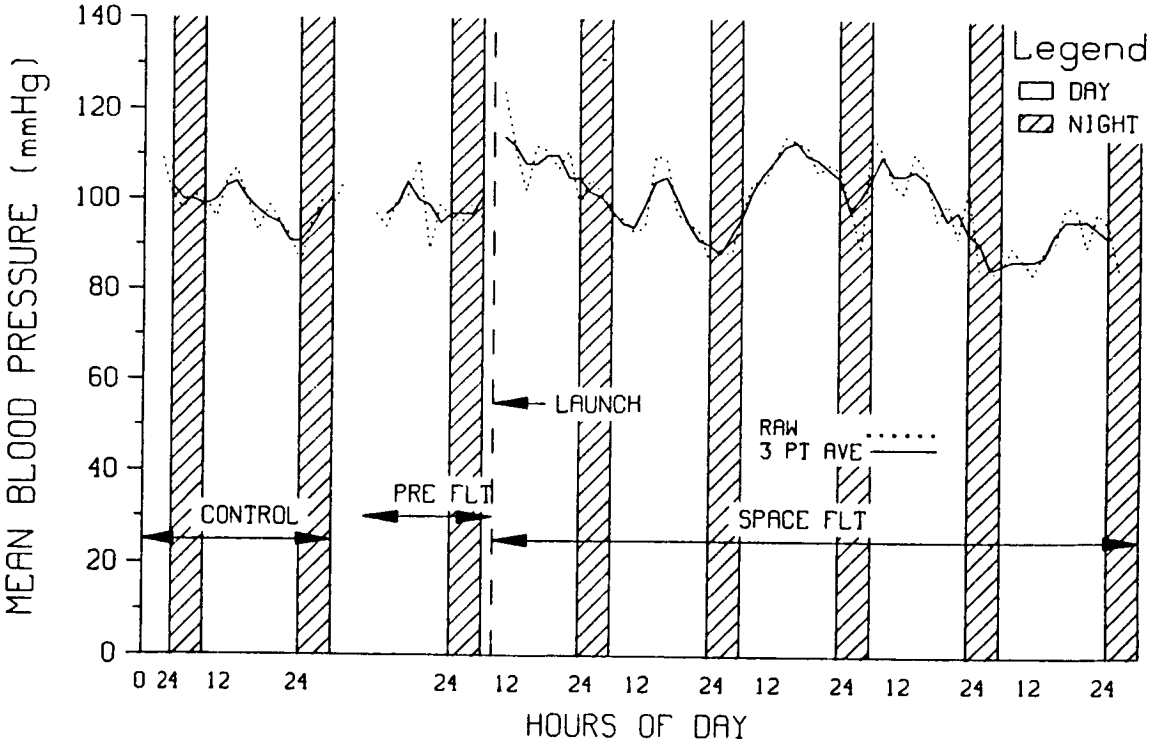

Figure 12.- Hemodynamics Cosmos spaceflight 1514, mean blood pressure.

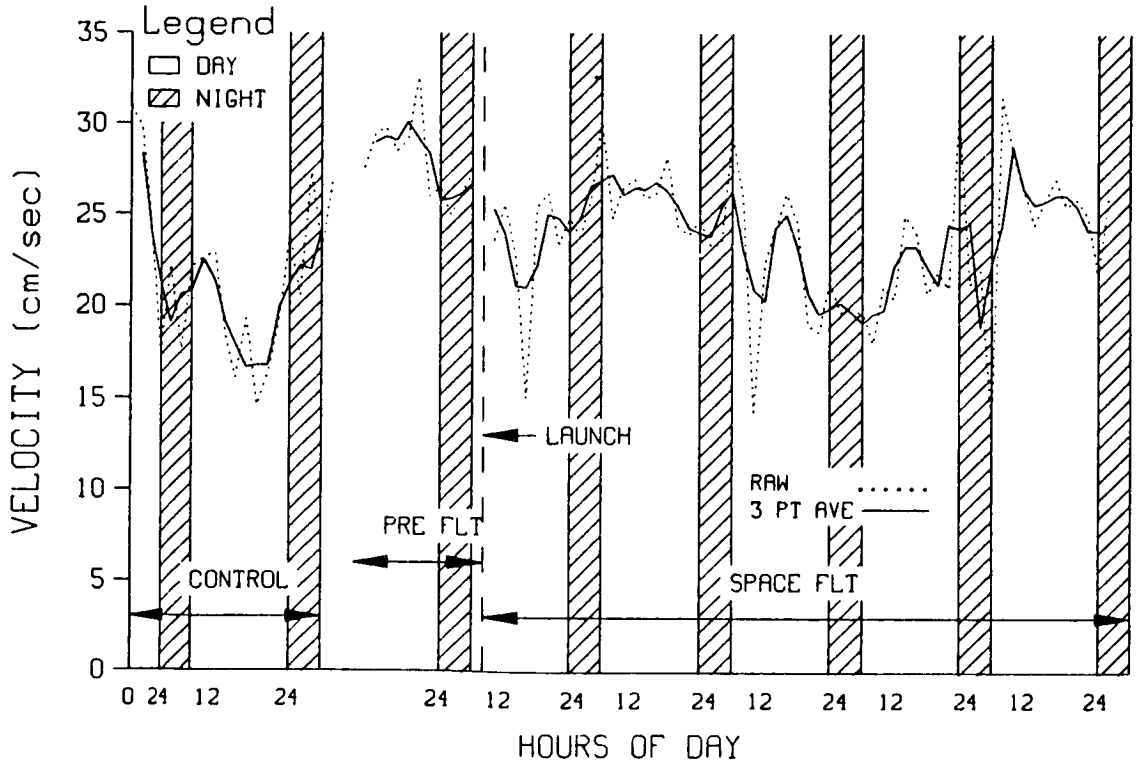

Figure 13.- Hemodynamics Cosmos spaceflight 1514, blood flow velocity.

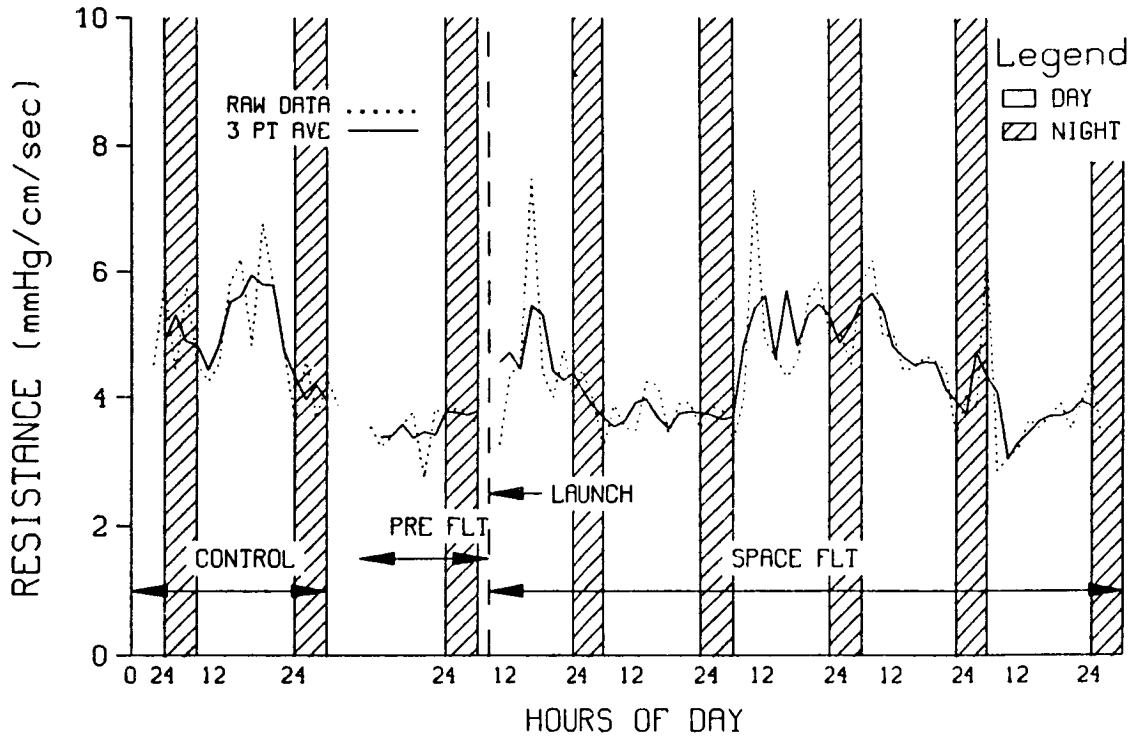

Figure 14.- Hemodynamics Cosmos spaceflight 1514, common carotid artery peripheral vascular resistance.

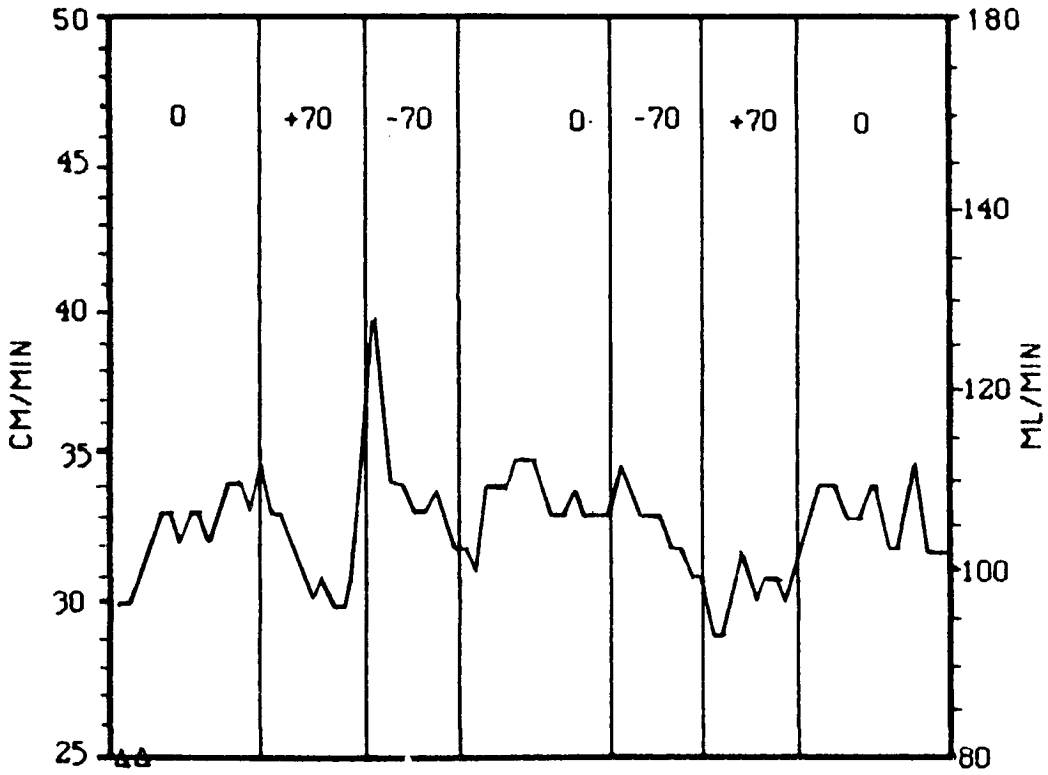

Figure 15.- Bion tilt: blood velocity and flow.

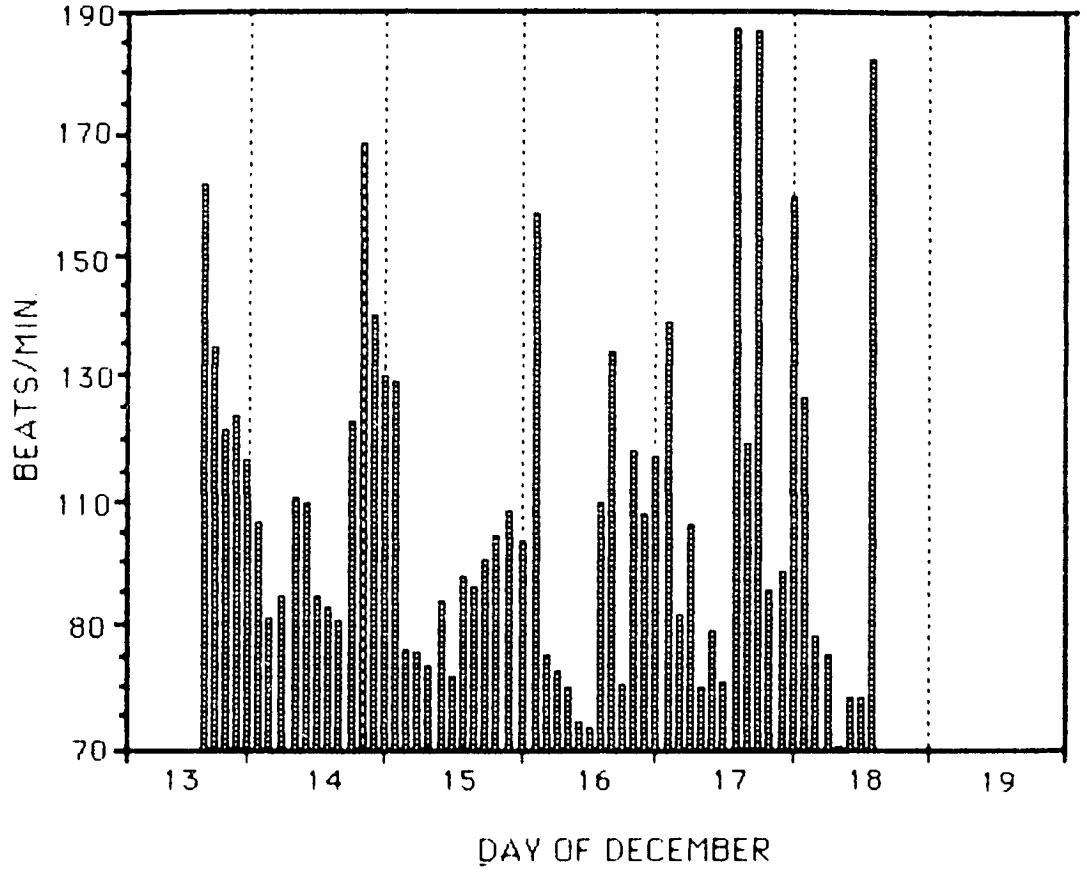

Figure 16.- Abrek heart rate data, 13 to 19 December 1983.

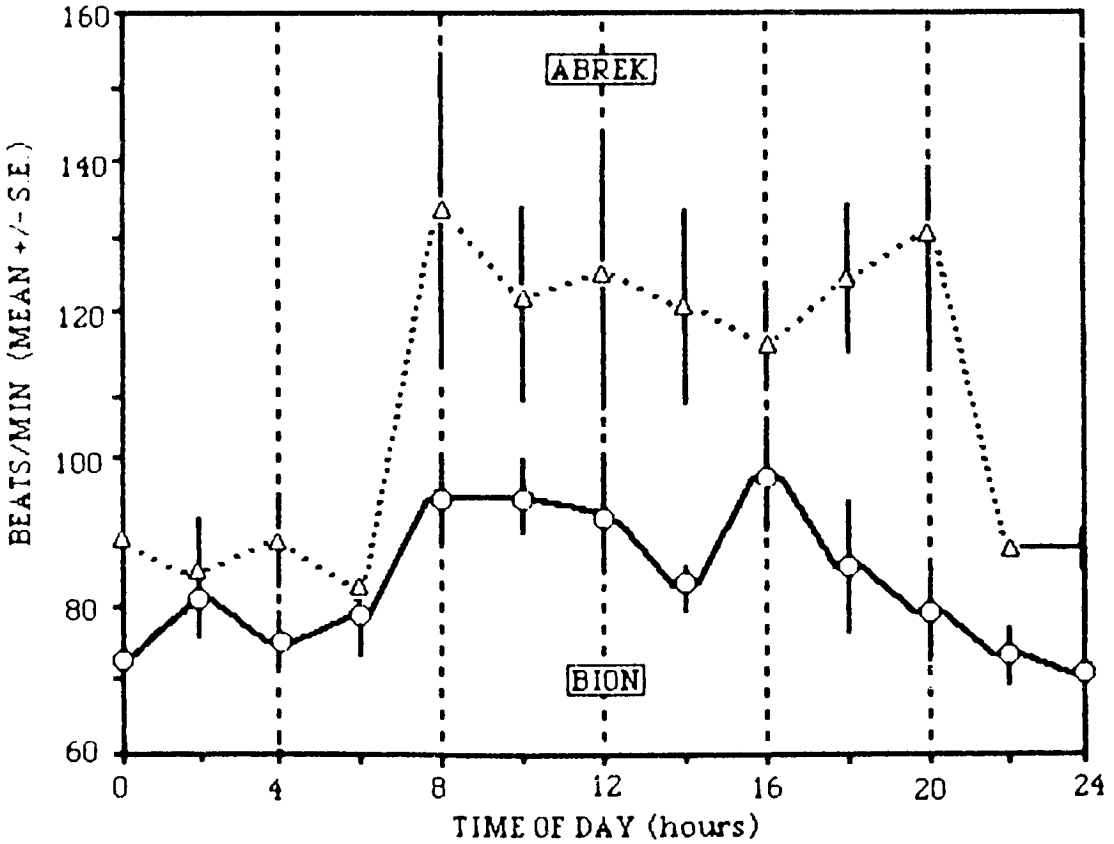

Figure 17.- Mean heart rate during flight: Bion vs. Abrek.

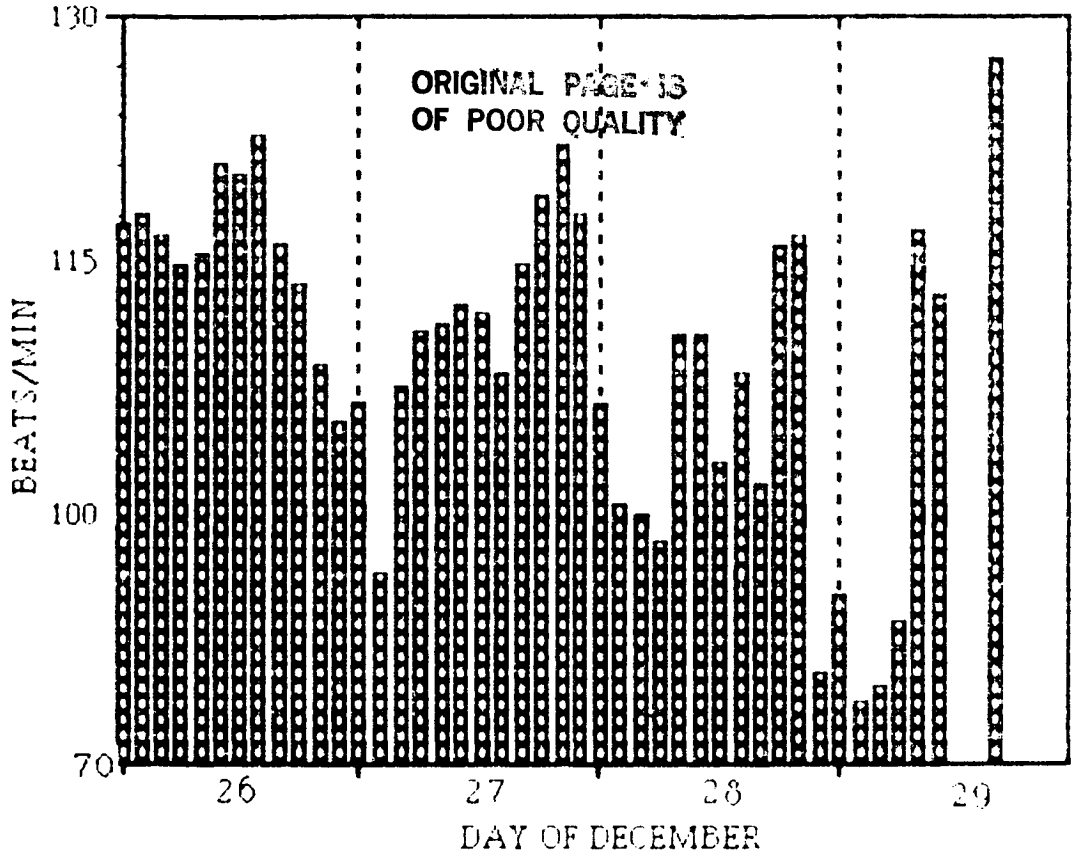

Figure 18.- Ariel heart rate data, 26 to 30 December 1983.

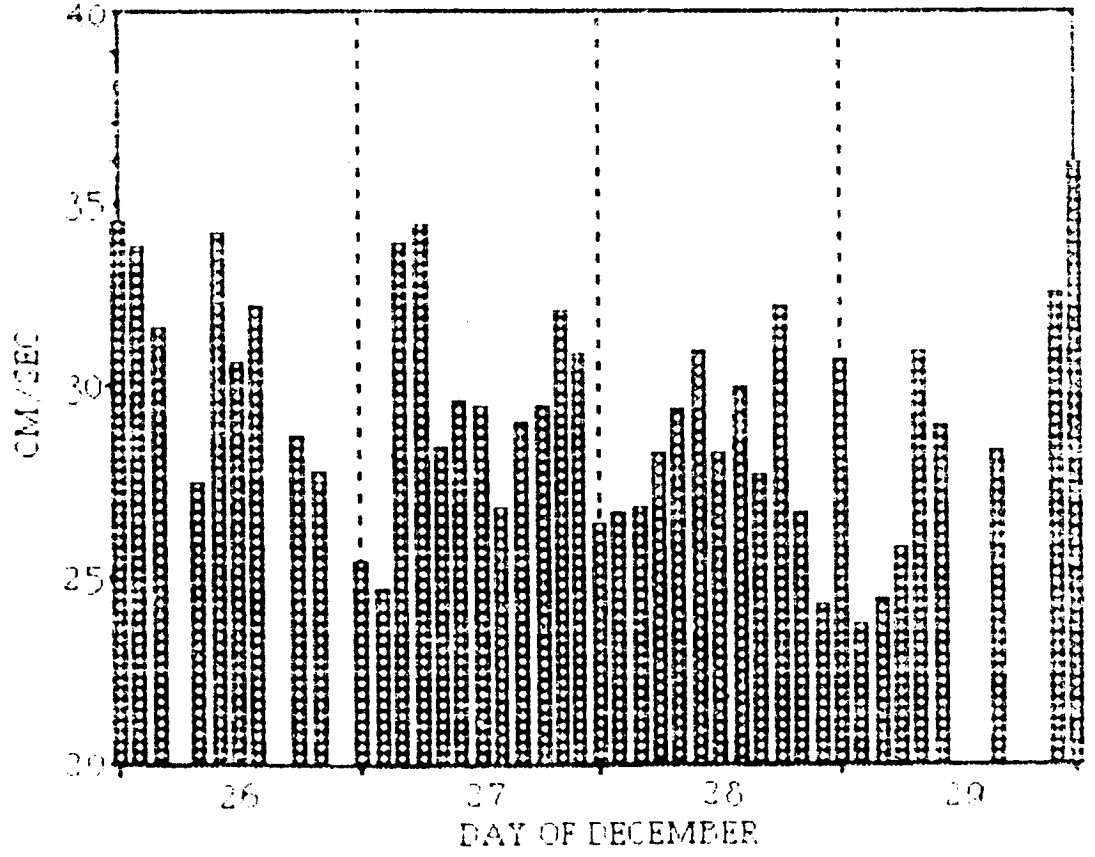

Figure 19.- Ariel mean flow data, 26 to 30 December 1983.

CALCIUM METABOLISM AND CORRELATED ENDOCRINE MEASUREMENTS IN PRIMATES DURING COSMOS '83

Prepared by:

Christopher E. Cann, Ph.D.
Department of Radiology
University of California
San Francisco, CA 94143

Christopher E. Cann, Ph.D.
University of California
San Francisco, CA

Patricia Patterson-Allen
NASA-Ames Research Center
Moffett Field, CA

Richard R. Adachi
NASA-Ames Research Center
Moffett Field, CA

Arkady Ushakov
Yuri Kondratyev
Alexander Rachmanoff
Viktor Oganov
Institute of Biomedical Problems
Moscow, USSR

SUMMARY

An experiment designed to measure the initial responses of the calcium homeostatic system in nonhuman primates to spaceflight was done. Results indicate that after five days of flight, the fraction of circulating calcium that comes from bone is increased; gross skeletal changes were not observed, but there is a suggestion of subtle changes as determined from high-quality radiographs.

INTRODUCTION

The problem of calcium loss from the body during spaceflight has long been recognized. The possibility of bone mineral decreases, as a response to weightlessness, was initially hypothesized based on the observation that osteoporosis developed following the disuse of poliomyelitis (Whedon and Shorr, 1957) and immobilization (Heaney, 1962). Such decreases have since been demonstrated following long-term spaceflight (Vogel et al., 1977; Gezenko, Genin, and Egorov, 1981). However, little is known about the initiating mechanisms of this loss of calcium and the early responses of the calcium homeostatic system to weightlessness. We can suggest two hypotheses: 1) a primary increase in bone resorption due to decreased mechanical stress on the bone, or 2) a primary renal calcium leak. The first mechanism would invoke homeostatic responses of slightly increased serum calcium, increased urinary calcium output, decreased serum PTH, decreased $1,25(OH)_2D_3$ synthesis, and decreased intestinal calcium absorption. The second process would include a slight decrease in serum calcium, increased serum PTH, and increased bone resorption followed by another set of responses similar to those seen if the primary mechanism was increased bone resorption.

All the data obtained to date from spaceflight are either anecdotal (such as a few serum samples from astronauts and cosmonauts) or were obtained in a manner which did not address the initiating mechanisms for disturbances in calcium homeostasis. The best human metabolic data were obtained during the Skylab missions, and they show that changes in urinary calcium output, for example, occur within the first 48 hours (fig. 1) of launch. The only other data available from spaceflight have been obtained from the Cosmos series of flights with rats, where decreases in bone formation and osteoblast precursor cell populations were noted (Morey and Baylink, 1978; Wronski and Morey, 1983; Roberts, Mozsary, and Morey, 1981) without any significant change in bone resorption (Cann and Adachi, 1983). However, in the skeletal system many of our findings about the juvenile rat-modeling system cannot be extrapolated to the primate adult remodeling system; we must study both humans and nonhuman primates to obtain this information. At the present state of knowledge, we cannot distinguish between the two hypotheses noted earlier. This present experiment was designed to test one aspect of the calcium homeostatic system: does weightlessness induce a primary increase in bone resorption in the remodeling skeleton of the nonhuman primate? By differentiating calcium of dietary origin from that of skeletal origin through the use of continuous tracer methodology, direct measurement of the inital response of the skeleton to zero g can be made. Correlative measures of endocrine response and skeletal status were planned to help interpret the tracer data.

METHODS

Tracer Studies

The basis of the continuous tracer technique, for the direct measurement of changes in bone resorption, is the fact that the skeleton can be considered "labeled" with stable isotopic tracers for calcium. A tracer is defined as a material which, when introduced into the system, is distinguishable from the bulk material, but does not change the properties of that material. Naturally occurring calcium is composed of the isotopes of mass 40,42,43,44,46 and 48 in varying abundances. Calcium-46 and calcium-48 have natural abundancies of 0.0033% and 0.185%, respectively, so their introduction to or removal from the body's miscible calcium pool alters their measured abundance but does not alter the bulk of the circulating calcium. In this experiment, calcium-48 was used as the tracer.

Circulating calcium comes from only two sources--diet and bone. By removing calcium-48 from the diet, the two sources can be distinguished, and the ratio of calcium coming from each source can be easily measured. This ratio is defined by the equilibrium circulating abundance of calcium-48 relative to the (initial) abundance of calcium-48 in natural calcium. It is exactly equal to the bone resorption normalized by calcium turnover.

The special diet used for this experiment was formulated by Y. Kondratyev. Calcium-48 was eliminated by replacing natural calcium salts with salts of 99.997% isotopically pure calcium-40 (specifically calcium-40-carbonate). Because the diet contained some natural products, there was a residual background of natural calcium representing approximately 20% of the total dietary calcium. A correction for this will be included in the final data analysis of the tracer study.

Tracer studies were done both for the bioengineering test (August/September 1983) and the flight. Four animals were used for the bioengineering test, and an initial pool of 12 animals was used for the flight and the synchronous control experiments. The time sequence for the design of the continuous tracer study is shown in figure 2. Animals were given the paste diet with natural calcium starting approximately 30 days preflight. They were started on the diet with calcium-40 (i.e., "free" of calcium-48) on L-15. The calcium-40 diet was continued for fifteen days preflight, five days inflight and seven days postflight, after which the paste diet with natural calcium was again given. These times were chosen based on results obtained from previous experiments with large primates (Cann, Young, and Nagel, 1978). These experiments showed that an equilibrium ratio of ^{48}Ca/total Ca in serum/urine is reached 8 to 10 days following the elimination or reduction of ^{48}Ca in the diet (fig. 3). Timing of samples was adjusted to provide near-optimal sampling, to give the kinetic curves for the decrease in ^{48}Ca ratio after the elimination of ^{48}Ca from the diet and its subsequent increase when ^{48}Ca was again introduced into the diet. The hypothetical curve in figure 4 shows what one would expect to measure if bone resorption increased early in flight.

Urine samples were obtained during preflight and postflight periods for the measurement of the isotopic abundance of ^{48}Ca. Ten-milliliter aliquots of urine were obtained for analysis (36 total samples from the bioengineering test and 96 samples from the flight/synchronous experiment). Urine pH was adjusted to 8 to 9 for each sample, and calcium was precipitated as the oxalate, washed, dissolved in dilute nitric acid and aliquots taken for determination of ^{48}Ca by neutron activation analysis. A 1.000-ml aliquot of the $Ca(NO_3)_2$ solution was sealed in a high-purity lab-grade polyethylene vial (Olympic Plastics, Los Angeles) and paired with a standard of 1.060-mg Ca (National Bureau of Standards Reference Material 915). The sample/standard pairs were irradiated in the Flexorabbit facility of the Berkeley Research Reactor for 10.0 minutes at a thermal neutron flux of 1.3×10^{13} cm^{-2} sec^{-1}. Standard/standard pairs were also irradiated at intervals to quantify the difference in neutron flux between the sample and standard positions in the reactor core (about 1.5-cm difference in vertical position); this difference in flux was about 3% and was included in the calculations. One hundred seconds after the end of irradiation, each sample was counted for 300 seconds using a high-purity germanium detector (15% relative efficiency, 1.8 keV FWHM at 1.33 MeV, peak:compton of 56:1) coupled to a DEC LSI 11/23-based analysis system. The system features included a 50-MHz ADC, 16-K channel by 16-bit histogramming memory, live-timer, and a high-resolution spectroscopy amplifier with pulse pileup rejection. This system allowed accurate counting of the 3084-keV photopeak of ^{49}Ca produced in the reaction $^{48}Ca\ (n,\gamma)\ ^{49}Ca$, even in a high-background activity of Na, Cl, Al and Mn. These elements are present in trace amounts in the sample, but they are made more significant because of the low amounts of calcium present (see Results). The comparator standards were counted in the same geometry as the standards for 300 seconds, starting 450 seconds after the end of irradiation. The area of the 3084-keV photopeak of ^{49}Ca was determined automatically at the end of the counting period and was printed out. Total mass of ^{48}Ca in each sample was calculated from sample and standard peak areas, known counting conditions, and the known mass of ^{48}Ca in the standard. A 0.200-ml aliquot of the initial $Ca(NO_3)_2$ solution was also taken for total calcium analysis by atomic absorption spectrophotometry. The ratio of ^{48}Ca/total Ca was determined from these measurements.

Dried fecal samples and diet samples were ashed at 600°C and the ash was dissolved in HCl. The samples were then treated, as were the urine samples, to determine ^{48}Ca/ total Ca in the feces and diet.

Endocrine Studies

During the bioengineering test, serum samples were obtained for ground-based endocrine measurements. A total of six samples were received; two each from two monkeys and one each from another two monkeys. Analyses for PTH, vitamin D metabolites and serum osteocalcin were done.

No serum samples were received from the flight experiment, so the planned endocrine studies were not done.

Radiologic Studies

Single lateral x rays were obtained for the right and left arms and legs of four monkeys: one flight animal, two synchronous control animals and one bioengineering test animal. The films were taken with a portable x-ray unit at 68 kVp with a focus-film distance of 85 cm. Exposures were made on OM-1 film with a Kodak Min-R screen to provide high contrast and good radiographic detail for bone. The films and test exposures were made by A. Rachmanoff and returned to the U.S. for development in an automatic processor (Kodak Industrial X-Omat, 3-minute processing). All 16 films (from the four monkeys) were well exposed.

RESULTS

Tracer Studies

All urine samples were analyzed initially for total calcium concentration to give an estimate of expected ^{48}Ca to optimize the neutron activation studies. A normal monkey on a diet with 300- to 400-mg Ca/day will excrete 50- to 100-mg Ca/day in the urine; even if we assume a 500- to 1000-ml/day urine volume, we would expect a calcium concentration of 0.1 mg/ml in the urine. Table 1 shows some urinary calcium values from the flight animals. The values range from 0.002 to 0.14 mg/ml with a mean value on the order of 0.02 to 0.03 mg/ml. This level, on the order of one-fifth of normal for urinary calcium, was completely unexpected and necessitated a redevelopment of analysis techniques for ^{48}Ca. Specifically, when calcium levels are so low, even minor contamination with calcium from the environment (such as from glassware or in water) will produce inaccurate measurements of the ^{48}Ca/total Ca ratio. A discussion of possible causes for this problem will be included later in this report.

Figure 5 shows the results from one of the flight animals (Abrek) for the tracer curve. The decline from a relative ^{48}Ca abundance of 1.0 at day L-21 to a value of approximately 0.55 prior to flight indicates that 55% of total circulating calcium (preflight) is coming from the bone. However, at L-3 there is a sudden increase in tracer abundance, perhaps related to elution of rapidly miscible calcium from the bone into the serum pool as a result of prelaunch stresses. This same anomalous tracer "spike" is seen on R+0, followed by a return to lower levels. The significance of this result will be discussed later.

Because of the extremely low calcium content of the urine specimens, the number of samples analyzed for ^{48}Ca with high confidence was reduced compared to the total number of samples received. Based on these samples, the results for pre- and post-flight tracer abundances were:

	Pre	Post
Abrek	0.55 ± 0.04	0.63 ± 0.05
Bion	0.48 ± 0.05	0.55 (one sample)

These differences were not statistically significant, but show a definite trend toward increased calcium release from bone in the flight or immediate postflight period.

Biochemical Studies

Urine specimens were also analyzed for osteocalcin (bone GLA-protein, a bone-specific noncollagenous protein), hydroxyproline and creatinine; results have been expressed per milligram creatinine for standardization and are presented in table 2. Figure 6 shows osteocalcin results for the two flight animals and for Abrek during the bioengineering test. While there are no remarkable changes between pre- and postflight means, the same "spike" occurs for osteocalcin at L-3 and R+0 as occurs for the ^{48}Ca tracer abundance. In contrast, no such increase occurs for hydroxyproline.

Radiographic Studies

The films obtained were all done postflight, primarily for assessment of the skeletal status (age, relative turnover, etc.). Of the four animals, number 1 (Tima-bioengineering test) and number 2 (Ariel-synchronous) were skeletally younger than numbers 3 (Teuton-synchronous) and 4 (Abrek-flight) as judged by the state of epiphyseal closure and the stage of development of the tibial tuberosity.

Because pre- and postflight films were not obtained, no attempt will be made at quantitative comparisons. However, some qualitative observations can be made along with reporting the quantitative data available. Table 3 presents the quantitative measurements. Qualitative assessment of the films for cortical porosity suggests that monkey 4 may be in a state of slightly increased bone turnover because of the presence of some intracortical striations in the radial and ulnar cortex. These striations are not present (monkeys 1 and 2) or only minimally visible (monkey 3) on the other animals. In addition, for approximately the same bone length, monkey 4 appears to have thinner cortices (for example, combined cortical thickness (CCT) for the left tibia is 4.8, 4.5, 5.3 and 3.4 mm for monkeys 1 to 4, respectively). This difference in monkey 4 may only be the result of a slighter skeletal build due to genetic differences. Because no preflight films were obtained, no statement can be made regarding bone loss. However, these results suggest that serial films may in fact be useful in later flights, both in selecting animals and for monitoring skeletal growth through flight.

Discussion

This experiment was designed to test the hypothesis that the initial reaction of the calcium homeostatic system to spaceflight (zero g) was a primary increase in bone resorption, and to study the homeostatic responses to this stimulus. Techniques which had been used successfully in immobilization studies with nonhuman primates (Cann, Young, and Nagel, 1978) were adapted for this study. Initial results from this flight suggest that bone resorption does increase; further analysis of the data and analysis of duplicate samples are necessary to better

characterize these results. As noted earlier, the absence of serum samples for endocrine analysis eliminated the possibility of fully interpreting the metabolic/tracer data; however, this was a secondary (although important) objective of the experiment. Fortuitously, the radiographs obtained postflight suggest that the use of radiographs would be valuable to follow dynamic changes in bone in young monkeys.

Figure 1 is a compilation of data taken from the Skylab experiments. A major point to be noted is that, even with a wide fluctuation in dietary calcium intake, urinary calcium output remained fairly constant over a 2- to 3-week period. Similar results have been noted in immobilized monkeys (Cann, Young, and Nagel, 1978). This observation means that the variations in dietary intake noted for the flight animals (i.e., decreased intake for the first couple of days of flight) should not have significantly perturbed the daily urinary calcium excretion. However, the very low level of urinary calcium observed in the specimens from this experiment and the wide variation when expressed as Ca/creatinine suggest a technical explanation. Often when a urine specimen is obtained, it may be at a pH higher than neutral, and calcium can precipitate out of this alkali urine as the phosphate or other compounds. It is not clear how the urine samples were obtained in this experiment, so this cannot be ruled out as an explanation for the low urinary calcium levels. The relative stability of the osteocalcin/creatinine and hydroxyproline/creatinine ratios further supports this hypothesis.

The ratio of ^{48}Ca/total Ca in the serum or urine can be affected by changes in the ratio of dietary to bone calcium coming into the serum pool if total dietary calcium intake is markedly reduced from its equilibrium preflight levels. However, this effect is transient and the ^{48}Ca/total Ca ratio is back to normal within about 48 hours after dietary intake returns to normal. Thus, in this experiment the data from R+0, R+1 and R+3 should be relatively unaffected by the reduced eating noted early in flight.

The dramatic increases in ^{48}Ca/total Ca abundance at L-3 and R+0 were unexpected, as were the similar increases in osteocalcin output. It is known that bone has a labile mineral component (rapidly exchangeable calcium). It is quite possible that the increased tracer abundance noted on these days is due to an elution of this calcium into the serum pool, mediated by pH or other changes in the bone fluid compartment. The fact that hydroxyproline output (bone matrix degradation) does not change in a similar manner suggests that we may use these techniques to separate osteoclastic resorption from mineral exchange on the bone surface. This is an exciting possibility which will be further explored.

Given some of the technical difficulties encountered in specimen collection and analysis, consideration should be given in follow-on studies to obtaining daily urine samples (fecal sampling frequency appears to be sufficient); this would minimize the noise in fitting the tracer curve and damp out any fluctuations which are noted. This might be accomplished by minor redesign of the animal holding cages currently in use at the Institute of Biomedical Problems.

Analysis of the radiographs obtained during this experiment suggests two refinements to experimental protocols: 1) preflight films could be used to match animals skeletally with their synchronous controls or other flight animals, so that they are all about the same skeletal age; and 2) a series of high-quality radiographs--two preflight, one immediate (1 to 2 days) postflight and one late (2 to 3 weeks) postflight--could be used to assess the changes in intracortical porosity due to the stimulus of spaceflight. The latter use was suggested by careful analysis of the postflight radiographs. It was not expected that the quality of the radiographs would be high enough to do this analysis, but it now appears that this may be feasible.

In summary, the results to date indicate that the methods used to study calcium metabolism during the spaceflight were sufficient to answer the questions asked. Technical difficulties encountered were partially overcome by some redundancy in the urine and fecal kinetics of ^{48}Ca; a careful analysis of the methodology used for specimen collection must be done to answer some questions raised by this study. Complete dietary intake data are necessary to fully interpret the data obtained so far. The correlative endocrine measurements will still be valuable, and should be done in later flights where tracer studies are done. Improvements in sample timing for both kinetic and radiographic studies may allow an interpretation of the data with much higher confidence. The final analysis of the current data set, yet to be done, will determine if the data obtained can be used to draw definitive conclusions about calcium metabolism in the juvenile nonhuman primate during spaceflight.

BIBLIOGRAPHY

Cann, C. E.: and Adachi, R. R.: Bone Resorption and Mineral Excretion in Rats During Spaceflight. Am. J. Physiol., vol. 244, 1983, pp. R327-331.

Cann, C. E.; Young, D. R.; and Nagel, D. D.: Regulation of Calcium Metabolism in Hypodynamic Monkeys. Final Report, NASA Contract NCA2-OR745-804, Oct. 1978.

Gezenko, O. G.; Genin, A. M.; and Egorov, A. D.: Major Medical Results of the Salyut-6-Soyuz 185-Day Spaceflight. 32nd Congress of International Astronautical Federation, Vol. II, Session D-5, Rome, Sept. 6-12, 1981.

Heaney, R. P.: Radiocalcium Metabolism in Disuse Osteoporosis in Man. Am. J. Med., vol. 33, 1962, p. 188.

Morey, E. R.; and Baylink, D. J.: Inhibition of Bone Formation During Spaceflight. Science, vol. 201, 1978, pp. 1138-1141.

Roberts, W. E.; Mozsary, P. G.; and Morey, E. R.: Suppression of Osteoblast Differentiation During Weightlessness. Physiologist, vol. 24 (suppl.), 1981, pp. S75-76.

Vogel, J. M.; Whittle, M. W.; Smith, M. C.; and Rambaut, P. C.: Bone Mineral Measurements-M078, Biomedical Results of Skylab. NASA SP 377, 1977, pp. 183-190.

Wheadon, G. D.; and Shorr, E.: Metabolic Studies in Paralytic Acute Anterior Poliomyelitis. II. Alterations in Calcium and Phosphorus Metabolism. J. Clin. Invest., vol. 36, 1957, p. 966.

Wronski, T. J.; and Morey, E. R.; Effect of Spaceflight on Periosteal Bone Formation in Rats. Am. J. Physiol., vol. 244, 1983, pp. R305-309.

TABLE 1.- URINARY CALCIUM IN FLIGHT MONKEYS (mg/ml)

	17660	18332
L-21	.1355	.0199
L-13	.0218	
L-12	.0066	.0060
L-8	.014	
L-7	.0244	.0636
L-5	.0081	.0093
L-3	.0041	.0099
R+0	.0044	.0058
R+1	.0477	.0105
R+3	.0016	
R+4	.0164	
R+7	.1252	
R+10	.0237	
R+12	.0162	
R+18	.0456	
R+21	.0154	

TABLE 2.- CHEMICAL/BIOCHEMICAL MEASUREMENTS IN URINE

	Calcium mg/mg Creat.		Hydroxyproline µM/m Creat.		Osteocalcin ng/mg Creat.	
	17660	18332	17660	18332	17660	18332
L-21	1.41	0.03	0.78	0.86	4.9	17.7
L-13	0.38		1.33		10.5	
L-12	0.09	0.30	1.07	(4.55)	13.3	78
L-8	0.20		0.91		43.3	
L-7	0.07	0.28	0.81	0.43	9.7	20.2
L-5	0.02	0.05		0.92	35	16.8
L-3	0.01	0.10	0.65		293	11,300
R+0	0.02	0.006		1.32	111	210
R+1	0.10	0.03	0.74	1.20	10.2	15
R+3	0.01		0.49		14.9	
R+4	0.06				42.9	
R+7	0.99		0.67		8.5	
R+10	0.09		0.92		12.8	
R+12	0.05		1.23		9.9	
R+18	0.27		0.55		24.8	
R+21	0.12		1.37		12.7	

TABLE 3.- QUANTITATIVE MEASUREMENTS FROM RADIOGRAPHS

Monkey Number	Tibia		Radius		Ulna	
	Left	Right	Left	Right	Left	Right
18641(#1-Tima)						
Length (cm)	11.9	12.0[c]	10.75	10.85	12.3	12.2
CCT (25%)[a]	1.8[d]	1.5	3.3	3.7	3.0	3.0
CCT (50%)[b]	4.8	4.8	3.8	3.9	3.7	4.0
18815(#2-Ariel)						
Length (cm)	10.45	10.45	10.0	9.9	11.2	11.2
CCT (25%)	1.6	2.0	3.1	3.1	2.7	2.9
CCT (50%)	4.5	4.7	3.4	3.5	3.4	3.3
18063(#3-Teuton)						
Length (cm)	12.1	12.15	11.05	11.1	12.55	12.7
CCT (25%)	1.7	1.7	4.1	3.9	3.5	3.6
CCT (50%)	5.3	5.5	4.8	4.6	3.9	3.7
17660(#4-Abrek)						
Length (cm)	11.3	11.4	10.4	10.4	11.7	11.65
CCT (25%)	1.3	1.3	2.8	3.1	2.8	2.9
CCT (50%)	3.4	3.6	3.6	3.3	3.7	3.5

[a]Combined cortical thickness at 25% bone length from distal (radius/ulna) or proximal (tibia)
[b]combined cortical thickness at midshaft
[c]film blurred from motion
[d]posterior cortical thickness only at tibial 25% site

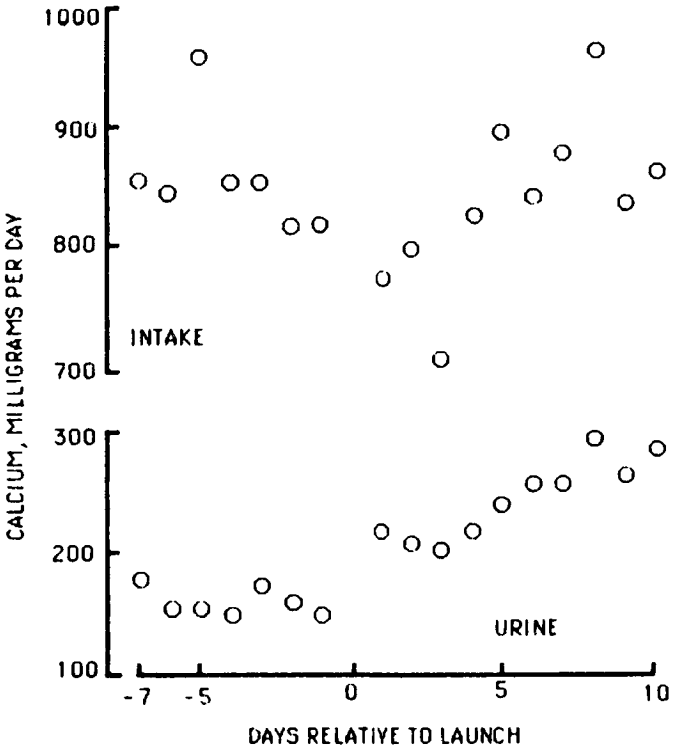

Figure 1.- Urinary calcium and calcium intake data (means) from the 9 Skylab astronauts for the 7 days immediately preflight and the 10 days inflight. Note stability of urinary output even with variation in intake during the initial 5-day inflight period.

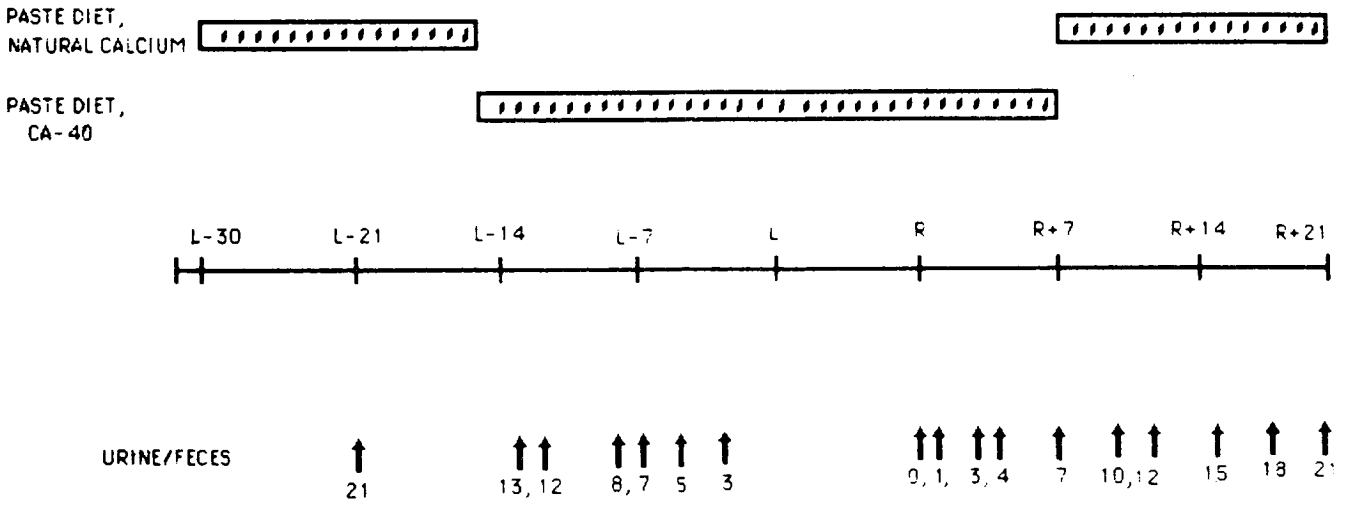

Figure 2.- Experiment timeline.

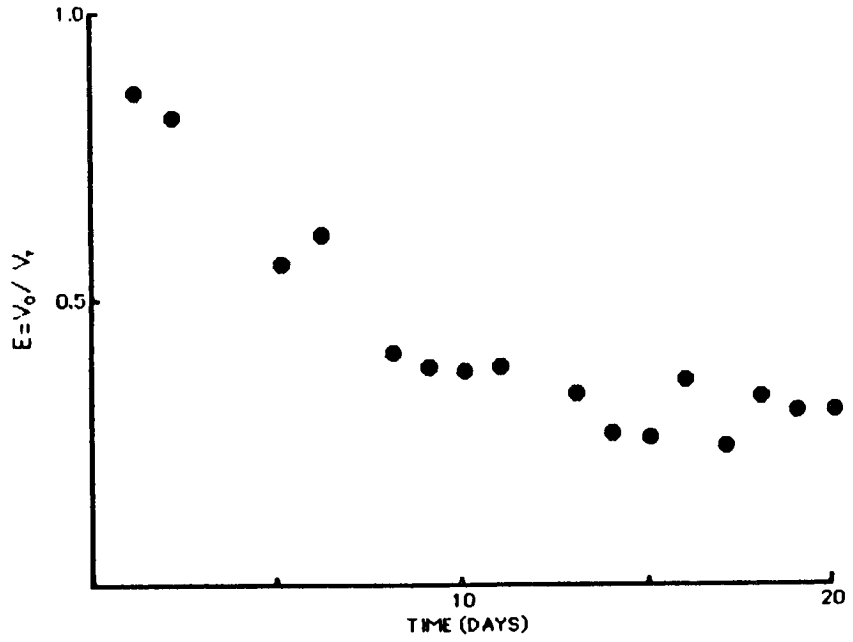

Figure 3.- Change in ratio of circulating ^{48}Ca relative to natural abundance (V_o/V_t) in a caged monkey following elimination of ^{48}Ca from the diet. ^{48}Ca abundance has reached a near-plateau level of 0.35, indicating 35% of calcium in the blood and urine is coming from bone.

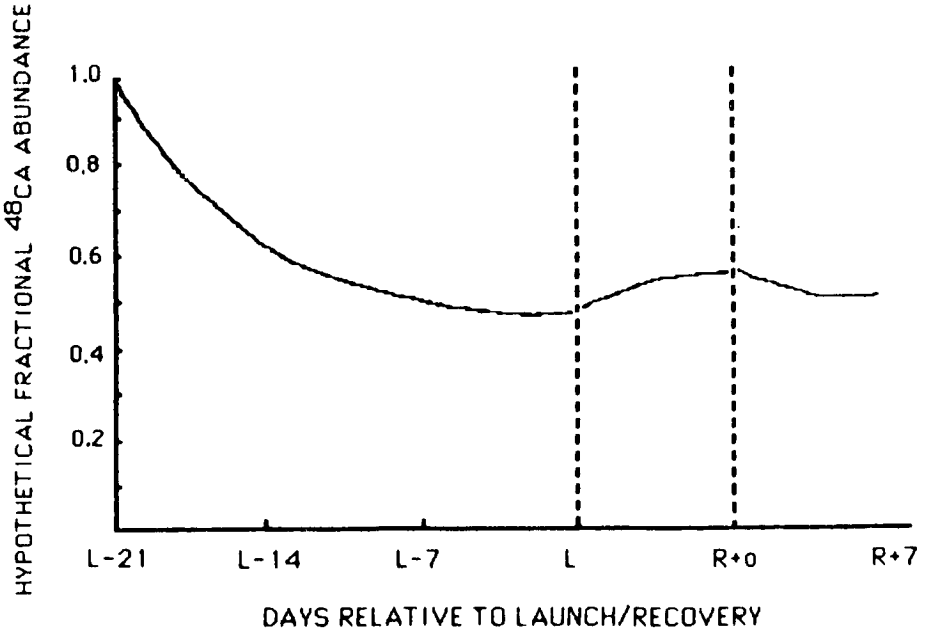

Figure 4.- Hypothetical fractional ^{48}Ca abundance curve for predicted stimulus due to spaceflight.

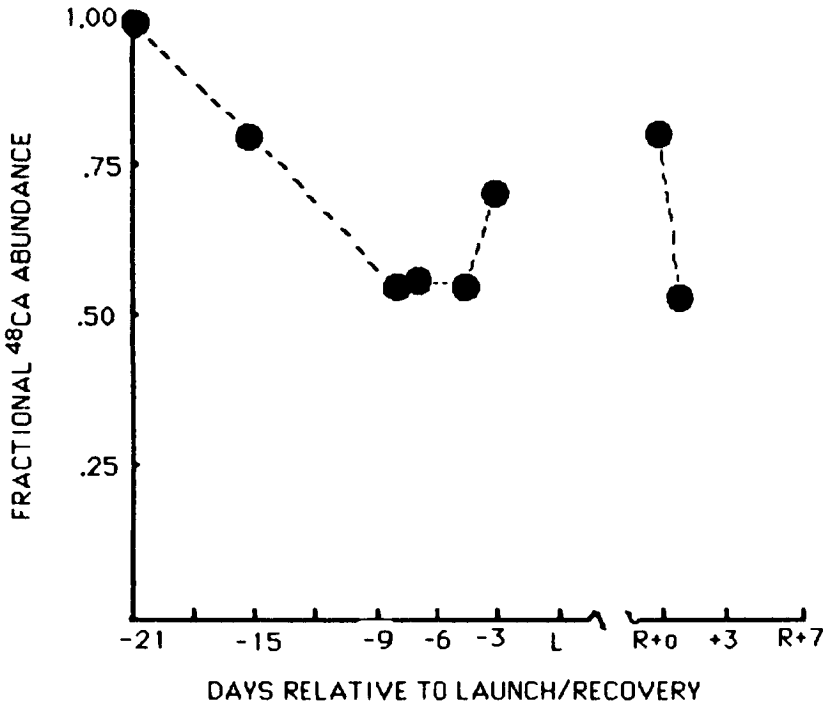

Figure 5.- Fractional ^{48}Ca abundance curve for one flight animal. Preflight data indicates 55% of circulating calcium comes from bone. The "spike" in abundance may be due to an exchange of calcium on bone surfaces.

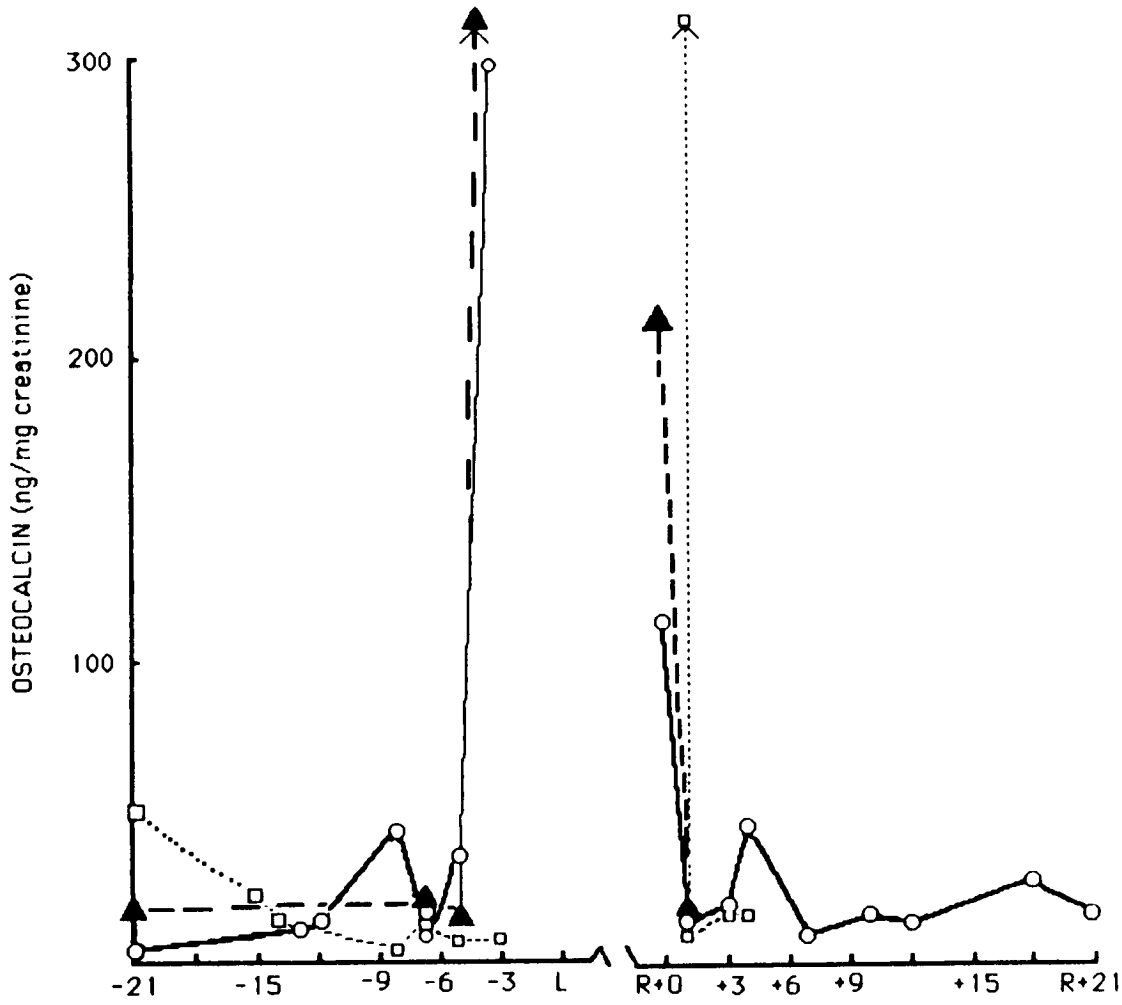

Figure 6.- Urinary osteocalcin output in flight monkeys 17660 (0) and 18322 (Δ), and in bioengineering test animal 17660 (□). Very high values may have been caused by either immobilization or stress responses.

EARLY POSTNATAL DEVELOPMENT OF RATS EXPOSED IN UTERO TO MICROGRAVITY

Jeffrey R. Alberts
Star Enterprises/
Indiana University
U.S.A.

L. V. Serova
Institute of Biomedical Problems
Ministry of Health
U.S.S.R.

J. Richard Keefe
BioSpace, Inc./
Case Western Reserve Univ.
U.S.A.

Zina Apenasenko
Institute of Biomedical problems
Ministry of Health
U.S.S.R.

SUMMARY

Five pregnant rats flown on Cosmos 1514 (Embryonic Days 13 to 18) were allowed to complete their pregnancies after recovery of the satellite. Four of the Flight females had normal deliveries of live offspring. These pups and their mothers were examined in a comprehensive, quantitative study of sensory and behavioral development. Two control groups were employed, viz., a Vivarium group and a Synchronous control group that was exposed to a 5-day mock flight. The postpartum cycle of lactation and maternal behavior was displayed by all dams. Flight and Synchronous females showed attenuated weight gains during their pregnancies. Flight offspring had higher rates of mortality and were smaller at birth, although well formed. Newborn, male Flight and Synchronous pups showed morphological signs of demasculinization, reflecting maternal stress during pregnancy. Sensory and motor functions were intact during postnatal development. Olfactory, tactile and vestibular perceptions were functional at birth. Audition and vision emerged at the normal postnatal time. High frequency (40 kHz) auditory detection appeared impaired, and there were signs of possible vestibular supersensitivity.

INTRODUCTION

The Soviet biosatellite Cosmos 1514 carried ten pregnant rats into orbit during days 13 to 18 of their 22-day gestation period. This was a bold and historic flight, the first occasion where mammalian development was challenged to proceed in the absence of terrestrial gravity.

The studies described in this report were part of a joint U.S./U.S.S.R. effort to ascertain if the basic processes of mammalian reproduction and development could be sustained during and subsequent to exposure to microgravity. More specifically, the present study was a broad program of research designed to both examine the adequacy of maternal care following space flight and evaluate the postnatal development of the infant rats.

The last trimester of the Norway rat's gestational period is a stage of formation and differentiation of sensory and motor systems vital to early survival and postnatal maturation. The present study represents a preliminary appraisal of the functional status of sensory and motor systems in the infant, and it charts some of the fundamental landmarks of maturation during the first 2 to 3 weeks of postnatal life.

MATERIALS AND METHODS

Animals. A total of 14 primiparous, Soviet Wistar rats and their litters were the subjects for these studies. The four dams in the Flight group were flown aboard the Cosmos 1514 satellite during days 13 through 18 of their pregnancies. The Synchronous control group (n = 5 dams) was housed in a compartment identical to that used for the Flight group. They were exposed to a regime of light and temperature cycles and to noise and accelerative levels mimicking those experienced by dams in the Flight group. These simulated flight conditions, on Earth, occurred during the same period of the Synchronous control group's pregnancies. The five dams in the Vivarium control group were transported to the launch site and back to the Moscow laboratories, but they were maintained in standard laboratory caging throughout their pregnancies.

Shortly after recovery of the biosatellite, Soviet scientists selected five of the ten rats on the flight for the present, postnatal experiment. The remaining five specimens were sacrificed for embryological studies. The five pregnant dams were transported to Moscow and housed temporarily in standard tubs, where they were maintained on a 16/8 LD cycle and the flight diet.

On the day after birth, rat dams and their offspring were transferred into specially designed cages that were monitored by a computer. Approximately two days later, the five Vivarium rats gave birth and they were housed similarly. The Synchronous control group, bred about 13 days after the Flight animals, entered the experiment after a parallel sequence of simulated flight conditions on Earth. The paste diet used for flight was the sole source of food for all three groups

throughout their pregnancies and early lactational period (see Mission Description for details).

All females (ns = 5 Flight, 5 Vivarium, 5 Synchronous control group) maintained their pregnancies for the full term. Four of the five Flight females delivered viable litters. The remaining female had an extended labor and delivered pups that were well formed, but nonviable (see reports of embryological studies).

Litters were culled to 8 pups each on the day of birth (Day 0), and the dam and her offspring were introduced into the maternity cages on Day 1. Additional sacrifices were made according to protocol.

Maternity Cages. The maternity cages used in this study (Star Enterprises, RMB-2) were designed to provide basic, normative data on maternal attendance in the nest, nest temperature, food intake, and the emission of high-frequency vocalizations by the pups. The cages (56 cm long, 42 cm high, 24 cm wide) were constructed from aluminum and Plexiglas. Each cage was divided into two sections, as illustrated in figure 1. The nest area was a pan, 21.6 cm long and 14 cm wide. Access to the nest was through a slot in one wall, 5.7 cm wide and 2.2 cm high. The slot was sufficient to contain the pups until about Day 15, but it was no obstacle to the dam. The floor of the nest was blanketed with wood shavings. The remainder of the cage was used by the dam for feeding from a glass bowl, drinking from a water bottle, and resting alone.

A round (0.95 cm diam), flat (0.32 cm), calibrated thermistor (YSI, Yellowsprings, OH) could be inserted into the center of the floor of the nest to measure nest temperature. In the ceiling, over the nest, was a small (8 mm) microphone for a QMC Bat detector (QMC, London, England). The detector was tuned to respond to pup cries at frequencies around 40 kHz.

The nest area was on one side of a fulcrum, and the floor of nest was depressed (about 3 mm) whenever the dam's weight was added to that of the litter. A microswitch recorded depressions of the nest floor. Daily adjustment of a counterweight compensated for growth of the litter, insuring that the weight of the dam was necessary and sufficient to actuate the microswitch beneath the nest floor.

The larger compartment of the cage contained the dam's daily ration of food and a drinking tube from which water was available ad libitum. Each day, an abundance of food was offered to each dam. Food intake was determined daily by weighing the bowl and its contents. Flight diet was used as the sole food until Day 10, postpartum. Thereafter, the dam's diet was supplemented with a variety of foodstuffs. Details and rationale for this procedure will be discussed in a later section.

A microcomputer system monitored the cages 24 hr/day and recorded (each 15 min) the number and duration of maternal visits to the nest. In addition, nest temperature and ultrasounds could be monitored simultaneously from as many as four cages. A video camera was positioned in front of two pairs of cages to make time-lapse recordings of mother-litter interactions in the nest.

Diet. Throughout this report, reference will be made to the "flight diet." This mixture, derived and prepared in Dr. Serova's laboratory, was used in previous Cosmos flights (Pace et al., 1981; Serova et al., Effect of Microgravity, 1984). It is a liquid paste which can be squeezed through feeding ports in the flight compartment. The diet is approximately 60% water, rendering it a source of both nutrients and fluid. Before and after the flight, the rats had access to water; while in the BIOS (flight) compartment, Flight and control group females derived both water and nutrition from this flight diet. The rats (Flight, Vivarium and Synchronous groups) in this study were maintained on this diet prior to, during, and after the spaceflight (or its simulation). After postpartum Day 10, however, this diet was supplemented with a variety of fresh foodstuffs: curds, nuts, vegetables and grasses.

Program of Experimentation. The studies described in this report comprise a broad program of analysis. The goal of the project was to evaluate the normalcy of infant rats that had been partially gestated in space. Normal growth and development of the infant rat, however, requires sustenance and nurturance from the mother. Thus, in order to interpret the studies of postnatal development, it is essential to first evaluate the quantity and quality of maternal care provided by dams in the Flight, Synchronous and Vivarium groups. These data will be presented and discussed in the next sections. Then, results of the infant studies will be presented and discussed. Because the infant studies involved a variety of tests and procedures, materials, methods, and results for each test will be presented under a single heading. To clarify the nature and range of this project, the full range of studies is shown in table 1.

MATERNAL CONDITION

The body weights of all pregnant female rats were equivalent at Launch, but five days later, at Recovery (Day 18 of pregnancy), there were significant differences in weight gain between groups (Serova et al., Cosmos 1514, 1984). Serova et al. (Cosmos 1514, 1984) reported that Flight females gained, on the average, only 5 gm, whereas Synchronous and Vivarium rats gained about 60 gm each. Nevertheless, by Postpartum Day 1, the beginning of the present study, there were marked differences across groups.

Body Weight. Rat dams were weighed by Dr. Serova each morning, on an O'Haus balance, to the nearest 1.0 gm. Figure 2 shows the body weight profiles, from postpartum Day 1 to 20. Note that there were significant differences in maternal body weights on Day 1, and these differences were sustained for at least the first 10 days. On Day 10, the flight diet was supplemented with a variety of foodstuffs (see Diet, above). Following dietary supplementation, maternal body weights converged across groups.

Food Intake. Maternal food intake was measured each morning by subtracting the amount of flight diet remaining in the dam's food dish from the amount offered to her the day before. Evaporative controls were not included. Figure 3 shows maternal food intake (median grams) from Day 1 to Day 10, postpartum. Days 11 to 20 are not shown because the amounts of supplemental diet eaten could not be accurately

measured. The food intake of mothers in each group were comparable, ranging from 39 to 51 gm on Day 1 to 65 to 80 gm on Day 8. Most evident was the similar pattern of overall increased intake, reflecting the increasing energetic demands of lactation.

To appreciate more thoroughly the relative metabolic performance of the three groups, maternal food intake was analyzed in two additional ways: (1) by ratio of amount eaten to maternal body weight; and (2) by ratio of amount eaten to weight of mother + weight of the entire litter (total biomass sustained). These ratios are useful indices for interpreting both the mother's responsivity to the demands of lactation and the growth patterns of offspring. Differences in the dams' body weights (fig. 2) make pertinent such ratios.

Tables 2 and 3 summarize maternal food intake, in terms of the above ratios, Days 1 to 10, postpartum. Figures 4 and 5 depict these data graphically and provide an overall summary. Looking at the summary histograms with each graph, it can be seen that the ratio of maternal food intake to maternal body weight ranged from 20.5% (Vivarium females) to 24.5% (Flight females)--not a significant difference. The data shown in figure 5, which are calculated to include the energetic requirements of the litter as well as the mother's body, reflect similar trends: Flight, 19.1%; Synchronous, 16.0%; and Vivarium 14.7%.

Water intake by the mother rats is shown in table 4. Because the past diet was hydrated, fluid intake was influenced by food intake. The amount of water taken from the spouts was therefore less than amounts usually seen in rats eating dry chow.

MATERNAL BEHAVIOR

Observations for the postnatal studies began on Day 1, postpartum. Figure 6 shows the amount of time spent in the nest by mother rats on each postpartum day, from Day 1 to Day 20. By correlating maternity cage data with video-taped tests, it was found that the 'nest time' measurement in this cage is a nearly perfect (.95) index of contact between dam and offspring (J. R. Alberts, unpublished observations, 1984). Contact time directly reflects the amount of maternal care directed at the offspring by the dam (Grota, 1973; Grota and Ader, 1969; Leon et al., 1978; and Rosenblatt and Lehrman, 1963).

Nest time decreased across the lactational cycle for both the Flight and control mothers. This is the normal profile for the cycle of maternal care in the rat (Larsen and Komisaruk, 1972; Plaut, 1974; and Rosenblatt and Lehrman, 1963). Time spent with the litter was somewhat higher for the Flight mothers relative to the controls. Nest time has been shown to be inversely related to the body mass of the litter and mother (Grota, 1973; Grota and Ader, 1969; and Leon et al., 1978). Thus, the behavior of the Flight mothers was appropriately modulated by their smaller mass and that of their offspring.

Figure 7 provides a more detailed view of the mother-litter interactions, with each graph providing an hourly account of maternal nest time and infant ultrasonic vocalization. For instance, the lower portion of figure 7 shows the amount of time spent in the nest by one Flight female (F71) during each hour of Postpartum Day 6. The upper portion of the graph shows levels of ultrasonic vocalizations emitted by the litter for each hour. Pup vocalizations are a stimulus for maternal approach and attention (Bell, 1979; and Noirot, 1972); maternal contact suppresses the emission of high frequency cries (Bell, 1979). It is apparent from the graphs in figure 7 that there was a general, inverse relationship between the occurrence of ultrasounds from the litter, and the time spent in the nest by the dam for each hour of the day. This pattern of results indicates that the behavior of the Flight mothers, like that of the controls, was appropriately correlated with the cries of the infants. In this manner, it can be seen that the flight experience did not eliminate the normal synchronization of maternal and infant behavior.

Both Flight and control dams exhibited circadian rhythmicities typical of maternal behavior (Grota, 1973; and Leon, 1978). The abscissa of each graph in figure 7 indicates the light and dark portions of day. It can be seen that the normal circadian pattern of maternal nest time was maintained in both the Flight and control groups, i.e., more mother-litter contact during the light portion of the day. In addition, the transition periods (light to dark and dark to light) were marked by a decrease in nest time. It appears that the circadian patterns of the Flight females may have been less pronounced than that of the control females. Note again, the total nest time by Flight females, Synchronous and Vivarium was greater (fig. 6) and that this difference in total time spent in the nest each day was provided by more contact time during the dark phase. Table 5 shows the average nest time/hr for dams in each group during the light and dark portions of the day. These data show the diminution of total nest time during the postnatal period and the proportion of time spent in the nest during the light and dark periods of the day.

On the basis of our inspection of these data, it appears that the circadian rhythmicity of maternal behavior, as seen in the global index of nest visitations, remained intact after exposure to microgravity and readaptation to 1-gravity. Note, however, that this is not intended to be a rigorous or definitive test of the female's endogenous rhythmicity; there were numerous environmental cues (zeitgebers) present, including the LD cycle, daily feeding, and daily rhythms of activity in the laboratory.

The time-lapse video records of maternal behavior proved to be unreadable, due to an incompatibility between the video camera and the electrical source. Thus, detailed visual information on maternal care is not available.

CONDITION OF NEWBORNS

Initial Body Weights. On the day of birth the litter was weighed as a unit. Beginning on Day 1, postpartum pups were marked and weighed individually. Pups were weighed on a Mettler top-loading balance (P400), sensitive to .01 gm. A large, warm

incubator, with arm ports, was used during weighing to reduce isolation stress in the litter and for individual pups. Pups were weighed and examined daily.

On Postnatal Day 1, the mean body weight of Flight pups was 6.25 gm; pups from the Vivarium control group were 7.06 gm, and the Synchronous pups had a mean weight of 6.02 gm. Mean body weights for both the Flight and Synchronous pups were significantly less than those of the Vivarium controls. Detailed inspection of these data revealed that the Flight pups not only had lower mean body weights, but they exhibited significantly more variance than either the Vivarium or Synchronous control pups. Table 6 shows the mean body weights and variance for Postnatal Days 1, 5, 10, 15 and 20. Bartlett's test for Homogeneity of Variance indicated that body weight variance was significantly different across groups, usually due to the range of weights in the Flight pups. On days 1 and 10, for example, variance in weight of Flight pups was nearly twice as great as that of the other groups [$F(2, 106) = 38.60$; $X^2 = 5.9$, and $F(2, 102) = 27.68$; $X^2 = 6.9$].

Gross Morphology. Pups were inspected each day at the time of weighing, to note their general appearance and to check for landmark events, such as eye-opening. Infant rats, partially gestated in space, appeared normal in proportion and general appearance. There were no allometric measures taken. Such measures might be useful in future studies, in light of the finding that Flight fetuses showed delayed skeletal development (Serova et al., Cosmos 1514, 1984; Serova et al., Effect of Microgravity, 1984; and Skuratova et al., 1984). Development of the pelage (fur) was equivalent across groups. Eye-opening occurred between Days 13 to 15 in Flight pups and Days 14 to 16 in controls.

Sexual Differentiation. On Day 1, each male pup was held gently under a dissecting microscope (16X) and a photograph was taken of the pup's anogenital region. In most cases, three photomicrographic samples were taken of each pup to reduce measurement error associated with differential stretching of the neonate's body. On each roll of film, photographs of a calibration scale were also taken for subsequent translation to actual linear distances. This was an adaptation of the method of Ward and Ward (Ward, 1972; and Ward, in press).

Sexual differentiation of male rat pups is revealed externally by anogenital (AG) distance, and it was not equivalent in all the males. In particular, male pups in the Flight and Synchronous groups displayed significantly smaller AG distances than male pups in the Vivarium group. The mean AG distance in male Vivarium pups was 1.76 mm ($n = 11$, S.E.M = 0.04) while the Flight group's was 1.42 mm (S.E.M. = 0.09, $t = 3.09$, $p < 0.01$, two-tailed test) and the Synchronous group's was 1.50 mm (S.E.M. = 0.04, $n = 16$, $t = 6.5$, $p < 0.001$ two-tailed test). AG distances were statistically equivalent between the Flight and Synchronous groups ($t = 0.73$, $p > 0.05$). Figure 8 shows these results.

Maternal stress during pregnancy can result in demasculinization of the male fetus, as reflected in decreased anogenital distance relative to the offspring of unstressed controls (Noirot, 1972; and Pace et al., 1981). Thus, these data suggest that Flight females showed signs of stress, but that this effect was not related to

their experience in space, since the same effect was observed in the Synchronous control group.

Growth. Figure 9 shows the growth curves for pups of all three groups, from postpartum Day 1 to Day 20. Both Flight and Synchronous pups were lighter at birth and lagged behind the Vivarium controls for the first week postpartum. Pups in the Synchronous group developed a slower growth trajectory than pups in the Flight and Vivarium groups. While no explanation for the latter result has been found, it suggests that the smaller size of the Flight pups was not a direct result of prenatal exposure to space conditions.

Mortality. Three pups in the Flight and Synchronous groups were sacrificed (on Days 4, 6, and 8) when it became clear that they were likely to die from failure to suckle or utilize milk; the pups were severely underweight and emaciated. They were the offspring of females F16 and F33. These dams had given birth to 13 and 9 pups, respectively, with one dead newborn in each litter. In addition, Flight female F25 produced a litter of 13 dead pups (see Serova et al., Cosmos 1514, 1984). In all, mortality among Flight offspring was 19%, compared to 0% in the Vivarium group and 2.5% in the Synchronous pups.

SENSORY AND MOTOR FUNCTION

The sensory and motor tests described below were designed for this project. The sensory tests were intended to demonstrate the presence of functional responsivity in selected modalities. Standardized stimuli were used. Parameters of stimulus intensity were intended to be suprathreshold for rat pups. Thus, the tests used here were not designed to assess the lower limits of sensitivity.

The sensory tests also provided useful data on motor development, particularly the development of postural control, strength, and interlimb coordination. Such data were analyzed directly from video records of the experiments.

Vestibular Tests. Surface Righting, Geotaxis, and Rotation tests were used to evaluate vestibular function in the pups. The Surface Righting test was administered on Days 2, 3, 4, 7, and 8. Geotaxis tests were given on Days 1, 5, 6, and 9, and the Rotation test was used on Days 2, 3, 5, 7, and 9.

Surface Righting Test. Surface Righting is a standard measure of vestibular and motor function (e.g., Altman and Sudarshan, 1975). During this postnatal testing, a pup was placed, belly up, on a soft (acrylic fur), level surface. It was held there by gentle pressure on the chest applied by the experimenter's finger. When properly aligned, the pup was released and given a maximum of 30 seconds to achieve a prone orientation. Each trial was recorded by a video camera located directly above the pup. Mirrors angled near the pup's head and along the side, provided simultaneous dorsal, lateral and frontal views for the video camera. Figure 10 illustrates the apparatus, which was also used for the Tilt Test,

(discussed below). To reduce temperature (cold) stress during testing, the animals and the apparatus were housed in a Plexiglas incubator and maintained at 32°C. The incubator was compatible with video recording, and it was equipped with ports to allow the experimenter to handle the subjects.

Table 7 shows the proportion of animals, in each group, that successfully righted themselves in this 30-second test. On Day 2, 25% of the Flight pups righted, whereas 31% of the Synchronous and 8% of the Vivarium pups successfully completed the test. These are statistically equivalent. We traced the age-related improvement of the righting response with age and found that it improved in all groups (table 7) until Day 7, when essentially all pups exhibited the righting response.

Average latencies, to achieve prone orientation from the supine, are shown in table 8. On Day 2 the Flight pups were the slowest to right themselves on the level surface. Flight pups required 11.2 seconds, whereas Vivarium and Synchronous pups righted themselves in 6.1 and 5.0 seconds, respectively. The significance of these differences is dubious, however, due to the variance and to the fact that such newborns do not reliably complete the response, thus adding to the ambiguity of the average latency measure. Righting responses became rapid in all groups by Day 7.

Infant rats placed in the supine position display stereotypical movements of various body parts. With age, these movements become integrated and coordinated, contributing to the development of the pups' righting reaction. Thus, it is pertinent to ask not only whether the pups showed the righting response, but how they right themselves at each age.

Our analysis of the pups' response in the righting test involved eight movement categories, illustrated in figure 11 and defined below:

1. Curl - Ventroflexion of the pup's body, involving the simultaneous compression of the rostral and caudal ends along the sagittal plane.

2. Curl/Roll - Ventroflexion, as above, maintained while the pup's body passively falls laterally to one side.

3. Rostral Twist - Rotation of the forelimbs to one side of the rostral end of the pup's body. The abdominal region and hindlimbs are not involved.

4. Caudal Twist - Rotation to one side of the caudal body of the pup, involving the hindlimbs and hips.

5. Partial Dorsoflexion - While the pup remains supine, it arches or hyperextends the anterior or posterior portions of the spine, in isolation or sequentially.

6. Partial Ventroflexion - While the pup remains supine, it moves the anterior or posterior portions of the body through the sagittal plane, in isolation or sequentially.

7. Active Roll - Coordinated, simultaneous or sequential rotation around the body axis, with the anterior and posterior regions moving simultaneously in the same direction.

8. Prone - Achievement of the prone position with all four paws on the surface.

Figure 12 provides a summary of the profile of movement reactions displayed by 2-day-old subjects during the first righting test. The overall patterns displayed in these histograms are typical of the infant rat. In 2-day-olds, the predominant movements, in response to placement in the supine position, are the curl and curl and roll (categories 1 and 2). In progressively older animals, these responses typically subside and are replaced by more isolated and differentiated movements, especially the twists (categories 3 and 4). In many cases, these twists are expressed and maintained in opposition to one another, resulting in the appearance of "squirming" movements. Coordinated, unidirectional responses, such as the roll (category 7), become the more effective, mature means of righting.

Geotaxis (Tilt) Test. Infant rats placed on an inclined plane tend to orient their body against gravity, a response termed "negative geotaxis." Altman and Sudarshan (1975) report that geotaxic responses in the infant rat become fully evident by Day 5, depending on the length of the test and angle of the substrate. After about Day 9, this test becomes less clear because the pup tends to turn and explore the test surface with diminished geotaxic responses.

For this postnatal testing, pups were grasped behind the shoulders and placed on a 20° incline. The surface was a soft, acrylic fur (nap length = 4 mm). The tilt table was inside an incubator, maintained at 32° C. The axis of the pup's body was parallel to the angle, facing down. Each trial lasted 30 seconds and was recorded with the overhead video camera and mirror arrangement described above.

The video records of the pups' reactions on the 20° tilt table were analyzed for those animals exhibiting negative geotaxis within 30 seconds. The response was defined as an active movement that turned the axis of the body at least 45° against the downward angle. This reaction requires perception of the tilt and sufficient strength and coordination to negotiate the turning movements. Thus, the negative geotaxis measure is a test of both sensory and motor competence. Because the newborn rat is usually not capable of emitting reliable responses on the tilt platform, scoring methods were adjusted to suit the characteristics of the infants. The animals were tested at various postnatal ages to evaluate the maturation of their responses.

On Day 1 postpartum, as a pup was being placed gently on the tilt platform, it was lowered with its body axis oriented horizontally. When it was within 2 cm of the platform, the pup was tipped so that its head was lower than the body. Using the video records (particularly from the side view in the mirror), it was determined whether the pup emitted a dorsoflexion of the neck (raising its head against the direction of change; see fig. 13). Only Flight and Vivarium pups were tested in

this manner, but equal numbers of pups in both groups, (67% (20/30) of the Flight pups and 59% (13/22) of the Vivarium group) showed this vestibular response. Lyon (1951) has successfully used a similar test to detect genetically related otoconial deficits in mice.

Infant pups can show other subtle responses on the Tilt platform, indicative of detection of vestibular and/or procrioceptive pertubation. The characteristic tail extension response of the tilted pup was also noted (see fig. 13). This reaction was infrequent among the Day 1 subjects (only 13% and 9% for Flight and Vivarium animals), but it became more common with age. During the Tilt test, on Day 5, 58% of the Flight and 51% of the Synchronous pups displayed the tail extension, whereas the response was seen in 95% (36/38) of the Vivarium pups. The developmental emergence of this difference, subsequent to equal performance earlier in life, may reflect motoric differences between groups. Indeed, this developmental divergence may be a reflection of the slower growth in the Flight and Synchronous groups.

Negative geotaxic responses emerged during the Day 5 test, as pups developed the strength and coordination to turn their bodies across the 20° tilt platform. These responses were seen in all three groups, as shown in table 9. On Day 5, the geotaxic response was displayed by 37% of the Vivarium pups and 23% and 18% of the Flight and Synchronous pups, respectively. These differences were not reliable, however, and fluctuated across the tests (see table 9).

Rotation Test. Pups were placed in the center of a turntable apparatus, with their thorax at the center of a 9 cm round arena. The turntable was in the testing incubator, with a video camera mounted overhead. There was an initial 30-second period to gauge the amount of head and body movement displayed by the pup, followed by a 30-second period of rotation at 33 rpm. The focus of this test was on the presence of an angular deviation of the head in response to the spin, illustrated in figure 14. Because the pup's eyes were sealed shut in all the age groups tested here, visual cues were not available and the pup's responses were based on detection of the angular momentum during rotation.

The first Rotation test was administered on Day 1. Sixty-six percent (19/29) of the Flight pups and 74% of the Vivarium group responded to the rotational stimulus (n.s., $p > 0.10$). On Day 2 the Rotation test was repeated. The responses for Flight, Vivarium, and Synchronous groups were 85%, 73% and 79%, respectively. On Day 5, Flight pups showed a significant increase in response. Five-day-old Flight pups emitted the head deflection in 96% (24/25) of the trials, whereas the Vivarium and Synchronous pups responded in only 62% and 73% of the tests ($X2 = 5.03$, $p < 0.05$). On Day 7 there were no significant differences. Figure 15 shows these results.

On Day 9 it was no longer appropriate to conduct the spin test, because the reflexive response had disappeared or was masked by autonomous movements in the pups. These movements tend to involve pivoting (in which the animal's side-to-side head movements and corresponding forelimb placements turn the front of its body while the rear limbs and hips remain in place) and walking (which involves interlimb

coordination of both the forelimbs and hindlimbs). The Day 9 test was used to make a 30-second video recording of each animal's dynamic adjustments to placement on the (motionless) platform. It was found that 9-day-olds, in all three groups, showed equivalent amounts of pivoting and walking, typical of their developmental stage (see fig. 16).

Tactile Sensitivity. After 1-day-old pups completed the first Surface Righting test, they were moved to a prone position and touched with a vonFrey hair (0.5 gm pressure). Because tactile sensitivity develops topographically in a rostral-to-caudal direction (Mozell, 1971), each pup's body was touched on the head, shoulders and flank. The trial was videotaped and movement responses were used to evaluate detection of the tactile stimulus.

There were two noteworthy results from this test. First, all pups evidenced tactile responsivity to the punctate stimulus. Regional sensitivity was intact across all body areas tested. The second pertinent observation was that the Flight, Vivarium and Synchronous pups were equally competent in their motor responses to the tactile stimuli. Any gross motor response (e.g., twitches, withdrawal, startle reaction) was treated as evidence of detection. Most interesting, however, was the demonstration of integrated, complex response patterns in these 1-day-old subjects. For instance, in response to tactile stimulation on the flank, pups demonstrated rudimentary hindlimb scratching movements accompanied by a lateral flexion of the body.

Development of Sniffing and Olfactory Detection. The mammalian sense of smell requires that airborne molecules be swept across the olfactory epithelium during cycles of inspiration and expiration. In an obligate nose-breather, such as the rat, respiration is inextricably linked to olfactory sampling. The term "sniffing" is used to describe a distinct type of nasal respiration, composed of a string of regular, rapid (> 5 cps) "nasal sampling epochs" (Alberts and May, Nasal Respiration, 1980; and Macrides and Chorover, 1971). There is evidence that the temporal parameters of nasal sampling are a component of the perceptual mechanisms of olfaction (Macrides and Chorover, 1971; Moulton, 1967; and Mozell, 1971); analysis of respiratory movements thus pertains to behavioral and neural arousal (Holst and Kolb, 1976; Komisaruk, 1970; and Larsson and Komisaruk, 1972), as well as sensory coding.

Olfactory perception in the rat is crucial to early survival and numerous aspects of adaptation to postnatal life (Alberts, 1984). The status of this sensory system in young pups was therefore examined and the development of respiratory rate, lability (maximums, minimums, durational changes), sniffing, and olfactory detection was traced during early postnatal life.

The rat pup's unconditioned sniffing response to suprathreshold olfactory stimulation (Alberts and May, Nasal Respiration, 1980) was used to measure olfactory detection. The olfactory stimulus was 100 µl of 10^{-3} amyl acetate. Previous research suggests that the development of the pup's sensitivity to this broad-spectrum odorant is similar to that for a biological stimulus (Alberts and May, Olfaction, 1980).

Respiratory rate was measured by strain-gauge plethysmography (Alberts and May, Nasal Respiration, 1980; and Alberts and May, Olfaction, 1980), using a Parks Electronics Plethysmograph and miniature, closed-loop, mercury-filled silastic strain gauges (3/8 in or 1/2 in, depending on pup size). The strain gauge was slipped around the pup's thoracic area and the infant was placed in a glass bowl, on a surface of wood shavings. This bowl was set within a small, heated fume hood (33° C) into which room air was drawn by two muffin fans. The exhaust was filtered through 450 gm of activated charcoal. Each trial consisted of three measurement periods. Pups were fitted with a strain gauge and placed in the test bowl within the heated hood. First, upon introduction of a pup into the test apparatus, a 30-second baseline measurement of respiration was recorded. Then a clean cotton swab was held for 10 seconds about 1 cm from the pup's nose. The swab was removed and loaded with 100 µl of 10^{-3} amyl acetate from a micropipette. The olfactory stimulus was then presented in the same manner as the blank control. Following withdrawal of the odorant, respiration was recorded for an additional 20 seconds.

Respiratory signals were recorded on a Brush chart recorder (paper speed 2 cm/second). An event marker was used to indicate the periods of presentation of the blank and the amyl acetate stimulus.

Figure 17 illustrates the average rates of respiration during the initial 30 seconds in the glass dish. The age-related rise in average respiration rate can be accounted for by more and longer bursts of sniffing, which is part of the development of arousal as exhibited in novel environments (Alberts and May, Nasal Respiration, 1980; and Welker, 1964). Table 10 provides a comprehensive view of the development of respiration rate and sniffing in 3-, 6-, and 10-day-old pups. These data are based on continuous respiratory recordings during the initial (readable) 30 seconds in the test chamber, and therefore reflect the animal's tendency to be aroused by the perception of environmental novelty. Under these conditions it is expected that pups between 1 and 11 days of age will show an increasing tendency to emit bursts of polypnea, and the duration of bursts will also increase (Alberts and May, Nasal Respiration, 1980; and Welker, 1964). The data in table 10 clearly fulfill this prediction. Mean respiratory rate (cps) increased, as did the total range of respiratory rates emitted during the 30-second trial. For instance, 3-day-old Flight pups ranged from 2 cps to 5 cps during this baseline measurement, with a median of 3.6 cps overall. Vivarium controls were nearly identical: 3.5 cps overall, consisting of one-second intervals that ranged in rate from 2 to 6 cps. Synchronous controls were slightly slower on Day 3 and equivalently faster during the Day 6 test. The small sample size precluded statistical tests, but it can be seen that all three groups overlapped on all parameters, suggesting overall equivalence.

The frequency of "spontaneous sniffing" during the 30-second trial was typically low in the 3-day-olds (e.g., $p = 0.05$ indicates 6 seconds of respiration, at 5 cps or more, out of 120-second observations). Table 10 shows the dramatic, age-related increase in the 6- and 10-day-olds. These measures were not extended beyond Day 10, after which a decline in baseline rate should be observed.

All pups responded to the amyl acetate signal, and the levels of sniffing induced by the suprathreshold stimulus were also equivalent across groups at each age. The maximum sniffing achieved was examined during two consecutive seconds within the 10 seconds of stimulus presentation. There was complete equivalence across all three groups. At 3 days of age, pups attained rates up to 7 cps in all groups. By 6 days of age, they achieved 8 cps.

Together, these data indicate that the Flight experience did not interfere with the development of nasal chemosensitivity in the pups. The development of neuromuscular control, as well as central excitatory states, appeared normal in all groups. These tests do not, however, represent stringent tests of olfactory abilities, as do threshold sensitivity, discrimination, and recognition. The crucial role of olfaction in the life of most mammals and the outstanding plasticity of this system, (especially in the perinatal period) make it desirable to investigate further the establishment of olfactory function during and after exposure to microgravity.

Auditory Sensitivity. Auditory detection of 4-kHz and 40-kHz tones (both at 90 dB) was tested in 14- and 19- to 20-day-old pups. The startle reflex was used to measure detection of the stimulus (Brunjes and Alberts, 1981). Each pup was placed on a ballistic stage contained within a warmed, aluminum chamber (43 by 29 by 29 cm) lined with acoustic foam. The two loudspeakers that generated the acoustic stimuli were equidistant from the animal (about 12 cm).

The voltage output of the ballistic stage was filtered and amplified with a Grass preamplifier and then displayed on a Brush chart recorder. Minute startle movements were visible as discrete peaks at least 2X baseline on the chart record. A signal marker indicated onset of the tones. Each tone was presented at least three times if there was no apparent response. Pups were given at least two minutes to habituate to the test apparatus before tones were presented. The tones were generated by a frequency oscillator, amplifier and attenuator (see description in Brunjes and Alberts, 1981).

Auditory sensitivity was first tested at 14 days of age, shortly after the external ears opened. The 4-kHz tone elicited responses from 100% (18/18) of the Flight pups and 68% (21/31) of the Vivarium control. Chi-square analysis indicated that this was a statistically significant difference ($X^2 = 7.29$, $p < 0.01$). There were no responses to the 40-kHz tone in either group at 14 days; this is to be expected, since it is typical for high-frequency sensitivity to develop later.

Tests at 19 to 20 days, with the 4-kHz stimulus, yielded equivalent levels of sensitivity: 69% (11/16) of the Flight pups responded, compared to 56% (10/18) for the Vivarium control (n.s., $X^2 = 0.62$, $p > 0.10$). In contrast, there were significant differences in the high-frequency tests with these pups. In response to the 40-kHz stimulus, only 38% (6/16) of the Flight group responded, whereas 72% (13/18) of the control showed detection ($X^2 = 4.14$, $p < 0.05$). Figure 18 summarizes these data.

Because of the small sample size for this experiment and the use of a response measure which is prone to "false negatives," (i.e., failure to reveal an animal that detects the stimulus), it is premature to conclude that the Flight animals had poorer high-frequency auditory sensitivity. Nevertheless, there is an apparent trend in these data and it might warrant further examination on both behavioral and anatomical levels.

Visual Acuity. Pups were placed individually in a clear, Plexiglas cylinder (10.8 cm high × 12.7 cm diam) that was located in the center of a larger cylindrical drum (60 cm high × 50 cm diam). The inside wall of the surrounding drum was covered with a vertical pattern of alternating black and white stripes, each subtending 1.5 deg of visual angle on the pup's retina. Figure 19 depicts this apparatus.

Previous research indicated that Sprague Dawley (albino) rat pups could resolve a 1.5° spatial frequency, as judged by their optomotor responses to slow rotation of the drum (Brunjes and Alberts, 1981). The pups' optomotor response (turning of the body in response to movement of the visual field) was incorporated as the measure of detection for this test. As in previous work, the striped drum was rotated at a rate of 6 rpm. A trial consisted of a 20-second period for habituation, a 20-second baseline period, a 20-second rotation period, an additional 20-second baseline period and a final 20-second rotation period in the direction opposite the first. Trials were videotaped for subsequent analysis.

The results of the vision test, shown in figure 20, showed clear responsivity in the Flighted pups, 93% (14/15) of which detected the 1.5° array. For the Vivarium pups, 87% (26/30) Chi-Square tests confirmed that these proportions were statistically equivalent ($X^2 = 0.45$, $p > 0.10$). Due to the high level of response in these two groups, it was unnecessary to test Synchronous litters.

DISCUSSION

Collectively, the results of this program of experimentation provide a preliminary picture of early postnatal mammalian development following a late, prenatal period of exposure to space conditions. The 5-day flight of Cosmos 1514, although not long in comparison to other satellite voyages, encompassed 23% of the rats' gestation period. The period selected for this experiment, Prenatal Days 13 to 18, contains numerous events critical to the establishment of the sensory and neural systems vital to survival.

It is clear from these preliminary studies that the absence of normal gravitational forces did not preclude the successful expression and completion of prenatal developmental events; postnatal development, subsequent to the microgravity experience, was capable of proceeding. This result, alone, is significant, because these are the first observations of mammalian ontogenesis subsequent to space flight. There remain specific issues and aspects of the results which merit discussion.

Variability and Mortality in Flight Pups. For measurements taken in these studies, pups in the Flight groups tended to evidence greater variability than

Vivarium or Synchronous controls. Such variances were analyzed for body weights at various points later in development (see table 5). The results indicated that, although rat pups can attain normal size after exposure to microgravity, some aspects of exposure can have long-lasting impact on the growth of pups. This effect may be related to individual genotype, or it may be more directly linked to an unidentified aspect of maternal care.

Another serious reminder that mammalian reproduction and development may prove to be dangerously vulnerable to prolonged (or differently timed) exposure to microgravity was the higher level of infant mortality among the Flight pups. The rate was 19% in comparison to 0% for the Vivarium and 2.5% for the Synchronous controls. Again, it is possible that this aspect of the data, like the variability among pups, was an effect translated via the Flight mothers. Additional experiments, using cross-fostering procedures, could be used to identify specific maternal contributions to altered development and those endogenous to the offspring.

Sensory Development after Exposure to Microgravity. Five sensory modalities of the developing rat pup were tested, namely the tactile, vestibular, olfactory, auditory and visual senses. It was determined that each of these systems attained function at the appropriate postnatal developmental stage. It must be understood, however, that the tests used were not comprehensive assessments of threshold levels or range of function. These were systematic, quantitative tests of detection in each modality. In addition, these studies were terminated by Day 20, postpartum. Subsequent development and the maintenance of function were not evaluated.

To the limits of interpretation of the testing regime, development of function appeared normal for the tactile, olfactory, and visual systems of the Flight pups. Tactile responsivity to strong, (probably noxious), punctate stimulation was found on the snout, shoulder, and flank of the 2-day-old. Three-day-olds showed normal levels of olfactory responsivity to amyl acetate, and their "nasal sampling" (sniffing), which is an important component of olfaction, was functionally intact. Normally, to find and suckle from nipples requires olfactory ability, and this was clearly present in the Flight pups.

Visual Acuity for a 1.5° pattern appeared intact shortly after eye-opening. Optokinetic responses are most revealing about function for peripheral visual processing, and more sophisticated measures are needed to evaluate higher levels of perceptual processing (Alberts, 1984).

Vestibular Function. Three tests of vestibular function were used: surface righting, geotaxis, and angular rotation. There were some trends in these data. To focus on the early tests, administered on Postnatal Days 2 and 3, it was found that Flight pups responded more to cues of rotation than did the controls. While the limited number of litters available for this study constrained the power of statistical analysis, the results suggest that the developing vestibular system, uninfluenced by gravitational cues, may become functionally supersensitive. Sensitivity of the system might be set developmentally by the level of activity during formation. Reduced activity may be a form of "deafferentation" (i.e., removal of input), which

has been shown to induce a heightened sensitivity in some neural systems (Mozell, 1971; and Narayanan et al., 1971). This is suggested as a novel hypothesis of denervation supersensitivity in vestibular function, following ontogenetic exposure to microgravity.

Auditory Function. The development of auditory function in most animals begins with early sensitivity to lower frequencies and progressively extends this sensitivity to higher frequencies (Alberts, 1984). This sequence was apparent in Flight and control rats. Although low-frequency sensitivity appeared equivalently intact during the early tests, high-frequency sensitivity (40 kHz) was lower in Flight pups on Days 19 to 20. Flight pups may have sustained a permanent deficit in their high-frequency perception or a mere developmental lag, leading to equivalent, but delayed function. The protocol used for the postnatal tests may have introduced some uncontrolled variability into these results. Pups were tested at predetermined points in relation to their day of birth, rather than in relation to the time of ear-opening. This was required by the overall schedule of testing. The visual acuity testing shares this procedural feature. There was a slightly different range in the time of eye-opening across groups which could be included in the determination of test dates (see Brunjes and Alberts, 1981). Future work might be based on more standard referents of sensory testing, such as the development of related landmark events (Brunjes and Alberts, 1981).

Motor Development. The present studies were not designed to focus on the interesting and important topic of motor development and microgravity. Most of the sensory tests indirectly measured coordinated movement or strength. A common response to tactile stimulation of the flank is a sterotypical, repetitive, "scratching" reaction with the neonate's ipsilateral rear leg. This was evidenced equally by Flight and control pups. The response is analogous to scratching, although the paw does not contact the body.

We also noted the incidence of poor motor control and ataxia in the rear legs of numerous pups. The majority of these, but not all, were pups born to Flight mothers. Some pups in the Synchronous litters also showed these symptoms, but to a milder degree. The appearance of the syndrome in the Synchronous pups indicates that this was not a space-specific effect. It correlated well with smaller, weaker-looking pups, and it was one of the reasons that the mothers' diets were supplemented with fresh vegetables and nuts on Day 10. These anomalous characteristics subsided after Day 10. It is not known if this was a dietary insufficiency, undernutrition related to maternal weight, or a stress-related effect. Each of these is an important possibility. The flight diet, although thoroughly tested with adult male and female (pregnant and nonpregnant) rats, had not been evaluated in the lactating animal. This may be a crucial factor for future studies, particularly those involving the interactions of reproductive effort and systematic stress.

Maternal Context of Postnatal Development. Maternal behavior of the rat, subsequent to a 5-day exposure to weightlessness and the melange of disruptive events associated with the study, was expressed well by all mothers. Most offspring survived, attesting to the sufficiency of the mothers' behavior, lactogenesis and

related aspects of her reproductive physiology. Observations of the maternal behavior of Flight, Synchronous and Vivarium dams suggest typical profiles: Circadian rhythmicity of nest time, patterned bouts, gradual decrease in nest time during the lactational cycle, and synchrony between infant vocalization and nest attendance.

There were several lines of evidence, however, indicating that the mothers were not equivalent during the postflight period. Most apparent were the large differences in body weight across groups. On the basis of the inspection of waste traps in the animal compartments, L. V. Serova (personal communication, Nov. 1984) reported that the animals had eaten their rations. This suggests the conditions of flight may have resulted in the differential utilization of nutrients by flight versus control animals. This is an unexplored topic. Regardless, it is important to note that the Vivarium dams, by the end of their pregnancies, had added about 20% more body mass than the Flight animals. The Synchronous animals were intermediate. Thus, ontogenetic effects observed in the Flight pups may have arisen, indirectly, through the altered metabolism of their mothers during pregnancy or after. Food intake of the lactating dam was evaluated in relation to their size and the size of the biomass of offspring. There was some evidence of enhanced relative intakes (figs. 4 and 5), but the increments were not large.

Maternal Stress. Nonspecific stress has previously been discussed as a potential factor that can appear in studies of weightlessness (Serova et al., Effect of Weightlessness, 1984). Indeed, Serova et al. (Effect of Weightlessness, 1984) described an experiment in which rats were centrifuged at 2 g during Days 14 to 21 of gestation, thereby approximating the same phase of intervention used in Cosmos 1514. Some of the effects observed in pregnant rats exposed to hypergravitational forces resembled those found after the microgravitational exposure associated with space flight. For example, the centrifuged adults sustained a 60-gm attenuation of growth relative to controls, which was equal to that seen in the present Cosmos study. There was greater mortality in the offspring of centrifuged females, and fetal bone development was delayed. As in Cosmos 1514, rats in the Synchronous control groups exhibited some of the effects seen in the centrifuged animals. These data support an interpretation of general stress reactions, rather than consequences specifically related to gravitational forces.

The morphometric measure of anogenital (AG) distance in male rat pups has been found to be an index of maternal stress during pregnancy. It was fortuitous that the flight period in this study corresponded to the portion of pregnancy when such data on stress effects have been collected (Pace et al., 1981; and Plaut, 1974). Test results, summarized in figure 8, indicate that the male offspring of Flight and Synchronous dams had significantly reduced AG distances. This can be interpreted as evidence of significant maternal stress during pregnancy, but not a form of stress related to the space environment, per se. This result, nevertheless calls attention to the scientific and ethical need to study and minimize stress to animals in the space habitat.

CONCLUSIONS

The results of this premiere study of mammalian development in microgravity are both clear and clearly important: Mammalian reproduction has passed its first direct test in space. The reproductive success of the Cosmos 1514 rats demonstrates that mammalian gestation can proceed in the absence of terrestrial gravity. Rats that were impregnated on Earth and flown for five days during the final trimester of pregnancy, delivered living, normally formed and ontogenetically competent offspring. Their postnatal development was generally normal and species-typical.

We have reported the findings of our detailed tests of sensory and motor function, and have discussed the interpretation of each measure that showed a noteworthy deviation from typical values or contrasted with one of the control groups.

The experiments described in this report are part of a more comprehensive study of the impact of space conditions on mammalian fetagenesis. Five of the ten Flight females, along with their counterparts in the control groups, were sacrificed at Recovery (Day E18). Keefe et al. (1985) described a striking profile of aberrations in neural development, most notably, the presence of mitotic figures in secondary (subventricular) cortical zones and within the inner plexiform layer of the eye. In addition, the cortical plates were thinner, the ventricular cavities were enlarged and the membranous labyrinths were reduced. These developmental anomalies were evident in each of the Flight fetuses. They were interpreted to have resulted from either retardation in development or as a secondary consequence of altered fetal fluid and electrolyte balance (Keefe et al., 1985).

The general well-being and functional patency of the newborn rats described in this report contrasts sharply with the picture of ontogenetic retardation or redirection displayed by the fetuses. The present results concur well with the anatomical picture of the postnatal studies (Keefe et al., 1985). That is, in contrast to the data derived from Flight animals sacrificed at Recovery, the anatomical and functional picture presented by the postnatal studies show ontogenetic normalcy. This suggests that the five-day interval between Recovery and birth of the Flight pups may have constituted an ontogenetically significant period of readaptation to gravity, during which time compensatory alterations in development removed or repaired the effects of ontogenetic perturbations exerted by the space environment. This is an important possibility that should be taken into account in the design and interpretation of subsequent studies.

Future experimentation should include studies of the impact of space conditions on other phases of the mammalian developmental cycle, as well as more detailed examination of the ontogenetic period addressed for the first time in the present study. The present results point to the likelihood of success for future studies and are an optimistic signal for the possibility that terrestrial life and reproduction can continue in new realms, never before encountered in its evolution.

BIBLIOGRAPHY

Alberts, J. R.: Sensory-Perceptual Development in the Norway Rat: A View Toward Comparative Studies. R. Kail and N. S. Spear, eds., Comparative Perspectives on Memory Development. L. Erbarm Asso. (New Jersey), 1984, pp. 65-101.

Alberts, J. R.; and May, B.: Development of Nasal Respiration and Sniffing in the Rat. Physiol. Behav, vol. 24, 1980, pp. 957-963.

Alberts, J. R.; and May, B.: Ontogeny of Olfaction: Development of the Rat's Sensitivity to Urine and Amyl Acetate. Physiol. Behav., vol. 24, 1980, pp. 965-970.

Altman, J.; and Sudarshan, K.: Postnatal Development of Locomotion in the Laboratory Rat. Anim. Behav., vol. 23, 1975, pp. 896-920.

Bell, R. W.: Ultrasonic Control of Maternal Behavior: Developmental Implications. Amer. Zool., vol. 19, 1979, pp. 413-418.

Brunjes, P. C.; and Alberts, J. R.: Early Auditory and Visual Function in Normal and Hyperthyroid Rats. Behav. Neural Bio., vol. 31, 1981, pp. 393-412.

Grota, L. J.: Effects of Litter Size, Age of Young and Parity on Foster Mother Behavior in Rattus norvegicus. Anim. Behav., vol. 21, 1973, pp. 78-82.

Grota, L. J.; and Ader, R.: Continuous Recording of Maternal Behavior in Rattus norvegicus. Anim. Behav., vol. 15, 1969, pp. 722-729.

Holst, D. V.; and Kolb, H.: Sniffing Frequency of Tupaia belangeri: A Measure of Central Nervous Activity (Arousal). J. Comp. Physiol., vol. 105, 1976, pp. 243-257.

Keefe, J. R.; Alberts, J. R.; Krasnov, I. B.; and Serova, L. V.: Developmental Morphology of the Eye, Vestibular System and Brain in 18-Day Fetal and Newborn Rats Exposed in Utero to Null Gravity During the Flight of Cosmos 1514, NASA TM-88223, 1986.

Komisaruk, B. R.: Synchrony Between Limbic System Theta Activity and Rhythmical Behavior in Rats. J. Comp. Physiol. Psychol., vol. 70, 1970, pp. 482-492.

Larsson, K.; and Komisaruk, B. R.: Abnormally Fast Vibrissa Movements Induced by Tetrabenazine in Rats. Psychopharmacologia, vol. 23, 1972, pp. 300-304.

Leon, M.; Crosskerry, P. G.; and Smith, G. K.: Thermal Control of Mother-Young Contact in Rats. Physiol. Behav., vol. 21, 1978, pp. 793-811.

Lyon, M.: Hereditary Absence of Otoliths in the House Mouse. J. Physiol., vol. 114, 1951, pp. 410-418.

Macrides, F.; and Chorover, S. L.: Olfactory Bulb Units: Activity Correlated with Inhalation Cycles and Odor Quality. Science, vol. 175, 1971, pp. 84-87.

Moulton, D. G.: Spatio-Temporal Patterning of Response in the Olfactory System. Olfaction and Taste II, T. Hayashi, ed., Pergamon (Oxford), 1967, pp. 109-116.

Mozell, M. M.: Spatial and Temporal Patterning. Handbook of Sensory Physiology IV, Chemical Senses, L. M. Biedler, ed., Springer-Verlag (New York), 1971, pp. 205-215.

Narayanan, C. H.; Fox, M. W.; and Hamburger, V.: Prenatal Development of Spontaneous and Evoked Activity in the Rat (Rattus norvegicus albinus). Behavior, vol. 29, 1971, pp. 100-131.

Noirot, E.: Ultrasounds and Maternal Behavior in Small Rodents. Dev. Psychobiol., vol. 5, 1972, pp. 371-387.

Pace, N.; Rahlmann, D. F.; Smith, A. H.; and Pitts, G. C.: Effects of the Cosmos 1129 Soviet Paste Diet on Body Composition in the Growing Rat. Environmental Physiology Laboratory Report, EPL 81-1, University of California, Berkeley, 1981.

Plaut, S. M.: Adult-Litter Relations in Rats Reared in Single- and Dual-Chambered Cages. Dev. Psychobiol., vol. 7, 1974, pp. 111-120.

Rosenblatt. J. S.: The Basis of Synchrony in the Behavioral Interaction Between the Mother and her Offspring in the Laboratory Rat. Determinants of Infant Behavior, Vol. 3, B. M. Foss, ed., Wiley (New York), 1965, pp. 3-41.

Rosenblatt, J. S.; and Lehrman, D. S.: Maternal Behavior of the Laboratory Rat. Maternal Behavior in Mammals, H. L. Rheingold, ed., Wiley (New York), 1963, pp. 8-57.

Serova, L. V.; Denisova, L. A.; Apenasenko, Z. I.; Bryantseva, L. A.; Chel'naya, N. A.; Oganov, U. S.; and Skuratova, S. A.: Preliminary Report on the Results of the Embryological Experiment with Mammals on the Cosmos 1514 Biosatellite. NASA TM 77617, 1984.

Serova, L. V.: Denisova, L. A.; Makeeva, V. F.; Chelnaya, N. A.; and Pustynnikova, A. M.: The Effect of Microgravity on the Prenatal Development of Mammals. The Physiologist, vol. 27, 1984, pp. SI07-S110.

Serova, L. V.; Kvetnansky, R.; Denisova, L. A.; and Chelnaya, N. A.: Effect of Weightlessness and Hypergravity on Ontogenesis in Mammals--Possible Function of Stress. Stress: The Role of Catecholamines and Other Neurotransmitters, E. Usdin, R. Kvetnansky, and J. Axelrod, eds., Gordon and Breach Science Publishers (New York), 1984, pp. 1049-1056.

Skuratova, S. A.; Oganov, V. S.; and Shirvinskaya, M. A.: Postnatal Differentiation of Skeletal Muscles of Newborn Rats Exposed to Weightlessness During Fetal Period. Results Symposium: Cosmos 1514 Studies, Moscow, 1984.

Sharpless, S. K.: Supersensitivity-like Phenomena in the Central Nervous System. Fed. Proc., vol. 34, 1975, pp. 1990-1997.

Sharpless, S. K.: Reorganization of Function in the Nervous System: Use and Disuse. Ann. Rev. Physiol., vol. 26, 1964, pp. 357-388.

Ward, I. L.: Prenatal Stress Feminizes and Demasculinizes the Behavior of Males. Science, vol. 175, 1972, pp. 82-84.

Ward, I. L.; and Ward, O. B.: Sexual Behavior Differentiation: Effects of Prenatal Manipulations in Rats. Neurobiology of Reproduction, N. Adler and D. Pfaff, eds., Plenum Press (New York), in press.

Welker, W. I.: Analysis of Sniffing in the Albino Rat. Behaviour, vol. 22, 1964, pp. 223-244.

TABLE 1.- PROGRAM OF EXPERIMENTATION: POSTNATAL STUDIES

Maternal Behavior
Maternal Condition
Body weight profile during lactation
Food and water intake
Condition of Newborns
Initial weights
Gross morphology
Sexual differentiation
Growth
Sensory and Motor Function
Vestibular tests
Rotation
Surface righting
Geotaxis
Tactile test
Olfactory tests
Responsivity
Respiratory patterns
Auditory test
Visual test

TABLE 2.- MATERNAL FOOD INTAKE/MATERNAL BODY WEIGHT

Postpartum day	Flight	Vivarium	Synchronous
1	16.8	12.6	16.4
2	18.1	13.8	18.2
3	20.1	18.4	21.2
4	20.0	19.3	23.3
5	23.0	26.4	23.3
6	26.0	26.4	22.9
7	27.6	21.6	25.0
8	26.2	22.0	23.8

TABLE 3.- MATERNAL FOOD INTAKE/MATERNAL BODY WEIGHT AND LITTER WEIGHT

Postpartum day	Flight	Vivarium	Synchronous
1	14.2	10.9	14.0
2	15.8	11.6	15.5
3	16.1	14.8	17.9
4	15.8	14.7	18.0
5	18.1	19.1	18.2
6	19.3	18.7	17.1
7	20.1	15.1	18.3
8	18.7	14.7	18.1

TABLE 4.- DAILY WATER INTAKE (ml) BY LACTATING DAMS

Day	Flight	Synchronous	Vivarium
1	11	10	11
2	13.5	10	19
3	16	12	18
4	9	10	16
5	19	9	13
6	17.5	11	12
7	18	13.5	8.5
8	11.5	12	23
9	11	11	17
10	15.5	11	14
11	22	23	18
12	21.5	24	15
13	13.5	20	12
14	15	23	23

TABLE 5.- MEDIAN PROPORTION OF TIME SPENT IN NEST DURING LIGHT (16 HR) AND DARK (8 HR) PHASES

Age (days)	Phase	Flight	Vivarium	Synchronous
2	Light	0.98	0.94	0.97
2	Dark	.86	.70	.75
5	Light	.88	.86	.94
5	Dark	.86	.64	.76
10	Light	.72	.74	.895
10	Dark	.82	.72	.80
12	Light	.79	.76	.85
12	Dark	.68	.76	.835

TABLE 6.- PUP BODY WEIGHTS

	Flight	Vivarium	Synchronous
Day 1			
Mean	6.25	7.06	6.022
Variance	0.48	.24	.215
$F_{(2,106)} = 38.6$; $X^2 = 5.9143$ (n.s.)			
Day 5			
Mean	11.28	13.14	11.63
Variance	4.39	2.25	.95
$F_{(2,104)} = 15.11$; $X^2 = 18.09$			
Day 10			
Mean	21.74	23.59	18.96
Variance	12.43	7.38	4.81
$F_{(2,102)} = 27.68$; $X^2 = 6.94$			
Day 15			
Mean	33.24	35.32	28.03
Variance	27.62	25.06	10.79
$F_{(2,96)} = 25.56$; $X^2 = 8.20$			
Day 20			
Mean	51.60	52.36	39.88
Variance	42.39	33.72	18.26
$F_{(2,96)} = 46.53$; $X^2 = 4.52$ (n.s.)			

F values refer to results of Bartlett's Test for Homogeneity of Variance.

TABLE 7.- PROPORTION OF PUPS TESTED THAT ACHIEVED PRONE POSITION DURING SURFACE RIGHTING TEST (30 sec)

Age (days)	Group	N	Righting, %
2	Flight	28	25
2	Vivarium	35	8
2	Synchronous	22	31
3	Flight	28	61
3	Vivarium	30	63
3	Synchronous	31	35
4	Flight	27	70
4	Vivarium	33	82
4	Synchronous	31	68
7	Flight	20	100
7	Vivarium	24	100
7	Synchronous	33	94
8	Flight	20	95
8	Vivarium	29	100
8	Synchronous	34	100

TABLE 8.- SURFACE Rrighting: LATENCIES (sec)

Days of age	Flight	Vivarium	Synchronous
2	11.2	6.1	5.0
4	8.5	5.0	7.1
7	3.8	2.9	6.1

TABLE 9.- PROPORTIONS OF PUPS TESTED THAT DISPLAYED NEGATIVE GEOTAXIS ON TILT TABLE (20°)

Age (days)	Group	N	Showing geotaxis, %
1	Flight	30	13
1	Vivarium	16	0
5	Flight	26	19
5	Vivarium	38	37
5	Synchronous	39	17
6	Flight	29	79
6	Vivarium	39	54
6	Synchronous	37	22
9	Flight	16	94
9	Vivarium	24	83
9	Synchronous	39	90

TABLE 10.- THE DEVELOPMENT OF RESPIRATORY RATE, RESPIRATORY RANGE, RESPIRATORY LABILITY AND THE OCCURRENCE OF POLYPNEA (SNIFFING), DURING THE INITIAL 30 sec IN A NOVEL ENVIRONMENT

Age (days)	n	Respiratory Rate (md. cps)	Respiratory range (min/max cps)	Probability of polypnea	Polypnea burst duration (sec)
Flight 3	4	3.6	2/5	0.05	1
Vivarium 3	4	3.5	2/6	.04	1
Synchronous 3	4	2.9	2/4	.01	0
Flight 6	4	3.5	3/6	.20	6
Vivarium 6	4	3.2	2/5	.03	5
Synchronous 6	4	4.2	2/7	.40	15
Flight 10	4	5.6	4/8	.81	27
Vivarium 10	4	5.1	3/8	.72	18
Synchronous 10	4	5.5	3/8	.60	23

Values shown are median cycles per second. All values computed from the pups' "initial 30-sec baseline" in a novel chamber. Median rate was calculated from a continuous 30-sec sample; the 2 values shown for range are the fastest and slowest single seconds (cps); sniffing, or polypnea, was defined as an episode of rhythmically regular respiration.

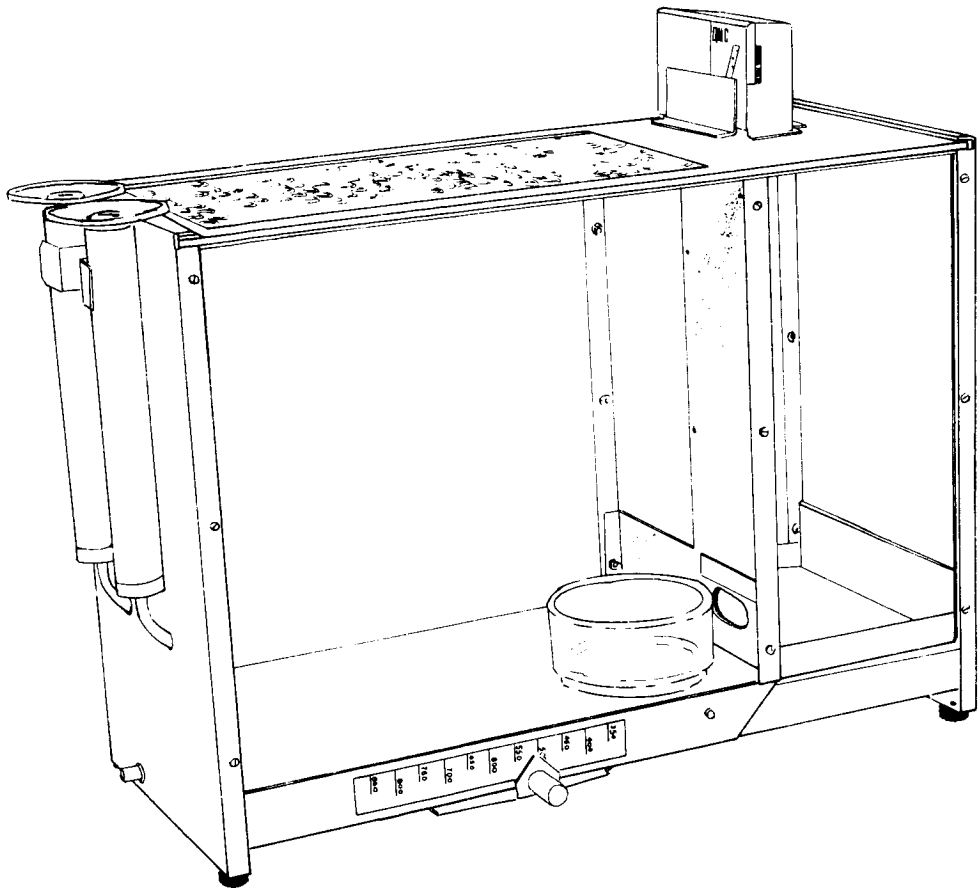

Figure 1.- Scale drawing of the cage used to house a rat dam and litter during the early postnatal period. The section depicted in the righthand portion of the cage was the nest area. The ceiling above the nest was a solid panel that could be equipped with a "bat detector" (shown in drawing) to record the emission of high-frequency vocalizations of the pups. A temperature probe could be inserted into the floor of the nest. (Only some cages have ultrasound and temperature recordings.) A microswitch was activated when the weight of the dam was added to that of the litter and depressed the floor under the nest. The electrical signal conveyed by the microswitch was used by a computer system to record the frequency and duration of maternal visits to the nest. A counterweight under the floor was adjusted each day to compensate for changes in the weight of the mother and pups. A notch was cut in one wall of the nest, permitting the mother to exit into the larger area (left) where her food and water were available.

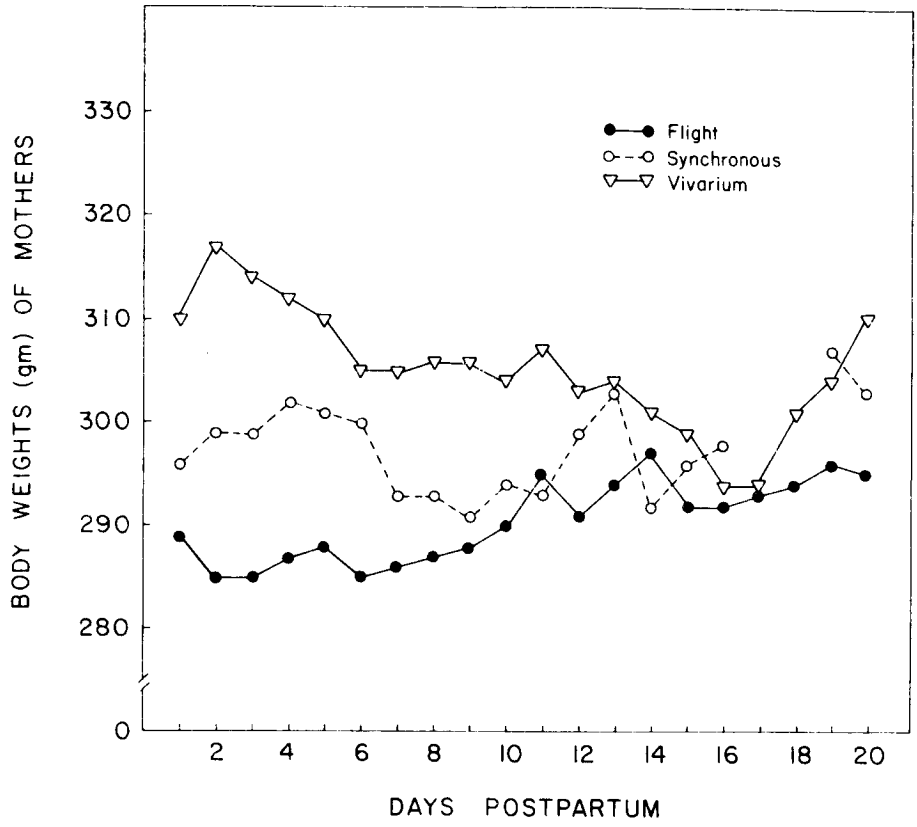

Figure 2.- Median body weights of Flight, Synchronous, and Vivarium group mothers from Day 1 postpartum through Day 20 (ns = 4, 5, 5, respectively).

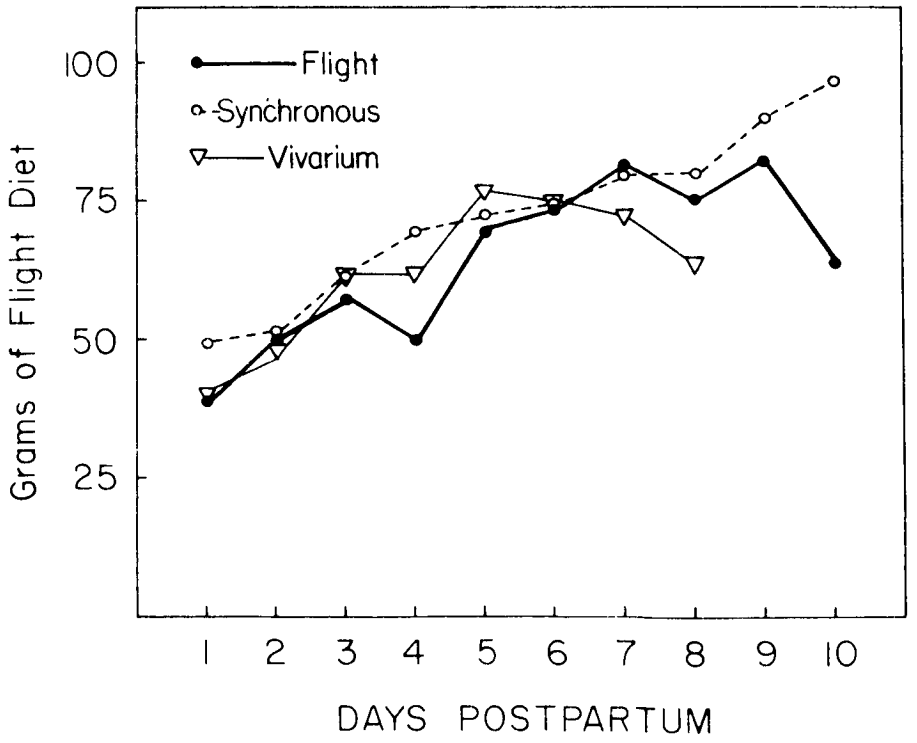

Figure 3.- Amount of flight diet (gm) eaten by mother rats during Days 1 to 10 postpartum. After Day 10, additional foodstuffs were added to the cages (see text) and accurate measurement of food intake was no longer possible.

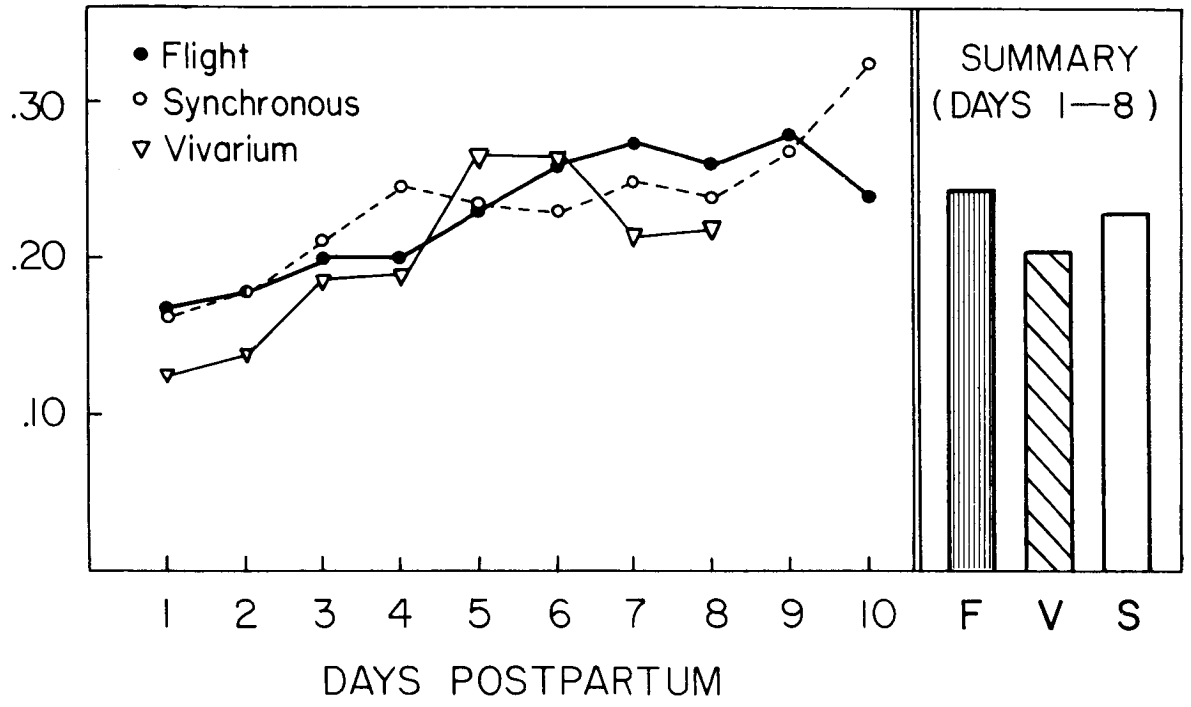

Figure 4.- Amount of food consumed per gram of maternal body weight intake (medians) by postpartum females. This calculation corrects for differences in mass of the mothers. The righthand panel summarizes the values for Days 1 to 8 postpartum.

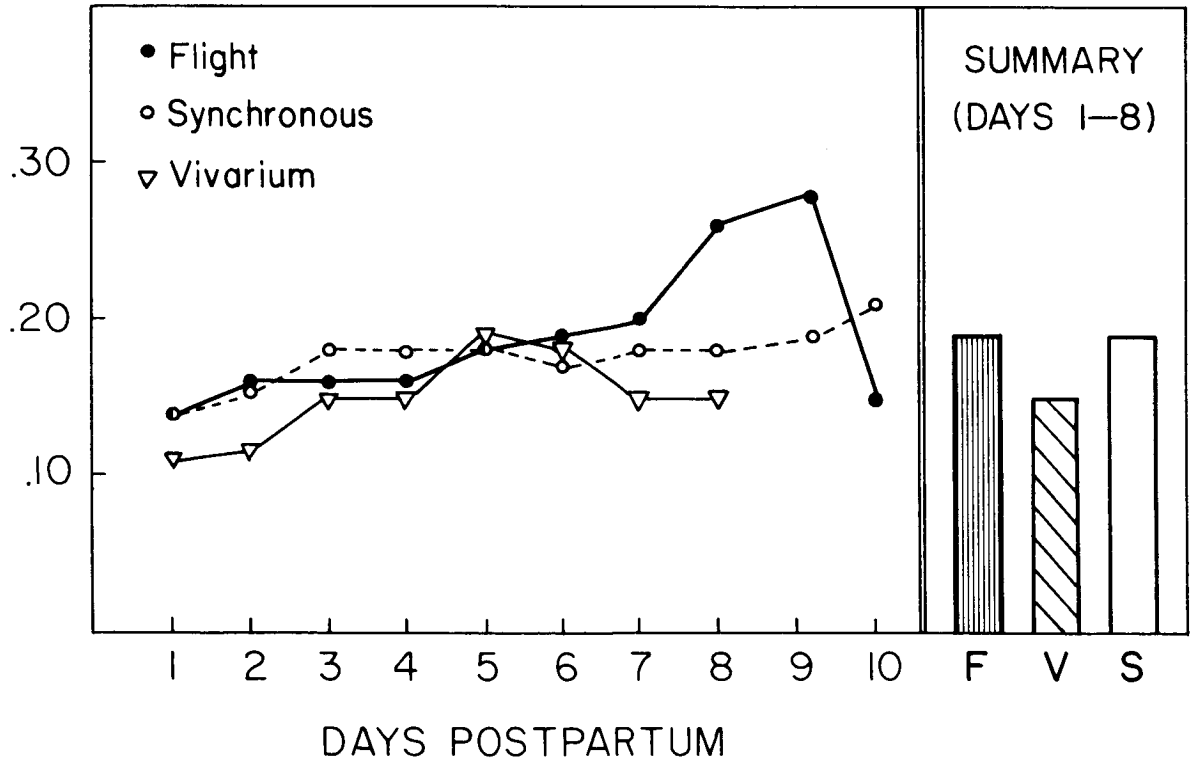

Figure 5.- Amount of flight diet consumed in relation to the total weight of the mother plus offspring. This calculation corrected for postflight differences in bodyweights in mothers and litters. The righthand panel summarizes the data for Days 1 to 8 postpartum.

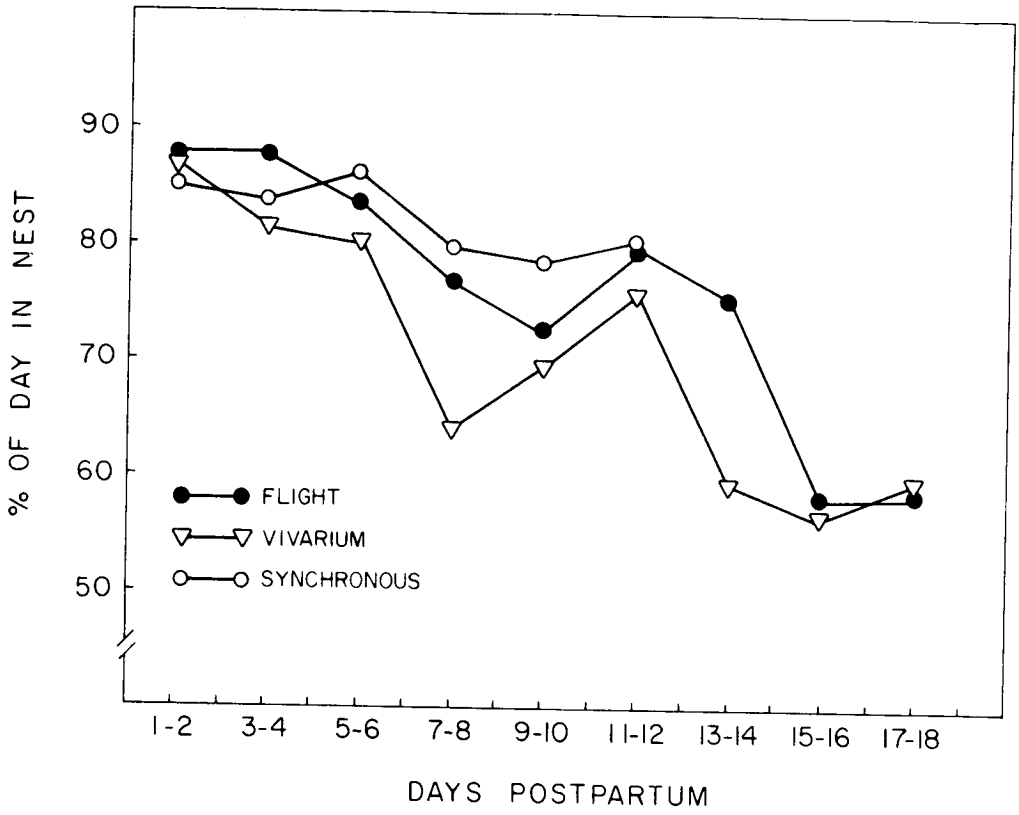

Figure 6.- Median duration of time spent in the nest by mothers, expressed as a portion of each day. Daily values are combined into two-day blocks.

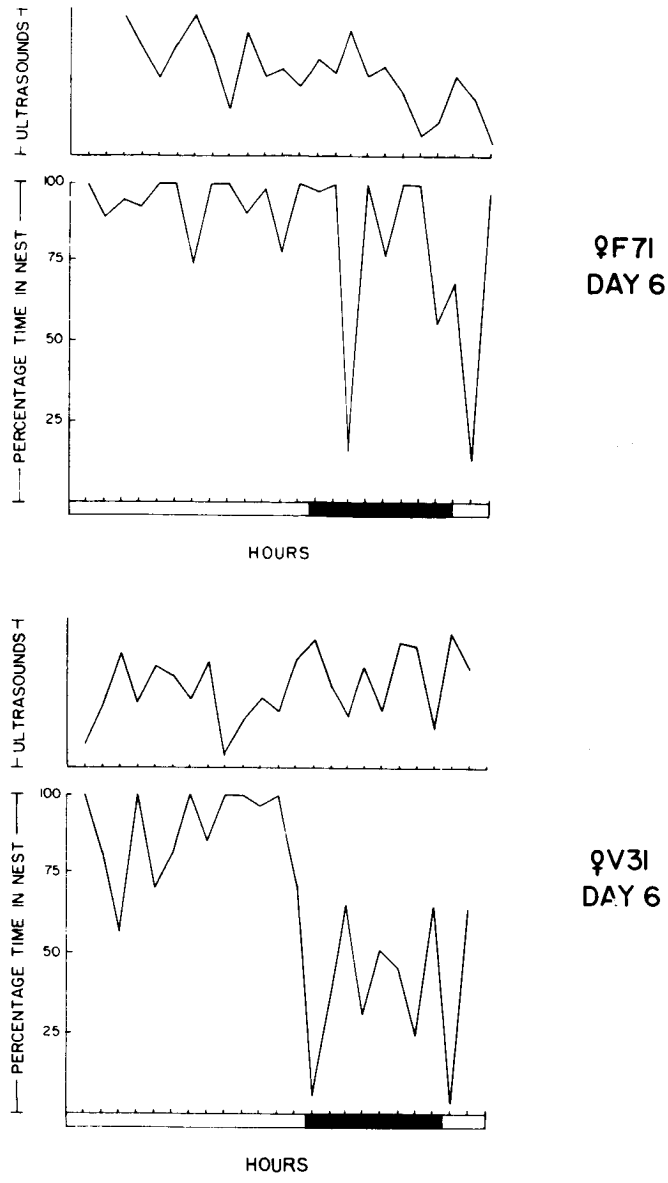

Figure 7.- Nest visitations by representative rat dams and the emission of high-frequency vocalizations by their pups, for each hour of Day 6 postpartum. The upper pair of graphs shows the litter's ultrasounds and maternal visits in the cage of Flight female F71. The lower pair of graphs represent the events in the cage of a Vivarium control subject and litter, V31. The dark bars along the abcissas indicate the period of darkness for the 24 hrs shown in each summary. These graphs indicate that the flight experience did not eliminate the typical circadian pattern of nest attendance typical of rat dams. The typical, inverse relationship between pup ultrasounds and maternal presence can be seen in the Flight dam, as in the control animal.

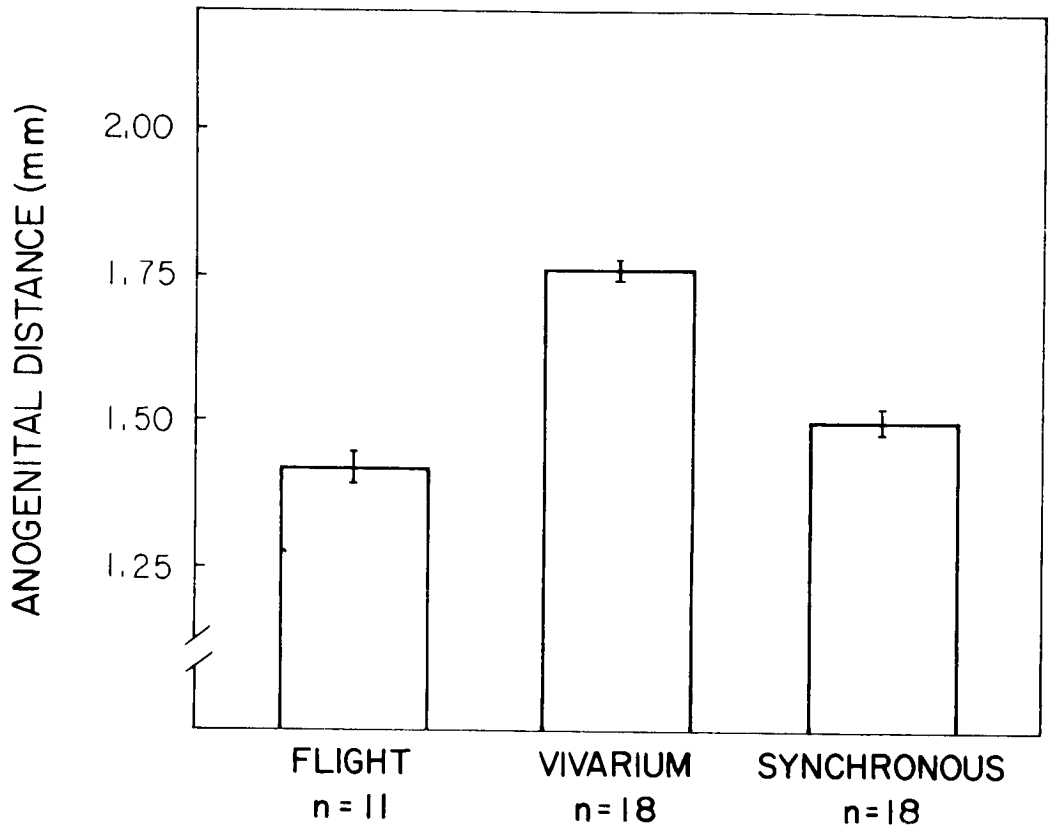

Figure 8.- Mean distance (mm) from the anal pore to the base of the phallus in male, Day 1 pups. Standard error of the means are shown by the vertical flags.

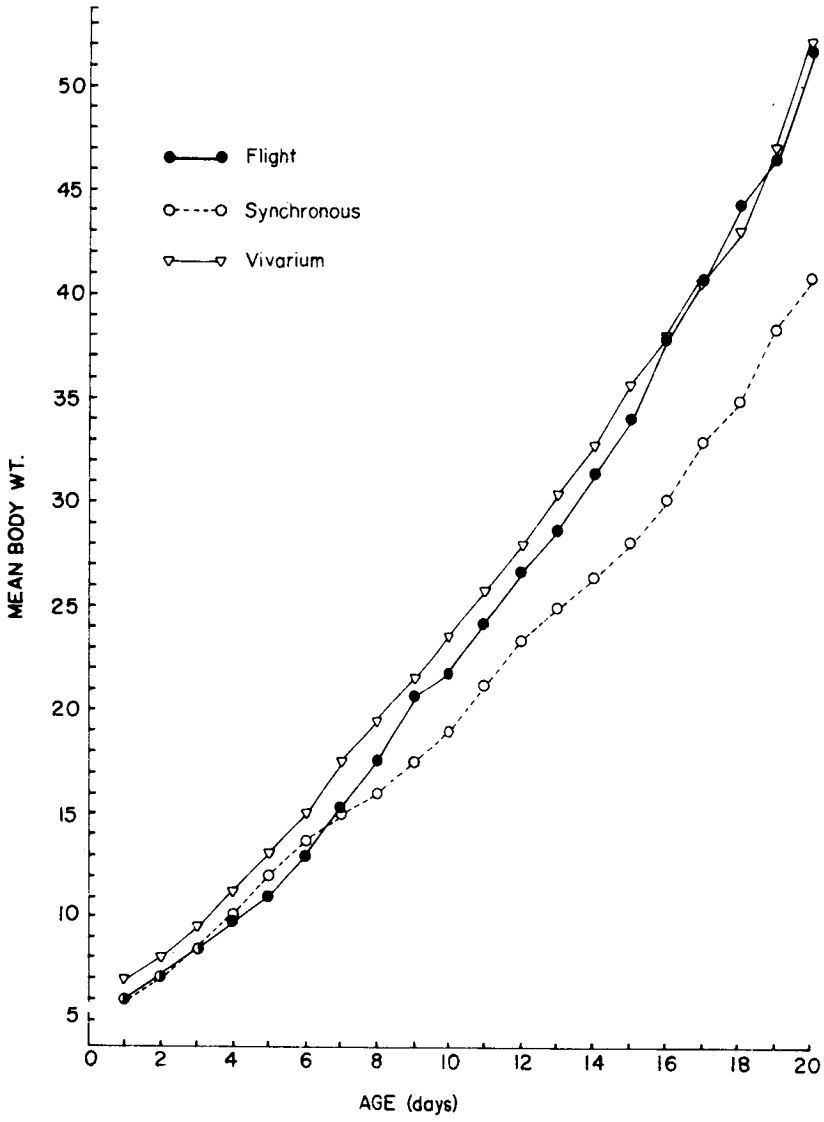

Figure 9.- Mean body weights of individual pups of Flight, Synchronous, and Vivarium mothers on Days 1 to 20 postpartum.

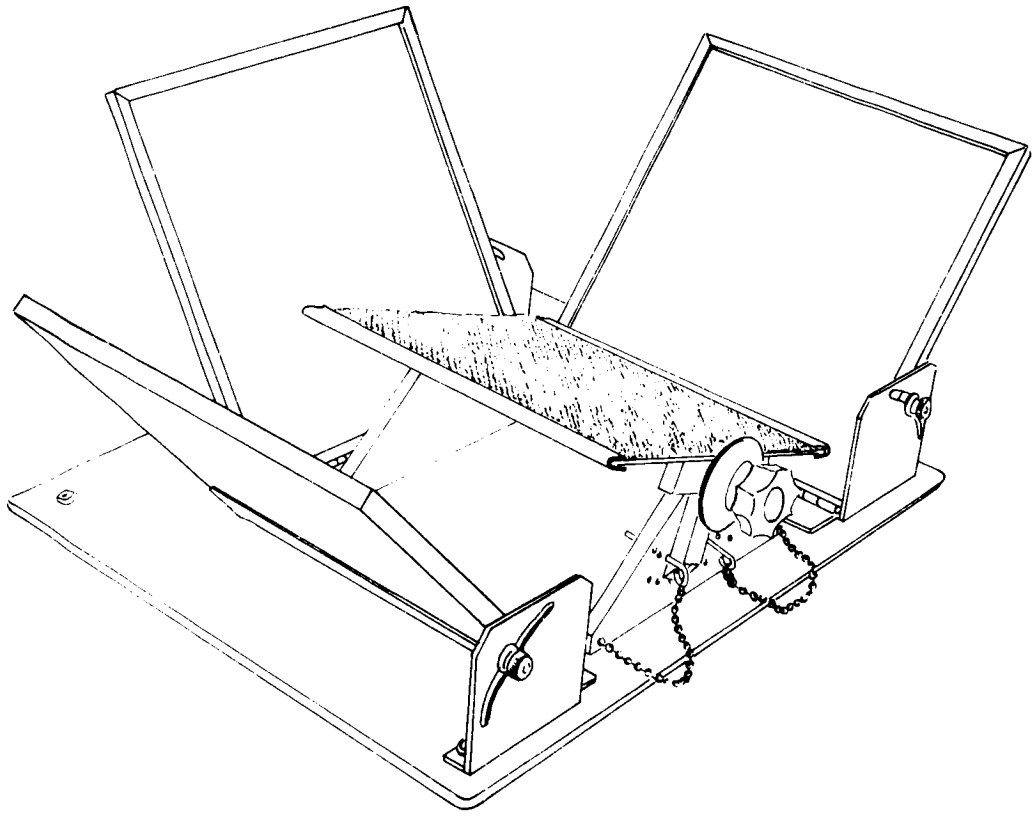

Figure 10.- Scale drawing of apparatus used in tests of negative geotaxis and surface righting. The pup was placed on an soft, acrylic mat that could be fixed at a 20° angle (shown) or as a level surface (for surface-righting tests). The adjustable panels surrounding the platform held mirrors that provided simultaneous frontal and side views of the subject to an overhead camera. This apparatus was contained within a warm incubator, to reduce thermal stress to the pups during testing.

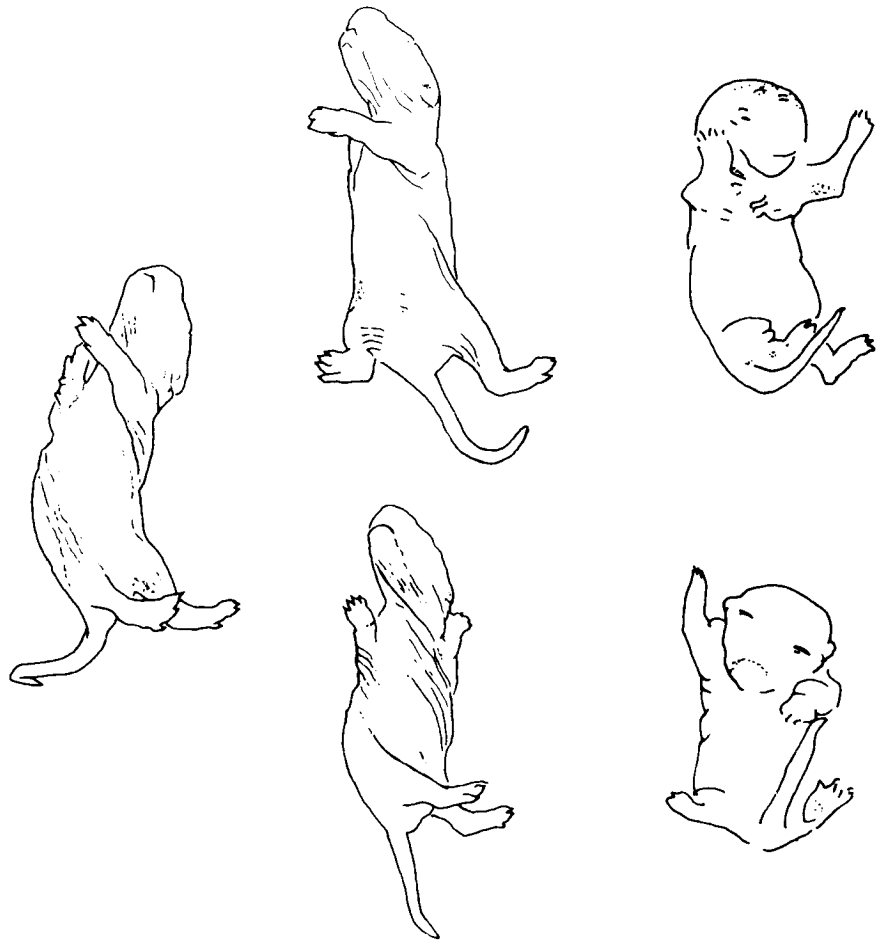

Figure 11.- Examples of movement categories examined in tests of surface righting. The two drawings on the top of the figure illustrate the Curl (category 1) and Curl/Roll (category 2) reactions. The drawings in the middle row illustrate examples of the Rostral (category 3) and Caudal Twist (category 4) as they occur in isolation. The lower drawing depicts these latter reactions occurring in unison and in opposing directions. (See text for discussion.)

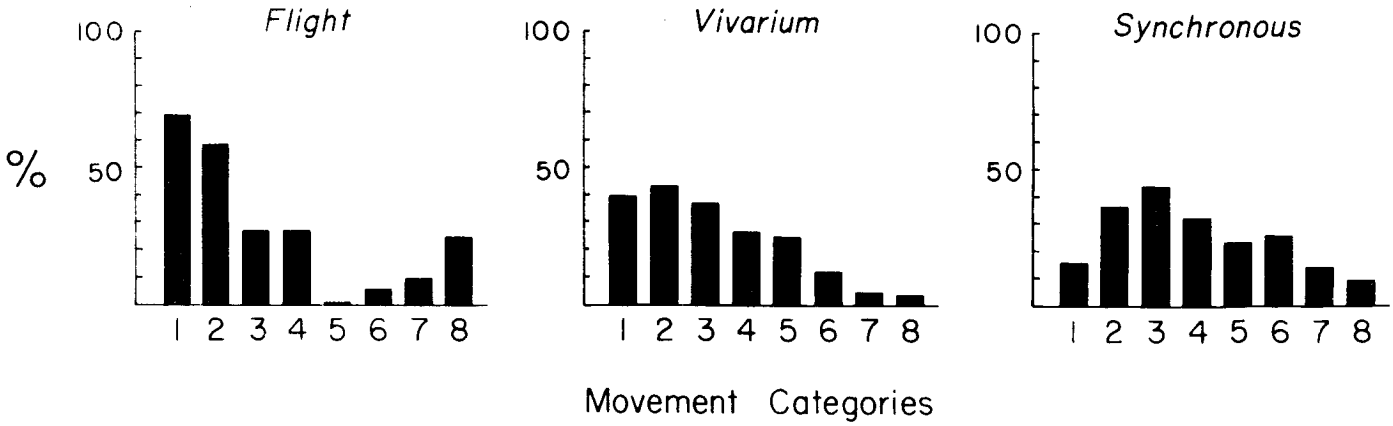

Figure 12.- Movements displayed by 2-day-old pups during the first postnatal test of surface righting. Each numerical category refers to a postural or movement classification (see text for details).

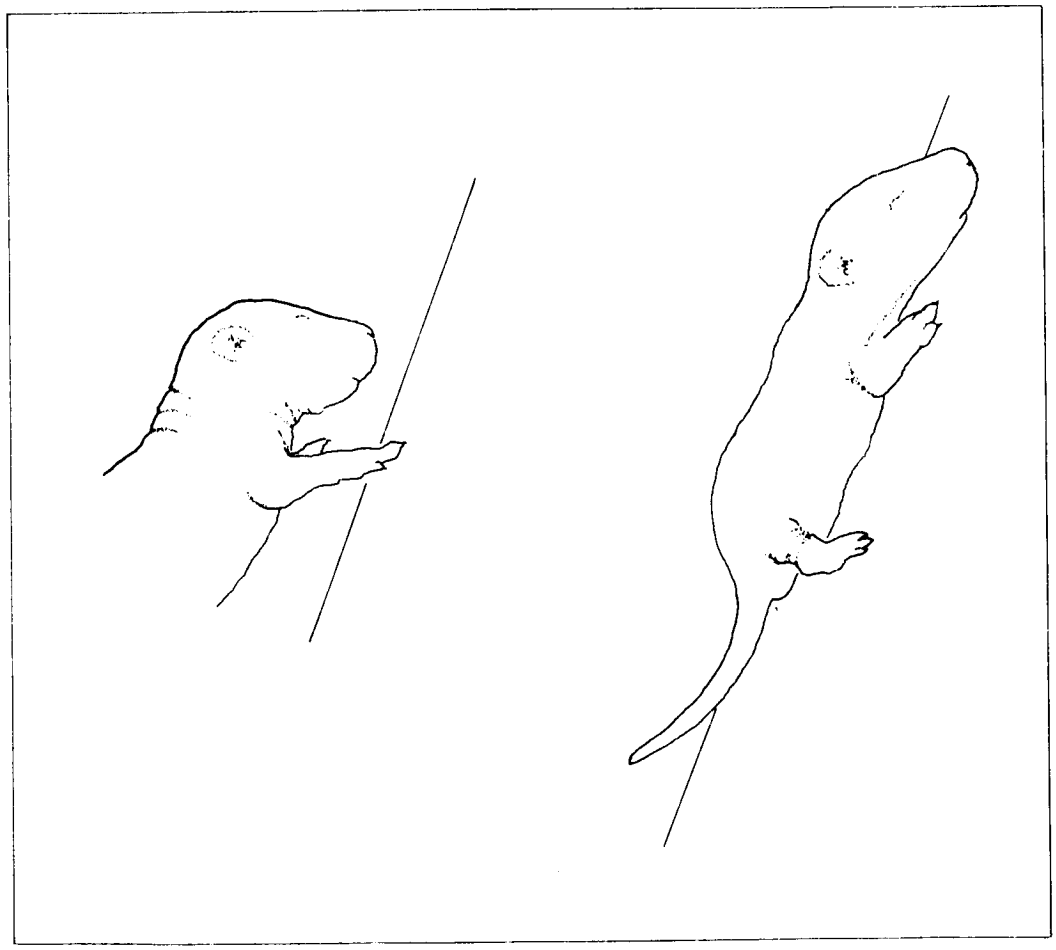

Figure 13.- Depiction of head raise and tail extension responses during two phases of vestibular testing. As a pup was lowered onto the tilt table, the experimenter tipped the hand-held animal so that its snout was lower than the rest of its body. Pups raise their heads in response to this vestibular signal of "falling." After being placed head-down at a 20° angle, one sign of detection of vestibular and/or proprioceptive perturbation is the extension of the tail, as depicted in the lower drawing.

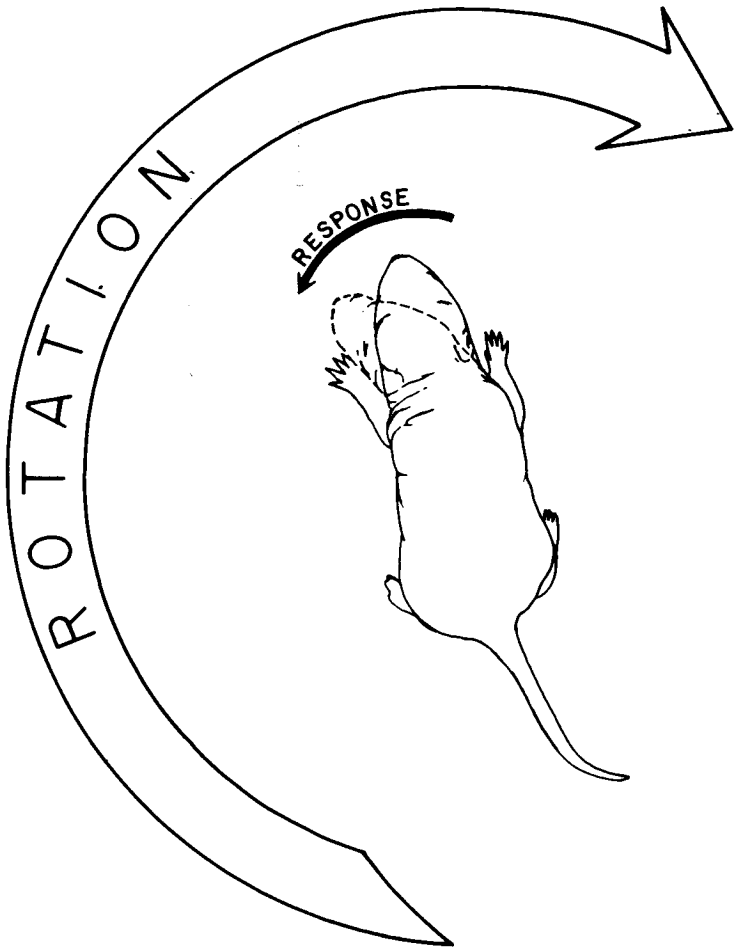

Figure 14.- Depiction of head deflection response, expressed in the direction counter to that of rotation. Rat pups, 1 to 5 days of age, reliably show this counter-rotational head movement. In older pups the reaction is replaced by more complex movements on the platform. The turntable apparatus used for this test was contained in a warm incubator to reduce thermal stress during testing.

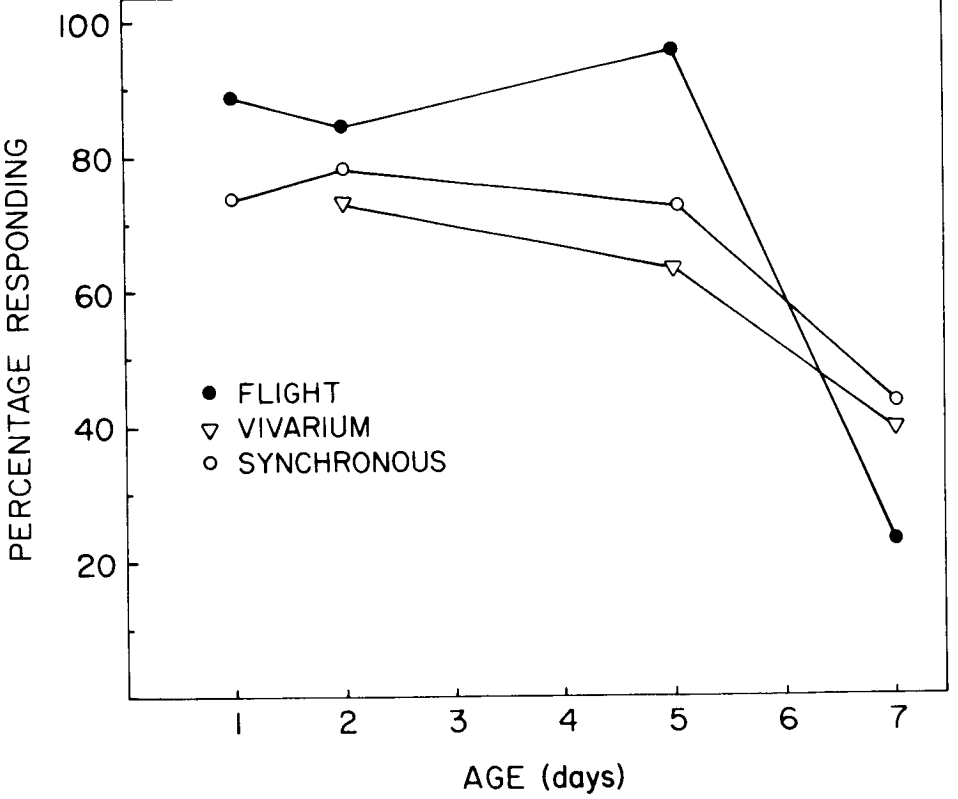

Figure 15.- Percentage of pups tested showing the head deflection response to rotation.

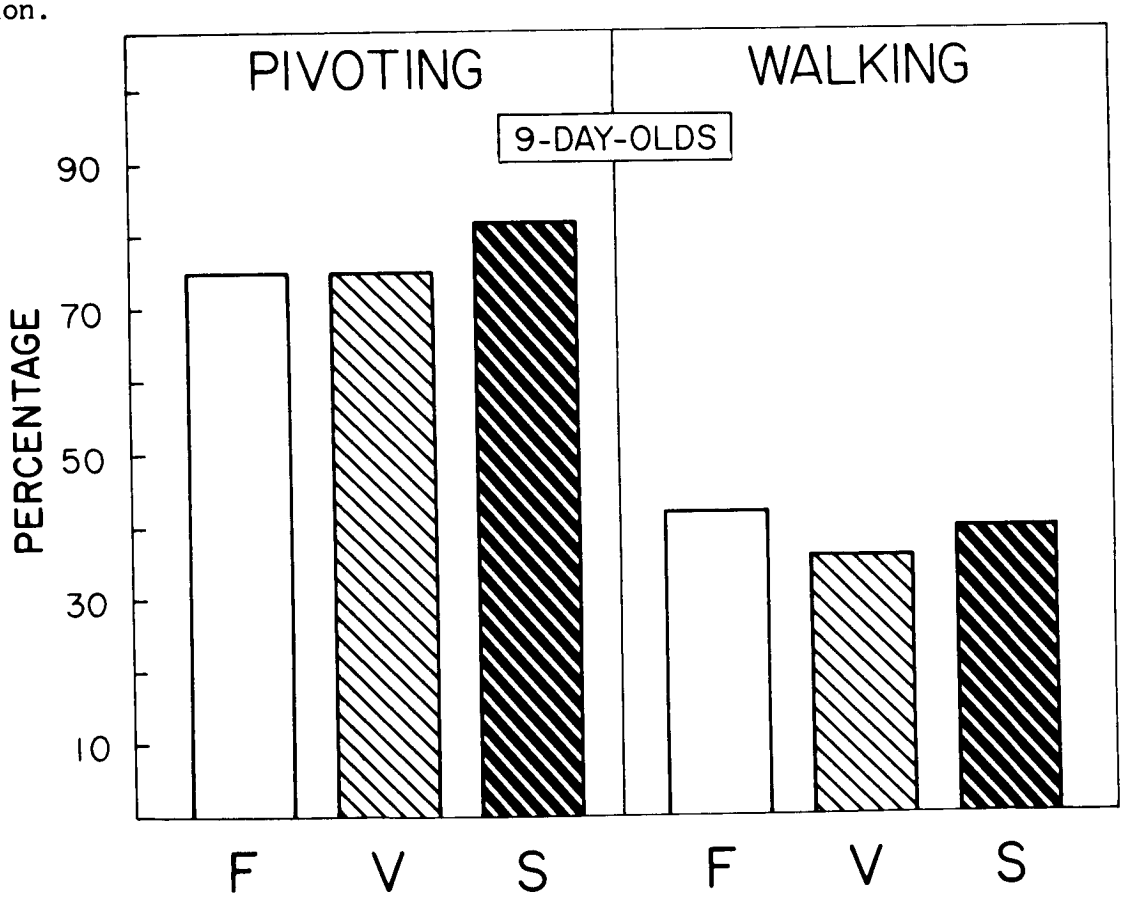

Figure 16.- Percentage of pups showing Pivoting (anterior body movements around a relatively fixed hindlimb base) and quadrapedal walking during test on postnatal Day 9.

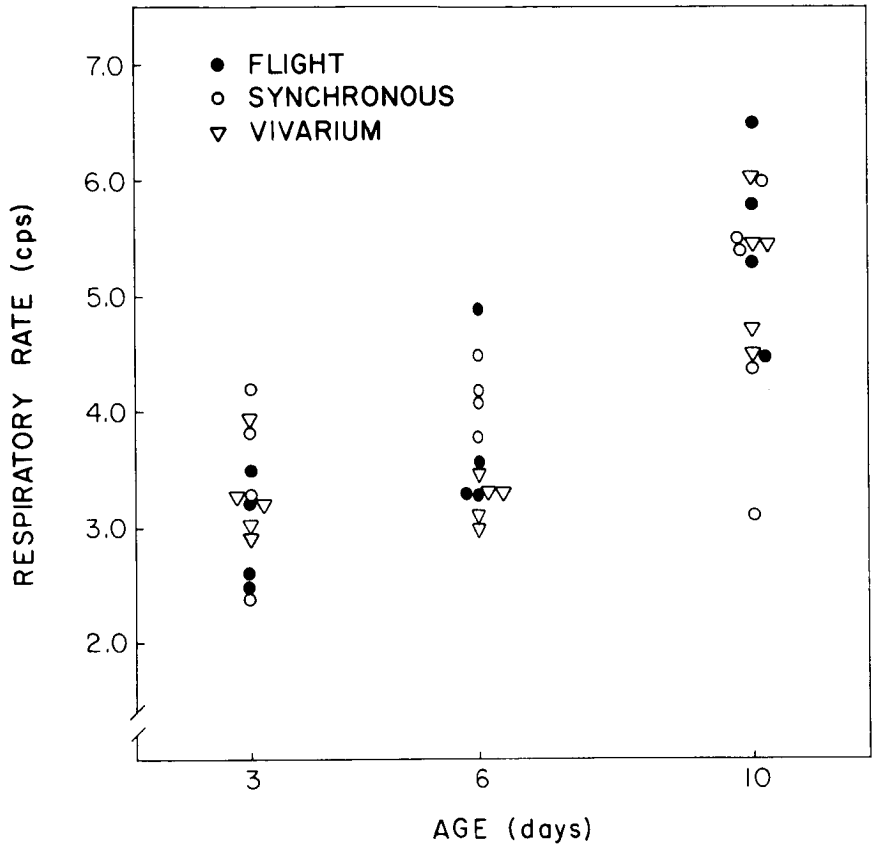

Figure 17.- Development of respiratory rate (cps) during the initial 30 seconds in a warm test compartment. Mean respiratory rates of individual pups tested a 3, 6, and 10 days of age are shown.

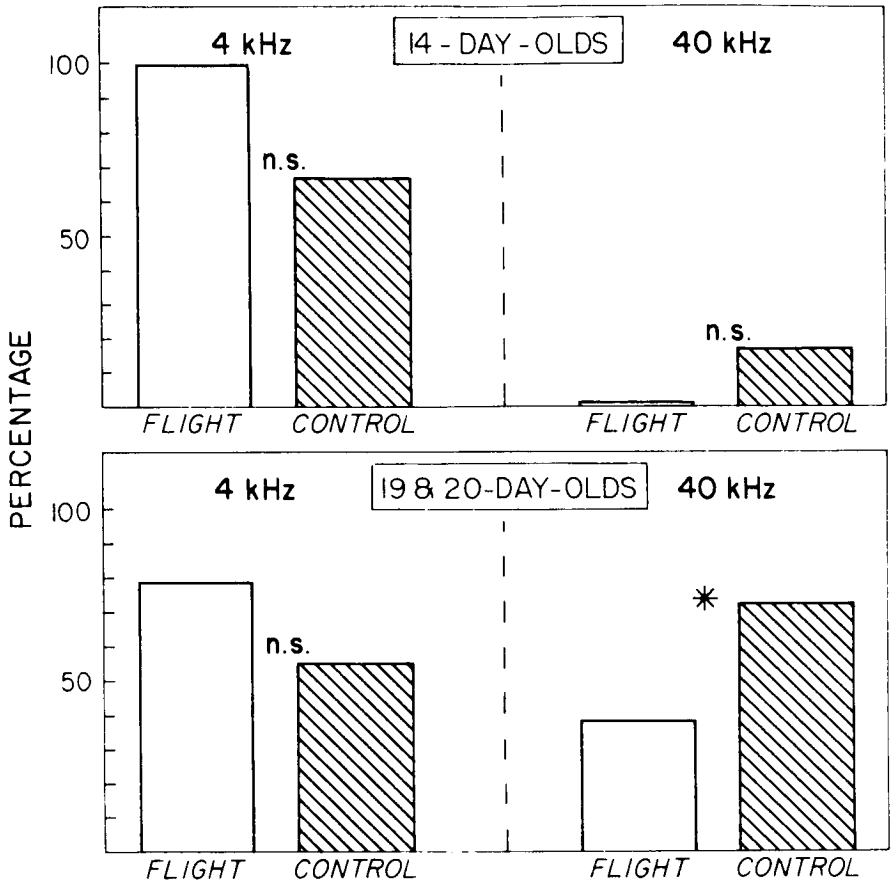

Figure 18.- Percentage of pups displaying a startle reaction to low (4 kHz) and high (40 kHz) tones, both at 90 db. Repeated tests were used, soon after ear-opening and about 3 days later, when sensitivity to higher frequencies improves.

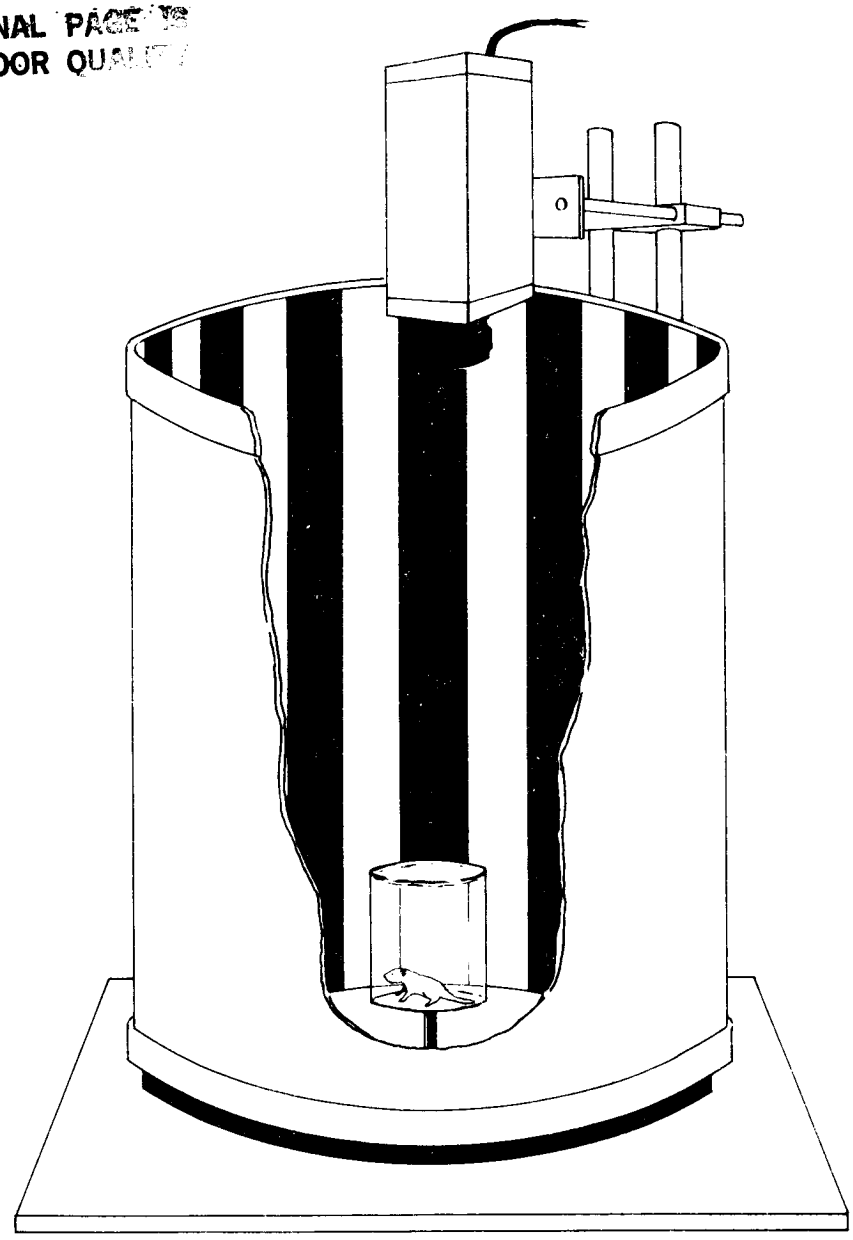

Figure 19.- Depiction of the optokinetic drum (cutaway to expose the inside) used to test visual acuity in rat pups. The subject was placed in the clear, cylindrical compartment near the bottom of the drum. The walls of the drum could be rotated slowly in either direction around the subject. The stripes on the inside wall (not drawn to scale) subtended 1.5° of visual angle on a retinal surface located at the inner wall of the subject's compartment. The movements of the pup were recorded via a video camera located above the subject.

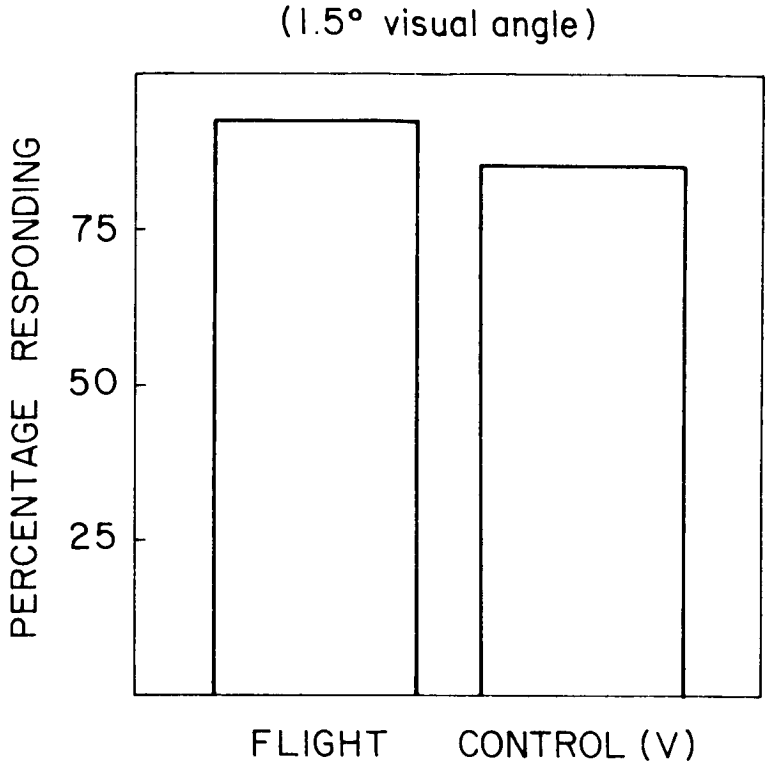

Figure 20.- Percentage of pups showing optokinetic response to a moving visual array. Flight and Vivarium pups were tested first and, because of their equivalent, excellent responses, it was not necessary to include pups from the Synchronous group.

DEVELOPMENTAL MORPHOLOGY OF THE EYE, VESTIBULAR SYSTEM AND BRAIN IN 18-DAY FETAL AND NEWBORN RATS EXPOSED IN UTERO TO NULL GRAVITY DURING THE FLIGHT OF COSMOS 1514

PRINCIPAL INVESTIGATORS

J. Richard Keefe, Ph.D.
BioSpace Incorporated
Case Western Reserve Univ.
Painesville, Ohio 44077

Jeffrey R. Alberts, Ph.D.
Star Enterprises
Indiana University
Bloomington, Indiana 47405

and

Igor B. Krasnov, Ph.D.
Institute of Biomedical Problems
Ministry of Health, U.S.S.R.
Moscow, U.S.S.R.

Lyubov V. Serova, Ph.D.
Institute of Biomedical Problems
Ministry of Health, U.S.S.R.
Moscow, U.S.S.R.

INTRODUCTION

The concept that gravity, an omnipresent environmental factor, must have played the role of a significant stressor in the evolution of mammalian developmental sequences, from the most subtle to the most major, can at last be tested under conditions of variable gravities from null to one during spaceflight.

To speak of gravitational impacts upon mammalian development, however, one must also speak of the potential for both direct and indirect effects. If it is assumed that female mammals demonstrate adaptive physiological responses to null-gravity exposure similar to those displayed by males that have flown, then questions of transplacental expression of a variety of systemic effects from null-gravity exposure become highly significant in evaluating the results of developmental studies under altered gravity.

Such an initial study of both direct and potentially indirect transplacental impacts of null-gravity exposure on mammalian development during the relatively stable midfetal period of E13 to E18 (days 13 to 18 of gestation) has been tested in two groups of five Wistar rats flown on COSMOS 1514. One group of five pregnant females was sacrificed at the recovery site, and the fetal heads (E18) were preserved for morphological studies. The second group of females was allowed to proceed to term, with four of five delivering litters. Samples of the offspring were derived by sacrifice of litter culls on postnatal day zero; samples from the remaining test population were taken on postnatal days 15 and 30.

The successful flight and recovery of ten pregnant rats in the COSMOS 1514 experiment represented a series of "FIRSTS" in Space Biology--the first experimental flight study of female mammals, the first spaceflight exposure of pregnant mammals with successful maintenance of all pregnancies for the flight duration, and the first spaceflight exposure of developing fetal stages for a higher vertebrate species. The COSMOS 1514 Neuro-Ontogeny experiment, through its sharing of specimens and data, also represented a new and major improvement in international cooperation during the design, implementation and interpretation of a complex biological experiment.

In summary, two highly significant observations can be made. First, there is nothing in the short-term (5 day), near-Earth spaceflight environment that critically impacts normal midfetal mammalian development, either directly or transplacentally. Second, spaceflight exposure during the midfetal period of gestation does not adversely impact the development of normal maternal characteristics. These two observations are very significant since they demonstrate that such exposures are not terminal in nature and, therefore, can support continuing experimental design.

As such, this project represents a truly "pioneering" effort. The present document represents a "status report" of an ongoing study, and it will present summary morphological data and interpretations from those specimens that have received adequate study.

C-3

HISTORICAL REVIEW

Although most previous flight projects have been severely limited by preflight operating constraints, by relative flight brevity and by minimal opportunity for "inflight" manipulation or sampling of the experimental population, they have offered insights into "windows of opportunity" existent within the broader science of developmental biology. The following brief summary endeavors to capture both the spirit of the individual project and the limiting factors impacting either the experiment design or its outcome.

If gravitational vectors have served as evolutionary drivers in mammalian development, then one should expect such effects to begin with the initial laying down and stabilization of oocyte cytoplasm, with particular reference to cytoskeletal organization and integration. Any subsequent rearrangement of cytoplasm, from fertilization through cleavage, should also be suspected of high gravitational sensitivity. Alterations to the cytoskeleton will likely continue to be expressed during development by varying patterns of cell migration, recognition and association, morphogenetic cell death and tissue plasticity. Pattern formation developed through cell-to-cell associations or cell surface features should be susceptible until persistent bonding forces, exceeding local gravity variations, are established. Finally, the role of intracellular calcium-control mechanisms and the potential inherent in the coevolution of calcium regulation (Lowenstam and Margulis, 1983) and gravity sensitivity must be evaluated.

SPACEFLIGHT STUDIES ON EARLY AMPHIBIAN DEVELOPMENT

One of the most widely studied (and contested!) effects of gravity upon early vertebrate development has been the study of the rotation of the yolk-laden portion of the fertilized amphibian egg and the establishment of initial axial symmetries (Ancel and Vintemberger, 1948; Schultz, 1894; Penners and Schleip, 1928; Young et al., 1971). Although varying from species to species, the period of maximum gravitational sensitivity appears to become evident during the second hour after fertilization and extends into the first cleavage period in some species. Such studies have been further complicated by the variety of experimental manipulations employed and the lack of consistency in their application. Many of the means of restricting rotation are themselves conducive to producing a range of developmental anomalies, with the severity of the abnormal development dependent upon the scalar range applied.

For example, Tremor and Souza (1972) demonstrated that gravity compensation (vectoral randomization), through horizontal clinostating of unrestrained fertilized eggs of Rana pipiens or Xenopus laevis, produced abnormal development only at certain rotational speeds (Tremor and Souza, 1976). Similar observations have been made in horizontally rotated fertilized eggs of Fundulus heteroclitus and

Gallus domesticus (Nace and Tremor, 1981; Egar, M. W., and Keefe, J. R., Simulation of Null-gravity by Continuous Rotation During Avian Development, 1984, unpublished results).

Fundamental to the understanding of the effects of gravity upon early development is the establishment of the structures responsible for detecting imposed gravitational fields. Malacinski (Radice et al., 1981; Malacinski, 1983) has proposed a "Density Compartment Model" utilizing a variety of cytological approaches. The model proposes compartmentalization of the cytoplasm, emphasizing yolk platelet composition of individual compartments and integrating the results of earlier experimental studies into a cytoplasmic gravity-detecting system capable of being experimentally tested.

It is also important to determine thresholds of gravity sensitivity throughout development. While alterations of the normal gravity vector during early critical time periods may produce developmental anomalies reflecting the sensitivity of the organism at that moment, the application of fractional-gravity loads over extended periods of development may have a more significant impact on development of the mature organism.

The earliest developmental studies to be undertaken in the U.S. space program were those of Young and Tremor, beginning in the mid-60's. In a series of studies (see table below), the earliest processes of fertilization, cleavage and early embryonic development was studied utilizing Sea Urchin (Arbacia) or frog eggs (Rana pipiens) intended to be fertilized inflight. Due to restrictions on hardware flight qualification and problems in maintaining viability of unfertilzed eggs in vitro over an indeterminate launchpad hold, these studies had to depend upon ground-based fertilization with chilling (43°F) of selected fertilized eggs until the time of launch. Such treatment was demonstrated to have no deleterious effects, although it resulted in delaying null-gravity exposure until after mid-first cleavage of all eggs.

CONCLUSIONS

Brief exposure to null gravity (ignoring spurious onboard inertial gravities) does not affect normal development from first cleavage through late gastrula stages in Rana pipiens.

The preceding sets of studies suffered from a variety of launch-time limitations. They required ground-based fertilization 12.5 hours before launch, selection of flight group eggs from those first showing fertilization rotation, chilling to 43°F to delay normal developmental processes, and elevation of incubator temperature to 70°F sometime after liftoff.

Since postfertilization rotation and early cytoplasmic organization could be affected by exposure to normal gravity vectors (in effect providing the fertilized egg with a "gravitational memory"), Souza and coworkers (Souza, K. A., SL-4 Frog Egg Experiment #256, 1983, unpublished experiment status description) are preparing an

experiment in which male and female gametes of Xenopus laevis will be flown and studied for successful inflight fertilization, egg rotation, development of bilateral symmetry, and growth through blastula and gastrula stages.

STUDIES OF EARLY AMPHIBIAN DEVELOPMENT

FLIGHT	YEAR	DURATION	SPECIMENS/STAGES
Gemini 3	1965	~5 hours	8 chambers of Arbacia (Young, 1971) Fertilize 4 pre/4 inflight. Time fix samples inflight. Hardware failure.
Gemini 8	1966	~11 hours	20 Rana eggs/4 chambers (Tremor and Young, 1968) Time fix inflight. Normal cleavage.
Gemini 12	1966	~4 days	20 Rana eggs/4 chamber. (Young, 1976) Time fix at 41/85 hrs = Normal embryo. 3/5 recovered live = normal. Live tadpoles = unexplained deaths.
Biosatellite 2	1967	~2 days	120 Rana eggs/16 chambers (Young et al., 1971) Time fix at intervals. Range of development: mid-first - neural plate. Live returned, followed controls.

SOVIET FROG WORK

Similar studies, conducted on Soyuz and Salyut flights from 1971 through 1981, and involving Rana, Xenopus and Brachydanio species, have recently been summarized by Vinnikov, Gazenko and colleagues (Vinnikov et al., 1983). All of these flight projects involved preflight, Earth-based fertilization with commencement of null-gravity exposure ranging from early blastulae through tail bud stages. This extensive series of experiments clearly demonstrates the capacity of the peripheral vestibular apparatus to undergo normal morphological development in the absence of an Earth-normal gravitational field.

DEVELOPMENT OF Fundulus heteroclitus

A demonstration project carried out on Skylab 3, in which 50 fertilized Fundulus eggs were exposed to spaceflight from late gastrula through hatching and early maturity, resulted in normal swimming behavior of the young fry. This was in

contrast to the disjointed, apparent vestibularly deafferentated, swimming of several young adult fish flown. This project was NOT intended to be an experiment and no provisions for feeding, inflight sampling or postflight analysis were provided. Postfacto postflight morphological analysis of the poorly preserved remnants suggested that, while the sensory maculae of the membranous labyrinth developed adequately, a developmental aberation of the otoconia may have taken place. This was perhaps a result of an altered inflight calcium balance, although no apparent disruption of the calcification process (normal in the developing cartilage of this species) was observed (Keefe, J. R., Report on Morphological Studies Performed on Skylab 3 Specimens, 1974, unpublished).

Two experiments, designed to more properly evaluate the effects of spaceflight upon the early developmental stages of Fundulus, were flown in 1975. The first was an American experiment on the joint Apollo-Soyuz Test Project (ASTP) while the second was a joint project with Soviet coinvestigators on the U.S.S.R. unmanned biological spaceflight COSMOS 782. In each of these experiments, five developmental stages of Fundulus, chosen for their relevance to vestibular system development in this species, were selected, and 100 timed embryos at each stage were packaged in plastic aquaria and flown for either 9 or 19 days, respectively.

The ASTP project (Scheld et al., 1976) consisted of a single flight package that was deployed during the mission which provided a stationary null-gravity exposure with normal lighting cycles. Five groups of embryos timed to be at postfertilization stages of 32 hours (mid-gastrula), 66 hours (initial statoliths), 128 hours (vestibular development complete), 216 hours (functional vestibular system), and 336 hours (able to hatch) at the time of liftoff were flown.

The COSMOS 782 experiment (Scheld et al., 1978) consisted of both null-gravity and gravity-compensated flight packages. The latter was mounted on a flight centrifuge which provided approximately 0.6 to 0.8 g. The fertilized eggs were prepared in a laboratory at NASA Johnson Space Center, chilled to 10°C and transported to the Moscow laboratories. There they were warmed at the suitable preflight times to produce timed stages matched to those previously described (32, 66, 128, 216, 336 hours postfertilization). The Soviet component of this joint project (Biological Studies, NASA TM 75769, 1980) consisted of four categories of developing Fundulus from the same population of fertilized, chilled and transported eggs : (a) null-gravity; (b) inflight 0.6 g; (c) preflight clinostat-adapted, inflight null-gravity; and, (d) preflight clinostat-adapted, inflight 0.6 to 0.8 g centrifuge.

Results from each of these projects were very encouraging. Development proceeded normally (if not more rapidly) and was attributed to the lack of metabolite stratification and even dispersal of the gas phase within the aquaria. Hatching rates and normalcy ratios were highest for the ASTP flight specimens. A contamination problem unrelated to flight caused severe developmental abnormalities in the COSMOS 782 population utilized by the U.S. NO significant deviations in vestibular morphology were reported by the U.S. investigators, although Soviet scientists reported variations in "otoconial membrane" morphology in certain groups which were attributed to spaceflight exposure.

Preliminary behavioral analyses of the ASTP flight specimens suggested unusual diving, stabilizing and righting responses. Postflight testing of flight specimens during periods of brief exposure to the null gravity of parabolic flights, however, was unable to confirm this observation (Baumgarten et al., 1975). The Soviet investigators on COSMOS 782, utilizing specimens of Fundulus that had been "experienced" to "null gravity" (by subjection to preflight clinostating), reported no significant differences from such preflight "null-gravity" experience.

Of continuing interest are the observations made by Soviet scientists during Cosmos 782 on an internally fertilizing, viviparous guppy (Lebistes reticulatus?). The female of this species internalizes and maintains the sperm mass, fertilizing ova on a continuing basis and retaining the developing eggs until a later (~21 days) release stage. In the flight experiment on COSMOS 782, these fish demonstrated normal fertilization and development during the preflight period. Those flight specimens on the centrifuge continued fertilization and development while the "weightless" variants (null gravity) were reported to have ceased the fertilization process coincident with flight liftoff. No eggs from fish of the later group were reported to have been fertilized during the spaceflight period proper, although normal fertilization was reported to be restored during the immediate postflight period.

The Soviet scientists (Gazenko et al., 1976) theorized that "...some flight factors inhibit the fertilization of oocytes." While these studies (unpublished) did not present any data on the early stages of embryogenesis in this species under conditions of null gravity, they do raise serious questions about the ability of normal vertebrate fertilization to proceed under spaceflight conditions. Although the results of these studies have not yet appeared in print, the fact that such work is continuing strongly suggests that there are fundamental problems with vertebrate fertilization in space.

STUDIES OF DEVELOPMENT ON COSMOS 1129

Three joint U.S./U.S.S.R. experiments relevant to the present discussion were performed on the 19-day flight of COSMOS 1129 (1979).

Pitts and co-workers (Pitts et al., 1982) studied the whole-body composition of young adult male rats subjected to the 19-day spaceflight exposure. Their data demonstrated that adaptive changes occurred, reflective of those previously reported in male flight crews from both countries. Changes of particular relevance to the present discussion included: decreased growth; marked diminution of extracellular water fraction; and a sizeable reduction in fat-free body fraction representing bone mineral.

These observations, when coupled with other studies on flight rats and man, suggest that inflight adaptive changes (fluid electrolyte balances, serum mineral and hormone levels), reflective of major physiological compensation for gravity

reduction, are cause for concern with respect to potential transplacental effects on normal mammalian development. Additionally, changes in distribution of body fluids, if they coincide with the vascular development of placentation, may be disruptive of this extremely sensitive developmental stage.

Sixty fertilized Coturnix eggs were flown in a flight incubator on COSMOS 1129. The incubator lost humidity during the latter half of the mission, resulting in the precocious death of the flight specimens. Although the processes of early development occurred in normal gravity prior to liftoff, the flight development of the quail, to the point of incubator failure, was adjudged to be normal by investigators from both countries (Keefe, 1981).

In an attempt to combine, in a single longitudinal study, the effects of null gravity upon the processes of mammalian copulation, insemination, fertilization, early embryogenesis, implantation, placentation and early fetogenesis, five female and two male Wistar rats were flown in a divided cage on COSMOS 1129. After the initial two-day acclimation period, the divider was opened and mating was presumed to have occurred.

The fact that neither the flight nor the synchronous ground control groups delivered any litters and that no fetuses were recovered from laparotomized flight females suggests that the factors impacting this experiment were not directly related to the spaceflight null-gravity exposure (Keefe, 1981; Serova, 1982).

* - * - * - * - * - * - * - *

The preceding summary of flight studies of vertebrate development reveals both the minimal time periods of exposure that have been studied and the paucity of studies on the myriad processes of mammalian development. It also illustrates the potential for affecting developmental processes via transplacental expression of an altered maternal physiology produced by adaptation to null-gravity loading. Finally, the summary demonstrates the total absence of studies on normal female mammals undergoing flight adaptation. It is in this context that the present mammalian development experiment from COSMOS 1514 was conceived.

I. EXPERIMENT OVERVIEW

On COSMOS 1514, two groups of five pregnant rats, gestation day 13 (E13) at liftoff, were flown in a common cage. GROUP I dams were sacrificed upon satellite recovery, early on gestation day 18 (E18), and the fetuses were recovered for morphological analyses. GROUP II dams continued to term, readapting to Earth-normal gravity before delivery. Four of the five dams delivered litters considered to be normal in number and sex ratio, although the pups were notably lighter in weight (Serova et al., 1984). Each of these litters was sampled, at birth and on postnatal days 15 and 30, for studies of cranial morphology. The present report describes the experimental protocol utilized for the study of perinatal cranial morphological

development of selected samples from both Groups (table 1) and it presents documentary evidence for an inflight effect acting upon the developing embryonic nervous system during the midfetal period. It is presently unclear whether this effect, expressed primarily in the population of mitotic neuroblasts, results from a direct effect of null gravity or results from an altered maternal physiology, acting adaptively across the placenta. Finally, this report demonstrates that the five-day postflight readaptation period resulted in the normalization of the flight effect on cranial morphology. All newborn flight specimens demonstrated normal morphology in the central nervous system, peripheral vestibular structures, pineal, pituitary and ocular structures.

II. EXPERIMENTAL DESIGN AND EXECUTION

A. Experimental Subjects

The experimental subjects for this study were Wistar-derived rats from a breeding colony maintained in the Moscow laboratories of the Institute for Biomedical Problems. All females were novice breeders and had not delivered a prior litter. For details see report by Dr. L. V. Serova (Serova et al., 1984).

B. Preflight Implementation, Flight and Recovery Activities

For details on the preflight implementation, see the report by Dr. Serova (Serova et al., 1984). In summary, pregnant females were placed on the COSMOS 1514 spacecraft late in the 12th day of gestation and launch was achieved early on day 13 of gestation. Recovery of the satellite and the specimens occurred early on the 18th day of gestation.

The ten pregnant females were assigned to two groups:

GROUP I consisted of five females that were sacrificed at the recovery site, laparotomized, and the fetuses realized intact in the uterine horns. For the purposes of the present study, the fifth fetus from each uterine horn was removed, examined grossly and decapitated, with the entire, unopened head placed in the modified Karnovsky biostabilizer (see Materials and Methods).

GROUP II consisted of the remaining five females that were allowed to proceed to normal term delivery following their return to the Moscow laboratories of the Institute for Biomedical Problems. These animals were maintained and monitored for birth activity by Dr. Serova, and her report should be consulted for details of the deliveries. Four of the five dams underwent "normal" birthing, delivering litters considered normal in pup number and sex ratio, but with a lengthened gestation age and lighter-than-normal birth weights (Serova et al., 1984).

For the purposes of the present study, six of the newborns (two each from three different dams) were sacrificed during the culling of the litters (to establish a standard nursing load for the analysis of postnatal behavioral development and the monitoring of maternal behavior characteristics (Alberts et al., 1986). In addition, two specimens each were prepared by decapitation sacrifice on postnatal days 15 and 30. ALL of these heads were opened along the dorsal midline of the skull, prior to immersion fixation in modified Karnovsky biostabilizer.

C. Postflight Processing

ALL flight-derived heads were initially stabilized for 24 hours at 4°C in a modified Karnovsky fixative and then were transferred to 10% neutral buffered formalin at 4°C for storage.

Control Groups: Two sets of Earth-normal gravity controls were established and maintained from the same animal source population. Synchronous controls were established from the "back-up" animal population and subjected to an exposure in a mock-up spacecraft under identical housing and feeding regimes. Due to the routine and normal delays in data transmission and programming of the mock-up spacecraft, this control group was carried on a five-day lag behind the flight specimens. Vivarium controls were established and maintained in the Moscow laboratory vivarium. It should be noted that the latter specimens had undergone transportation to and from the launch site. This is considered to be of significance in their role as standard normal controls. In addition, the vivarium control specimens, which consisted of a second potential flight group should a liftoff delay occur, lagged behind the flighted counterparts by two days.

Controls were sacrificed on a matching schedule with the flight specimens, with the following noteworthy exception: due to a delay in transit of fresh biostabilizer chemicals, ALL Group I flight specimens were initially fixed in a different batch of stabilizer than either of their control groups. ALL Group II specimens were fixed in biostabilizer aliquots prepared freshly on the day prior to sacrifice of the flight specimens. Thus, newborn flight, synchronous and vivarium specimens were fixed in aliquots of the IDENTICAL fixative even though they varied by several days at time of sacrifice.

All heads were stored, at 4°C in 10% neutral buffered formalin, for varying periods of time prior to their transport to the U.S. laboratory. In the instance of the Group I heads, this period extended for nearly three months. This lengthy storage may have contributed to the extreme degree of tissue hardness encountered in all Group I specimens.

During transportation to the U.S., specimens were maintained in a temperature-controlled container. On arrival at our laboratory, all heads were subjected to gross photography, extensive washing to remove excess formalin, thorough decalcification with DECAL and gradual dehydration over a period of two weeks to ensure complete removal of all water from the tissues.

Since a large number of specimens had been realized, it was elected to embed these in three alternative embedments for three sectioning planes. Embedding of all Group I specimens was carried out in Araldite 502, Spurr low-viscosity epoxy resin (due to the hardness of the blocks) and Paraplast paraffin. Embedding of specimens was achieved by multiple infiltrations of fresh embedding medium over a period of two weeks for the plastics and three days for the paraffin material.

Embedding selection for Group II specimens was more dictated by head size. Newborn heads were embedded in the same three embedding compounds, following initial bisection in the desired sectioning plane. All 15- and 30-day postnatal specimens required embedding in paraffin due to their size. Each of the latter specimens was also either bisected or quartered, depending upon the desired sectioning orientation.

Materials and Methods

Three sets of pregnant dams were established to support FLIGHT, SYNCHRONOUS CONTROL and VIVARIUM CONTROL groups. Vivarium "control" animals were two-day lags of flight specimens, while the Synchronous controls lagged by thirteen days. NEITHER control group was initially processed as controls with the flight groups.

ALL specimens consisted of whole heads, initially fixed by Dr. Igor Krasnov using a modified Karnovsky biostabilizing fluid. Storage and transport were in 10% neutral-buffered formalin. The following standard protocol, including fixtive preparation, was followed by Dr. Krasnov in obtaining the samples:

GROUP I: Decapitate fetus, transfer entire unopened head to 60 cc of cold (4-8°C) primary fixative (see appendix) contained in labelled containers.

GROUP II: Decapitate postnatal pups (Newborn, PN15 and PN30), reflect skull, transfer entire opened head to 90 cc of cold (4-8°C) primary fixative (see appendix) contained in labelled containers.

The PRIMARY FIXATION for both groups was to be at 4-8°C for a period of at least 12 hrs, but not to exceed 24 hrs. Such time periods allow adequate initial fixation but prevent excessive hardening of the tissues.

ALL heads were transferred from primary fixative to labelled mesh bags (one head/bag) and placed in containers of cold (4-8°C) storage fixative (see appendix). These containers were designed to hold specimens from both Flight and Vivarium groups in common storage fixative, to serve as internal controls during both storage and transport. A temperature of 4-8°C was maintained during the prolonged storage in the U.S.S.R. and during transport to the U.S. laboratory.

Decalcification, Embedding and Processing Steps

Upon receipt in the U.S. laboratory, each of the COSMOS 1514 heads was processed in the GENERAL pattern outlined below, although specific heads may have received somewhat different times in various stages due to their size or maturity (e.g., postnatal 15 and 30d). IN EACH INSTANCE, FLIGHT HEADS WERE PROCESSED SIMULTANEOUSLY WITH MATCHED VIVARIUM AND SYNCHRONOUS CONTROL HEADS. Each processed head was assigned a single TISSUE PROCESSING SHEET, on which EACH STEP was recorded as it occurred. Notations of date and time, as well as any novel environment (e.g., temperature variation) or unique specimen observations were also recorded. The processing data were also stored in protected computer files.

Pattern of Processing

1. Store at 4-6°C until processing begun. (Processing on older heads delayed to force similar times in storage fixative.)

2. Wash in running cold (7°C) tap water for 3-6 hours. (NOTE: pH of the transport fixative was measured at this point and varied from 6.05 to 6.91.)

3. Immerse in DECALCIFYING SOLUTION (DECAL^{TM}) for AT LEAST 18 hours. Provide fresh solution every 24 hours. NOTE: The decalcification time variable is dependent upon both specimen's HEAD SIZE and DEVELOPMENTAL AGE. Timing of this step is monitored by testing individual decalcifying fluids each morning (see appendix).

4. Remove heads from transport bags and transfer to individual, labelled, processing containers. The transport label prepared by Dr. Krasnov and a new, coded, label were carried with the tissues throughout all subsequent procedures.

5. Wash in running cold (7°C) tap water for 3-6 hours. (NOTE: Any trimming or blocking of head and photography of entire head is performed during this interval.)

6. Dehydrate whole heads (COSMOS 1514 #'s 1-10, 11-20, 21-30, 31-48) or blocked heads (COSMOS 1514 #'s 49-60) through ascending concentrations of ethanol for the MINIMUM times indicated, which vary dependent upon relative size of head:

70% ethanol/glass distilled water	(24 hour minimum) **
95% ethanol/glass distilled water	(12-24 hour minimum)
100% ethanol [200 proof!]	(8-12 hour minimum) ***
100% ethanol [200 proof!]	(8-12 hour minimum)
100% ethanol [200 proof!]	(8 hour minimum)

** NOTE: Can store for several weeks in 70% without hardening of tissues.
*** NOTE: Three complete changes of 200 PROOF ALWAYS utilized!

7. Subsequent processing steps depend upon the embedding medium selected. To optimize sectioning and staining routines for the specimens from COSMOS 1514, THREE DIFFERENT EMBEDDING protocols were chosen: ParaPlast paraffin, Araldite 502 epoxy resin and Spurr low viscosity (see appendix).

8. Sectioning of blocks is dependent upon

A. EMBEDMENT - plastic vs paraffin

Serial paraffin sections are cut at 7 to 10 micra with sharpened metal knives on a Spencer 820 microtome. Araldite 502 and Spurr Epoxy resin serial sections are cut at three micra with either standard glass or Ralph knives on either an LKB Ultratome II, LKB Pyramitome or Sorvall JB-4 microtomes.

B. ORIENTATION of section plane selected

Three standard anatomical planes are produced:

Transverse	(cross) sections
Sagittal	(longitudinal) sections
Coronal	(horizontal) sections

9. Serial sectioning is utilized to produce a complete series in each plane. Sections are mounted on chemically cleaned, thinly albumenized glass slides as follows:

Survey slide #1: sections #'d 1 8 15 22 29 36

LEFT SIDE		RIGHT SIDE
Section 2 3 4	Slide 1	Section 5 6 7
Section 9 10 11	*Slide 2*	Section 12 13 14
Section 16 17 18	Slide 3	Section 19 20 21
Section 23 24 25	*Slide 4*	Section 26 27 28
Section 30 31 32	Slide 5	Section 33 34 35

Survey slide #2: sections #'d 37 44 etc.....

LEFT SIDE		RIGHT SIDE
Section 38 39 40	*Slide 6*	Section 41 42 43

etc.

The SURVEY SLIDES are stained with a routine Hematoxylin and Eosin and are intended to be utilized strictly for monitoring progress through the block during the sectioning process. Slide sets indicated by *Slide #* above have been encased in slide boxes and shipped to the U.S.S.R.

10. Most slides are stained on one side with the Bodian Silver Proteinate technique and on the other side with Azure II (see appendix for protocols).

This side of slide	SLIDE	This side of slide
stained with Azure II	LABEL	stained with Protargol

RESULTS

The present document must be viewed as a report of work that is yet in progress. The material realized from the most unique flight of COSMOS 1514 is extensive (table I). Due to the deep significance of the results of this experiment for the implementation of future flight experiments, progress through the complement of specimens has been exhaustive and has been done with great care. The current status

of our efforts on each of the specimens is displayed in table II for Group I and table III for Group II specimens.

The results to date, of the studies on Group I specimens, reveal an effect of spaceflight that is exerted upon the normal developmental progression of neuronal maturation. This effect is reflected in three primary aspects of development:

(1) the comparative overall systemic immaturity of the flight specimens most evident in ocular, vestibular and cortical structures;

(2) the presence of abnormal mitotic figures in or near neuronal regions displaying high levels of neuroblast generation and migration along radial sustentacular elements, such as the neural retina and cerebral plates; and,

(3) the apparent volumetric disturbances reflected in ocular, vestibular, cochlear and ventricular cavities, as well as in the disturbances in the normal development of their neuronal and non-neuronal complements.

Morphometric analyses have been stymied by the excessive degree of both intragroup and intergroup variability. This is compounded in the analysis of Group I specimens, since the flight animals were initially biostabilized in a different fixative fluid than either of their control counterparts, prohibiting the ruling-out of possible osmotic fixation effects. Thus, while apparent volumetric differences are visually evident (see for comparison figs. 1 to 20), there are, at best, only trends in the morphometric data due to the high degree of variance. Efforts to resolve this problem, utilizing more refined analytical techniques, are continuing.

The analysis of Group II specimens presents a different and more heartening status. Progress in this experimental group has been severely slowed by the failure to observe any significant differences or problems in the newborn pups derived from the flight dams. The gravity of the observation of normal development resulting from five days of Earth-normal readaptation has caused numerous analyses to be repeated. Initial morphometric analysis, while still showing extensive intergroup variability, fails to demonstrate any consistent difference patterns between newborn flight and control groups.

RESULTS OF GROUP I STUDIES

Cerebral Hemispheres

The continued development of the cerebral hemispheres, during the late fetal period, was not grossly impacted by an exposure of the dams to spaceflight conditions. The hemispheres of all Group I flight specimens were at an earlier developmental stage, with thinner regional cortical plates and marginal zones, although an apparently normal developmental progression from telencephalic outgrowth through

full initial zonation has occurred (figs. 1 to 3). All cortical zones (ventricular, subventricular, intermediate and marginal) were present but thinner. While all ependymal mitoses appeared normal and the cytological organization did not appear to be disrupted, the brain ventricles appeared enlarged when compared with controls, with an actively mitotic ependymal lining (ventricular zone). The choroid plexus appeared swollen, suggesting a potential hyperplastic fluid response (fig. 4).

Aberrant mitotic figures (figs. 5 to 8) have been observed, in most of the actively differentiating regions of the cortex near and in the secondary zones (subventricular) of Group I flight specimens, amid the normal cohort of proliferative cells. The number of aberrant cells and their location (in regions in which the principal developmental process is displacement of newly formed neuroblasts along radial glial fibers) strongly suggest that these cells did not result from the events of reentry, but rather resulted from a failure to complete cytokinesis sometime during the spaceflight exposure. There have been no such aberrant mitotic cells observed in any of the Group I control specimens.

Vestibular Periphery

The peripheral vestibular apparatus of Group I flight specimens showed an apparently normal developmental progression from the otocyst through initial partition, with all primary structures present.

All Group I flight specimens appeared to be at an earlier developmental stage than their control counterparts. This was evidenced by the incomplete separation of utricular and saccular maculae, a higher mitotic activity in presumptive sensory regions than is normal for an E18 specimen, and fewer differentiated hair cells, frequently displaying only kinocilia. Otoconial precursors on the forming otolithic membrane were present, but smaller and sparser than their control counterparts (figs. 9 to 13). The cupulae of the cristae were forming but were relatively primitive (figs. 14 and 15). The vestibular ganglia were smaller and less developed in the flight specimens.

Preliminary volumetric studies suggest an appreciably smaller membranous labyrinth with the cartilaginous precursor of the bony labyrinth normal in shape, but with enlarged internal spaces similar to that normally observed in E16- to E17-day embryos. Although both endolymphatic and perilymphatic cavities were markedly distended, these observations suggest that either endolymph production had not yet been equilibrated with the perilymph, possibly as a result of some alteration in fluid electrolyte regulation, or the flight specimens were retarded by approximately 24 to 36 hours in their vestibular development.

The Eye

The visual organs of all Group I flight specimens appeared to be at earlier developmental stages than the vivarium controls by more than a full day. As an

example, the eyelids have not yet fused in any of the flight specimens--normally observed by day 18 of gestation--while nearly all of the control specimens show full eyelid fusion (figs. 16 and 17). The eyes followed a normal developmental progression from cup invagination through initial retinal layering and differentiation, and they were not grossly impacted by spaceflight exposure during the late embryogenic period. Lens invagination and differentiation were behind the control specimens in developmental staging. Lens compaction was notably different, suggesting an intraocular fluid imbalance, possibly in the transport mechanism.

The appearance of a "ring optic cavity," at the level of the forming ora serrata (figs. 16, 18 to 20), is reflective of either a fluid electrolyte imbalance, an irregularity in the development of the ciliary fluid transport complex, or a failure in the cytological differentiation of surface features along the retinal-pigment epithelial interface. This developmental disruption has been observed in ALL flight specimens, but in NONE of the controls.

Mitotic activity in eyes derived from flight specimens was notably different from the control specimens. The proliferation of scattered cells throughout the posterior pigment epithelium (figs. 21 and 22) is NOT NORMAL for this developmental age, and it was not observed in any of the control specimens. Aberrant mitotic figures (figs. 23 to 28) have been observed in nonproliferative retinal zones such as the forming inner plexiform layer. The presence of ring-shaped and primarily metaphase figures in this region suggests a failure to complete normal cytokinesis prior to cellular migration along the radial Mueller fibers. The ora zone (developing ora serrata) cells showed normal patterning, although the differentiated status of the outer layer cells and the width of the ora zone were notably more primitive than that observed in the control specimens (figs. 16, 19, 20, 29, 30).

Many of these observations on the visual organ may be the result of an altered fluid electrolyte balance which has impacted the full development of intraocular turgor pressure. These differences may also merely reflect a delay in the development of the visual organ.

Interesting Miscellaneous Observations

The cartilaginous precursors of the bony skull were normal in shape and extent, but the cranial surface-to-volume ratio appeared larger, suggesting an earlier developmental stage. Both the mandible and maxillae appeared normal in shape and size, although the tooth primordia appeared to be at much earlier developmental stages. The palatal shelves have fully completed elevation and appeared to be normally fused in the midline (figs. 31 to 33).

The pituitary parenchyma was primarily tubulocystic, not solid cords as would be expected in an 18-day fetus (figs. 34 and 35). The flight specimens showed an elevated mitotic level, with a retarded cytodifferentiation in which chromophils were not distinguished and chromophobes were not apparent. These observations are consistent with the concept of a retarded development.

The pineal showed a distended central stalk cavity with only very preliminary convolutions (figs. 36 and 37). Cellular differentiation was not yet occurring, suggesting a developmental stage younger than 18 days.

External ear structures appeared normal, with the external auditory canal closed with periderm and an enlarged Eustachian tube and middle ear cavity (fig. 38). The cochlea (figs. 39 to 41) showed normal developmental progression, but at an earlier developmental stage than the controls. For example, the hair cells were frequently not yet evident. Preliminary volumetric analysis indicates an enlarged cochlear cavity, but with a slightly reduced Cochlear duct (Scala media)--an observation that could, again, reflect an imbalance in fluid electrolytes.

RESULTS OF GROUP II STUDIES

The results from the study of the Group II specimens must be restricted to the newborn specimens (see table 3). After repeated anlyses of the members of this population, no differences have been observed between the flight and control group members.

Preliminary morphometric analysis also fails to reveal either specific differences or suggestive trends towards differences among or between the three groups of specimens. Both intragroup and intergroup variances are also markedly lower than observed in the Group I specimens.

A comparison of comparable regions from flight and control specimens is presented for the eyes (figs. 42 and 43), with special emphasis on the maturing ora serrata zone (figs. 44 and 45), the cochlear duct (figs. 46 to 48), peripheral vestibular apparatus (featuring maculae of utricle and saccule (figs. 49 to 53)), otolithic membrane (figs. 54 to 56), and cristae of the semicircular canals (figs. 57 to 60).

It should be stressed that there is no evidence of either the continued presence or an effect of the abnormal mitotic neuroblasts demonstrated, in both cortical and retinal layers, in all of the the Group I flight specimens.

While the principal concern with the analysis of this group was the inability to display any differences in the flight population, the apparent ability of the flight specimens to reverse any effects of the spaceflight during the immediate postflight interval was heartening. What continues to be most frustrating is the knowledge that, while these flight specimens consistently showed lower birth weights than their control counterparts, the component elements of our analysis failed to demonstrate any effect of this difference.

The results of this experiment have thus far demonstrated that, even though this exposure period occurred at a time when no new structures were being initiated, there is (are) some factor(s) in the spaceflight environment that impact the processes of normal neuronal cytodifferentiation and are expressed the generative staging of organ maturation. At the present time and with the present material, it is uncertain whether these effects are the result of the direct exposure to the null-gravity environment or an expression of the spaceflight environment acting directly upon the dam and indirectly, via the placenta, upon the developing fetus.

However, one should be heartened that spaceflight exposure of the flight dams did not result in either the premature termination of pregnancy or the gross deformation of the developing fetuses. Such a demonstration facilitates the planning of future mammalian developmental studies.

Furthermore, postflight readaptation to Earth-normal gravity appears to relieve the effects evident at the termination of the flight exposure, perhaps reflective of the plasticity of the maternal-fetal unit at this developmental stage. The apparent differences in organ volumes (such as in the eye, membranous labyrinth and cerebral ventricles) do not continue to show expression following adaptation and birthing. Differences in developmental staging, approximating a 24- to 30-hour developmental deficiency in all flight specimens in Group I, appear to have been reduced, perhaps via the mechanism of a longer gestation duration.

There is no evidence in the newborn specimens for a continued presence of the abnormal mitotic figures observed in all of the Group I flight specimens, nor does there appear to be a persistent deficit in the developmental regions (neural retina and cerebral cortex) showing these abnormal features at the termination of the spaceflight. Future work in this area should concentrate on the causative mechanisms of the observed cell deaths and their potential impact at more critical developmental intervals. Such intervals should include gestational days 8 through 12, during which interval disruptive mitoses would have a greater potential for disruption of normal neurogenesis. Further analytical efforts should be devoted to the immediate perinatal period and the possible effects of the abnormal mitotic events upon the pattern and extent of normal cell death.

The establishment of the complex central nervous system of mammals, an exercise in precision and plasticity, is demonstrated by the following: (1) precise timing of cellular birthdates from specifically designated generative sites; (2) precision migratory movements of newly generated neuroblasts along radial guidance substrates from their generative sources, frequently over extensive distances through complex developing systems, to properly defined terminal structures with aggregates of like kind; (3) precise cytodifferentiation with suitably plastic expression of membrane properties, transmitter characteristics and cellular morphology dependent to an as yet unknown degree upon the functional loading of the system; and, (4) establishing proper, but regulatable (again dependent upon functional loading of the system),

connectivity with relating structures and tracts. Failure in precision during any of these processes is believed to provide the groundwork for aberrant neural relationships that may result in the death of the organism or unusual behavior responsiveness to otherwise normal stimuli. It has only been in recent years that the degree of plasticity in these otherwise precise sequential processes that appears to be dependent upon the functional loading of the maturing system, has been appreciated.

This combination of both precision and plasticity in the development of the mammalian central nervous system strongly suggests the potential for both evolutionary modifiability and phenotypic regulation, dependent upon the system requirements of the perinatal developmental environment. Such regulation would require the system capability of modifying the responsive neuronal population. This may take the form of an elevation in the apparent rate of production of relevant neuroblasts, modulation of the phenotypic expression of the individual neuronal population during perinatal cytodifferentiation and maturation or modification of the systemic integration through synaptic field compression or expansion. Any modulation in the responsive production of neurons would require changes in either the rate, length of time or site of production of neuroblasts. Such evidence has not been observed in any mammalian species. The mammalian central nervous system appears to have evolved a different mechanism to modulate the production of neurons in response to variations in functional loading of both sensory and motor systems through a process of regular overproduction of neuroblasts with subsequent degeneration of superfluous neurons during the processes of perinatal maturation. Such cell death has been observed for decades but only recently been positively correlated with changes in the functional loading of the affected system. This is of paramount significance to gravitational biologists since exposure to the gravitational vectors in spaceflight provides opportunities for modulation of the sensory loading of both vestibular and proprioceptive systems during selected developmental intervals.

Future perinatal studies under conditions of null gravity possess unique attributes for testing the functional loading hypothesis; future experimenters should direct their attention to the analysis of this phenomenon in their experimental design.

APPENDIX

FIXATIVE PREPARATION PROTOCOL

PRIMARY FIXATIVE [BIOSTABILIZER = KARNOVSKY (HALF-STRENGTH)]

Composition and Directions for Preparation:

For 500 cc of primary fixative: place 10 gm Paraformaldehyde powder in 125 cc glass-distilled water, STIR and HEAT until temperature = 60-65°C, remove from heat and, with continued stirring, ADD 1.5 cc 1 N NaOH (the solution should clarify). With continued stirring, ADD 150 cc 8% Glutaraldehyde and 225 cc 0.2 M Cacodylate buffer, pH 7.2 (see below). Continue stirring and ADD 0.25 cc 0.1 M $CaCl_2$ and 0.25 cc 0.1 M $MgCl_2$.

Preparation of 0.2 M cacodylate buffer:

To 500 cc of glass-distilled water dissolve with constant stirring 16 gm Cacodylic acid, sodium salt. Adjust pH to 7.2 with ~8 cc of 1 N HCl. STORE IN REFRIGERATOR.

SECONDARY (STORAGE) FIXATIVE: 10% NEUTRAL BUFFERED FORMALIN (NBF)

Composition, Preparation and Storage:

Heat 2000 cc glass-distilled water to 60-65°C and dissolve (constant stirring) 13.0 gm anhydrous sodium phosphate, dibasic and 8.0 gm sodium phosphate, monobasic. Add 80 gm Paraformaldehyde and continue stirring for 20 min at 60-65°C. Add 20 cc of 1 N NaOH. Solution should clear with slight residual murkiness. REFRIGERATE AT ONCE!

TEST FOR COMPLETE DECALCIFICATION

a. Extract 5 ml of used decalcifying fluid from container.

b. Add 5 ml of 5% ammonium hydroxide (aqueous solution) and 5 ml of 5% ammonium oxalate (aqueous solution).

c. Mix thoroughly and let stand 15-30 minutes at room temperature. NONMILKY (clear!) = indicates complete decalcification. CLOUDY = incomplete decalcification, continue with fresh decalcification solution for another 24 hours and check again.

A. PARAFFIN embedding (standard process utilizing ParaPlast)

a. Tissues are CLEARED in methyl salicylate (several changes required until entire head cleared).

b. 50:50 methyl salicylate and fresh filtered ParaPlast.

c. Infiltrate with fresh ParaPlast at 57 ±0.5°C. May require as many as 20 changes of ParaPlast.

d. Orient and cast in fresh ParaPlast.

B. ARALDITE 502 epoxy resin (after Luft)

a. Heads are intermisced in propylene oxide (two changes @ 3-6 hours/change) (size dependent!).

b. 50:50 propylene oxide:Araldite 502 (complete) (overnight at room temperature).

c. 25:75 propylene oxide:Araldite 502 (complete) (24 hours at room temperature).

d. Fresh Araldite 502 (complete) (all day at room temperature).

e. Fresh Araldite 502 (complete), orient in molds (overnight at 37°C).

f. Check orientation and transfer to 60°C for 24 hrs.

Araldite 502 Media Composition

27 cc Araldite 502 Resin
23 cc dodecenyl succinic anhydride (DDSA)
0.8 cc 2,4,6-tri(dimethylaminomethyl)phenol (DMP-30)

Add above quantities in sequence and stir with glass rod for at least 30 minutes at room temperature.

NOTE: Although large quantities of complete Araldite 502 media can be made in advance and aliquots frozen until required, moisture condensation during the thawing can cause embedding problems. For this reason FRESH Araldite was always prepared for each use!

C. SPURR EPOXY RESIN (after Spurr, mod. by Doane 1974)

a. 50:50 Absolute ethanol:Spurr (complete) (24 hours in desiccator at room temperature).

b. Fresh Spurr (complete) (24 hours in desiccator at room temperatore)

c. Fresh Spurr (complete) - orient heads in casting molds (6 hours at 37°C) (24 hours at 65°C) (24 hours at 70°C).

Spurr Embedding Composition

10.0 gm	Vinylcyclohexene dioxide
6.0 gm	diglycidyl ether of polypropyleneglycol (DER 736)
26.0 gm	nonenyl succinic anhydride
0.2 gm	dimethylaminoethanol (DMAE)

Low viscosity, longer pot life facilitating impregnation of dense (heavily fixed) and unusually large tissue blocks.

STAINING PROTOCOLS

Bodian (Protargol) Stain for Epoxy Sections

PRECAUTIONS: For this procedure use only glass vessels and jars cleaned with chrome-sulfuric acid, washed with MICRO detergent and scrupulously rinsed with glass-distilled water. We label each piece of glassware with a diamond marker pencil restricting that glassware to use with only that one specific chemical solution. Such glassware need be washed only with MICRO and rinsed following each use WITH THE EXCEPTION of the glassware used for the silver solution which must be soaked overnight in chrome-sulfuric acid each time it is used. Transfer of slides between staining solutions is by using a SEPARATE pair of NYLON FORCEPS. These forceps are restricted to particular staining step, rinsed after each use and regularly cleaned by dipping them into chrome-sulfuric cleaner followed by thorough rinsing in glass-distilled water.

EQUIPMENT REQUIRED: This procedure takes eight acid-cleaned Coplin glass staining jars, four pair of forceps and additional Coplin jars for desired counterstain.

PREPARATION OF STAINING SOLUTIONS

(NOTE: Quantities set for run of FIVE sets of 10 slides)

SILVER PROTEIN SOLUTION: Prepare five Coplin jars each as follows:

50 cc glass-distilled water
0.50 gm silver proteinate

Sprinkle the silver proteinate as a "dust" on the surface of the jar. DO NOT STIR! Allow ~1 hour for solvation before beginning the staining process.

REDUCER: 250 cc glass-distilled water
12.50 gm sodium sulfite
1.25 gm potassium metaborate
2.50 gm hydroquinone

OXALIC ACID: 250 cc glass-distilled water
2.50 gm Oxalic acid

SODIUM THIOSULFATE: 250 cc glass-distilled water
12.50 gm sodium thiosulfate

ALL of the above solutions MUST be prepared FRESH each use!

GOLD CHLORIDE: 250 cc glass-distilled water
2.50 gm Gold Chloride

(NOTE: Store in Coplin Jar with glass lid, wrapped in Parafilm and exterior aluminum foil at 4-6°C. Filter through Watman #1 if contamination evident. AVOID METALLIC CONTAMINANTS and LIGHT!)

BODIAN PROCEDURE

1. Using clean plastic gloves, cut a piece of clean 2-mil copper foil to fit the width of a Coplin staining jar (~2.5 × 4.5 cm weighing ~2 grams) and fold the foil to fit the glass jar. Using a new dissecting needle, extensively perforate the foil to increase the surface area exposed to the silver solution and facilitate circulation of the staining solution.

2. Load 10 slides/holder, fold the foil around the ends of the slides, gently lower the foil/slide combination into the silver solution, cover the jar with a glass lid and place the jar in a 38°C oven for 18 hours.

3. Rinse carefully with three changes of fresh glass-distilled water (~one minute/change).

4. Place slides in REDUCING SOLUTION for 10 minutes.

5. Rinse carefully with three changes of fresh glass-distilled water (~one minute/change).

6. Transfer slides to GOLD CHLORIDE SOLUTION for 6-10 minutes (dependent upon section thickness).

7. Rinse carefully with three changes of fresh glass-distilled water (~one minute/change).

8. Transfer slides to OXALIC ACID SOLUTION for 3-4 minutes. (Step complete when sections turn "battle-ship gray"!)

9. Rinse carefully with four changes of fresh glass-distilled water (~one minute/change).

10. Transfer slides to SODIUM THIOSULFATE SOLUTION for 10 minutes.

11. Rinse carefully with three changes of fresh glass-distilled water (~one minute/change).

12. May counterstain with Azure II (or Aniline Blue).

13. Dry slides with canned air blasts.

14. Coverslip with Permount or Preservaslide.

AZURE II STAIN FOR EPOXY SECTIONS

Ten slides (five each of matched FLIGHT and VIVARIUM) are racked and stained for 1 minute in AZURE II (0.25% Azure II in 0.5% sodium tetraborate) maintained at 60°C. The slides are rinsed in three changes of glass-distilled water, shaken then dried on a hotplate at 60°C and coverslipped with Corning No. 1 coverglasses using either Permount or Preservaslide mountants.

BIBLIOGRAPHY

Alberts, J. R.; Serova, L. V.; Keefe, J. R.; and Apenasenko, Z.: Early Postnatal Development of Rats Derived from Cosmos 1514. NASA TM 88223, 1986.

Ancel, P.; and Vintemberger, P.: Recherches sur le determinisme de la symetrie bilaterale dans l'oeuf des amphibiens. Bull. Biol. France et Belg., Suppl. 31, 1948, pp. 1-182.

Baumgarten, R. J.; Simmonds, R. C.; Boyd, J. F.; and Garriott, O. K.: Effects of Prolonged Weightlessness on the Swimming Patterns of Fish Aboard Skylab 3. Aviat. Space. Env. Med., vol. 46, 1975, pp. 902-906.

Biological Studies on the Kosmos Biosatellites: Trans. of "Biologicheskiye Issledovaniya na biosputnikakh 'KOSMOS'," Y. A. Il'yin and G. P. Parfenov, eds., NASA TM 75769, 1980.

Gazenko, O. G.; Butenko, R. G.; Rubin, F. A.; and Belousov, L. V.: Predvaritel'nyye rezul'taty issledovaniy na biosputnika "Kosmos-782" (Preliminary Results of Studies on the Biosatellite "Kosmos 782"), Preliminary Results Report on COSMOS 782, NASA TT F 15500, 1976, pp. 74-76.

Keefe, J. R.: Experiment K-313: Rat and Quail Ontogenesis. NASA TM 81289, 1981, pp. 325-362.

Lowenstam, H. A.; and Margulis, L.: Evolutionary Prerequisites for Early Phanerozoic Calcareous Skeletons. Biosystems, vol. 12, 1980, pp. 27-41. (See also: The Regulatory Functions of Calcium and the Potential Role of Calcium in Mediating Gravitational Responses in Cells and Tissues, S. J. Roux, ed., 1983, NASA CP 2286.)

Malacinski, G. M.: Cytoplasmic Rearrangements Associated with Amphibian Egg Symmetrization. NASA Space Biology Annual Symposium, 1983, pp. 65-66.

Nace, G. W.; and Tremor, J. W.: Clinostat Exposure and Symmetrization of Frog Eggs. Physiologist, vol. 24, 1981, pp. S77-8.

Penners, A.; and Schleip, W.: Die Entwicklung der Schultzeschen Dopplebildungen aus dem Ei von Rana fusca. Zeitschr. wiss. Zool., 1928, vol. 130, pp. 305-454, and vol. 131, pp. 1-156.

Pitts, G. C.; Pace, N.; Smith, A. H.; Ushakov, A. S.; and Smirnova, T. A.: Body Composition Data from the Rat Subjects of Cosmos 1129 Experiment K-316. Contract Report EPL 82-1 filed by Environmental Physiology Laboratory, Univ. of California, Berkeley, 1982. (See also Pitts, G. C.; Ushakov, A. S.; Pace, N.; Smith, A. H.; Rahlmann, D. F.; and Smirnova, T. A.: Effects of Weightlessness on Body Composition in the Rat. Am. J. Physiol., vol. 244, 1983, pp. R332-R337.

Radice, G. P.; Neff, A. W.; and Malacinski, G. M.: The Intracellular Responses of Frog Eggs to Novel Orientations to Gravity. Physiologist, vol. 24, 1981, pp. S79-80.

Scheld, H. W.; Boyd, J. F.; Bozarth, G. A.; Conner, J. A.; Eichler, V. B.; Fuller, P. M.; Hoffman, R. B.; Keefe, J. R.; Kuchnow, K. P.; and Oppenheimer, J. M.: Killifish Hatching and Orientation. NASA SP 412, 1976, pp. 19-1 to 19-14.

Scheld, H. W.; Keefe, J. R.; Boyd, J. F.; Fuller, P. M.; and Oppenheimer, J. M.: Killifish Development in Zero-G on Cosmos 782. NASA TM 78525, 1978, pp. 179-199.

Schultz, O.: Die kunstliche Erzeugung von Dopplebildungen bei Froschlarven mit Hilfe abnormer Gravitationswirkung. Roux' Arch. Entwick. Mech., vol. 1, 1894, pp. 269-305.

Serova, L. V.: Paper Before 4th Annual Meeting of IUPS Commission on Gravitational Physiology. Physiologist, vol. 25, 1982, pp. 9-12.

Serova, L. V.; Denisova, L. A.; Apenasenko, Z. I.; Bryantseva, L. A.; Chel'naya, N. A.; Oganov, U. S.; and Skuratova, S. A.: Preliminary Report on the Results of the Embryological Experiment with Mammals on the Kosmos 1514 Biosatellite. NASA TM 77617, 1984.

Tremor, J. W.; and Souza, K. A.: The Influence of Clinostat Rotation on the Fertilized Amphibian Egg. Space Life Sci., vol. 3, 1972, pp. 179-191.

Tremor, J. W.; and Young, R. W.: The Effect of Weightlessness on the Dividing Egg of Rana pipiens. Bioscience, vol. 18, 1968, pp. 609-615.

Vinnikov, Ya. A.; Gazenko, O. G.; Lychakov, D. V.; and Palmbach, L. R.: Formation of the Vestibular Apparatus in Weightlessness. Development of Auditory and Vestibular Systems, R. Romand, ed., Academic Press (New York), 1983, pp. 537-560.

Young, R. W.: Gravity and Embryonic Development. Life Sciences and Space Research, vol. XIV, 1976, pp. 69-75.

Young, R. W.: Sea Urchin Egg Fertilization and Development. Gemini Program Biomedical Science Experiments Summary. NASA TM X-58074, 1971, pp. 245-247.

Young, R. W.; Tremor, J. W.; Willoughby, R.; Corbett, R. L.; Souza, K. A.; and Sebesta, P. D.: The Effect of Weightlessness on the Dividing Eggs of Rana pipiens. The Experiments of Biosatellite II, J. F. Saunders, ed., NASA SP 204, 1971, pp. 251-271.

TABLE 1.- COSMOS 1514 NEURO-ONTOGENY SPECIMEN STATUS

Group I					Group II				
Hd.#	Group	Pup/Dam	Emb	Plane	Hd.#	Group	Pup/Dam	Emb	Plane
1	F E18	5L/24	Aral	Trans	31	F NB	8/71	Aral	Trans
2	F E18	5R/24	Aral	Sagit	32	F NB	7/71	Spur	Trans
3	F E18	5L/83	Spur	Trans	33	F NB	1/79	Para	Trans
4	F E18	5R/83	Spur	Sagit	34	F NB	3/79	Aral	Coron
5	F E18	5L/69	Para	Trans	35	F NB	15/16	Spur	Coron
6	F E18	5R/69	Para	Trans	36	F NB	12/16	Para	Coron
7	F E18	5L/4	Aral	Coron	37	S NB	85/58	Aral	Trans
8	F E18	5R/4	Spur	Coron	38	S NB	86/58	Para	Trans
9	F E18	5L/13	Spur	Coron	39	S NB	78/65	Spur	Coron
10	F E18	5R/13	Para	Coron	40	S NB	80/65	Para	Coron
11	S E18	5L/71	Aral	Trans	41	V NB	55/81	Aral	Trans
12	S E18	5R/71	Aral	Sagit	42	V NB	56/81	Para	Coron
13	S E18	5L/44	Spur	Trans	43	V NB	75/43	Para	Trans
14	S E18	5R/44	Spur	Sagit	44	V NB	76/43	Aral	Coron
15	S E18	5L/64	Para	Trans	45	V NB	68/42	Spur	Coron
16	S E18	5R/64	Para	Trans	46	V NB	71/36	Spur	Trans
17	S E18	5L/86	Aral	Coron	47	V NB	19/95	Aral	Trans
18	S E18	5R/86	Spur	Coron	48	V NB	22/95	Para	Coron
19	S E18	5L/39	Spur	Coron	49	V 15d	7/31?	Para	Coron
20	S E18	5R/39	Para	Coron	50	S 15d	2/57?	Para	Coron
21	V E18	5L/6	Aral	Trans	51	S 15d	1/58?	Para	Trans
22	V E18	5R/6	Aral	Sagit	52	V 15d	2/52?	Para	Trans
23	V E18	5L/42	Spur	Trans	53	F 15d	3/79	Para	Coron
24	V E18	5R/42	Spur	Sagit	54	F 15d	6/71	Para	Trans
25	V E18	5L/27	Para	Trans	55	F 30d	3/79	Para	Trans
26	V E18	5R/27	Para	Trans	56	F 30d	6/79	Para	Coron
27	V E18	5L/28	Aral	Coron	57	S 30d	58/46	Para	Trans
28	V E18	5R/28	Spur	Coron	58	S 30d	56/65	Para	Coron
29	V E18	5L/29	Spur	Coron	59	V 30d	33/5	Para	Trans
30	V E18	5R/29	Para	Coron	60	V 30d	26/31	Para	Coron

Para = Paraffin
Spur = Spurr epoxy
Aral = Araldite 502

Trans = Transverse (cross) section
Sagit = Sagittal (longitudinal) section
Coron = Coronal (horizontal) section

TABLE 2.- COSMOS 1514 GROUP I SPECIMEN STATUS

Hd.#	Group	Pup/Dam	Emb	Plane	Status	Stain	#Slides	US/USSR
				Flight Specimens				
1	F E18	5L/24	Aral	Trans	Completed	Az/Prot	424	E O
2	F E18	5R/24	Aral	Sagit	Completed	Azure II	260	O E
3	F E18	5L/83	Spur	Trans	Stored			
4	F E18	5R/83	Spur	Sagit	Stored			
5	F E18	5L/69	Para	Trans	Completed	Prot	68	E O
6	F E18	5R/69	Para	Trans	Completed	Prot	48	O E
7	F E18	5L/4	Aral	Coron	Completed	Az/Prot	279	O E
8	F E18	5R/4	Spur	Coron	Stored			
9	F E18	5L/13	Spur	Coron	Stored			
10	F E18	5R/13	Para	Coron	Completed	H+E	82	O E
				Synchronous Controls				
11	S E18	5L/71	Aral	Trans	Completed	Az/Prot	455	E O
12	S E18	5R/71	Aral	Sagit	Analysis	Azure II	275	O E
13	S E18	5L/44	Spur	Trans	Stored			
14	S E18	5R/44	Spur	Sagit	Stored			
15	S E18	5L/64	Para	Trans	Completed	Prot	86	O E
16	S E18	5R/64	Para	Trans	Completed	Prot	82	O E
17	S E18	5L/86	Aral	Coron	Sectioned			
18	S E18	5R/86	Spur	Coron	Stored			
19	S E18	5L/39	Spur	Coron	Stored			
20	S E18	5R/39	Para	Coron	Completed	H+E	85	O E
				Vivarium Controls				
21	V E18	5L/6	Aral	Trans	Completed	Az/Prot	355	E O
22	V E18	5R/6	Aral	Sagit	Completed	Azure II	283	O E
23	V E18	5L/42	Spur	Trans	Stored			
24	V E18	5R/42	Spur	Sagit	Stored			
25	V E18	5L/27	Para	Trans	Completed	Protargol	83	O E
26	V E18	5R/27	Para	Trans	Completed	Prot	93	O E
27	V E18	5L/28	Aral	Coron	Completed	Az/Prot	476	E O
28	V E18	5R/28	Spur	Coron	Stored			
29	V E18	5L/29	Spur	Coron	Stored			
30	V E18	5R/29	Para	Coron	Completed	H+E	65	O E

Para = Paraffin
Spur = Spurr epoxy
Aral = Araldite 502

Trans = Transverse (cross) section
Sagit = Sagittal (longitudinal) section
Coron = Coronal (horizontal) section

TABLE 3.- COSMOS 1514 GROUP II SPECIMEN STATUS

Hd.#	Group	Pup/Dam	Emb	Plane	Status	Stain	#Slides	US/USSR
			Newborn Flight Specimens					
31	F NB	8/71	Aral	Trans	Completed	Az/H+E	410	E O
32	F NB	7/71	Spur	Trans	Stored			
33	F NB	1/79	Para	Trans	Completed	Protargol	-	O E
34	F NB	3/79	Aral	Coron	Completed	Azure II	-	E O
35	F NB	15/16	Spur	Coron	Stored			
36	F NB	12/16	Para	Coron	Completed	H+E/Prot	167	O E
			Newborn Synchronous Controls					
37	S NB	85/58	Aral	Trans	Completed	Az/H+E	222	E O
38	S NB	86/58	Para	Trans	Completed	H+E	-	O E
39	S NB	78/65	Spur	Coron	Stored			
40	S NB	80/65	Para	Coron	Completed	H+E	-	O E
			Newborn Vivarium Controls					
41	V NB	55/81	Aral	Trans	Completed	Az/H+E	344	E O
42	V NB	56/81	Para	Coron	Completed	H+E	-	E O
43	V NB	75/43	Para	Trans	Completed	Prot/H+E	229	O E
44	V NB	76/43	Aral	Coron	Stored			
45	V NB	68/42	Spur	Coron	Stored			
46	V NB	71/36	Spur	Trans	Stored			
47	V NB	19/95	Aral	Trans	Stored			
48	V NB	22/95	Para	Coron	Completed	H+E	-	E O
			PN14-Day Specimens					
49	V 15d	7/31?	Para	Coron	Analysis	H+E	-	E O
50	S 15d	2/57?	Para	Coron	Completed	Prot	-	O E
51	S 15d	1/58?	Para	Trans	Stored			
52	V 15d	2/52?	Para	Trans	Stored			
53	F 15d	3/79	Para	Coron	Analysis	Prot	-	O E
54	F 15d	6/71	Para	Trans	Stored			
			PN30-Day Specimens					
55	F 30d	3/79	Para	Trans	Stored			
56	F 30d	6/79	Para	Coron	Analysis	Prot	-	E O
57	S 30d	58/46	Para	Trans	Stored			
58	S 30d	56/65	Para	Coron	Analysis	Prot	-	E O
59	V 30d	33/5	Para	Trans	Stored			
60	V 30d	26/31	Para	Coron	Analysis	H+E	-	O E

Para = Paraffin
Spur = Spurr epoxy
Aral = Araldite 502

Transverse (cross) section
Sagittal (longitudinal) section
Coronal (horizontal) section

Plate 1

Figure 1: Low-power view of developing telencephalic isocortex from an 18-day fetal control specimen. Note the degree of cortical layering with a prominent outer cortical Layer 1 and forming intermediate zone (arrow). The choroid plexus (CP) is minimally represented in this section, selected for the maximum ventricular area (STAR).

Figure 2: Low-power view of forming cerebral isocortex from a flight specimen selected to illustrate the maximum state of cortical development observed in the present study. Note the choroid plexus (CP) extending into the enlarged ventricle (STAR). Contrast the state of cortical development in this specimen with that from a more typical flight specimen, illustrated in figure 3.

	Animal #	Section plane	Stain	Magnification
Figure 1:	Synchronous #20	Coronal	Hematoxylin/Eosin	(100x; bar = 100 μ)
Figure 2:	Flight #5	Transverse	Protargol	(100x; bar = 100 μ)

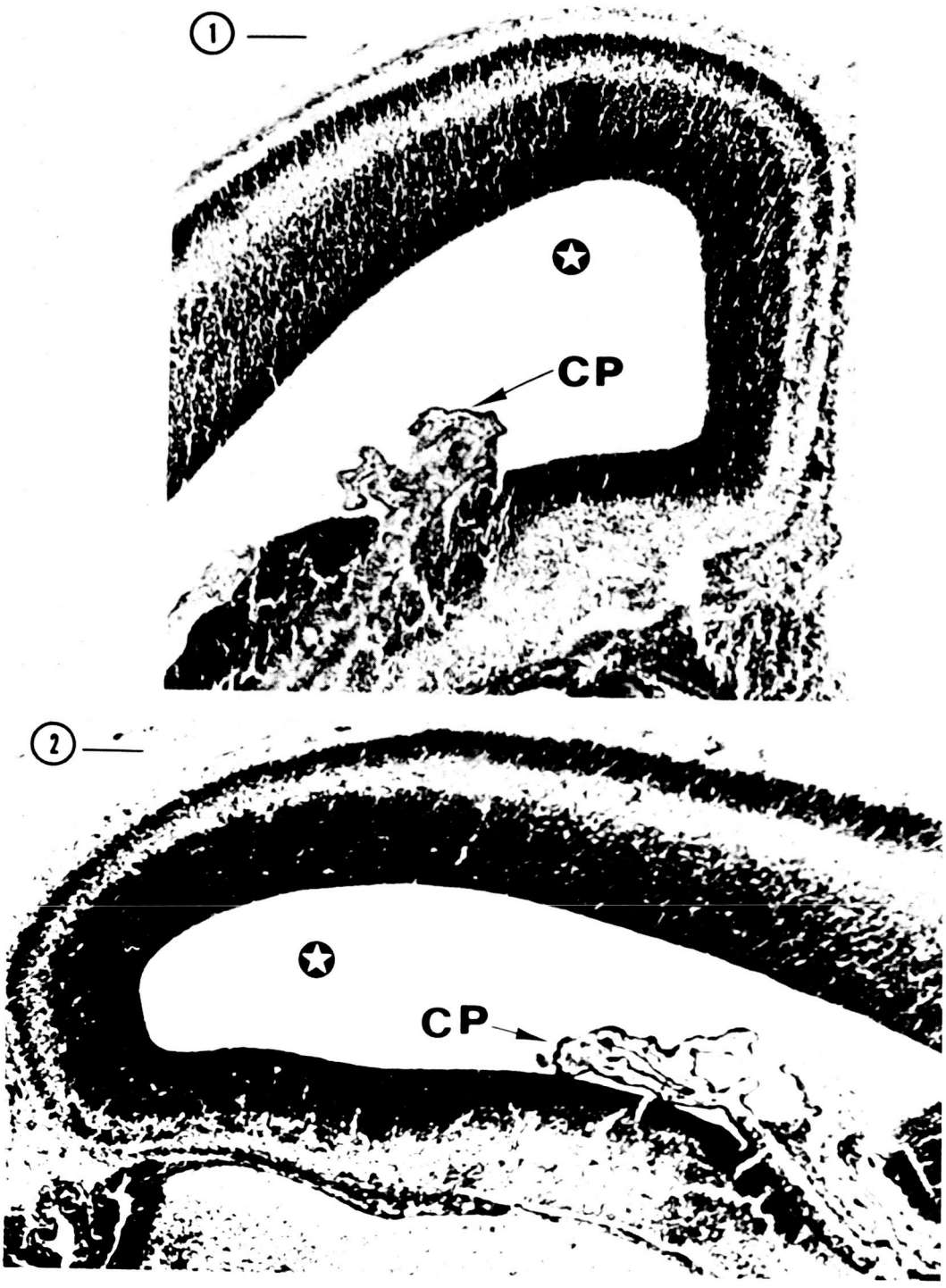

Plate 2

Figure 3: This section of the right cerebral hemisphere from a typical flight specimen displays the enlarged lateral ventricle (STAR) and a portion of the choroid plexus (CP). The status of isocortical differentiation is reflected by the degree of cortical layering shown near the top of the figure. Cortical zonation, numbered from the outer cortical layer (1) to the inner ventricular lining (5), while becoming evident, is more typical of that from a 17-day fetal rat isocortex. Zones evident in this optimally displayed region include: (1) marginal zone (with initial Layer 1 neurons); (2) intermediate zone of initial neuronal fibers; (3) migrating cortical plate neurons; (4) region of forming subventricular zone; and, (5) a ventricular zone, the site of active neuronal proliferation. These zones are illustrated in greater cytological detail in figure 6.

The regions outlined by rectangles are illustrated in greater detail in figures 4, 5 and 6.

Figure 4: This section from the medial striatal surface illustrates the distended, vacuolated nature of the cells of the choroid plexus (CP) as it extends into the lateral ventricle. The ependymal lining (E) of the striatal surface is minimally active in mitosis and does not contribute significant numbers of neuroblasts that require subsequent migration to exteriorized laminated structures. It is significant that no aberrant mitotic activity has been observed in such regions.

	Animal #	Section plane	Stain	Magnification
Figure 3:	Flight #7	Coronal	Azure II	(100x; bar = 100 μ)
Figure 4:	Flight #7	Coronal	Azure II	(1000x; bar = 10 μ)

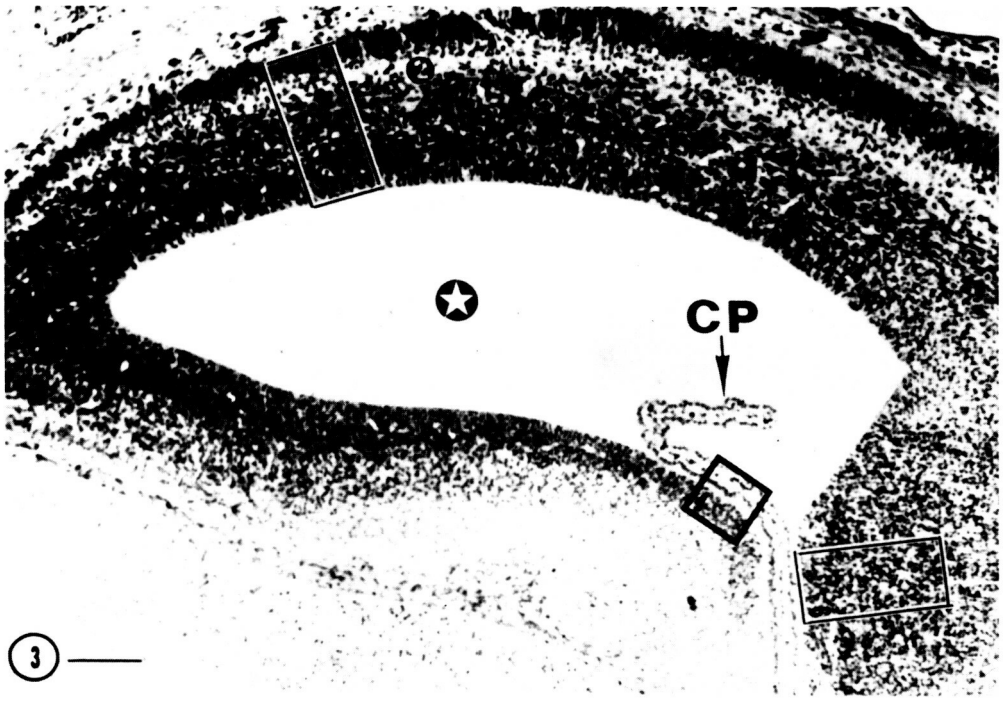

Plate 3

Figure 5: Region of optimally differentiated isocortex from a flight specimen. The inner aspects of the marginal zone (M) consist of columns of migrating neuroblasts arrayed along radial glial cells exiting the lighter-staining outer intermediate zone. The ventricular zone (V) is separated from the incipient subventricular zone (S) by a dashed line.

Note the presence of directional patterns within the three zones. The formation of neuroblasts from the ependymal surface (along bottom left) is followed by their vertical displacement within the ventricular zone (V). The forming subventricular zone (S) demonstrates the more lateral displacement, from right to left in this plane of isocortex, of the actively migrating neuroblasts into the intermediate zone. Passage of neuroblasts into the marginal columns is usually accompanied by initial neuronal cytodifferentiation and elaboration of cellular processes, which contribute to the formation of the lighter-staining outer intermediate zone.

An aberrant mitotic neuroblast is shown (arrow) within the forming subventricular region. The rectangular outline is illustrated in greater detail on the right (fig. 5a).

Figure 5a: Detail of the rectangular region from figure 5. The ventricular zone (lower half) is distinguished from the forming subventricular zone by a dashed line. An aberrant neuroblast (circle), frozen in late anaphase or very early telophase, is contained within the initial aspects of the subventricular zone.

Figure 6: Detail from a more primitive region of forming isocortex (for reference see rectangle on lower right of fig. 3). The forming subventricular zone is markedly less differentiated in this region (note the absence of displacement patterns) and is separated from the more active ventricular zone by a dashed line. The mitotically active ependymal surface of the ventricular zone is highlighted by arrows. Rectangular area is displayed in greater cytological detail in figure 6a.

Figure 6a: Four aberrant mitotic neuroblasts are encircled. Note that all of these cells are located within the forming subventricular zone. Such aberrant cells are only observed in flight specimens and are most commonly observed in this zone. Note that the lower two aberrant cells represent polar views and occur at the interface between the zones, possibly reflective of the migratory patterns in this region.

	Animal #	Section plane	Stain	Magnification
Figure 5:	Flight #7	Coronal	Azure II	(500x; bar = 100 μ)
Figure 5a:	Flight #7	Coronal	Azure II	(1000x; bar = 10 μ)
Figure 6:	Flight #7	Coronal	Azure II	(500x; bar = 100 μ)
Figure 6a:	Flight #7	Coronal	Azure II	(1000x; bar = 10 μ)

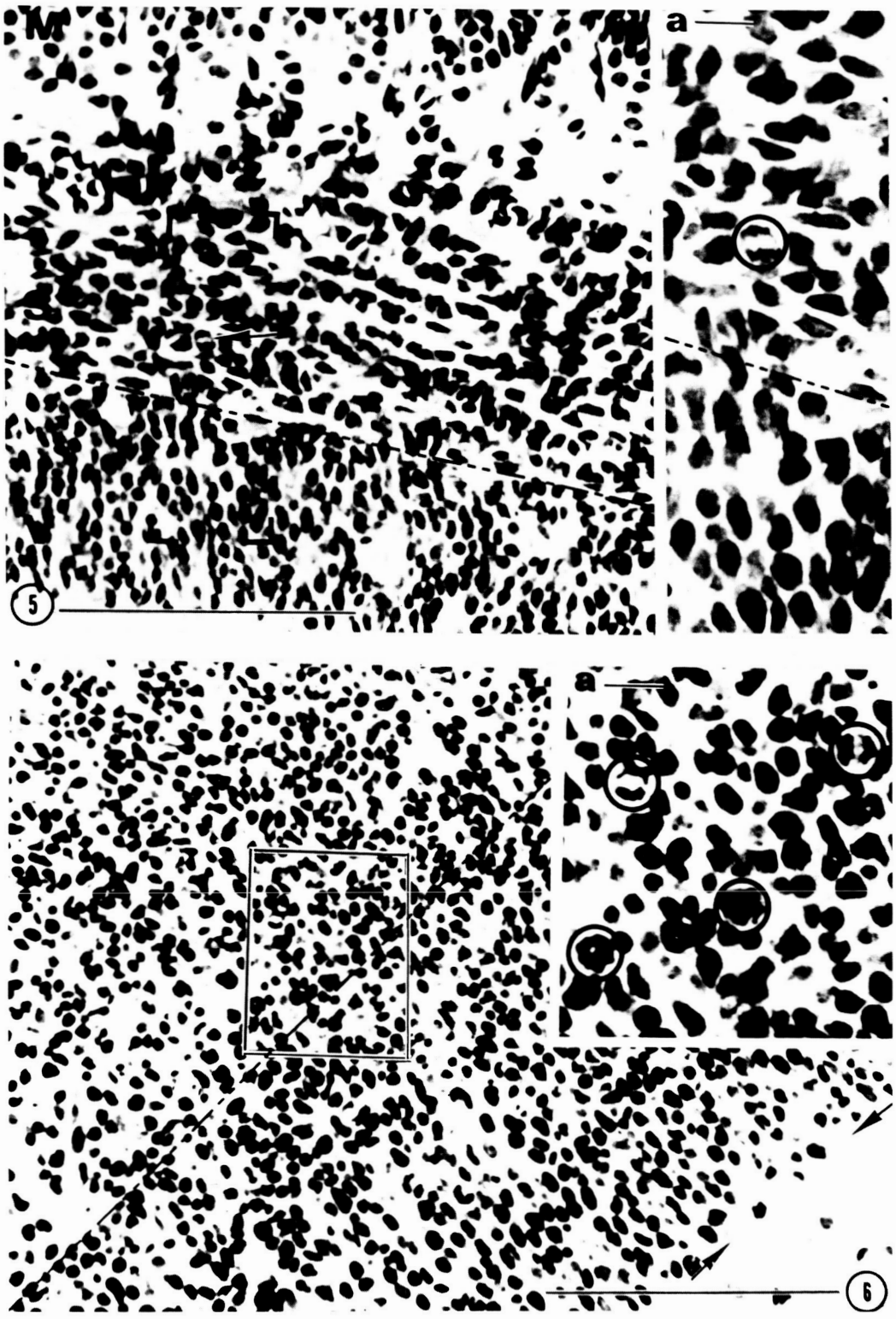

Plate 4

Figure 7: Region of forming isocortex from hippocampal region of flight specimen. The mitotically active ventricular surface is arrayed along the right edge, while the forming subventricular zone is not yet clearly demarcated in this region. Extensive masses of migrating neuroblasts are displayed, moving from the ventricular zone on the right towards the left. Highly patterned migration is not evident at this developmental stage, suggesting an age status of approximately 17 days.

While the entire field contains numerous examples of aberrant mitotic neuroblasts, the area within the rectangle has been selected to reveal several at greater detail in figure 8.

Figure 8: This section, featured in the rectangle on figure 7, contains portions of 14 aberrant mitotic neuroblasts. Three of these are highlighted by circles, with the two on the right side lying within the outermost region of the ventricular zone. A single aberrant neuroblast in late telophase is featured (double arrows).

	Animal #	Section plane	Stain	Magnification
Figure 7:	Flight #7	Coronal	Azure II	(500x; bar = 100 μ)
Figure 8:	Flight #7	Coronal	Azure II	(1000x; bar = 10 μ)

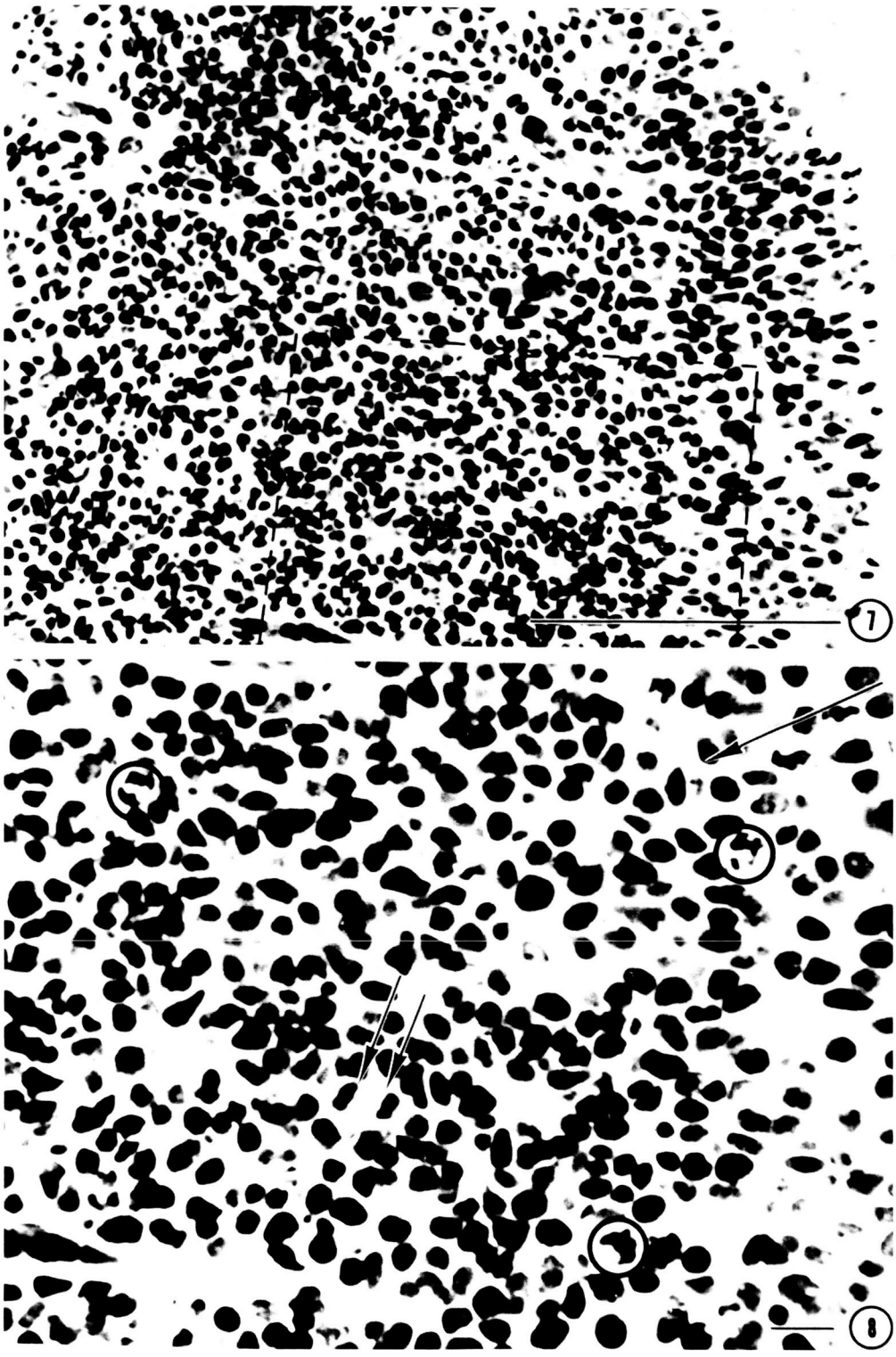

Plate 5

Figure 9: Section through forming cochlear helicotrema of control specimen, featuring one and one-half complete turns of the cochlear duct (C) contained within a well-defined cartilaginous labyrinth that is partially calcified (CA).

Figure 10: Section through cochlear helicotrema from a flight specimen, comparable to figure 9. Note the diminished extent of calcified cartilage of the presumptive labyrinth (CA) and the incomplete full turn of the cochlear duct (C). The area contained within the rectangle, illustrated in greater cytological detail in figure 14, displays large numbers of migrating ganglion cell precursors reflective of status usually observed in late 16-day embryos. The immaturity of both the sacculus (SA) and utricle (UT) is demonstrated in greater detail in figures 11 and 12.

	Animal #	Section plane	Stain	Magnification
Figure 9:	Vivarium #27	Coronal	Azure II	(100x; bar = 100 μ)
Figure 10:	Flight #7	Coronal	Azure II	(100x; bar = 100 μ)

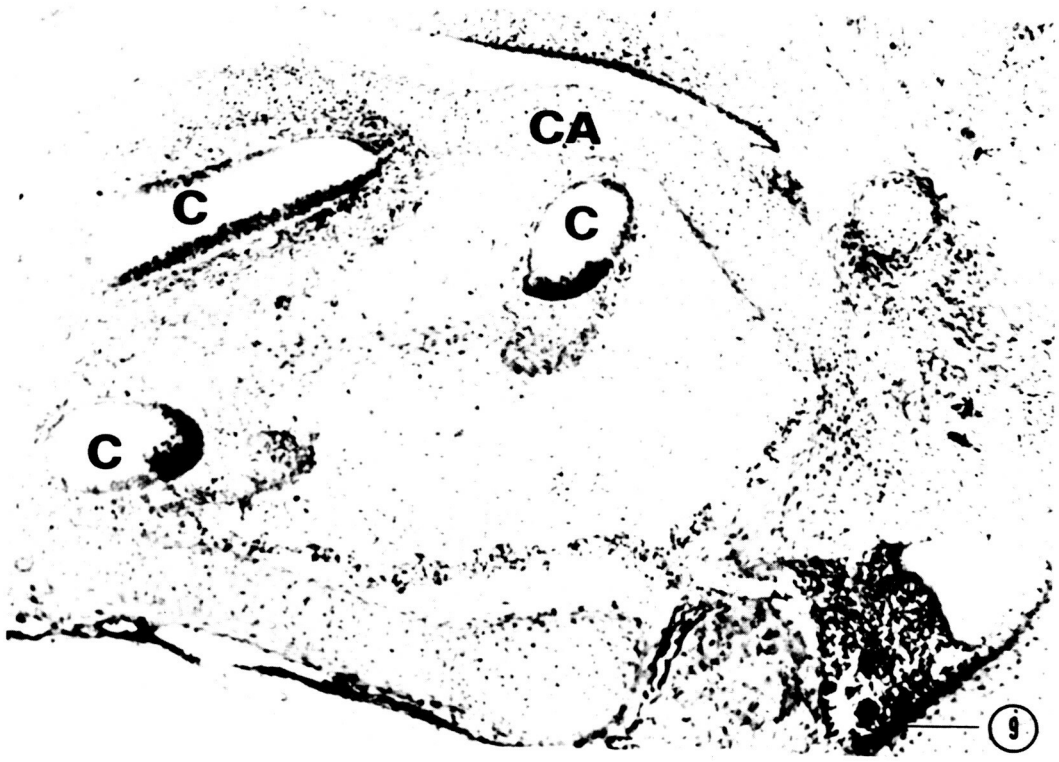

Plate 6

Figure 11: Detail of utricular macula from a flight specimen. The differentiated extent of the macula is contained within the dashed lines. Mitotic activity (M) continues along both the marginal surface of the macula as well as within the central macular regions. Note the columnar nature of the cells comprising the membranous labyrinth and the marked immaturity of the otolithic membrane.

Figure 12: Cytological detail from a section adjacent to that of figure 11. The majority of hair cells are in a very early differentiative state (h), with dense cytoplasmic staining. Occasional hair cells (H) show fuller expression of their cytological differentiation, evidenced by nuclear rounding and cytoplasmic staining. Note the extensive lateral cavitation associated with the bases of the forming hair cells. This is normal in 16- to 17-day specimens.

Note the relative immaturity of the basement membrane underlying the macula and the near total absence of otoconia from the otolithic membrane (OM). Mitotic cell (M).

Contrast the immaturity of this preparation with that of a comparable control section illustrated in figure 13.

	Animal #	Section plane	Stain	Magnification
Figure 11:	Flight #7	Coronal	Azure II	(500x; bar = 100 μ)
Figure 12:	Flight #7	Coronal	Azure II	(1000x; bar = 10 μ)

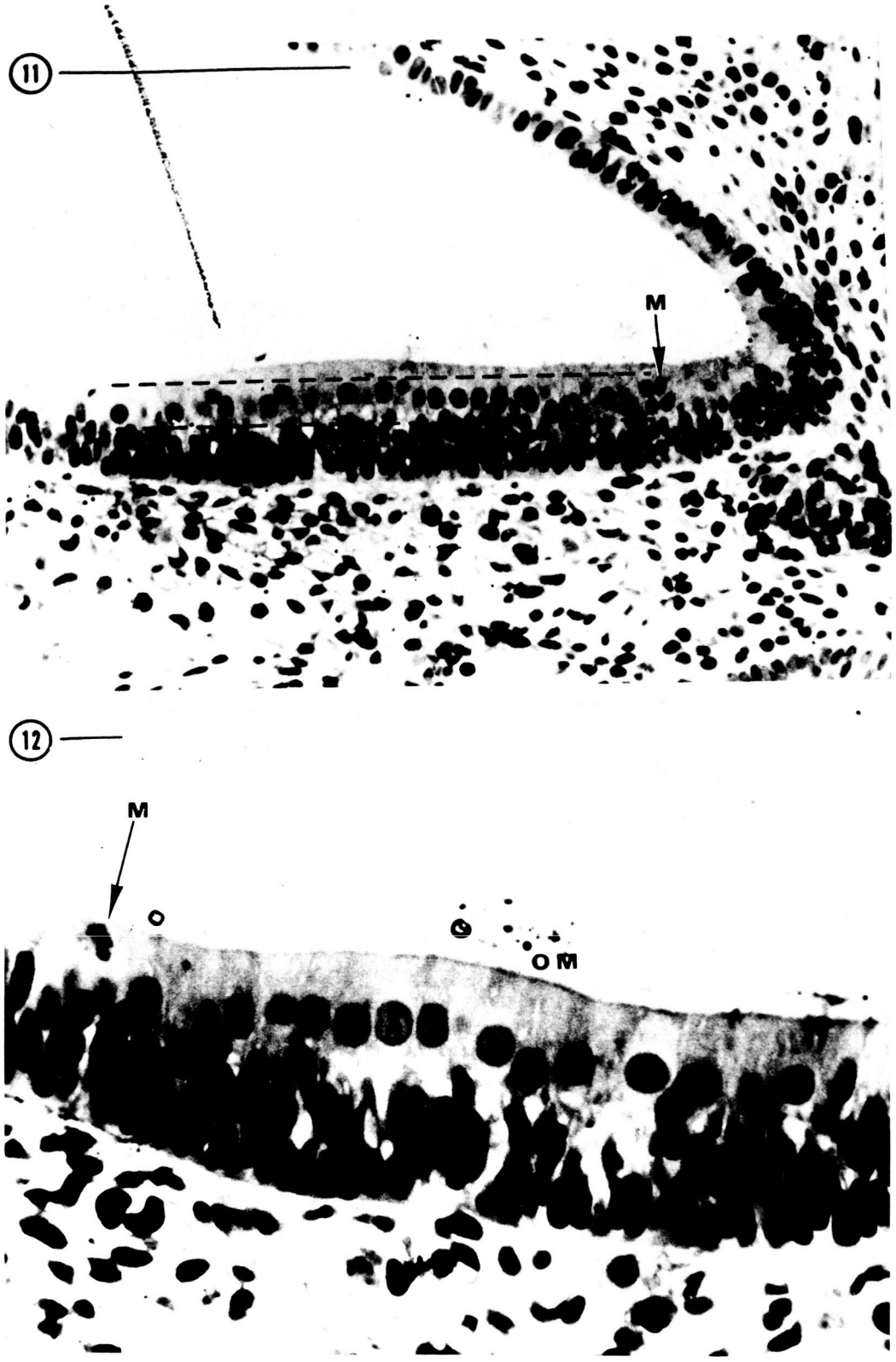

Plate 7

Figure 13: Section through utricular macula of a control specimen comparable in location and magnification to that displayed in figure 12. Note the presence of numbers of differentiated hair cells (H) among prominent sustentacular elements (S). The otolithic membrane (OM) consists of an extensive array of stereocilia enmeshed in a prominent matrix bearing numerous primary otoconia. The mitotic activity (M) is most evident along the lumenal surface, reflective of interkinetic nuclear migration characteristic of this epithelium. The basement membrane and adjacent vascularization are well formed.

Note the absence of lateral cavitation at the bases of the hair cells.

Figure 14: Detail of outlined region from the helicotrema illustrated in figure 10. Note the total absence of hair cell differentiation, characteristic of a totally proliferative population. The migrating ganglion cells, filling the lower third of the figure, have yet to condense into the spiral ganglion. Both observations are characteristic of late 16-day specimens.

	Animal #	Section plane	Stain	Magnification
Figure 13:	Vivarium #27	Coronal	Azure II	(1000x; bar = 10 μ)
Figure 14:	Flight #7	Coronal	Azure II	(500x; bar = 100 μ)

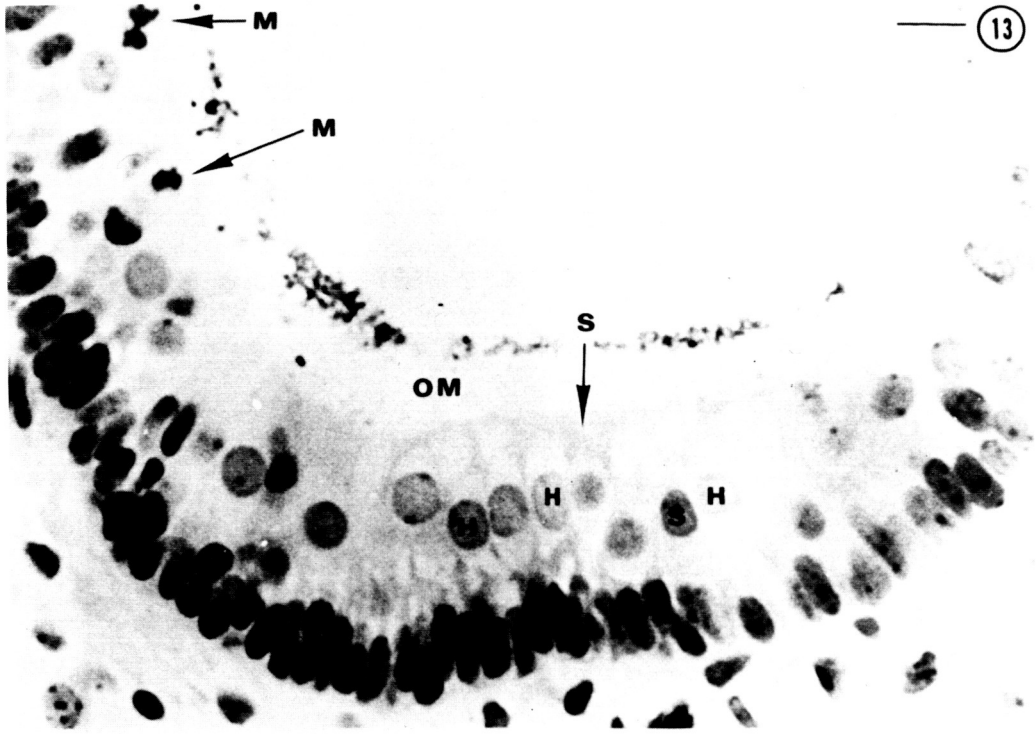

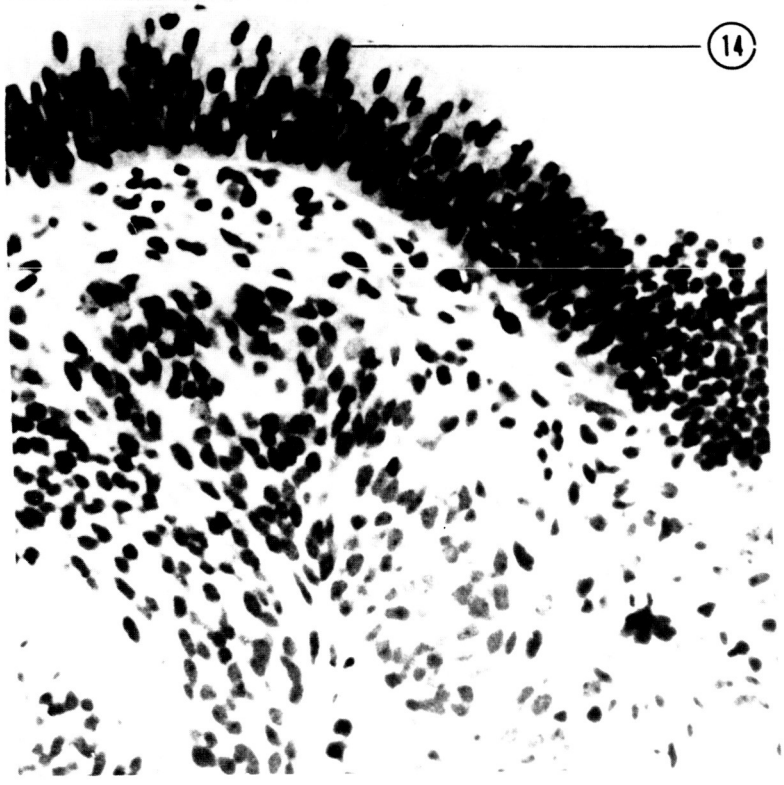

Plate 8

Figure 15a: Detail of crista of lateral semicircular canal from a control specimen. Note the condensation of both the crest and ampulla, as well as the initial cytological differentiation (arrow) of hair cells. Contrast the degree of condensation and differentiation in the early calcifying cartilaginous labyrinth (CA) with that of the flight specimen illustrated in figure 15b. Note also the differentiated status of the connective tissue of the labyrinth (STAR) and the cytological differentiation of the endolymphatic duct (E).

Figure 15b: Detail of ampulla of the left lateral semicircular canal and crista from a flight specimen. NOTE THE DOUBLED MAGNIFICATION necessary to establish a comparable image. The lack of cytological differentiation in both the crest (arrow) and lining of the endolymphatic duct (E), along with the immature quality of the connective tissue (STARS) and cartilage (CA), are reflective of the overall immaturity of this flight specimen.

	Animal #	Section plane	Stain	Magnification
Figure 15a:	Vivarium #27	Coronal	Azure II	(250x; bar = 100 μ)
Figure 15b:	Flight #5	Transverse	Protargol	(500x; bar = 100 μ)

Plate 9

Figure 16: Coronal section through the eye of a control specimen at the level of the optic nerve. The fusion of the eyelids (arrows) is typical of the 18-day specimen. Note the size of the anterior chamber (A), restricted by the normal protrusion of the well-differentiated lens (L). This feature, coupled with the compaction of the vitreous humor (V), degree of retinal differentiation and integrity of the anterior retinal structures are reflective of a fully closed choroid fissure and the development of an adequate intraocular turgor pressure.

Figure 17: Coronal section through the eye of a flight specimen at the level of the optic nerve (ON). CONTRAST THIS FIGURE WITH THAT OF FIGURE 16.

Note the failure of the eyelids to fuse (arrow), the enlarged anterior chamber (A), the immaturity of the lens differentiation (L), the enlarged vitreous cavity (V) and the presence of a defect in closure between the neural retina and pigment epithelium (STAR). Such features are characteristic of eyes from embryos failing to complete closure of the choroid fissure or unable to establish proper intraocular turgor.

	Animal #	Section plane	Stain	Magnification
Figure 16:	Vivarium #27	Coronal	Azure II	(100x; bar = 100 μ)
Figure 17:	Flight #7	Coronal	Azure II	(100x; bar = 100 μ)

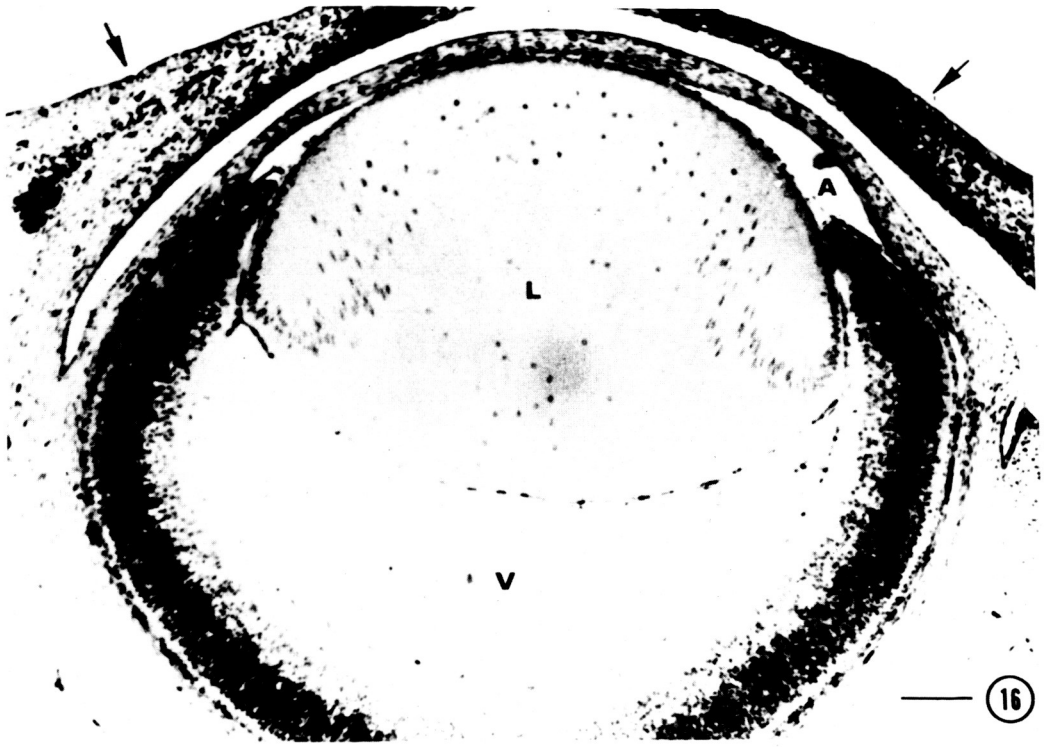

16

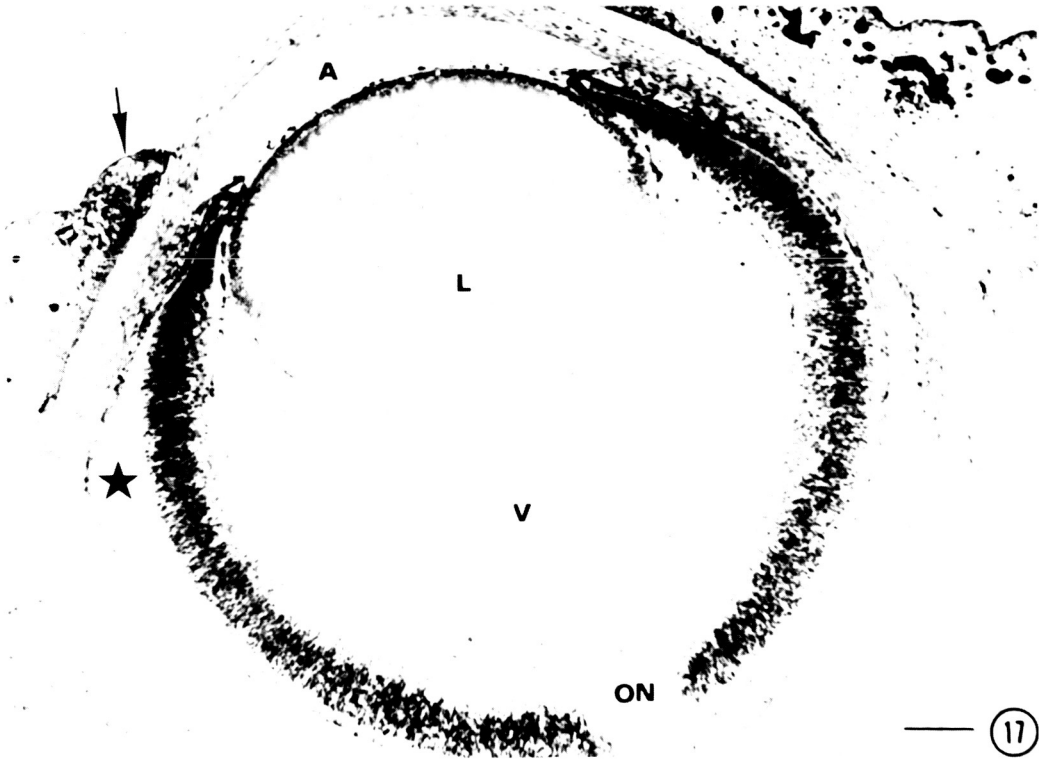

17

Plate 10

Figure 18: Detail of the anterior retinal margin from the flight specimen displayed in figure 17. Note the persistence of a remnant of the optic ventricle (STAR) between the pigment epithelium and neural retina. The neural retina, although clearly showing radial Mueller fibers (arrows), lacks the normal rounding of the anterior region comprising the ora serrata (OS). Vitreous humor (V), lens (L).

Figure 19: Detail of the posterior aspect of the persistent optic ventricle (STAR) between the neural retina (NR) and the pigment epithelium (PE). Note the thickness of the cells of the pigment epithelium and the lack of alignment in the adjacent connective tissue; conditions reflective of a lack of adequate intraocular turgor pressure.

The ganglion cell layer demonstrates an array of neurons undergoing cell death (arrows). Such cell death is normally more confined to the production of the plexiform layers and is not normally extensive within the ganglion cell layer proper. Vitreous humor (V).

	Animal #	Section plane	Stain	Magnification
Figure 18:	Flight #7	Coronal	Azure II	(250x; bar = 100 μ)
Figure 19:	Flight #7	Coronal	Azure II	(500x; bar = 100 μ)

Plate 11

Figure 20: Detail of neural retina from the central region of figure 19. The pigment epithelium is demarcated by the dashed lines. Proliferative activity within the developing neural retina is normally confined to cells in the region of the outer limiting membrane, approximating the pigment epithelium. Two such mitotic figures are illustrated by the arrows. During cytodifferentiation, the neuroblasts leave the outer surface and migrate along the radial glial fibers of Mueller towards the vitreal surface (V), establishing inner layers of differentiating neurons. Thus, differentiation is from vitreal towards scleral (left side) aspects of the retina. The majority of nuclei illustrated within the right portion of the retina represent differentiating retinal ganglion cells.

A single aberrant mitotic neuroblast is contained within the frame. Mitotic cells are never observed in this region under normal developmental conditions and none has been observed in any of the control specimens. Both eyes from each of the Group I flight specimens presented such features. The location and morphology of these cells strongly suggest that they have failed to complete cytokinesis before commencing their migratory dispersement.

Figure 21: Detail of the region of the optic nerve from the flight specimen illustrated in figure 17. The pigment epithelium (P) of all flight specimens is unusually cuboidal, suggesting a failure to come under expanding intraocular pressure. Fibers of the forming optic nerve (ON) must pass through the pigment epithelium, exiting the eye to enter the brain. The pigment epithelium remains actively mitotic around this exit site (arrow). Such activity is not normal for an 18-day embryo and has not been observed in any of the control specimens. (For detail see fig. 22.)

	Animal #	Section plane	Stain	Magnification
Figure 20:	Flight #7	Coronal	Azure II	(1000x; bar = 10 μ)
Figure 21:	Flight #7	Coronal	Azure II	(500x; bar = 100 μ)

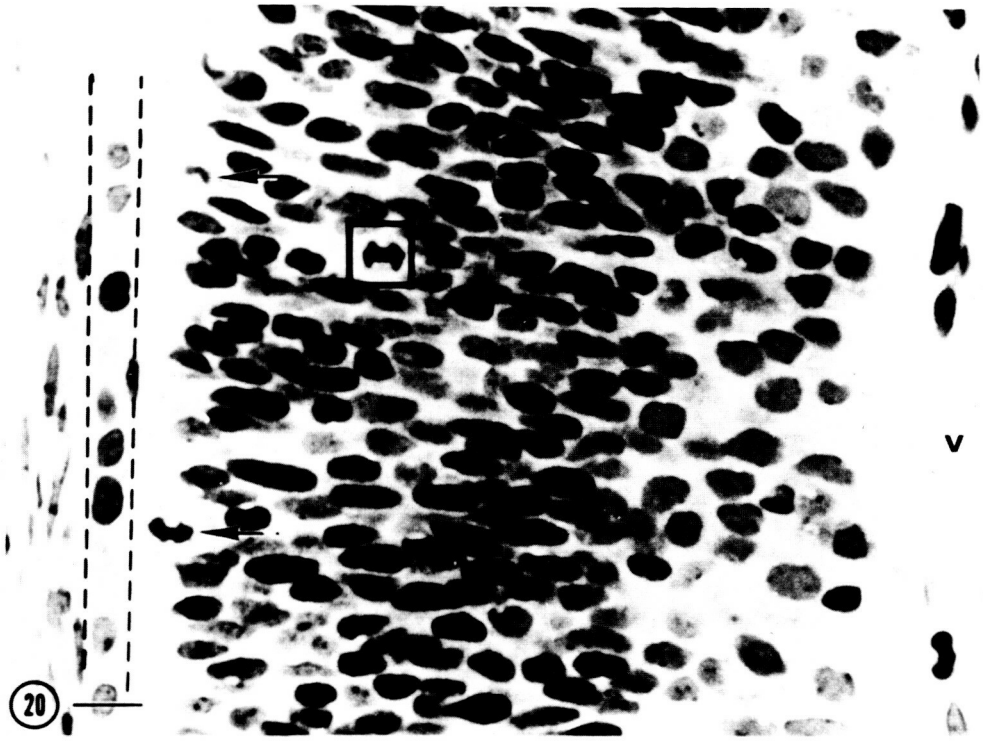

Plate 12

Figure 22a: Detail of mitotic pigment epithelial cells (arrow) from optic nerve region (ON) of the flight specimen illustrated in figure 21. Note again the cuboidal nature of the adjacent pigment epithelial cells (P).

Figure 22b: Portion of the retinal-pigment epithelial interface from a flight specimen, illustrating the normal location for mitotic activity within the external limiting membrane of the retina (arrow). The mitotic pigment epithelial cell (P) is not normal for an 18-day embryo. Such mitotic pigment epithelial cells have not been observed in any of the control specimens.

Figure 23: Control specimen chosen to illustrate the normal pattern of neuroblast proliferation and cytodifferentiation in an 18-day embryonic retina. The vitreal surface (V) and the pigment epithelium (P) establish the limits for the retina. Proliferation occurs at the outer retinal surface (arrows), with migration of the newly formed neuroblasts directed internally through the mass of proliferating neuroblasts (thick band of dark nuclei). At the 18-day stage, many of the older neuroblasts have achieved their internal position and are differentiating (lightly stained nuclei) to produce the ganglion cell layer (G), while the inner plexiform layer (IPL) is being carved out of the tissue via the mechanism of cell death.

Note the attenuation of the connective tissue and vascular elements of the choroid along the outer surface of the pigment epithelium (p). Such attenuation is reflective of the imposition of normal intraocular turgor pressure.

	Animal #	Section plane	Stain	Magnification
Figure 22a:	Flight #7	Coronal	Azure II	(1000x; bar = 10 μ)
Figure 22b:	Flight #7	Coronal	Azure II	(1000x; bar = 10 μ)
Figure 23:	Vivarium #27	Coronal	Azure II	(500x; bar = 100 μ)

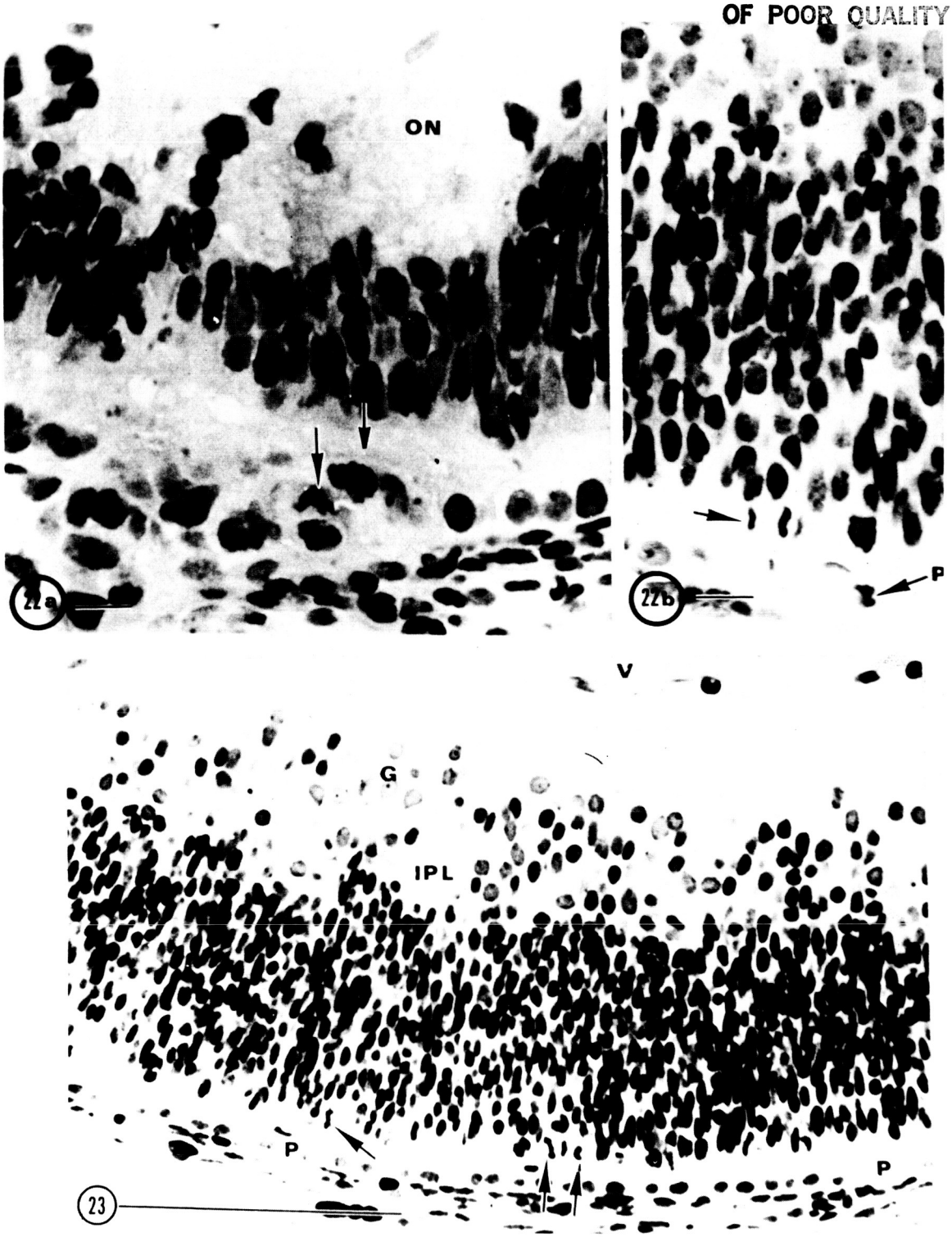

Plate 13

Figure 24: Retina from a flight specimen selected from a region comparable to the control retina illustrated in figure 23. Note the increased thickness of the retina, the elevation of retinal mitotic activity and the minimal attenuation of choroid connective tissues (bottom of illustration). Such features are reflective of a decrease in intraocular turgor pressure.

A single aberrant mitotic neuroblast is enclosed within the central rectangle.

Figure 25: Detail of outer retinal region from the flight specimen illustrated in figure 24. The retinal surface, bordering upon the pigment epithelium (P), contains mitotic neuroblasts (arrows). The central mitotic figure appears abnormal in its chromatid separation.

An aberrant mitotic neuroblast (star), undergoing migration along a radial glial fiber with a cohort of apparently normal neuroblasts, appears to have failed to complete cytokinesis. Such aberrant mitoses were observed in all flight specimens but were never encountered in any of the controls.

	Animal #	Section plane	Stain	Magnification
Figure 24:	Flight #7	Coronal	Azure II	(500x; bar = 100 μ)
Figure 25:	Flight #7	Coronal	Azure II	(1000x; bar = 10 μ)

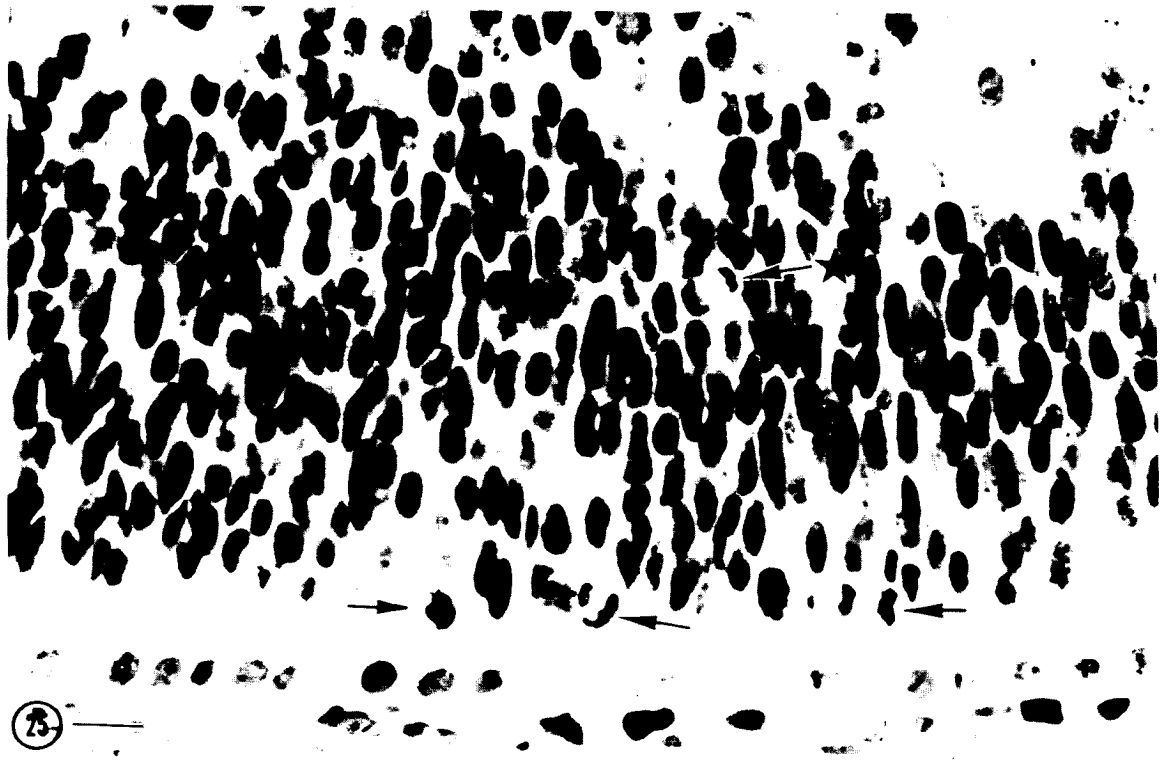

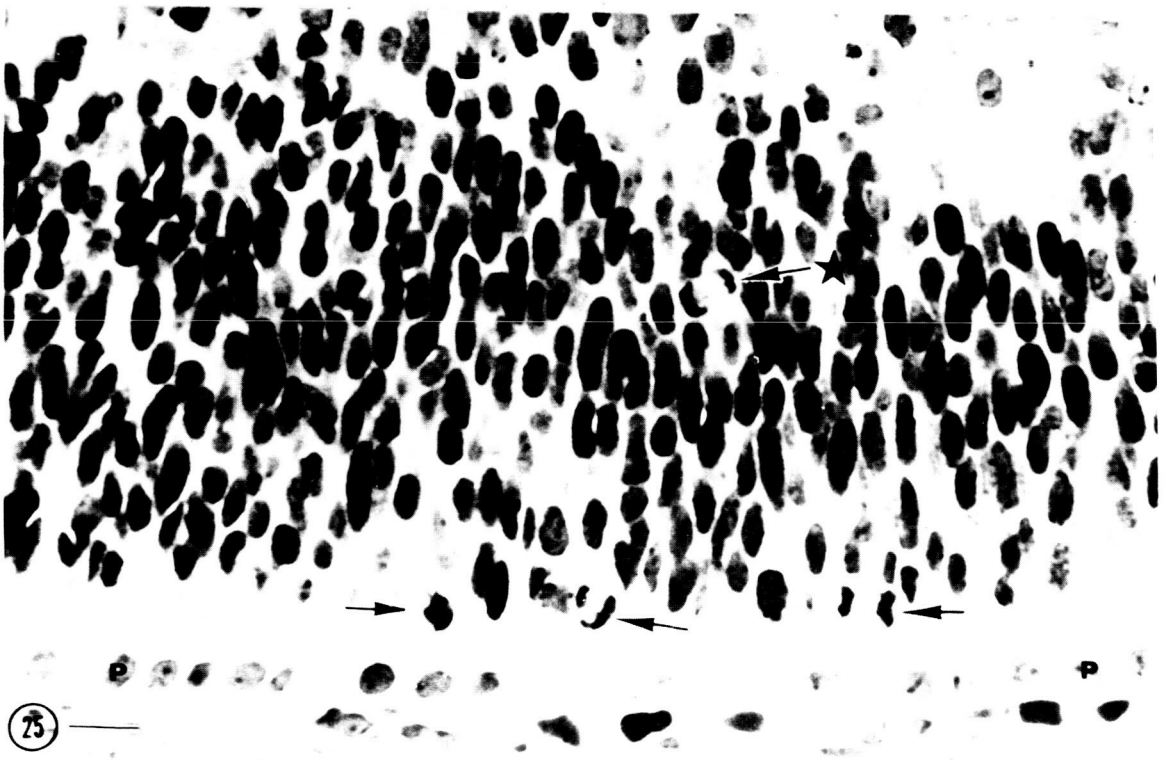

Plate 14

Figure 26: Transverse section through the eye of a flight specimen. Several features suggest that this eye is from a late 16-day embryo: (1) failure of eyelid closure and fusion (arrows); (2) enlargement of the anterior chamber (A); (3) diminished size of vitreous cavity (V); and (4) persistence of portions of the primitive optic ventricle (STARS) (originally separated the inner neural retina from the outer pigment epithelium) as a "ring-shaped" optic cavity. Lens, L.

Figure 27: Detail of the anterior dorsal portion of the eyeball from the flight specimen illustrated in figure 26. The persistence of the primitive optic ventricle (STAR) between the pigment epithelium (P) and the ora zone (OZ) of the forming anterior neural retina has been observed in all flight specimens and in none of the controls. The ora zone (OZ), the condensing anterior proliferative band of neural retina, is considerably larger and more primitive than that observed in the control specimens (for comparison, see figs. 29 and 30) suggesting a more primitive embryonic state.

Figure 28: Cytological detail of proliferating posterior neural retina from the flight specimen illustrated in figure 26. Note the pigment epithelium (P), the proliferating neuroblasts of the external limiting membrane (arrows) and the aberrant mitotic neuroblast (rectangle). Such cells are aberrant in both position and mitotic form (frozen in late anaphase) and have not been observed in any of the control specimens.

	Animal #	Section plane	Stain	Magnification
Figure 26:	Flight #1	Transverse	Azure II	(100x; bar = 100 μ)
Figure 27:	Flight #1	Transverse	Azure II	(250x; bar = 100 μ)
Figure 28:	Flight #1	Transverse	Azure II	(1000x; bar = 10 μ)

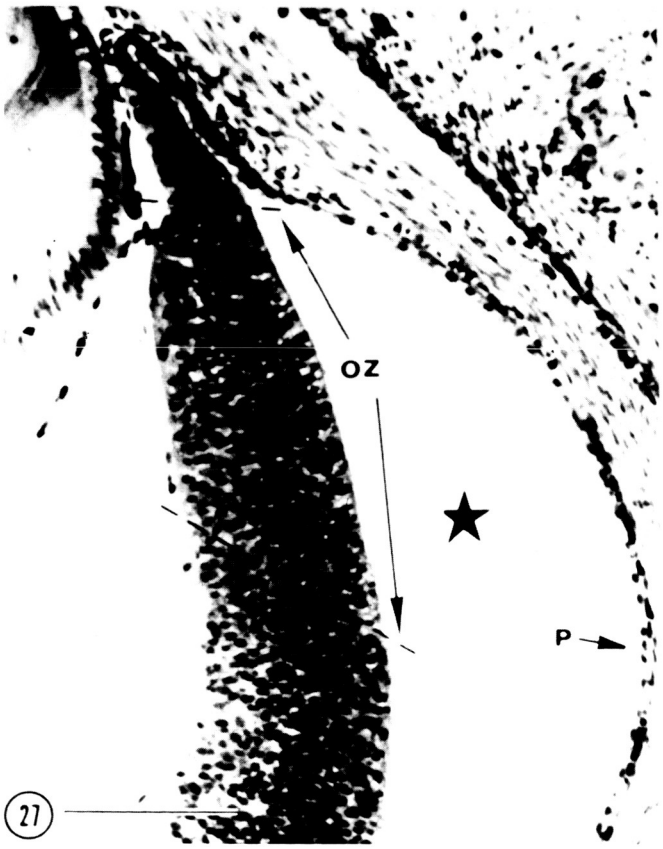

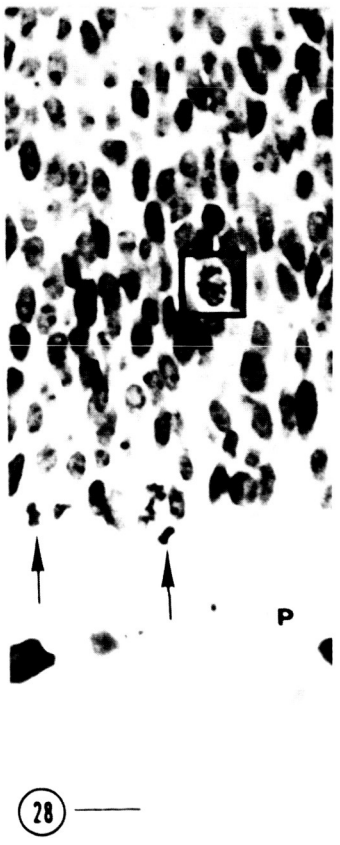

Plate 15

Figure 29: Detail of the anterior ventral region of the eye from the control specimen featured in figure 16. The ora zone (OZ) represents the anterior-most condensation of the differentiating neural retina and is the only region remaining in which proliferation is the sole developmental activity. This region will continue to condense, disappearing shortly after birth with the final establishment of the ora serrata of the retina. Note its wedge-shape and recall that this is a single section through a cylindrical tissue wedge.

Note the absence of extracellular spaces in the adjacent retinal tissues, the close approximation of the retina and pigment epithelium (P), and the condensation of both the fibers and cells of the cornea (C). Anterior chamber (A); Lens (1); Vitreous cavity (V).

Figure 30: Detail of the anterior dorsal region of the eye from the flight specimen illustrated in figure 26. The ora zone extends from the dashed line to the right edge of the picture and contains predominantly proliferative retina. There is an extensive amount of extracellular space within the retinae of all flight specimens (arrows). Note the persistent cavity of the optic ventricle (STAR), separating the pigment epithelium (P) from the ora zone, and the early differentiated state of the cornea (C). Anterior chamber (A); Lens (L); Vitreous cavity (V).

	Animal #	Section plane	Stain	Magnification
Figure 29:	Vivarium #27	Coronal	Azure II	(500x; bar = 100 μ)
Figure 30:	Flight #1	Transverse	Azure II	(500x; bar = 100 μ)

Plate 16

Figure 31: Note the immaturity of the periocular connective tissue (STARS) and cartilage of the cranial vault (CA) in this flight specimen. The size of the optic nerve (ON) and the extraocular muscle suggests a 17-day embryo.

Figure 32: The pituitary structure of this flight specimen is indicative of a late 16- or early 17-day embryo. Note the retention of the cleft of Rathke's pouch (C), the small neurohypophysis (N) (although the infundibular recess has been closed), and the primitive intermediate portion. The adenohypophysis (A) is closely associated with the sphenoid cartilage (CA). For detail of the Adenohypophysis, see figures 35 and 36. Oropharynx, O.

	Animal #	Section plane	Stain	Magnification
Figure 31:	Flight #10	Coronal	Hematoxylin and eosin	(100x; bar = 100 μ)
Figure 32:	Flight #7	Coronal	Azure II	(100x; bar = 100 μ)

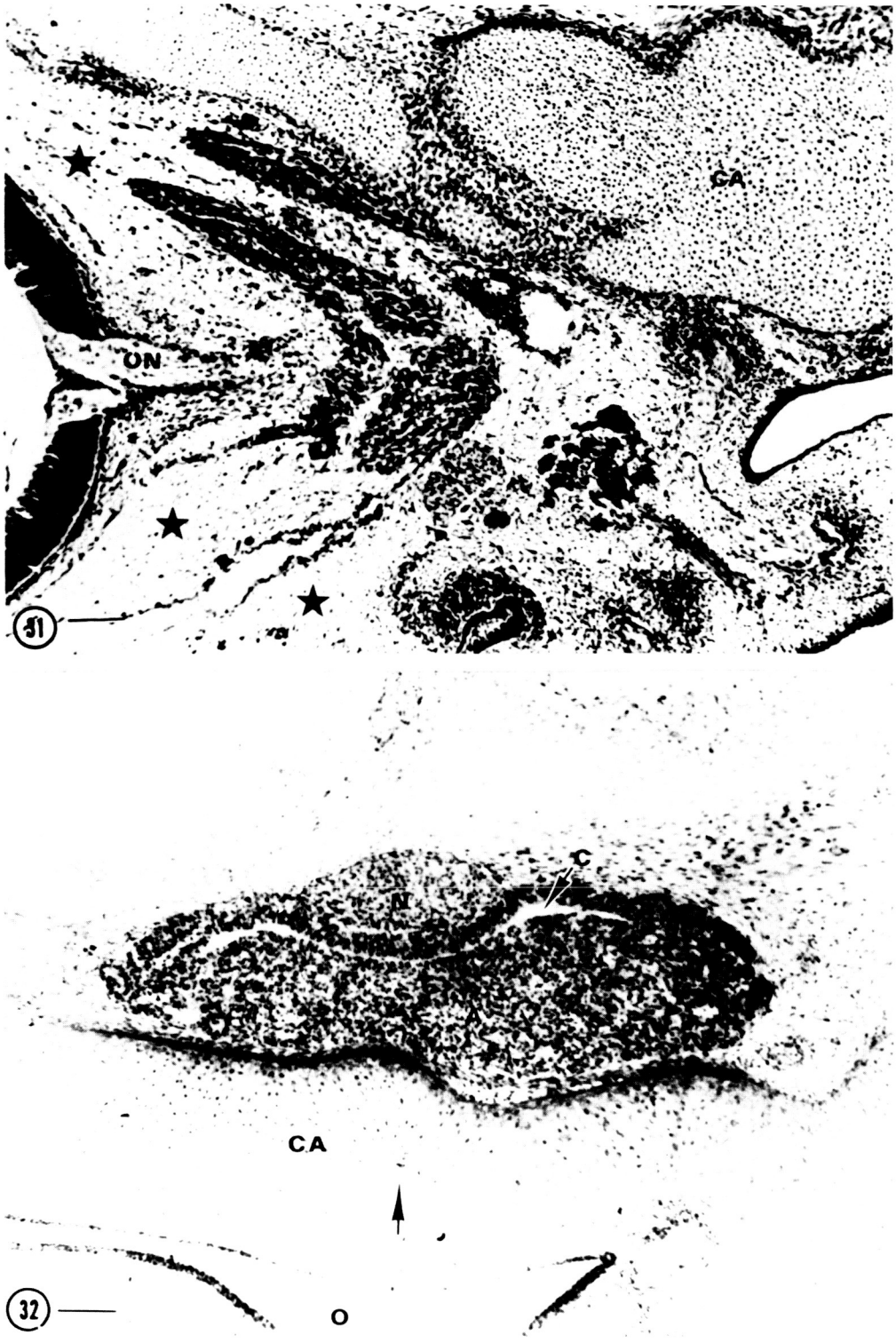

Plate 17

Figure 33: Section through the oral cavity of a flight specimen. The tongue (T) occupies most of the oral cavity, which is limited on the superior surface (left) by the condensing mesenchyme and cartilage of the palatal shelves (STARS) which have achieved midline fusion. The mandible (B) is forming in relation to Meckel's cartilage.

The image presented from a flight specimen displays a morphology usually associated with a 17-day rat fetus, but is otherwise normal.

Figure 34: Detail of forming mandible wings from the flight specimen illustrated in figure 33. Note the well-defined Meckel's cartilage (CA) and the forming lateral bony walls of the mandible (B = primitive Haversian channels of the bone). There is extensive osteoclastic remodeling in process (arrows). Branches of the inferior alveolar nerve are also evident (NE). The degree of development is synonymous with that of a 17-day rat fetus.

	Animal #	Section plane	Stain	Magnification
Figure 33:	Flight #10	Coronal	Hematoxylin and eosin	(100x; bar = 100 μ)
Figure 34:	Flight #10	Coronal	Hematoxylin and eosin	(500x; bar = 100 μ)

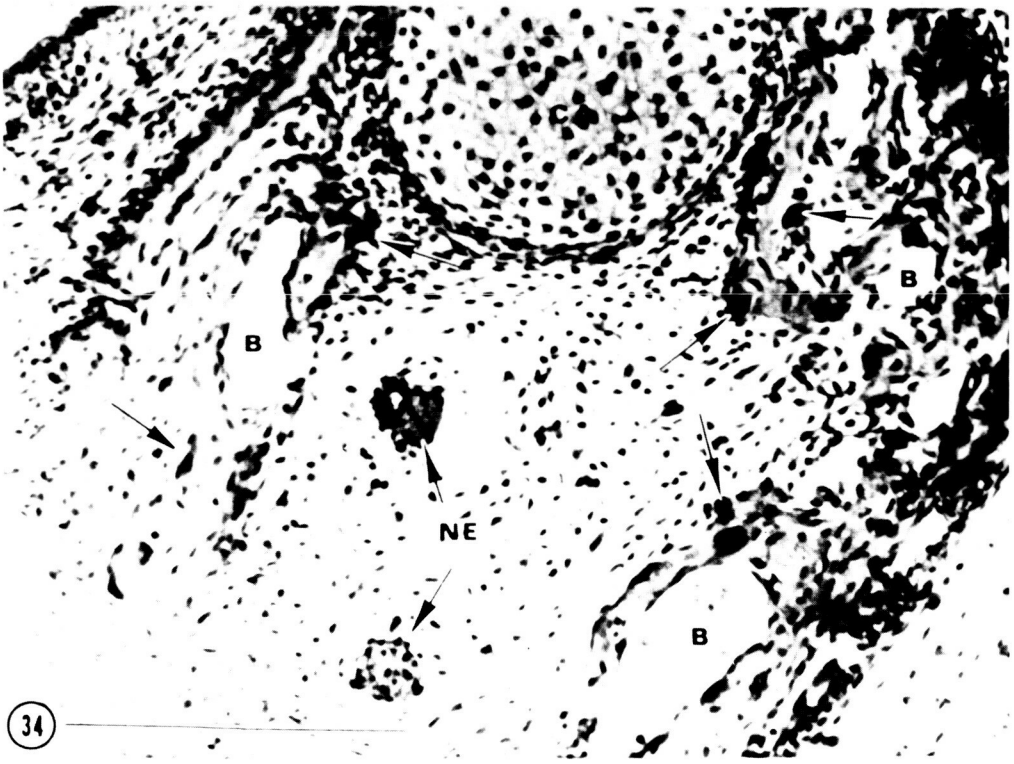

Plate 18

Figure 35: Detail of adenohypophysis from the flight specimen illustrated in figure 32. Note the differentiation of scattered tubular glands in the more mature central region. Cytodifferentiation is lagging behind that of a normal 18-day rat fetus.

A portion of the small intermediate lobe is evident at the top of the figure, bounding the cavity of Rathke's pouch (slit extending across figure).

Figure 36: Detail of a lateral portion of the adenohypophysis from the flight specimen illustrated in figures 32 and 35. Note the extensive mitotic activity (M), the lack of any cytodifferentiation and the initial development of a capillary network (B). The establishment of the capillary network normally signals the onset of tubular cytodifferentiation and is typical of a late 16-day rat fetus.

	Animal #	Section plane	Stain	Magnification
Figure 35:	Flight #7	Coronal	Azure II	(500x; bar = 100 μ)
Figure 36:	Flight #7	Coronal	Azure II	(1000x; bar = 10 μ)

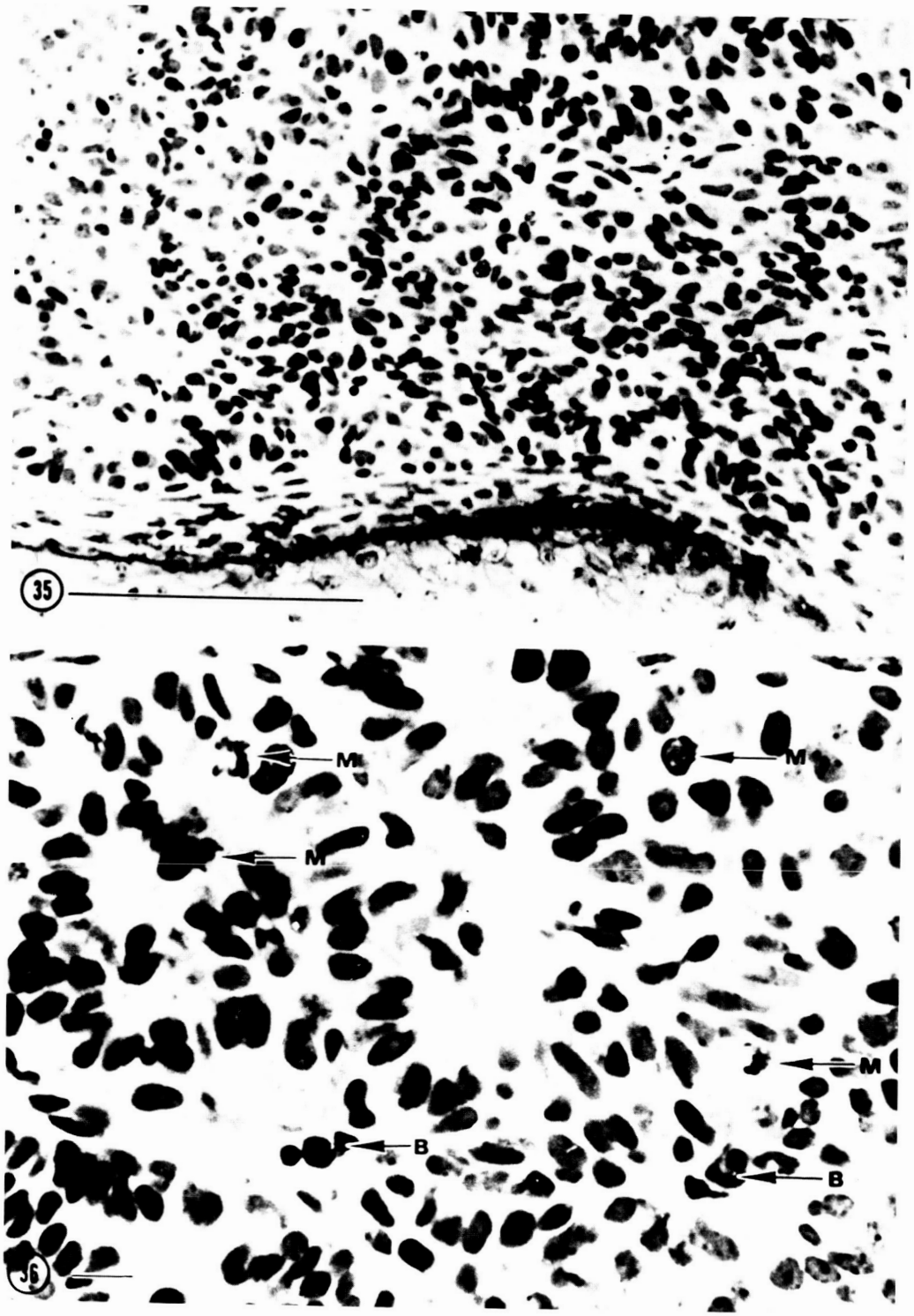

Plate 19

Figure 37: Portion of the evaginating epiphysis cerebri (pineal gland) from a flight specimen. Note the continued patency of the cavity with the 3rd ventricle (to the right). This pathway is closed in all of the control specimens.

Figure 38: Detail of portion of the evaginating pineal gland from the flight specimen illustrated in figure 37. Note that the walls of the vesicle are yet entirely proliferative, with several mitotic figures emphasized (arrows). This structure has yet to initiate cytodifferentiation and is typical of that usually observed in late 16-day to early 17-day rat fetuses.

	Animal #	Section plane	Stain	Magnification
Figure 37:	Flight #7	Coronal	Azure II	(250x; bar = 100 μ)
Figure 38:	Flight #7	Coronal	Azure II	(500x; bar = 100 μ)

Plate 20

Figure 39: External auditory structure development in a control specimen. The external auditory meatus (EA) is sealed with periderm. The tubotympanic recess of the eustachian tube (P) is approximating the cartilaginous precursor of the malleus (CC), which is undergoing calcification. The cartilaginous precursor of the bony labyrinth (CA) is shown enclosing the first one and one-half turns of the cochlea (upper left corner).

Figure 40: External auditory features from a flight specimen include a markedly reduced cartilaginous labyrinth (CA), an abbreviated tubotympanic recess (P), with the adjacent primordium of the malleus, and slightly more than one full turn of the cochlea. The common vestibular precursor of the utricle and saccule are also evident. This development is delayed approximately one full day from that shown in the control illustrated in figure 39.

	Animal #	Section plane	Stain	Magnification
Figure 39:	Vivarium #27	Coronal	Azure II	(100x; bar = 100 μ)
Figure 40:	Flight #7	Coronal	Azure II	(100x; bar = 100 μ)

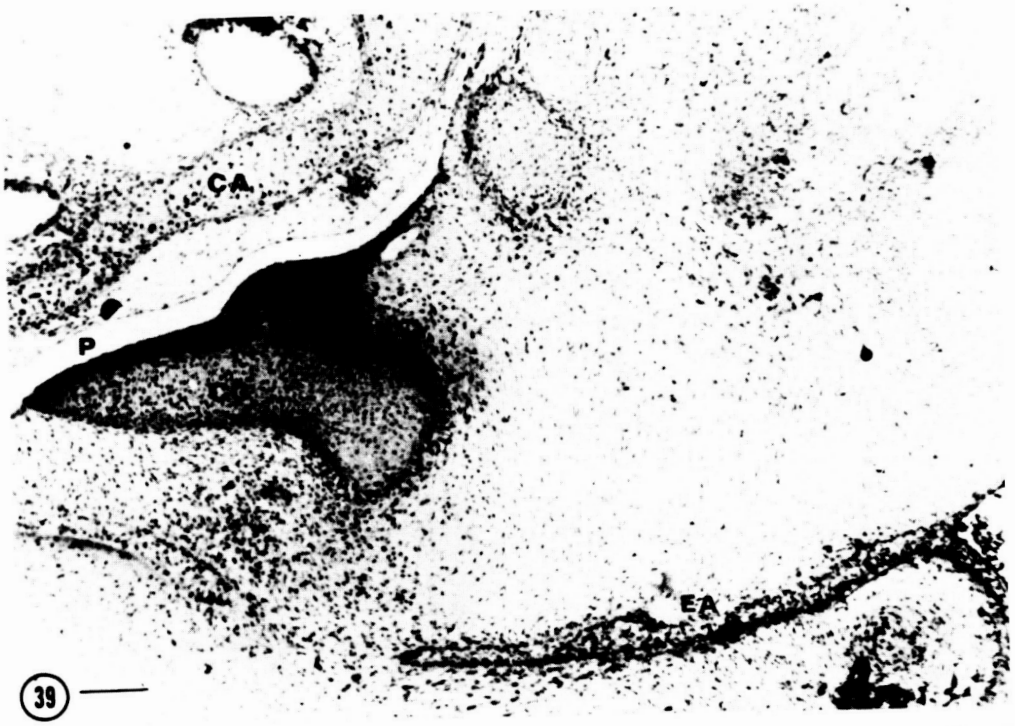

39

40

Plate 21

Figure 41: Detail of the maximal cochlear duct (CD) differentiation observed in a flight specimen displaying an actively mitotic neuroepithelium, immature cartilaginous labyrinth (CA) and scattered initial hair cells (HC). The basilar membrane (B) is beginning to become established and initial cavitation of the mesenchyme, to form the Scalae, is evident around the vascular elements (V). This picture is one usually encountered in late 16-day rat fetuses.

Figure 42: Coronal section derived from the eye of a newborn flight specimen. The eyes in all newborn flight specimens were morphologically normal. The separating of neural retina and its infolding from the pigment epithelium resulting in a presumptive optic cavity (OC) is entirely artifactual. Lens, L; Vitreous cavity, VC.

	Animal #	Section plane	Stain	Magnification
Figure 41:	Flight #7	Coronal	Azure II	(250x; bar = 100 μ)
Figure 42:	Flight #36	Coronal	Protargol	(80x; bar = 100 μ)

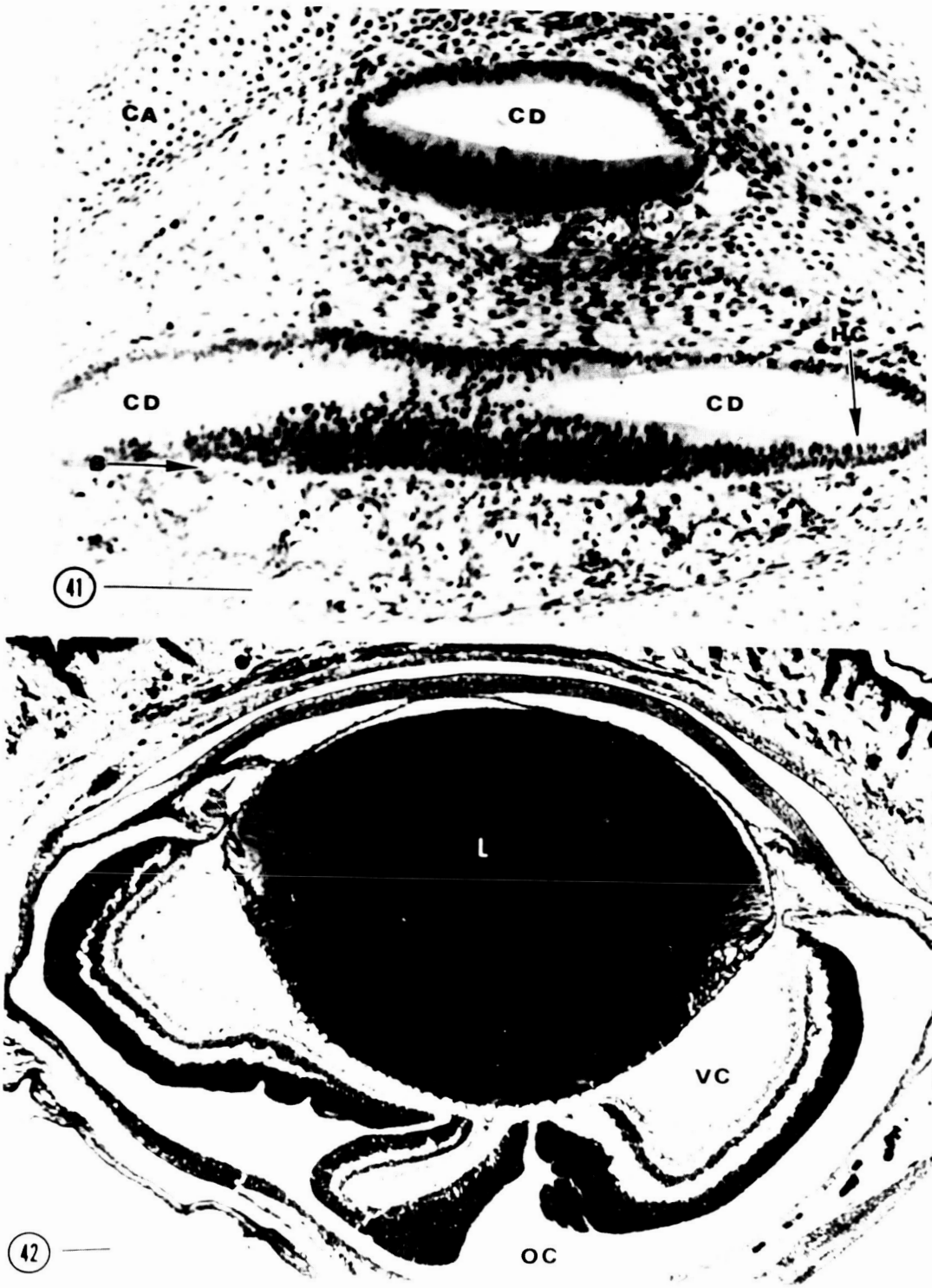

Plate 22

Figure 43: The ora zone (OZ) is slightly enlarged and the nuclear layer of the retina (NL) slightly thicker than normal in this eye from a newborn flight specimen. The separation between neural retina and pigment epithelium (O) is artifactual. Lens, L; Vitreous cavity, VC.

Figure 44: Cytological details from the retina of a newborn flight specimen. Bordering the vitreal surface (V), the retina shows a well-developed ganglion cell layer separated from the differentiating outer nuclear layer (NL) by a moderately developed inner plexiform layer (arrow). The cells comprising both the outer limiting membrane (OLM) and the pigment epithelium (PE) are mitotically inactive as is appropriate for this stage. The separation of retina from pigment epithelium is an artifact of the preparative process.

	Animal #	Section plane	Stain	Magnification
Figure 43:	Flight #33	Coronal	Protargol	(100x; bar = 100 μ)
Figure 44:	Flight #36	Coronal	Protargol	(425x; bar = 100 μ)

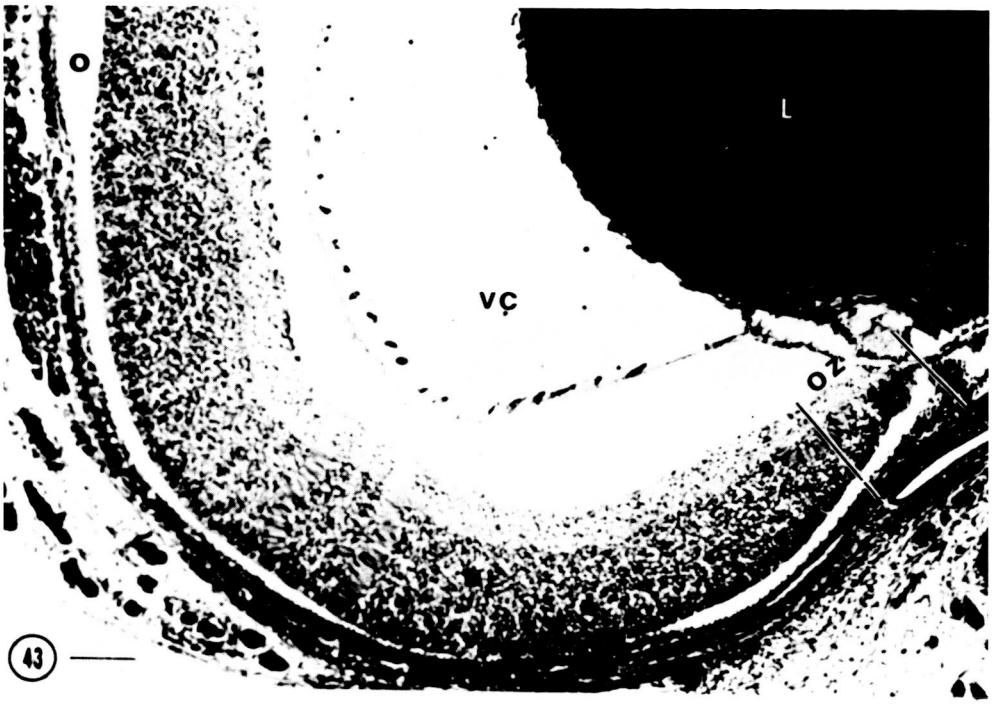

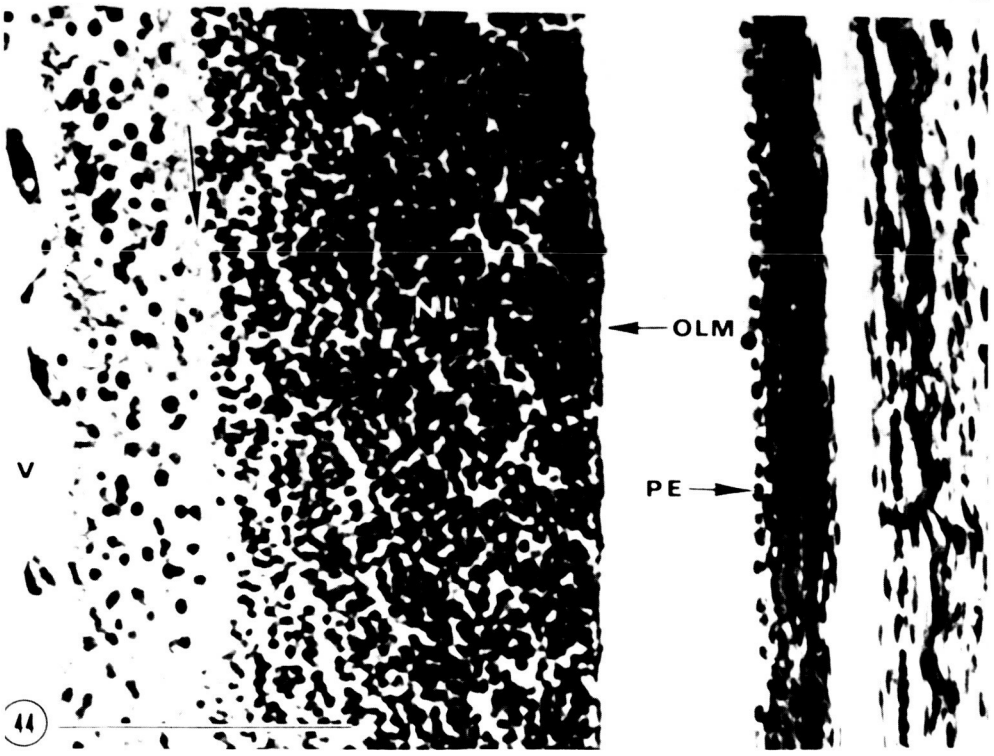

Plate 23

Figure 45: Sample of hippocampal region from a newborn flight specimen. The allocortex is typically differentiated with full expression of the cytoarchitectonic divisions of the hippocampal formation.

Figure 46: Sample of adenohypophysis from a newborn flight specimen, showing excellent cytodifferentiation of acidophils (A), basophils (B) and chromophobes (C), with only scattered mitotic figures (M). Note the well-developed capillary networks (arrows).

	Animal #	Section plane	Stain	Magnification
Figure 45:	Flight #36	Coronal	Protargol	(80x; bar = 100 μ)
Figure 46:	Flight #31	Transverse	Azure II	(1400x; bar = 10 μ)

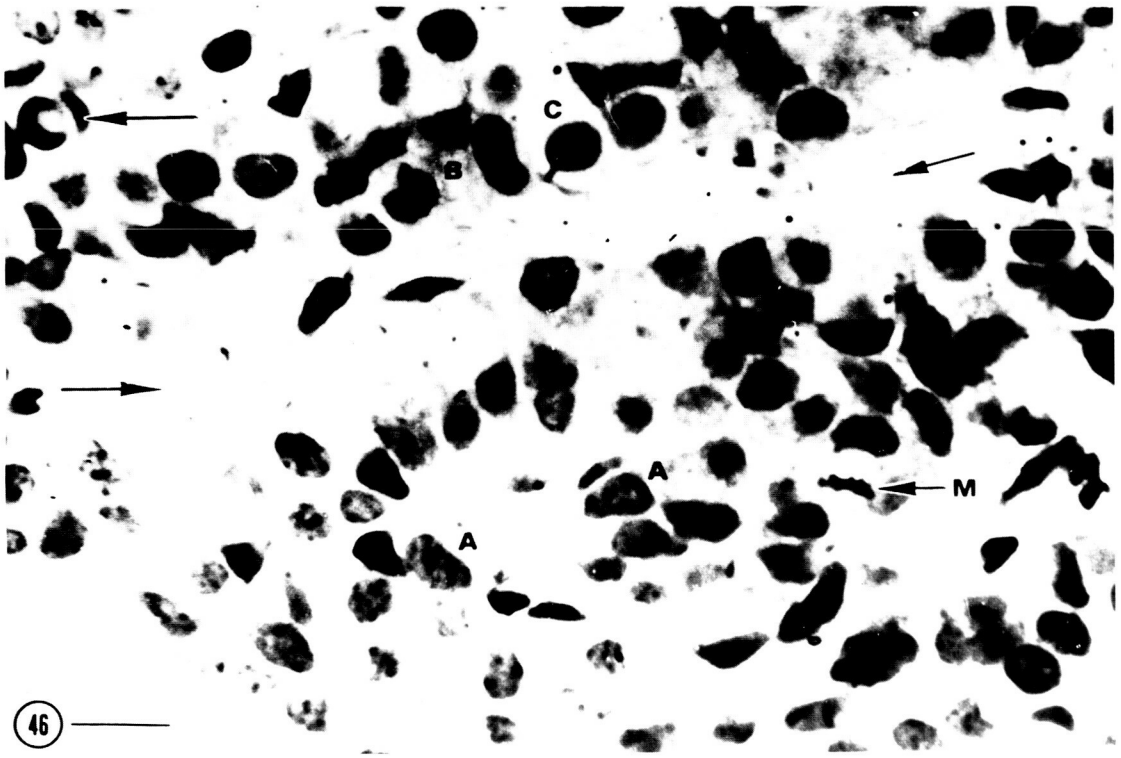

Plate 24

Figure 47: Section through the bony roof of the oral cavity from a newborn flight specimen, featuring the fused midline and bony elaboration of the palate, with paired upper tooth primordia (D).

Figure 48: Cartilage of peri-aural region from a newborn flight specimen. Note the calcification of the labyrinth (CA), as well as the cartilaginous precursors of the middle ear bones: stapes (ST), incus (IN), and Malleus (MA). The cartilage precursors of the middle ear bones are just commencing the elaboration of their articular surfaces.

	Animal #	Section plane	Stain	Magnification
Figure 47:	Flight #36	Coronal	Hematoxylin and Eosin	(80x; bar = 100 µ)
Figure 48:	Flight #31	Transverse	Azure II	(80x; bar = 100 µ)

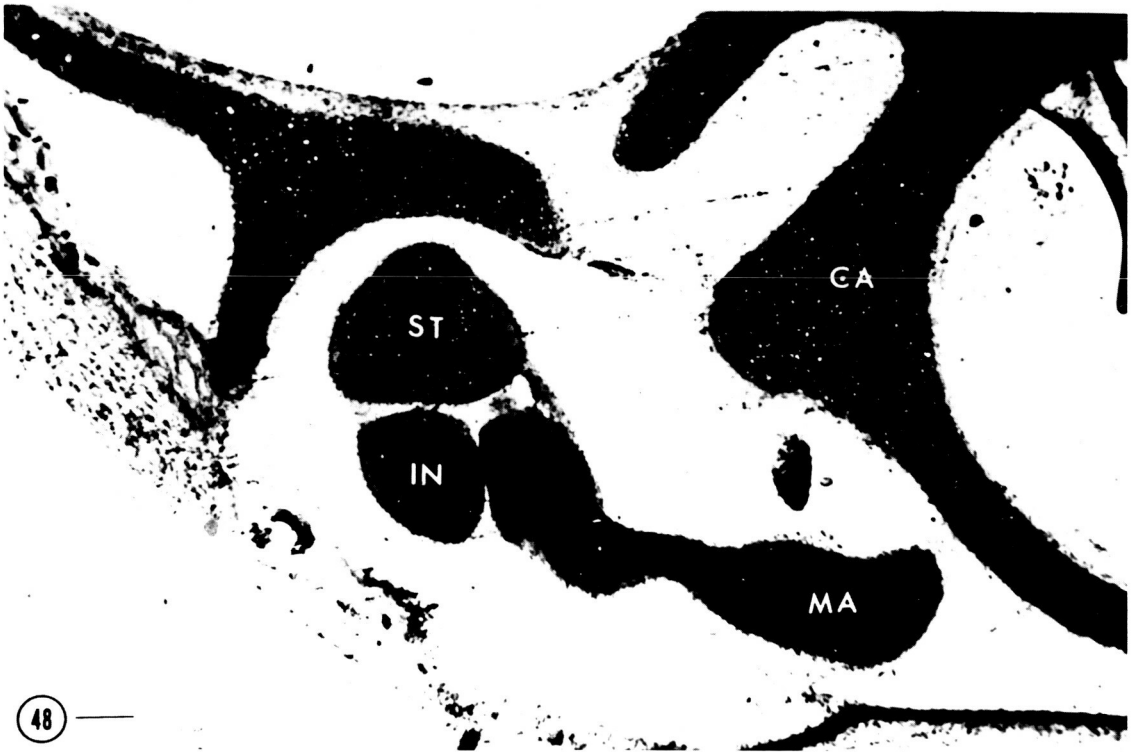

Plate 25

Figure 49: Detail of the process of dentinogenesis from a newborn flight specimen. The normalcy of this process strongly supports the adequacy of the nutrition provided. The clearly aligned stratum intermedium overlies the highly differentiated ameloblasts (A). Note the well-developed enamel (E), dentin (D) and predentin (pD). The separation (stars) of the odontoblastic layer (O) from the predentin (PD) is an artifact of the preparative process, as is the separation of the odontoblasts from the dental papilla.

Figure 50: Normal processes of endochondral ossification from a newborn flight specimen. Calcified cartilage (c) is being overlain by newly formed bone (B), with the erosion of the cartilage producing significant marrow cavities (M).

	Animal #	Section plane	Stain	Magnification
Figure 49:	Flight #36	Coronal	Hematoxylin and Eosin	(350x; bar = 100 μ)
Figure 50:	Flight #31	Transverse	Azure II	(350x; bar = 100 μ)

Plate 26

Figure 51: The cochlea from a newborn flight specimen is normally developed, with full expression of the cochlear duct (stars) and clearly defined scalae vestibuli (SV) and tympani (ST). The innervation pattern is normal as is the cartilaginous coiling. Note the utricle on the left and the cartilaginous precursor of the malleus (M) at the lower right.

Figure 52: In this transverse preparation from a newborn flight specimen, note the common crus (COM) of the semicircular canals (SC), the utricle (UT) and the highly calcified cartilaginous capsule (CA). Each of these structures is normal in its timing of cytodifferentiation. For greater detail of the utriculus, see figures 55 through 58.

	Animal #	Section plane	Stain	Magnification
Figure 51:	Flight #36	Coronal	Protargol	(80x; bar = 100 μ)
Figure 52:	Flight #31	Transverse	Azure II	(80x; bar = 100 μ)

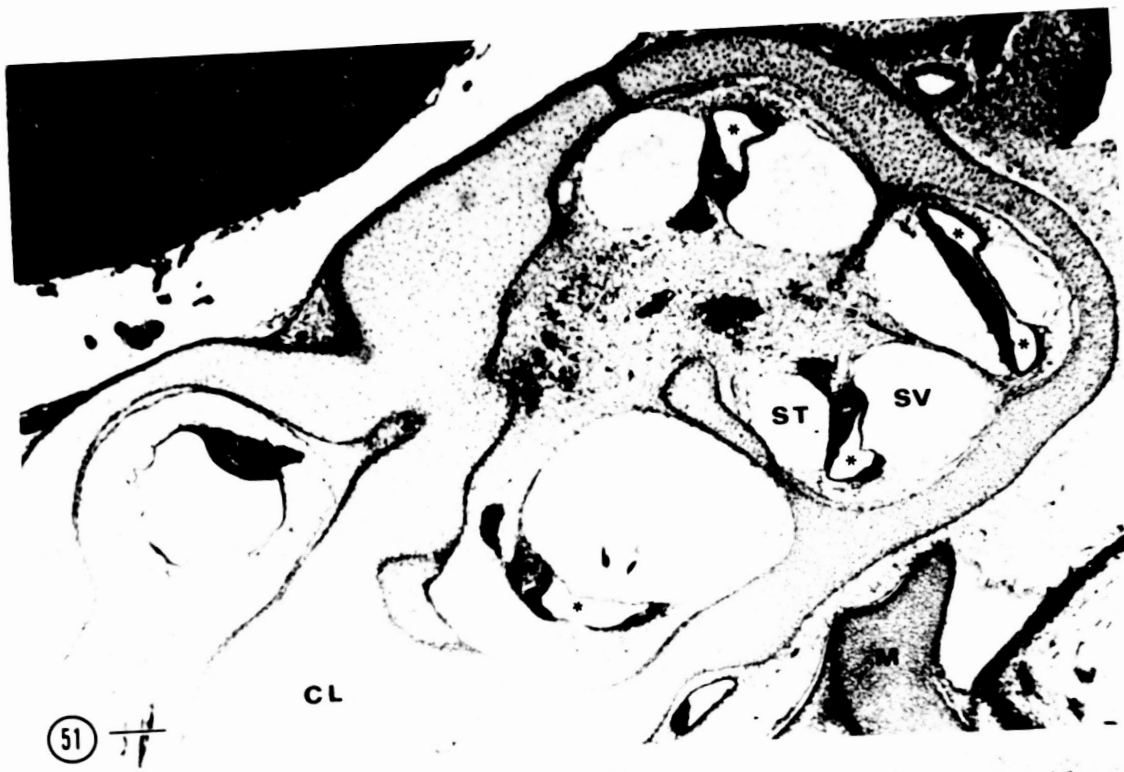

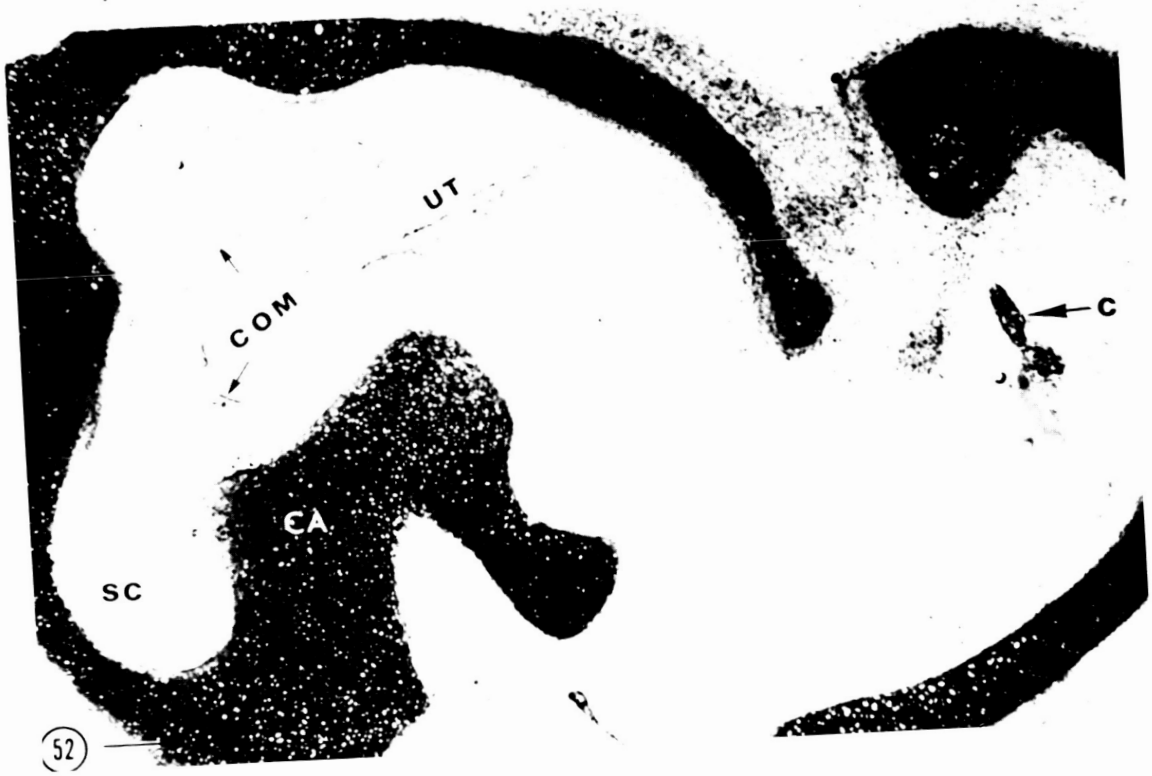

Plate 27

Figure 53: Detail of one cochlear turn from the newborn flight specimen illustrated in figure 51. The spiral limbus (arrow) is moderately developed. The cochlear duct (D) is well separated from the scale vestibuli (SV) by the dual epithelial sheets comprising the vestibular membrane (VM). A loosely organized basilar membrane separates the scala tympani (ST) from the sensory Organ of Corti (star). The highly vascular stria vascularis (StV) is functionally differentiated.

Figure 54: Transverse section through the core of the osseous spiral lamina from a newborn flight specimen. Note the spiral array (V) of bipolar ganglion cells comprising the spiral ganglia.

	Animal #	Section plane	Stain	Magnification
Figure 53:	Flight #36	Coronal	Hematoxylin and Eosin	(250x; bar = 100 μ)
Figure 54:	Flight #31	Transverse	Azure II	(350x; bar = 100 μ)

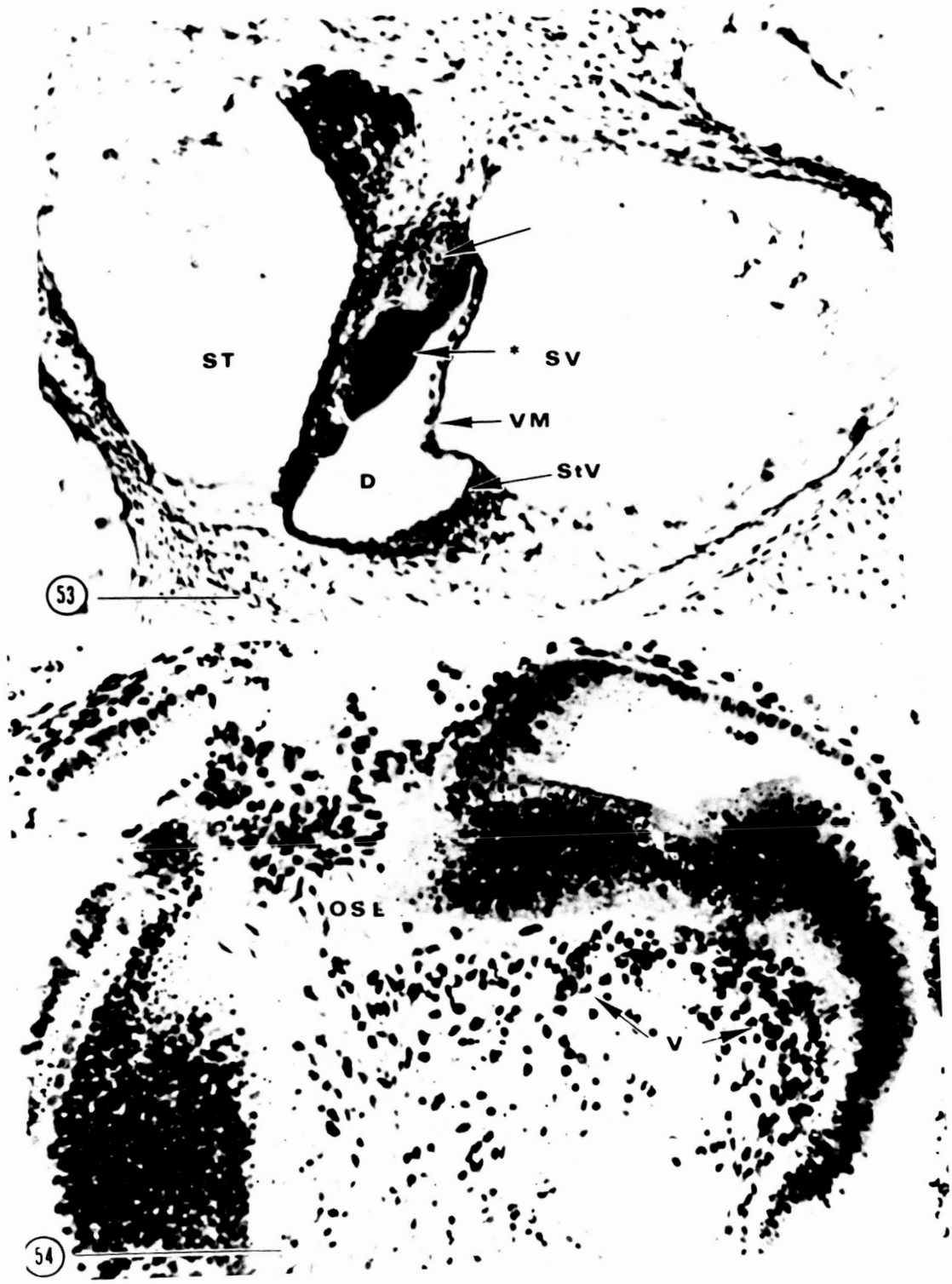

Plate 28

Figure 55: Note the degree of cartilaginous calcification (CA) and endochondral ossification (arrow) from this newborn flight specimen. The membranous labyrinth clearly shows a primitive split-base crest (C), contributing to both the ampulla of the superior semicircular canal (SSC) and the ampulla of the lateral semicircular canal (LSC).

The utricular macula (UT) is overlain with an otolithic membrane featuring two categories of otoconia: a more posterior large size class (a) and a more anterior set of smaller otoconia (b). This region is displayed in figure 57 for greater cytological detail.

Figure 56: Detail of the macula of the saccule from a newborn flight specimen. Note the basally located nuclei of the sustentacular cells (s) which permeate the sensory epithelium, culminating with the apical cytoplasmic expansions forming the limiting membrane (LM). Embedded among the sustentacular cells are two categories of sensory hair cells (a and b), primarily evidenced by their nuclear differences. The hair cells extend clumps of stereocilia (H) into the supportive mass of the otolithic membrane (OM), which carries two size categories of otoconia.

A prominent basement membrane (arrows) firmly anchors the sensory macula to the underlying connective tissue bearing a rich capillary plexus infiltrated with numerous fine nerve processes.

	Animal #	Section plane	Stain	Magnification
Figure 55:	Flight #31	Transverse	Azure II	(100x; bar = 100 μ)
Figure 56:	Flight #3	Transverse	Azure II	(850x; bar = 10 μ)

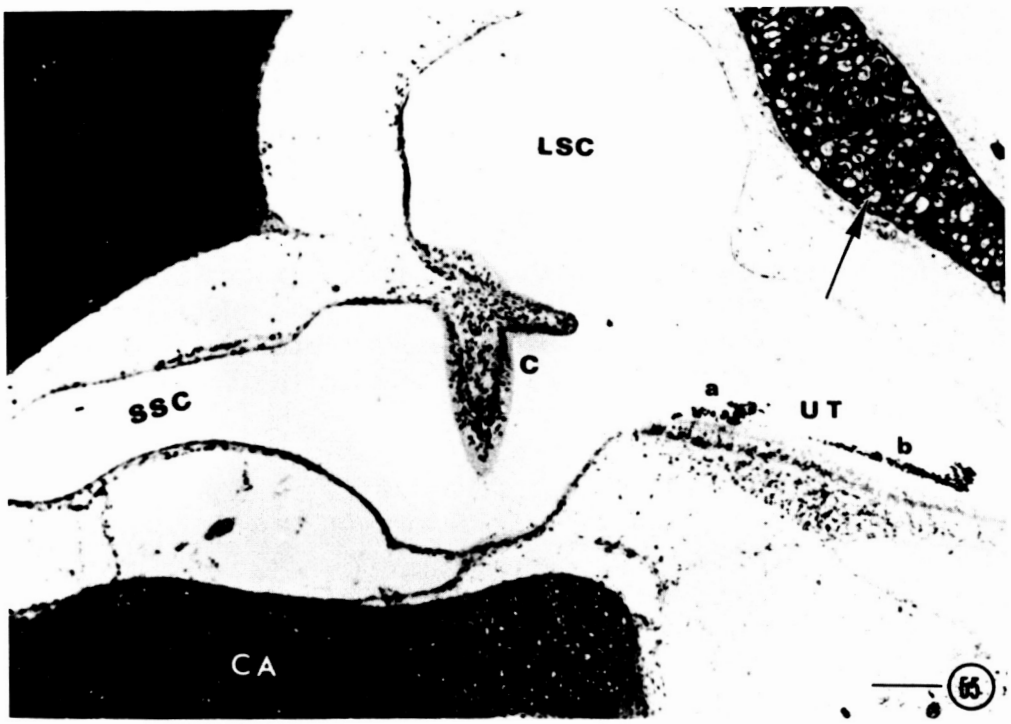

Plate 29

Figure 57: Detail of the utricular macula from the newborn flight specimen illustrated in figure 55. Note the thickened basement membrane (B) firmly anchoring the sensory macula upon the richly vascular connective tissue.

Prominent hair cells (three at arrows) are well differentiated. The otolithic membrane (OM) shows clear separation of two size categories of otoconia (a and b). The larger otoconia are more posteriorly located.

Figure 58: Portion of utricular macula, comparable to that illustrated in figure 57, taken from a newborn control specimen. Again, note the prminent basement membrane (B), differentiated hair cells (arrows) and otolithic membrane (OM) with two size categories of otoconia. The larger otoconia (a) are also arrayed along the more posterior surface of the sensory macula.

	Animal #	Section plane	Stain	Magnification
Figure 57:	Flight #31	Transverse	Azure II	(500x; bar = 100 μ)
Figure 58:	Synchronous #37	Transverse	Azure II	(50x; bar = 100 μ)

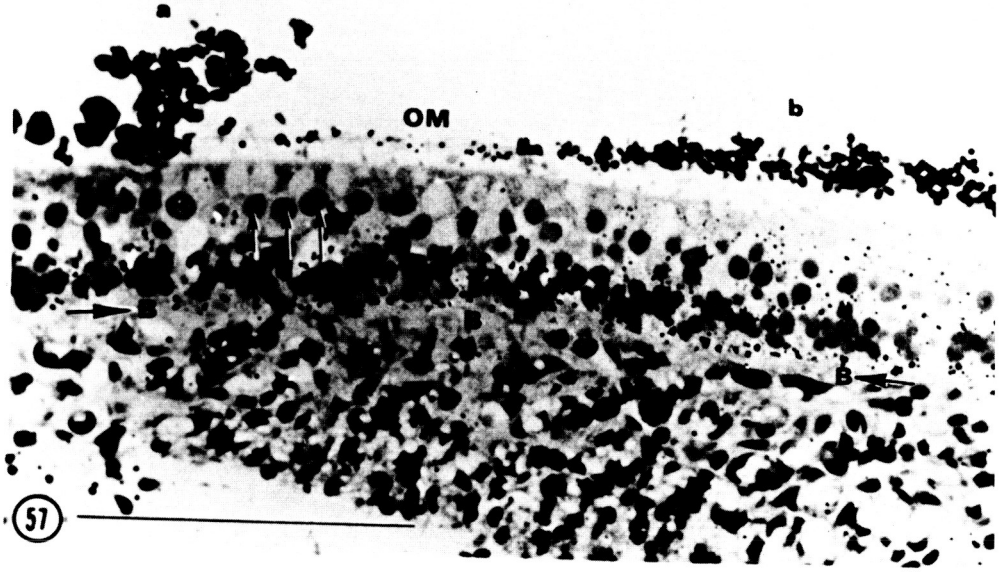

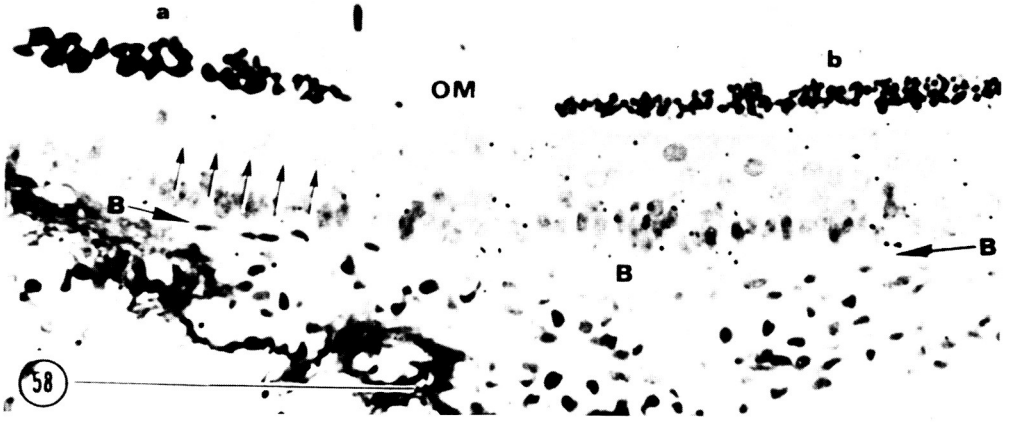

Plate 30

Figure 59: Coronal section through the left labyrinth of a newborn flight specimen. The protargol stain clearly reveals both the major vestibular (VN) and cochlear (CN) nerve branches of the eighth nerve, as well as many of its smaller branches supplying the sensory macula of the utricle (UT) and the sensory crest of the ampulla of the lateral semicircular canal (Ca). The calcified cartilage of the labyrinth (CA) and the precursors of the malleus (M) and incus (IN) is well compacted.

Figure 60: Detail of the sensory crest from the alteral semicircular canal of the newborn flight specimen illustrated in figure 59. Note the penetration of the prominent basement membrane (B) by numerous nerve processes (N) to establish synaptic relations with the differentiated sensory hair cells (H).

	Animal #	Section plane	Stain	Magnification
Figure 59:	Flight #36	Coronal	Protargol	(80x; bar = 100 μ)
Figure 60:	Flight #36	Coronal	Protargol	(850x; bar = 10 μ)

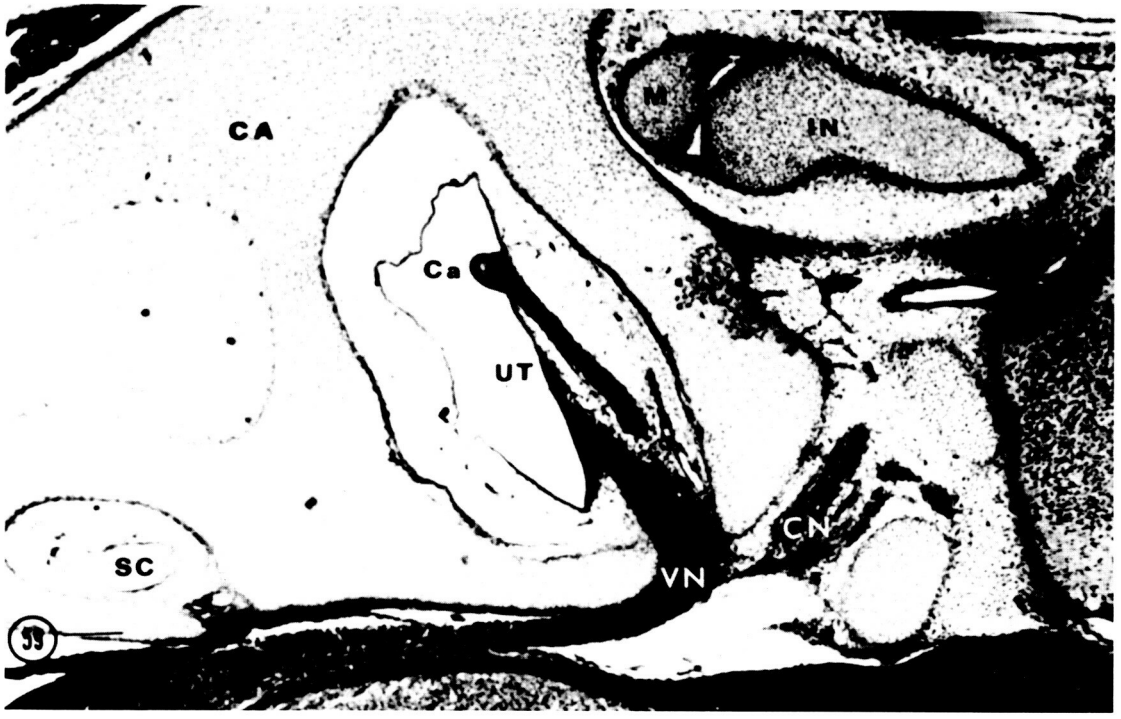

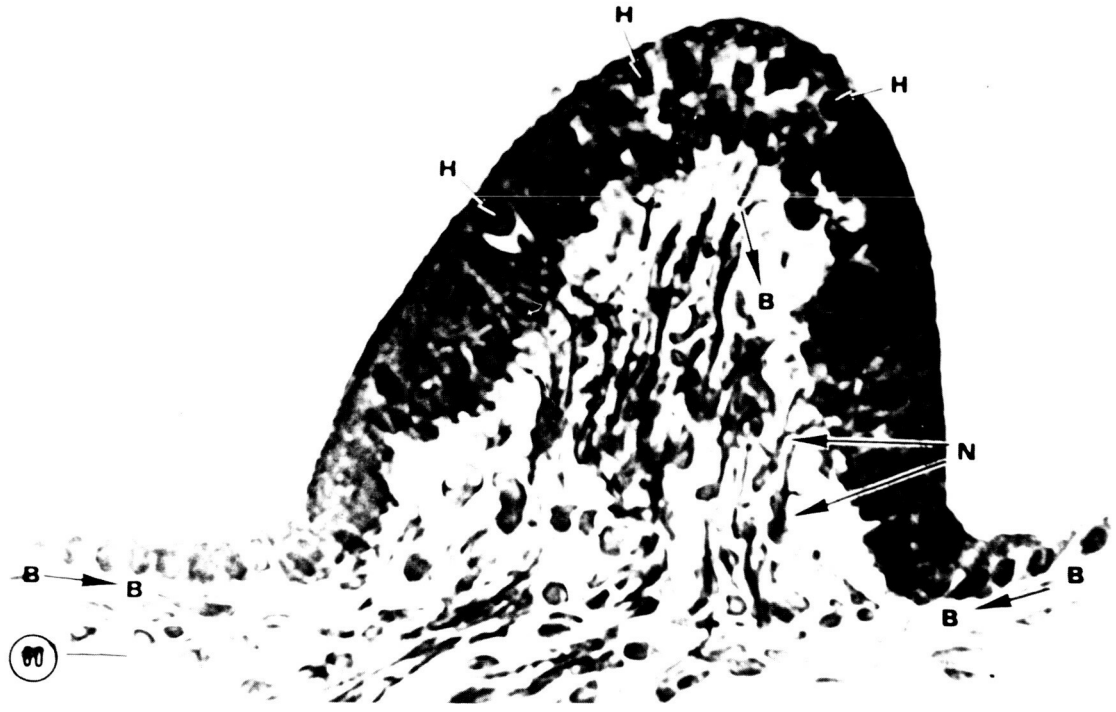

1. Report No.	2. Government Accession No.	3. Recipient's Catalog No.
NASA TM-88223		

4. Title and Subtitle	5. Report Date
FINAL REPORTS OF U.S. MONKEY AND RAT EXPERIMENTS FLOWN ON THE SOVIET SATELLITE COSMOS 1514	May 1986
	6. Performing Organization Code
7. Author(s)	8. Performing Organization Report No.
Richard C. Mains and Edward W. Gomersall (Eds.)	A-86147
	10. Work Unit No.
9. Performing Organization Name and Address	
Ames Research Center Moffett Field, CA 94035	11. Contract or Grant No.
	13. Type of Report and Period Covered
12. Sponsoring Agency Name and Address	Technical Memorandum
National Aeronautics and Space Administration Washington, DC 20546	14. Sponsoring Agency Code 805-94-00-01

15. Supplementary Notes

Point of contact: C. Schatte, M/S 240A-3, Ames Research Center, Moffett Field, CA 94035, (415)694-6748 or FTS 464-6748

16. Abstract

On December 14, 1983, the U.S.S.R. launched Cosmos 1514, an unmanned spacecraft carrying biological and radiation physics experiments from nine countries, including five from the United States. This was the fourth flight with U.S. experiments aboard one of the U.S.S.R.'s unmanned spacecraft. Earlier flights carried a variety of biological specimens and lasted 18.5 to 19.5 days. The Cosmos 1514 flight was limited to 5 days' duration because it was the first nonhuman primate flight for the U.S.S.R. Cosmos 1514 marked a significant departure from earlier flights both in terms of Soviet goals and the degree of cooperation between the U.S.S.R. and the United States. This flight included more than 60 experiments on fish, crawfish eggs, plants and seeds, 10 Wistar pregnant rats, and 2 young adult rhesus monkeys as human surrogates. After 5 days in orbit, the spacecraft landed in Central Asia where a Soviet recovery team began recovery operations. U.S. specialists participated in postflight data transfer and specimen transfer to the United States, and conducted rat neonatal behavioral studies. An overview of the mission is presented focusing on preflight, on-orbit, and postflight activities pertinent to the five U.S. experiments aboard Cosmos 1514.

17. Key Words (Suggested by Author(s))	18. Distribution Statement
Space biology Microgravity Soviet biosatellite Cosmos 1514 satellite	Unlimited Subject Category - 51

19. Security Classif. (of this report)	20. Security Classif. (of this page)	21. No. of Pages	22. Price*
Unclassified	Unclassified	282	A13

*For sale by the National Technical Information Service, Springfield, Virginia 22161

GPO 686-725/58250